Cellular Compartmentation Effects in Receptor-mediated Signal Transduction

by

Jason Michael Haugh

B.S., Chemical Engineering
North Carolina State University, 1994

Submitted to the department of Chemical Engineering
in partial fulfillment of the requirements for the degree of

Doctor of Philosophy in Chemical Engineering

at the

Massachusetts Institute of Technology

September 1999

Signature of Author .....
Department of Chemical Engineering
June 2, 1999

Certified by .....
Douglas A. Lauffenburger
Professor of Chemical Engineering
Thesis Supervisor

Accepted by .....
Robert E. Cohen
St. Laurent Professor of Chemical Engineering
Chairman, Committee for Graduate Students

Cellular Compartmentation Effects in Receptor-mediated Signal Transduction

by

Jason Michael Haugh

Submitted to the Department of Chemical Engineering on June 2, 1999
in partial fulfillment of the requirements for the degree of
Doctor of Philosophy in Chemical Engineering

Abstract

Cells survey their environment primarily through the engagement of specific cell surface receptor proteins. Ligated receptors participate in signal transduction by initiating intracellular reactions involving heterologous proteins and metobolites. A quantitative understanding of these signaling processes is the key to controlling cell functional responses, including survival and growth, migration, differentiation, and secretion. One issue of particular importance is how the structural organization of the cell can affect these events, by regulating the subcellular localization of signaling molecules. For example, many signaling receptors are internalized into the cell upon activation, leading to their delivery from the plasma membrane to intracellular organelles called endosomes.

Receptors in complex with cytosolic proteins almost invariably target membrane-associated molecules, including certain membrane lipids, Ras and related small GTPases, heterotrimeric G-proteins, and Src family tyrosine kinases, to carry out signaling functions. Based on theoretical modeling efforts, it is asserted that the membrane localization of these molecules impacts the organization of signaling interactions in two major ways: 1) it allows amplification of signaling via recruitment of enzymes from the cytosol to the membrane, which is expected to completely synergize with allosteric effects and covalent modifications like phosphorylation, and 2) it allows variations in membrane component concentrations and formation of microdomains to arise based on the chemical interactions between different membrane lipids. The latter would also affect the composition of endosomes relative to the plasma membrane, environments that are physically separated. For these reasons, unstructured models of intracellular signal transduction pathways are likely to be inadequate.

Experimental work involved the investigation of how the internalization of epidermal growth factor receptor (EGFR), a prominent receptor tyrosine kinase in mammals, affects the magnitude of signaling through distinct pathways involving phospholipase C (PLC) and the Ras GTPase. For both pathways, the binding and tyrosine phosphorylation of cytosolic proteins (PLC-γ1 for the PLC pathway and Shc for the Ras pathway) were not affected by receptor compartmentation in endosomes for a given level of total receptor activation. However, at the level of membrane target modification, endosome-associated PLC-γ1 could not hydrolyze its lipid substrate phosphatidylinositol (4,5)-bisphosphate (PIP_2), while the membrane-associated protein Ras was efficiently activated by internal EGFR in the same cell line. This provides evidence that receptors in different compartments may not have access to the same membrane-associated signaling molecules, and that internalization can select for the activation of certain pathways.

Thesis Supervisor: Douglas A. Lauffenburger
Title: Professor of Chemical Engineering

Acknowledgments

I am extremely grateful to my advisor, Douglas Lauffenburger, for his wisdom, encouragement and patience during the completion of this project. I would also like to thank all DAL lab members past and present, especially Cartikeya Reddy, Dave Schaffer, Lily Chu, Marti Ware, Sean Palecek, Mark Powers, Chase Orsello, Eric Fallon, Anand Asthagiri, Anne Dewitt, Casim Sarkar, Michael Lässle, and Doug "Pointspread" Osborne for fostering a lighthearted atmosphere on the 3rd floor and for helpful discussions. I will miss you guys, but I will still be in P.P.E.with picks ready to go. I am indebted to our collaborator on the project, Alan Wells, for immeasurable help and advice, as well as Kiran Gupta, Mark Van Epps-Fung, and Heng Xie from his lab for technical assistance. Excellent assistance in lab was also provided by Alarice Huang, an undergraduate student from the Biology department, who helped with this project. More great advice and encouragement was provided by the other members of my thesis committee: Professors William Deen, Gregory Stephanopoulos, and Lawrence Stern. While I owe a great debt to a lot of people, I was personally kept out of debt by the National Science Foundation Graduate Fellowship Program, the National Science Foundation Biotechnology Program, and the Merck/MIT Collaboration, who funded my research. Finally, I want to thank my parents, Martin and Deborah Haugh, and especially my wife, Ruthie, for their support and love during these last five years.

Table of Contents

Tables and Figures

CHAPTER 1
Introduction and Background

Living cells react to perturbations in their environment. Such responses include survival and proliferation, migration, or differentiation of cell function. The goal of *cell engineering* is to quantitatively control these behaviors through manipulation of the cellular environment and the ability of the cell to respond to it. Realization of this goal would allow rational design of pharmaceuticals and gene therapies at the cellular level, use of engineered cells themselves as therapeutic agents, tailoring of biomaterials for tissue engineering applications, and optimization of commercial protein production. The primary way in which cells survey their surroundings is through reversible binding of cell surface receptors. These proteins span the cell membrane and present docking sites for specific ligand molecules. Once a complex of ligand and receptor has formed, the receptor is able to initiate multiple chemical reactions. These reactions eventually trigger the activation of genes and expression of protein products, changes in cell metabolism, and modification of cellular structure. Thus, this process of *signal transduction*, or *signaling*, is the biochemical integration of all the information perceived by the cell.

1.1 Epidermal Growth Factor Receptor (EGFR) and its Ligands

The 170 kDa epidermal growth factor receptor (EGFR) is the best-characterized of a class of signaling receptors called receptor tyrosine kinases (RTKs), which contain a domain with intrinsic enzymatic activity that is able to selectively phosphorylate protein substrates on tyrosine residues. Other RTKs include the receptors for insulin, insulin-like growth factor, platelet-derived growth factor (PDGF), fibroblast growth factor, and nerve growth factor (van der Geer et al., 1994). The relavent structural details of the EGFR are illustrated in Figure 1.1. The functional domains of the EGFR include the extracellular ligand-binding (ecto) domain, which contains dual cysteine-rich regions that cooperate to bind growth factor ligands, short transmembrane and juxtamembrane regions, the kinase domain, and a cytosolic regulatory domain. Early studies of EGFR function indicated that its tyrosine kinase activity is fully responsible for its biological function (Chen et al., 1987). EGFR is the first member of the erbB receptor family of RTKs. The other members are erbB-2, erbB-3, and erbB-4.

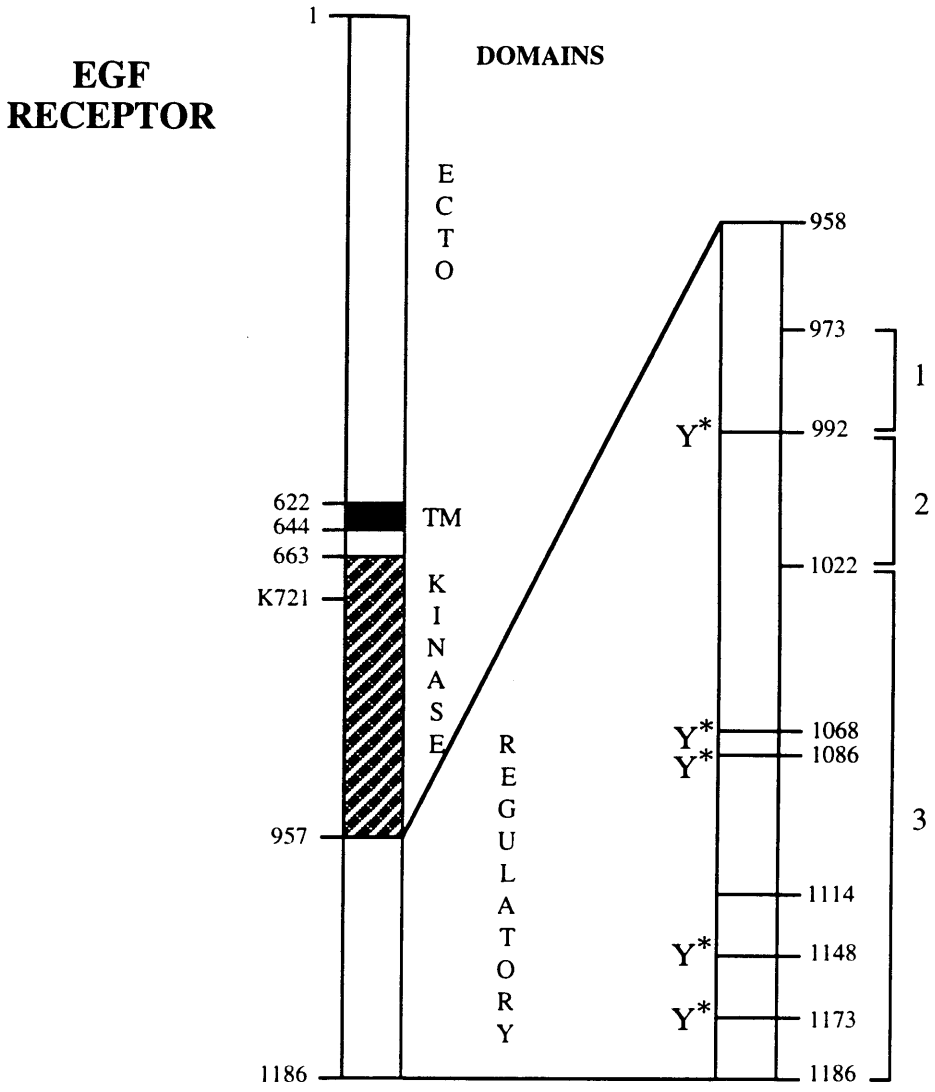

Figure 1.1 Structure/Function of the Epidermal Growth Factor Receptor (EGFR). The sites of tyrosine autophosphorylation are indicated by asterisks. Each of the regions designated 1, 2, and 3 provide gain of function when added onto truncated, internalization-deficient receptors. TM, transmembrane segment. Adapted from Chang et al., 1993.

The proto-oncogene erbB-2 is found to be overexpressed in multiple human tumors (particularly those of the breast), has no known ligand, and is transactivated by activated EGFR (Hynes and Stern, 1994; Dougall et al., 1994). ErbB-3 and -4 have differing ligand specificities from EGFR, and, interestingly, erbB-3 lacks intrinsic tyrosine kinase activity (Carraway and Cantley, 1994; Chen et al., 1996b).

Epidermal growth factor (EGF) is synthesized as a 1207 amino acid precursor, while the functional secreted form is 53 amino acids (Scott et al., 1983; Bell et al., 1986). EGF is capable of stimulating a spectrum of responses, including proliferation and migration, in many cells of epithelial origin, including keratinacytes and fibroblasts. Discovered more than 30 years ago, roles for this cytokine have been identified in tissue organization during development and wound healing (Carpenter and Wahl, 1990; Pittelkow, 1992). EGF binds reversibly to the EGFR with 1:1 stoichiometry (Weber et al., 1984), stimulating receptor tyrosine kinase activity, homo- and hetero-dimerization, and endocytic internalizaton, with the outcome of multiple signaling pathways regulating the cell behavioral response (Lund et al., 1990b; Lemmon and Schlessinger, 1994; van der Geer et al., 1994). TGFα, amphiregulin, heparin-binding EGF, and betacellulin are among other ligands which belong to the EGF family and bind EGFR; the EGF family member neu differentiation factor (NDF) does not bind to EGFR, but rather to erbB-3 and -4 (Carpenter and Wahl, 1990; Kimura et al., 1990).

1.2 Regulation of EGFR Function by Phosphorylation

EGFR kinase activity, associated with residues 663-957, is activated upon ligand association, and the first substrate to be phosphorylated is the receptor itself. The kinase machinery autophosphorylates tyrosines in the C-terminal regulatory region (Figure 1.1), which can be considered to occur instantaneously upon receptor ligation (Hunter and Cooper, 1981); the kinetics of EGFR kinase activity (Cheng and Koland, 1996) are very rapid compared to those of ligand binding. The autophosphorylation sites of EGFR compete with other substrates for the kinase, suggesting a mechanism by which phosphorylation relieves an inhibition of kinase activity by the regulatory domain of the EGFR (Bertics and Gill, 1985; Bertics et al., 1985; Walton et al., 1990). Tyrosine phosphorylation is reversed by protein tyrosine phosphatases (PTPs) (Tonks and Charbonneau, 1989; Fischer et al., 1991; Sun and Tonks, 1994; Neel and Tonks, 1997), although much less is known about phosphatases than kinases in general. Some PTPs that

modulate RPTK activity are membrane proteins (Kulas et al., 1996b; Kulas et al., 1996a), implying a high frequency of potentially reactive collisions with RTKs.

Y1173 is the preferred autophosphorylation site of the EGFR, with nearly 1:1 phosphorylation per bound receptor. Y1148 and Y1068 are secondary sites, while Y992 and 1086 are phosphorylated at very low stoichiometry (Downward et al., 1984; Margolis et al., 1989; Walton et al., 1990). Unoccupied receptors are either not able to be phosphorylated or are summarily dephosphorylated by phosphatases, so there is a stoichiometric relationship between ligated and tyrosine-phosphorylated EGFR (Lund and Wiley, 1994).

A large body of evidence suggests that EGFR signaling is attenuated by heterologous phosphorylation on serine and threonine residues. In particular, T654, T669, S671, and S1046/7 have been identified as phosphorylation sites that regulate EGFR function, although the relative importance of each is debatable. Activation of protein kinase C (PKC) has been shown to correlate with T654 phosphorylation, affinity downmodulation, and abrogation of EGF-induced responses, representing a negative feedback loop that can be selectively blocked by the T654A mutation (Fearn and King, 1985; Lin et al., 1986; Welsh et al., 1991). PDGF agonization of its receptor also potentiates phosphorylation of EGFR T654, but in a PKC-independent manner (Davis and Czech, 1987). Interestingly, depletion of PKC in human fibroblasts by long-term exposure to phorbol esters does not affect the observed modulation of affinity, indicating other mechanisms (Wiley et al., 1989). T654 phosphorylation in response to phorbol ester treatment significantly attenuates EGFR kinase activity (Lund et al., 1990a). Thus, while affinity may be only modestly reduced, the biological activity of receptors desensitized in this manner may be seriously compromised in some cases. Another study examined T669 and S671 phosphorylation by mutating these sites to alanine. While these receptors bound ligand and were autophosphorylated normally, they were impaired in their ability to internalize (see below) inducibly (Heisermann et al., 1990). Interestingly, EGFR T669 is phosphorylated by a mitogen-activated protein kinase (MAPK) *in vitro*, suggesting a feedback loop (Northwood et al., 1991; Takishima et al., 1991). Finally, alanine mutation of S1046/7 also inhibited internalization and prevented desensitization of EGFR-mediated phosphorylation of an exogenous substrate *in vitro* (Countaway et al., 1992; Theroux et al., 1992). Taken together, serine/threonine phosphorylation can compromise the biological activity of EGFR in varying ways.

1.3 EGFR-mediated Signal Transduction Pathways

Intracellular proteins that participate in signaling cascades recognize autophosphorylated residues on EGFR and other RTKs. These physical interactions are achieved through the src homology 2 (SH2) and phosphotyrosine-binding (PTB) modular domains of signaling proteins (Pawson, 1995; van der Geer and Pawson, 1995), which derive specificity from the primary structure of the receptor around the target tyrosine (Songyang and Cantley, 1995; Zhou et al., 1995). The three major potential implications of these binding events, as illustrated in Figure 1.2, are: 1) allosteric activation of the protein substrate, 2) an increase in the frequency of phosphorylation of the bound substrate by the receptor kinase, and 3) recruitment to the membrane that enhances associations with downstream targets there. Allostery, covalent modification, and membrane localization are all likely to play a role in any given signaling pathway at the receptor level, and these contributions can be synergistic.

EGFR mediates the activation of three major signaling pathways: the phospholipase C (PLC), the Ras/mitogen-activated protein kinase (Ras/MAPK), and phosphatidylinositol 3-kinase [PI(3)K] pathways (Table 1.1). EGFR elicits activation of the γ1 isoform of PLC in fibroblasts, which catalyzes the hydrolysis of the acidic phospholipid phosphatidylinositol (4,5)-bisphosphate (PIP_2) (Rhee and Choi, 1992). The products of this reaction are diacylglycerol (DAG), which remains in the membrane and activates the serine/threonine kinase protein kinase C (PKC), and inositol (1,4,5)-triphosphate (IP_3), which cooperatively releases calcium from intracellular stores (Toker, 1998). Also, proteins with pleckstrin homology (PH) domains bind to PIP_2 or other lipids with high affinity (Lemmon et al., 1996; Lemmon et al., 1997), and PLC-mediated hydrolysis releases associated proteins into the cytosol. Binding of PLC-γ1 to autophosphorylated EGFR enhances the tyrosine phosphorylation of PLC-γ1 by the receptor kinase, predictably by reducing the Michaelis constant K_M (Margolis et al., 1990; Rotin et al., 1992; Zhu et al., 1992). Phosphorylation by EGFR activates the enzyme *in vivo*, apparently by allowing it to hydrolyze PIP_2 bound by other proteins (Goldschmidt-Clermont et al., 1991). Since PIP_2 is a membrane lipid, recruitment to activated EGFR would presumably also modulate PLC by membrane localization (Fig. 1.2).

Previous studies using EGFR-expressing NR6 fibroblasts have identified the molecular requirements for PLC activation and its role in cellular function. Using signaling-restrictive EGFR mutants, it was determined that EGFR kinase activity and autophosphorylation sites are strictly required for modulation of PLC activity *in vivo* (Margolis et al., 1990; Vega et al., 1992; Chen et al., 1994b).

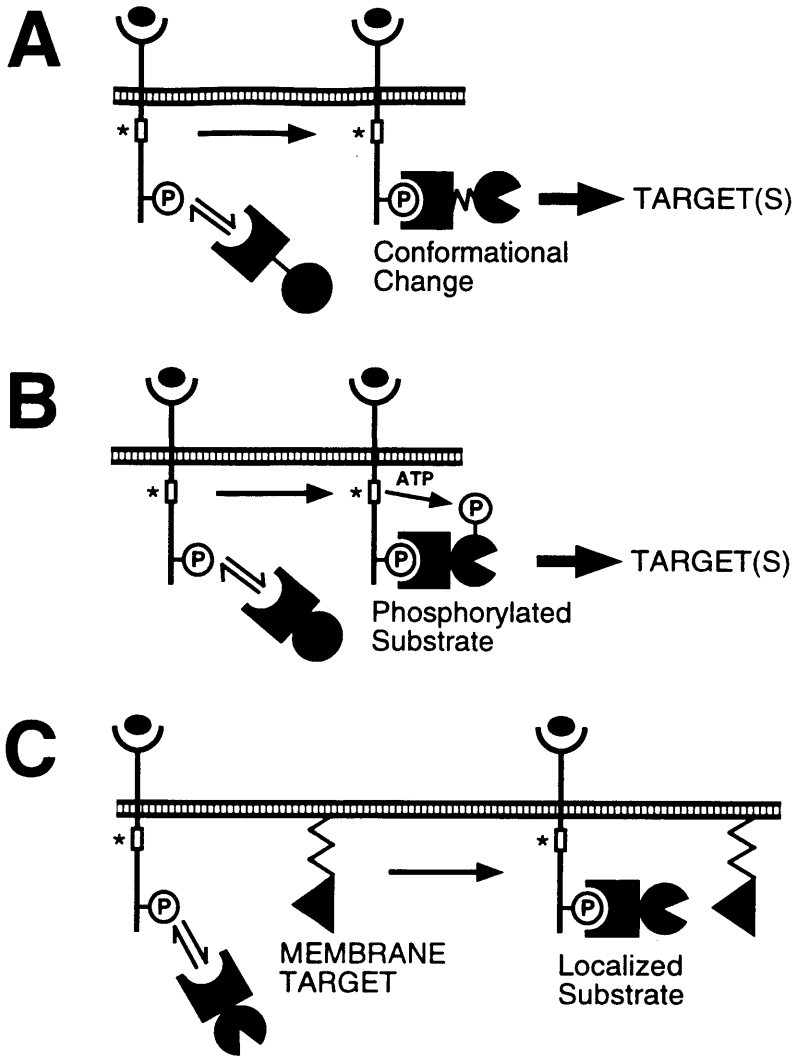

Figure 1.2 Mechanisms of RTK-mediated Activation of Protein Substrates. A, allostery. Upon association of a substrate molecule with an autophosphorylated receptor, a conformational change is transmitted from the binding domain of the substrate to its catalytic domain. The activity of the catalytic domain towards downstream targets is affected by this structural change. B, increase in phosphorylation frequency. Receptor binding brings the substrate in prolonged proximity to the active kinase domain of the receptor, resulting in a significant increase in the rate at which the substrate is phosphorylated. The activity of the substrate's catalytic domain towards downstream targets is affected by the phosphorylation state of the substrate. C, membrane localization. The catalytic domain of the substrate is already fully active per se, but the localization of a substrate molecule to a cellular membrane enhances its search for targets residing there.

Substrate	Binding Domains	Tyrosine-Phosphorylated?	Target	Product(s)
PLC-γ1	2xSH2	Y	PIP_2	DAG + IP_3
Grb2-Sos	SH2	N	Ras-GDP	Ras-GTP
Shc	SH2, PTB	Y	Grb2-Sos/ Ras-GDP	Ras-GTP
PI(3)K	2xSH2	Y	PIP_2	PIP_3

Table 1.1 Signaling Functions of EGFR-binding Proteins. The enzymes phospholipase C-γ1 (PLC-γ1) and phosphatidylinositol 3-kinase [PI(3)K] target the membrane lipid phosphatidylinositol (4,5)-bisphosphate (PIP_2) for hydrolysis and phosphorylation, respectively. The Grb2-Sos complex, aided by tyrosine-phosphorylated Shc, targets the membrane-tethered Ras-GTPase for nucleotide exchange (GTP for GDP) and activation.

PLC-restrictive receptor mutants also failed to elicit cell migration in response to EGF, and inhibition of PLC activity by PLC-specific drug and PLC antisense treatments blocked cell motility (Chen et al., 1994a; Chen et al., 1994b). In these cells, PLC-mediated PIP_2 hydrolysis leads to liberation of the actin-modifying protein gelsolin into the cytosol. Inhibition of PLC blocked gelsolin release from the membrane, and treatment with antisense gelsolin inhibited cell migration, linking EGFR-mediated PLC activity to dynamic changes in the cytoskeleton that affect migration (Chen et al., 1996a).

The Ras GTPase (21 kDa) is highly conserved in eukaryotes (Bourne et al., 1991), and is targeted for insertion in the plasma membrane by a series of posttranslational modifications (Willumsen et al., 1984; Willumsen et al., 1996). In the GTP-bound active state, Ras initiates the Raf/MEK/MAPK kinase cascade and activates other GTPases to control cell growth, differentiation, and cytoskeletal organization in various cell types (Vojtek and Der, 1998). Ras hydrolyzes GTP to GDP, which shuts off these signals, and the rate of hydrolysis is regulated by GTPase activating proteins (GAPs) (Zhang et al., 1990; McCormick, 1996). Mutations which hinder the ability of Ras to hydrolyze GTP are transforming, and such mutations are implicated in a high percentage of human tumors (Bos, 1989). In fibroblasts, activation of the Ras pathway by EGFR is mediated by a complex of Grb2 and Sos proteins. Grb2 is a ~23 kDa protein comprised almost entirely of one SH2 and two SH3 domains (Chardin et al., 1995), which ubiquitously coprecipitates with EGFR and PDGF receptor via its SH2 domain. Grb2 is not phosphorylated by RTKs and does not have enzymatic activity; its function is to serve as an adaptor that links other proteins such as Sos to RTKs via its SH3 domains (Lowenstein et al., 1992; Olivier et al., 1993; Simon et al., 1993; Buday and Downward, 1993a; Chardin et al., 1993; Egan et al., 1993; Gale et al., 1993; Li et al., 1993; Rozakis-Adcock et al., 1993). Homologs of Sos (Son of Sevenless) are guanine nucleotide exchange factors (GEFs) for the Ras GTPase (Wolfman and Macara, 1990; Bonfini et al., 1992; Bowtell et al., 1992).

Sos, as a GNP exchange factor, mediates the activation of Ras by stimulating the dissociation of GDP and GTP from Ras (Feig, 1994). The exchange is completed when Ras binds another GNP molecule from the pool of free nucleotides; this favors the active state *in vivo* since GTP is in > 10-fold excess over GDP in the cytosol (Lai et al., 1993). The activation of Ras in response to RTK ligands, characterized almost exclusively in fibroblasts, involves an increase in the exchange of nucleotides on Ras (Buday and Downward, 1993b; Medema et al., 1993). On the other hand, stimulated cells of hematopoietic lineage do not show such an increase in nucleotide exchange activity even though Ras is activated quite efficiently, suggesting a decrease in GAP activity (Downward

et al., 1990; Torti et al., 1992). *In vitro* studies demonstrate that Grb2 and mammalian homologs of Sos can form highly stable complexes; the SH3 domains of Grb2 both contribute to tight binding of proline rich sequences in Sos independently of Grb2 SH2 occupation (Cussac et al., 1994; Lemmon et al., 1994). While these studies suggest a precoupled heterodimer, coprecipitation of Sos and Grb2 is increased significantly in response to EGF in Rat 1 cells, suggesting that the interaction is regulated to some degree *in vivo* (Buday and Downward, 1993a). Importantly, the *in vitro* exchange activity of Sos does not depend on whether the protein is purified from quiescent or EGF-stimulated cells, nor is it affected by the presence of EGFR and/or Grb2 *in vitro*, suggesting that the Grb2-Sos or EGFR-Grb2-Sos complexes by themselves do not have enhanced exchange activity (Buday and Downward, 1993a). Sos is not tyrosine-phosphorylated by RTKs and does not seem to be activated allosterically in a direct fashion by RTK and Grb2 interactions alone, begging the question of how the activity of Sos might be regulated by RTKs. A change in localization of Grb2-Sos from cytosol to membrane is observed in response to EGF, suggesting that the presence of Sos in complexes with EGFR has the effect of bringing GEF activity closer to the constitutively membrane-associated Ras (Buday and Downward, 1993a). Indeed, it was found that constitutive targeting of Sos to the membrane is transforming in a Ras-dependent and RTK-independent fashion (Aronheim et al., 1994; Quilliam et al., 1994), confirming that location at the membrane is sufficient for modulating Ras activation.

The 110 kDa mammalian phosphatidylinositol 3-kinases [PI(3)Ks] phosphorylate phosphatidylinositol (PI) lipids on the D3 position, producing PI 3-P, $PI(3,4)P_2$, and PIP_3. The last two products are upregulated in response to RTK ligands (Auger et al., 1989) and seem to be instrumental in triggering cell proliferation, cytoskeletal organization, and survival (Carpenter and Cantley, 1996; Vanhaesebroeck et al., 1997; Carpenter, 1996; Toker and Cantley, 1997). Induction of PI(3)K activity associated with the α and β isoforms of p110 is observed in lysates of PDGF- and EGF-stimulated cells *in vitro* (Auger et al., 1989; Bjorge et al., 1990), and this activity coprecipitates with an 85 kDa protein recognized by anti-phosphotyrosine antibodies in PDGF-stimulated cells (Kaplan et al., 1987). Upon cloning of p85, it was discovered that there are two isoforms (α and β). These form stable heterodimers with p110 *in vivo* and have dual SH2 domains that associate with autophosphorylated RTKs upon ligand stimulation *in vitro* (Escobedo et al., 1991; Skolnik et al., 1991; Hu et al., 1992; McGlade et al., 1992). While specific high affinity binding to PDGF receptors is primarily controlled by the C-terminal SH2 domain of p85 (Klippel et al., 1992), binding of both SH2 domains likely proffers stable binding and/or maximal PI(3)K activity *in vivo* (Cooper and Kashishian, 1993; Rordorf-Nikolic et

al., 1995). While EGF clearly stimulates PI(3)K *in vivo*, and binding to autophosphorylated EGFR can be demonstrated *in vitro*, whether p85 can directly bind to EGFR *in vivo* has been questioned.

Binding of p85 SH2 domains induces a conformational change in p85, which is associated with an increase in p110 activity (Shoelson et al., 1993). This is accomplished via the p110 binding domain of p85, located between the SH2 domains; binding of this domain by itself is sufficient to activate p110 (Cooper and Kashishian, 1993; Klippel et al., 1993). A chimera of this domain fused with p110 is a constitutively active mutant (p110*), allowing study of PI(3)K-mediated downstream signaling (Hu et al., 1995). As previously discussed, RTK binding also localizes substrates to cellular membranes. Since the direct targets of PI(3)K are membrane lipids, a consequence of receptor binding would be that these target lipids would see a higher concentration of enzyme, yielding enhancement of the observed PI(3)K activity over and above that caused by the conformational change in p85 (allosteric effects). To test this, p110 constructs were modified with post-translational lipid modification signal peptides that target proteins to the plasma membrane, in tandem with the activating chimera; while the lipid-modified p110* has ~ 50% of the *in vitro* PI(3)K activity as p110*, it is significantly more potent in producing 3'-phosphorylated lipids and activating downstream effectors *in vivo* (Klippel et al., 1996). Membrane targeting alone is also sufficient to increase downstream signaling *in vivo*, albeit to a level lower than the membrane-localized, activated p110* (Reif et al., 1996; Klippel et al., 1996). These results suggest that allosteric and locational effects are synergistic in the potentiation of PI(3)K activity.

1.4 Intracellular Trafficking of EGFR and its Ligands

A complicating issue in the regulation of EGFR-mediated signaling is that ligated receptors do not necessarily stay at the plasma membrane the whole time they are activated. Many of these receptor-ligand complexes are inducibly internalized (receptor-mediated endocytosis) on the time scale of minutes by entrapment in specialized, clathrin-coated pits in the membrane (Trowbridge et al., 1993). This entrapment is mediated by adaptor proteins, which link endocytic motifs exposed in the cytoplasmic domain of a ligated receptor to the clathrin cage. These pits invaginate and pinch off to form vesicles (~ 50 nm), which deliver receptor and ligand molecules to intracellular trafficking organelles known as sorting endosomes (100-500 nm). It is in endosomes that receptor and ligand molecules are sorted for recycling back to the cell surface or destruction in proteolytic

lysosomes (Figure 1.3). This allows the cell to control the number of receptor and ligand molecules available for long-term signaling (Mellman, 1996).

The specific rate of receptor internalization is characterized by the endocytic rate constant k_e (Wiley and Cunningham, 1982):

$$C_i = k_e \int_0^t C_s dt \approx k_e \sum \left(\frac{C_{s,f} + C_{s,i}}{2} \right) (t_f - t_i) \qquad (1.1),$$

where C_i and C_s are the amount of ligand inside and on the surface of cells, respectively, and t is time. The value of k_e can be determined by measuring C_s and C_i experimentally, employing the addition of radioiodinated ligand at time zero and construction of an InSur (Internal-Surface) plot, in which internal radioactivity C_i is graphed *versus* the numerical integral of surface-associated radioactivity C_s with respect to time (eqn. 1.1). For EGFR, factors other than ligand binding influence the entrapment of receptors in clathrin-coated pits and therefore k_e. Deletion of three regions of the EGFR cytosolic regulatory domain (Figure 1.3) yield successive loss of endocytic function (Chang et al., 1993). For example, cells expressing a c'973 truncated EGFR internalize EGF at the same basal rate as that of non-activating anti-EGFR antibody internalization by wild-type EGFR. This basal rate is consistent with random inclusion in coated pits (Wiley, 1985). EGFR kinase activity is also required for internalization (Chen et al., 1987; Lamaze and Schmid, 1995). However, while receptor autophosphorylation has a positive effect on internalization, it is not a strict requirement for induced endocytosis, suggesting a role for a heterologous substrate of the EGFR kinase (Lund and Wiley, 1994).

As mentioned above, receptor-mediated endocytosis is strongly influenced by ligand-dependent interactions of the receptor with cytoplasmic adaptor molecules. Thus, the cell's ability to downregulate its ligated receptors is "saturable" in cell lines overexpressing EGFR, presumably since the accessory proteins that immobilize receptors in clathrin-coated pits become stoichiometrically limiting (Wiley, 1988; Lund et al., 1990b). This effect can be assessed by plotting the endocytic rate constant k_e *versus* the average C_s for different ligand concentrations. Saturation is characterized by a drop in k_e for increasing C_s. Experiments of this nature were performed using radioiodinated EGF and EGFR-expressing NR6 fibroblasts. The parental NR6 line is devoid of EGFR mRNA and protein (Pruss and Herschman, 1977). The results (Figure 1.4) show that EGF internalization mediated by wild-type EGFR is saturable. The basal internalization rate, assessed for c'973 truncated EGFR, exhibits a constant, reduced value of k_e.

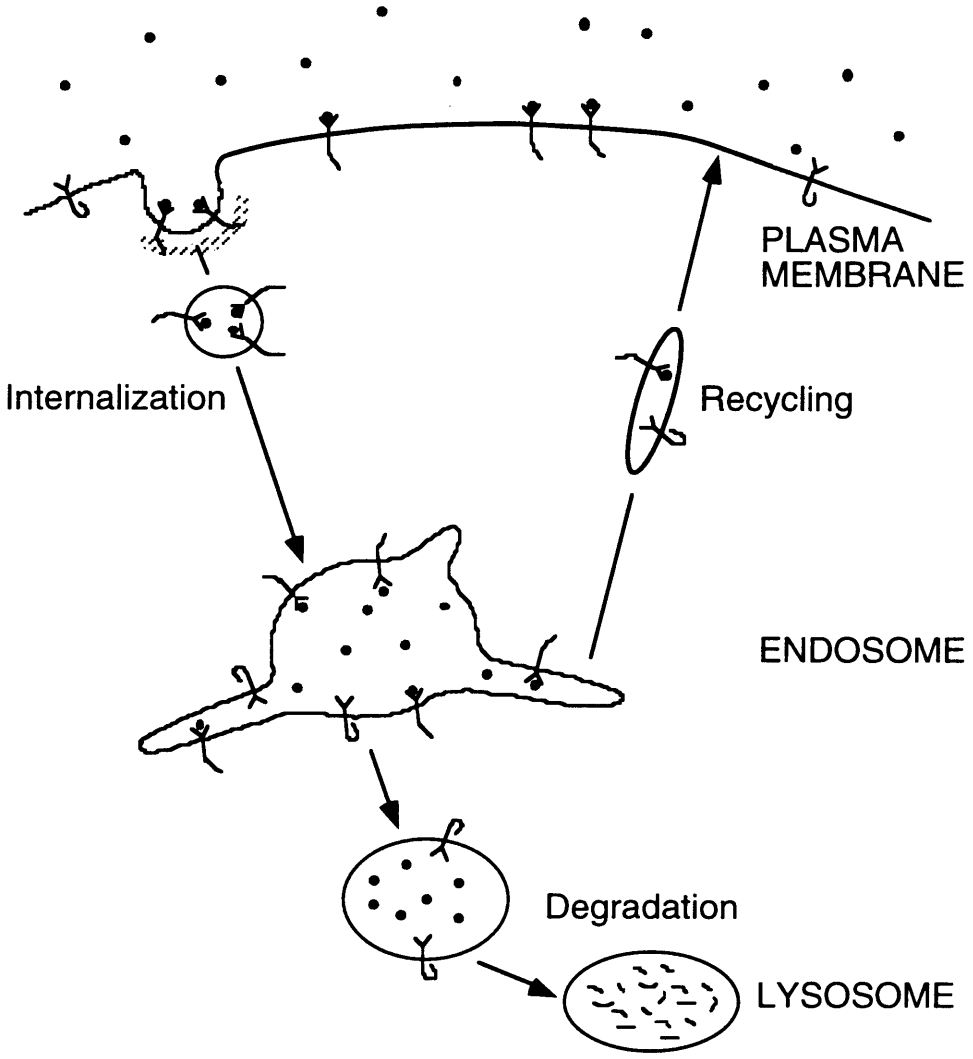

Figure 1.3 Endocytic Trafficking. The binding of cytokines to cognate receptors is often concomitant with the specific entrapment of the receptor in specialized clathrin-coated pits in the plasma membrane. Upon invagination the coated pit pinches off, and the resulting endocytic vesicle fuses with an early endosome, delivering receptor-ligand complexes and other components of the plasma membrane. It is here that receptors and ligands are sorted for either *recycling* back to the cell surface or *degradation*. Long protruding endosomal tubules collect molecules for return to the surface, while molecules that remain in the vesicular portion of the endosome are routed for degradation in lysosomes, which employ proteolytic enzymes to break down ligands and receptors.

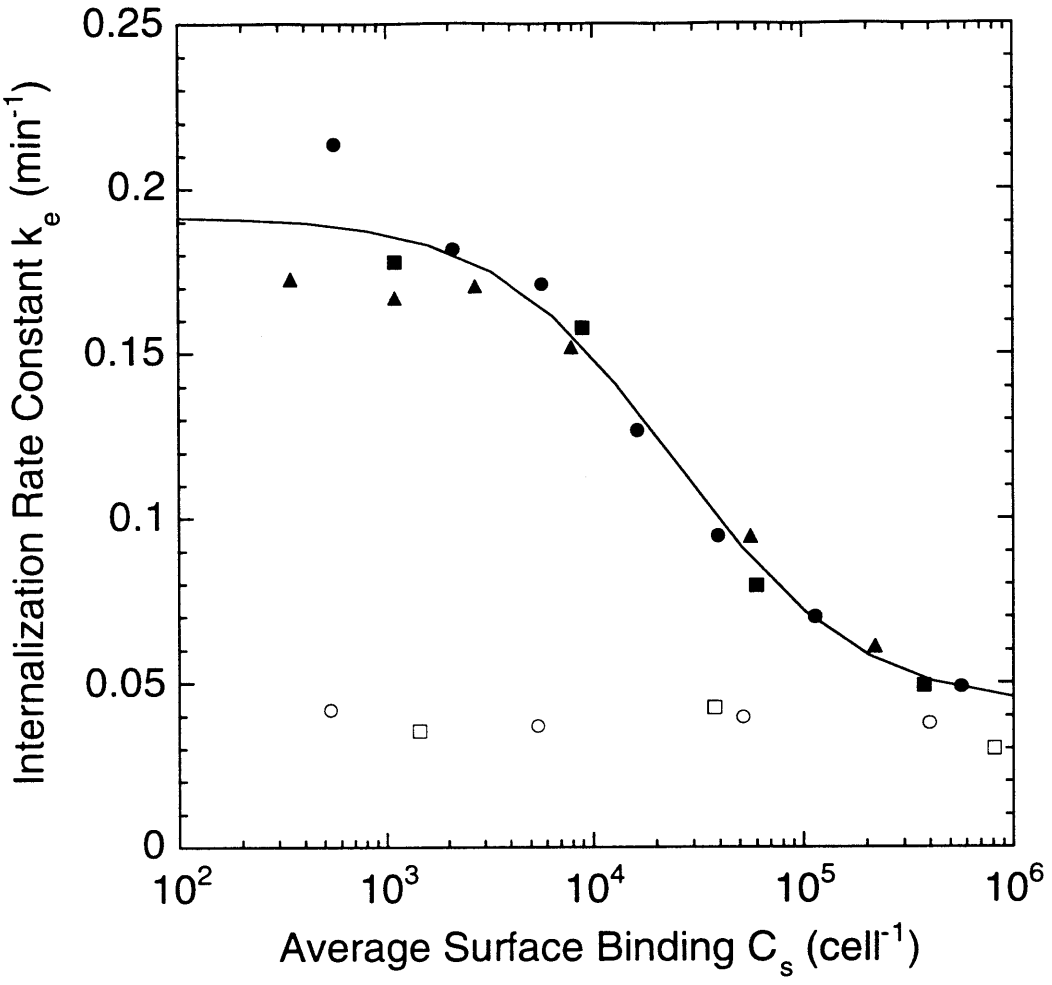

Figure 1.4 Saturation of Internalization in EGFR-expressing NR6 Fibroblasts. EGF was radioiodinated using Iodobeads (Pierce), according to the manufacturer's protocol. NR6 fibroblasts expressing wild-type (closed symbols) or c'973-truncated (open symbols) EGFR were exposed to ^{125}I-EGF at various concentrations for times of 1, 2, 3, 4, and 5 minutes, and surface and internal ligand were discriminated by pH 3 acid washing (Wiley and Cunningham, 1982). The endocytic rate constant k_e was calculated as described in the main text. The solid curve is the fit of the wild-type data to eqn. 1.2.

This plot can be analyzed theoretically by imposing a model for the interaction between ligated EGFR and a finite number of internalization components (Lund et al., 1990b):

$$k_e = \frac{(\lambda P_T + k_t K_{cp}^{-1}) + k_t C_s}{(P_T + K_{cp}^{-1}) + C_s} \qquad (1.2),$$

where λ and k_t are the rates of coated-pit invagination and basal endocytosis, respectively, K_{cp} is an affinity constant characterizing the interaction with internalization components at steady state, and P_T is the total number of these components.

During the intracellular trafficking of EGFR, the sorting and degradative compartments become increasingly acidified. While the physiological pH encountered in the extracellular environment of most cells is 7.4, sorting endosomes and lysosomes contain proton pumps that decrease the pH of the lumen to roughly 5.5-6.5 and 4, respectively (Mellman et al., 1986). Acidification can affect the activity of proteolytic enzymes, as well as the ability of the ligand to remain complexed with the receptor after internalization. For this reason, sorting endosomes have been called the compartment for uncoupling of receptor and ligand (CURL) (Dunn and Hubbard, 1984). Both the geometry of endosomes and specific interactions with endosomal proteins are believed to have a strong influence on the sorting of ligands and receptors. Lipids and other "membrane phase" components are predominantly routed into recycling tubules, while soluble "fluid phase" components in the endosomal lumen are predominantly retained in the vesicular portion of an endosome and routed for degradation. For example, transferrin remains tightly complexed with its receptor in endosomes, and this ligand is constitutively recycled along with its receptor. In contrast, low-density lipoprotein dissociates from its receptor at endosomal pH, and this ligand is degraded while its receptor is free to return to the cell surface (Ghosh et al., 1994). The EGFR ligands EGF and TGFα exhibit a marked difference in their receptor-binding affinities at pH 6.0, implying that EGF can occupy more receptors in endsomes than TGFα (French et al., 1995). This is likely due to the fact that TGFα contains five histidine residues, whereas EGF only has two, giving TGFα the much higher isoelectric point. This impacts the differential intracellular processing of these ligands (Ebner and Derynck, 1991), as detailed below.

The relative fluxes of ligand to recycling and degradative fates can be assessed experimentally by measuring the *ligand recycling fraction* (the fraction of radiolabeled ligand exocytosed by the cell that is intact) under steady state conditions (Figure 1.5). Nondissociative ligands can achieve recycling fractions even lower than fluid or membrane phase ligands if the ligated receptor is recognized by accessory proteins in the vesicular portion of an endosome, yielding endosomal retention. In this case, the receptor is also routed for degradation, yielding downregulation of total receptor number.

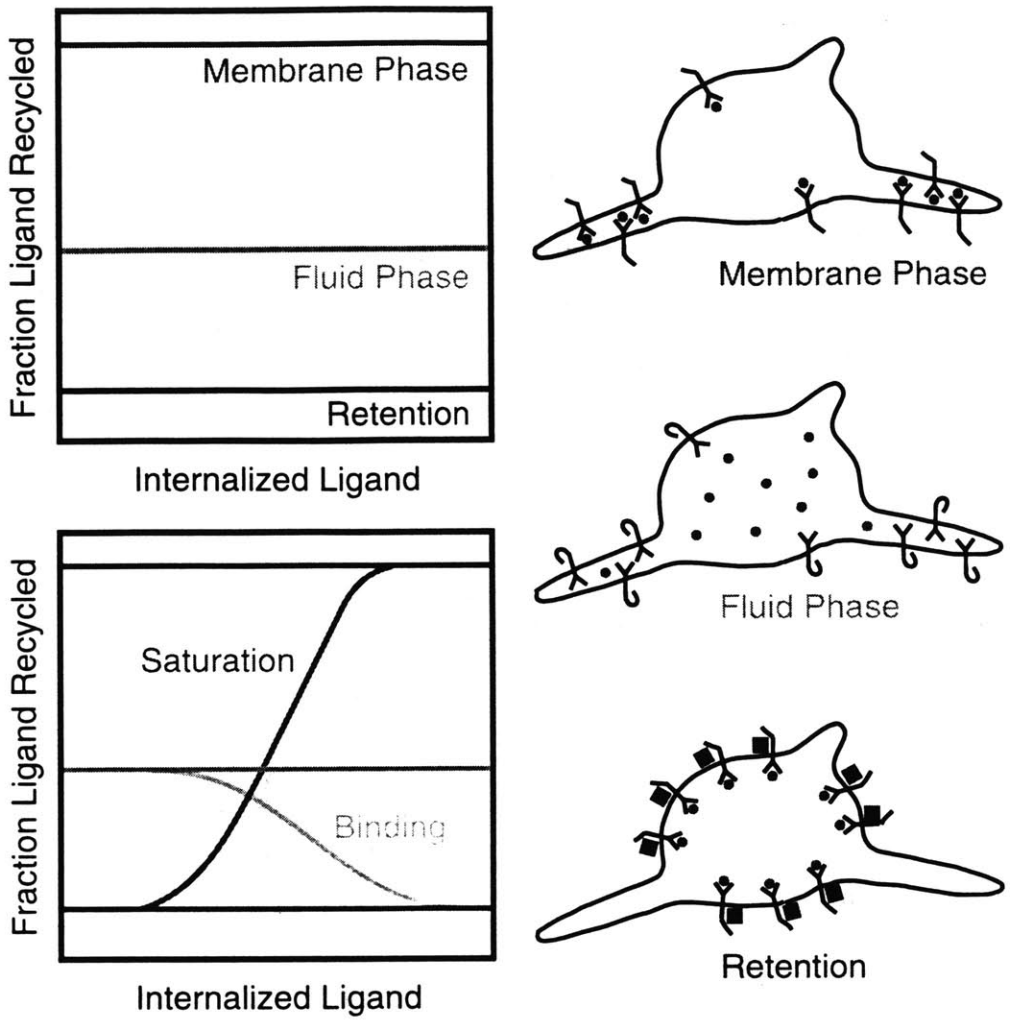

Figure 1.5 Mechanistic Analysis of Endosomal Sorting. Lipids and other "membrane phase" components are predominantly routed into recycling tubules, while soluble "fluid phase" components in the endosomal lumen are predominantly retained in the vesicular portion of an endosome and routed for degradation. The relative fluxes of ligand to recycling and degradative fates can be assessed experimentally by measuring the *ligand recycling fraction* (the fraction of radiolabeled ligand exocytosed by the cell that is intact) under steady state conditions. Nondissociative cytokines can achieve recycling fractions even lower than fluid or membrane phase ligands if the ligated receptor is recognized by accessory proteins in the vesicular portion of an endosome, yielding endosomal retention (top graph). As the level of internalized ligand increases, a dissociative ligand such as TGFα will bind some receptors (leading to retention of ligand and receptor), and a nondissociative ligand such as EGF will occupy enough receptors to saturate the limited number of accessory retention proteins (bottom graph).

For example, EGF is retained in endosomes in an occupancy-dependent manner (Herbst et al., 1994; French et al., 1994). This process requires regions of the EGFR cytosolic domain distinct from those regulating endocytosis (Opresko et al., 1995) and has been linked to the interaction of ligated EGFR with an accessory sorting nexin (Kurten et al., 1996).

Intermediate behaviors have been observed for EGF and TGFα in B82 fibroblasts; when the ligand recycling fraction is plotted *versus* the level of total intracellular ligand, the TGFα curve exhibits a slightly negative slope while the EGF curve clearly exhibits a positive slope. Counterintuitively, TGFα exhibits a higher recycling fraction at low levels of internal ligand, while EGF exhibits a higher recycling fraction at high levels of internal ligand (French et al., 1995). The current model adequately explains these subtle aspects of sorting (Figure 1.5): as the level of internalized ligand increases, a dissociative ligand such as TGFα will bind some receptors (leading to retention of ligand and receptor), and a nondissociative ligand such as EGF will occupy enough receptors to saturate the limited number of accessory retention proteins (French and Lauffenburger, 1996). Therefore, both receptor endocytosis and intracellular degradation are saturable in cells overexpressing EGFR, which has been linked to cell transformation and tumorigenesis (Wells et al., 1990; Masui et al., 1991; Reddy et al., 1994; Lenferink et al., 1998; Worthylake et al., 1999). Display of high receptor numbers leads to significant signal generation at low agonist concentrations, conditions under which only a small fraction of surface receptors are ligated and therefore subject to internalization and downregulation. When receptor overexpressors experience chronic agonist stimulation, the normal attenuation of signaling by receptor downregulation is mitigated by saturation of both specific internalization and intracellular degradation.

1.5 Thesis Topic

Acidification of endosomes causes many ligands, including TGFα, to dissociate from their receptors in endosomes, allowing the receptor to be sorted by default towards recycling to the plasma membrane. Unlike TGFα, EGF remains tightly complexed to EGFR in endosomes of multiple cell types (Kay et al., 1986; Carpentier et al., 1987). While this adequately explains the observed difference in postendocytic processing of the two ligands, it was not known whether internal receptor-ligand complexes could participate in signaling reactions. Receptor trafficking certainly downregulates the total numbers of receptors and ligands available for signaling in the long term, but internalization could also

have a short-term effect, either positive or negative, on signaling through the localization of a receptor pool in internal compartments.

The specific aims of my thesis project were 1) to assess whether the compartmentalization of EGFR in endosomes *versus* the plasma membrane can affect the magnitude of signaling through specific pathways, and 2) to mechanistically determine the molecular bases for any observed differences. This line of investigation basically tackles the following fundamental question: how structured should a model of receptor-mediated signaling (and therefore cell function) be (Bailey, 1998)?

1.6 Previous Studies Relating EGFR Trafficking and Signaling

Knauer and colleagues proposed a model in which there is a linear relationship between cell growth rate (or DNA synthesis rate) and the level of EGFR-ligand complexes on the surface C_s (Knauer et al., 1984). Using a mathematical model validated previously (Wiley and Cunningham, 1981), they related C_s to the extracellular ligand concentration [L] at pseudo-steady state:

$$\text{Response} = \gamma C_s = \frac{\gamma V_s k_f [L]}{k_{eR}(k_r + k_{eC}) + k_{eC} k_f [L]} \qquad (1.3),$$

where V_s is the rate of *de novo* receptor synthesis, k_f and k_r are association and dissociation rate constants for the receptor-ligand interaction, respectively, and k_{eR} and k_{eC} are basal and induced endocytic rate constants, respectively. γ can be considered the intrinsic mitogenic signal generation coefficient, a phenomenological parameter. The above model agreed well with experimental data obtained for the DNA synthesis rate (measured by incorporation of ^{3}H-thymidine) of human foreskin fibroblasts stimulated with EGF (Knauer et al., 1984). However, an interesting feature of the trafficking model is that internal complexes C_i is related to C_s at steady state by a proportionality constant, such that the following model would be equally valid:

$$\text{Response} = \gamma_s C_s + \gamma_i C_i = \left(\gamma_s + \frac{\gamma_i k_{eC}}{k_{deg}} \right) C_s \qquad (1.4),$$

where k_{deg} is the rate constant describing lysosomal degradation of internal complexes. Other models have also been developed with a similar flavor, but including effects such as saturation of internalization (Starbuck and Lauffenburger, 1992).

As mentioned above, it has been established that the interaction of EGF with the EGFR is relatively insensitive to endosomal acidification. In multiple cell types, the

internal pool of EGF-ligated EGFR remains phosphorylated on tyrosine, and these autophosphorylation sites are accessible to cytosolic proteins (Lai et al., 1989; Sorkin and Carpenter, 1991; Wada et al., 1992). This suggested that EGFR could carry out signaling functions in endosomes. In fact, in the case of Shc in rat liver parenchyma, the endosome-associated pool of the protein adaptor Shc exhibited a phosphorylation stoichiometry at maximal internalized EGF/EGFR exceeding that seen at the plasma membrane for any receptor density (Di Guglielmo et al., 1994). However, internalization of EGFR does not seem to lead to a uniform up- or down-regulation of substrate phosphorylation, indicating some degree of specificity (Vieira et al., 1996).

Interestingly, previous studies relating receptor internalization and signaling have not assessed how endosomal localization affects the function of cytosolic enzymes recruited by the EGFR. This function is to modify their substrates, *which are with few exceptions membrane-associated molecules*. This implies that the composition of endosomal membranes, compared to that of the plasma membrane, can be an important factor in determining the potential role of internal EGFR in signaling. In other words, this would in part determine the relative values of γ_s and γ_i in eqn. 1.4.

1.7 Thesis Overview

The possible role of internalized EGFR in signal transduction was examined both theoretically and experimentally. To answer the question of interest, it was first important to address the more fundamental issue of how subcellular location in general can influence signaling reactions. The depiction of Fig. 1.2C implies that recruitment to a membrane, be it the plasma membrane or endosomal membranes, can affect the dynamics of signaling. This was addressed theoretically by analyzing reaction and diffusion of molecules in two and three dimensions, to see how receptor-mediated membrane recruitment of a cytosolic enzyme can impact the association rate with a membrane-associated target (Chapter 2). To expand that effort to examine internalization of RTKs, another model was formulated that takes into account the binding of a cytosolic enzyme to both surface and internal receptors, phosphorylation/dephosphorylation of the enzyme, and the concentration profile of phosphorylated molecules in the cytosol (Chapter 3). Thus, signal transduction was analyzed using theory of reaction kinetics and transport phenomena, both fundamentals of chemical engineering.

Experimentally, quantitative measurements of signaling pathways were made using EGFR-expressing NR6 fibroblasts. The overall methodology was to construct a

relationship between signaling and the total level of EGFR autophosphorylation (surface and internal), the *activation-response* relationship. Unlike a dose-response curve, in which the cellular response is plotted *versus* ligand concentration, this methodology accounts for differing ligand affinities and feedback modulation of the EGFR. This analysis was performed under conditions that manipulated the relative numbers of EGFR at the surface and in internal compartments. If the location of the receptor does not affect signaling, then all points on an activation-response plot will fall on the same curve. If receptor location does matter, then internal receptor activation shifts the curve to the left (internal superior to surface) or right (internal inferior to surface). Two distinct signaling pathways were investigated: the phospholipase C (PLC) pathway (Chapter 4) and the Ras/MAPK pathway (Chapter 5).

Finally, a second generation mathematical model was formulated to address specific aspects of the PLC pathway (Chapter 6). This was motivated by experimental observations that could not be explained using the generalized analysis of Chapter 3. The model accounted for not only modulation of the enzyme PLC-γ1 by the EGFR, but also the regulation of the level of its lipid substrate PIP_2, and it can mimic effectively the experimental results. Importantly, the agreement of the model with experiment allowed the included molecular mechanisms, some controversial, to be scrutinized. Models of this type should be useful in the design of drug therapies and other biomedical intervention strategies.

1.8 References

Aronheim, A., Engelberg, D., Li, N., Al-Alawi, N., Schlessinger, J. and Karin, M. (1994). Membrane targeting of the nucleotide exchange factor Sos is sufficient for activating the Ras signaling pathway. *Cell*, 78: 949-961.

Auger, K.R., Serunian, L.A., Soltoff, S.P., Libby, P. and Cantley, L.C. (1989). PDGF-dependent tyrosine phosphorylation stimulates production of novel phosphoinositides in intact cells. *Cell*, 57: 167-175.

Bailey, J.E. (1998). Mathematical modeling and analysis in biochemical engineering: past accomplishments and future opportunities. *Biotechnol. Prog.*, 14: 8-20.

Bell, G.I., Fong, N.M., Wornstead, M.A., Caput, D.F., Ku, L., Urdea, M.S., Rall, L.B. and Sanchez-Pescador, R. (1986). Human epidermal growth factor precursor: cDNA sequence, expression in vitro and gene organization. *Nucleic Acids Res.*, 14: 8427-8446.

Bertics, P.J. and Gill, G.N. (1985). Self-phosphorylation enhances the protein-tyrosine kinase activity of the epidermal growth factor receptor. *J. Biol. Chem.*, 260: 14642-14647.

Bertics, P.J., Weber, W., Cochet, C. and Gill, G.N. (1985). Regulation of the epidermal growth factor receptor by phosphorylation. *J. Cell. Biochem.*, 29: 195-208.

Bjorge, J.D., Chan, T., Antczak, M., Kung, H. and Fujita, D.J. (1990). Activated type I phosphatidylinositol kinase is associated with the epidermal growth factor (EGF) receptor following EGF stimulation. *Proc. Natl. Acad. Sci. USA*, 87: 3816-3820.

Bonfini, L., Karlovich, C., Dasgupta, C. and Banerjee, U. (1992). The Son of Sevenless gene product: a putative activator of Ras. *Science*, 255: 603-605.

Bos, J.L. (1989). Ras oncogenes in human cancer: a review. *Cancer Res.*, 49: 4682-4689.

Bourne, H.R., Sanders, D.A. and McCormick, F. (1991). The GTPase superfamily: conserved structure and molecular mechanism. *Nature*, 349: 117-127.

Bowtell, D., Fu, P., Simon, M. and Senior, P. (1992). Identification of murine homologues of the *Drosophila* Son of Sevenless gene: potential activators of Ras. *Proc. Natl. Acad. Sci. USA*, 89: 6511-6515.

Buday, L. and Downward, J. (1993a). Epidermal growth factor regulates p21ras through the formation of a complex of receptor, Grb2 adapter protein, and Sos nucleotide exchange factor. *Cell*, 73: 611-620.

Buday, L. and Downward, J. (1993b). Epidermal growth factor regulates the exchange rate of guanine nucleotides on $p21^{ras}$ in fibroblasts. *Mol. Cell. Biol.*, 13: 1903-1910.

Carpenter, C.L. (1996). Intracellular signals and the cytoskeleton: the interactions of phosphoinositide kinases and small G proteins in adherence, ruffling and motility. *Sem. Cell Developmental Biol.*, 7: 691-697.

Carpenter, C.L. and Cantley, L.C. (1996). Phosphoinositide kinases. *Curr. Opin. Cell Biol.*, 8: 153-158.

Carpenter, G. and Wahl, M.I. (1990). "The epidermal growth factor family." in *Peptide Growth Factors and Their Receptors*, eds. Sporn, M. B. and Roberts, A. B. New York: Springer-Verlag, pp. 69-171.

Carpentier, J., White, M.F., Orci, L. and Kahn, R.C. (1987). Direct visualization of the phosphorylated epidermal growth factor receptor during its internalization in A-431 cells. *J. Cell. Biol.*, 105: 2751-2762.

Carraway, K.L. and Cantley, L.C. (1994). A neu acquaintance for erbB3 and erbB4: a role for receptor heterodimerization in growth signalling. *Cell*, 78: 5-8.

Chang, C., Lazar, C.S., Walsh, B.J., Komuro, M., Collawn, J.F., Kuhn, L.A., Tainer, J.A., Trowbridge, I.S., Farquhar, M.G., Rosenfeld, M.G., Wiley, H.S. and Gill, G.N. (1993). Ligand-induced internalization of the epidermal growth factor receptor is mediated by multiple endocytic codes analogous to the tyrosine motif found in constitutively internalized receptors. *J. Biol. Chem.*, 268: 19312-19320.

Chardin, P., Camonis, J.H., Gale, N., Van Aelst, L., Schlessinger, J., Wigler, M.H. and Bar-Sagi, D. (1993). Human Sos-1: a guanine nucleotide exchange factor for Ras that binds to Grb2. *Science*, 260: 1338-1343.

Chardin, P., Cussac, D., Maignan, S. and Ducruix, A. (1995). The Grb2 adaptor. *FEBS Letters*, 369: 47-51.

Chen, P., Gupta, K. and Wells, A. (1994a). Cell movement elicited by epidermal growth factor receptor requires kinase and autophosphorylation but is separable from mitogenesis. *J. Cell Biol.*, 124: 547-555.

Chen, P., Murphy-Ullrich, J.E. and Wells, A. (1996a). A role for gelsolin in actuating epidermal growth factor receptor-mediated cell motility. *J. Cell Biol.*, 134: 689-698.

Chen, P., Xie, H., Sekar, M.C., Gupta, K. and Wells, A. (1994b). Epidermal growth factor receptor-mediated cell motility: phospholipase C activity is required, but mitogen-activated protein kinase activity is not sufficient for induced cell movement. *J. Cell Biol.*, 127: 847-857.

Chen, W.S., Lazar, C.S., Poenie, M., Tsien, R.Y., Gill, G.N. and Rosenfeld, M.G. (1987). Requirement for intrinsic protein tyrosine kinase in the immediate and late actions of the EGF receptor. *Nature*, 328: 820-823.

Chen, X., Levkowitz, G., Tzahar, E., Karunagaran, D., Lavi, S., Ben-Baruch, N., Leitner, O., Ratzkin, B.J., Bacus, S.S. and Yarden, Y. (1996b). An immunological approach reveals biological differences between the two NDF/heregulin receptors, ErbB-3 and ErbB-4. *J. Biol. Chem.*, 271: 7620-7629.

Cheng, K. and Koland, J.G. (1996). Nucleotide binding by the epidermal growth factor receptor protein-tyrosine kinase. *J. Biol. Chem.*, 271: 311-318.

Cooper, J.A. and Kashishian, A. (1993). In vivo binding properties of SH2 domains from GTPase-activating proteins and phosphatidylinositol 3-kinase. *Mol. Cell. Biol.*, 13: 1737-1745.

Countaway, J.L., Nairn, A.C. and Davis, R.J. (1992). Mechanism of desensitization of the epidermal growth factor receptor protein-tyrosine kinase. *J. Biol. Chem.*, 267: 1129-1140.

Cussac, D., Frech, M. and Chardin, P. (1994). Binding of the Grb2 SH2 domain to phosphotyrosine motifs does not change the affinity of its SH3 domains for Sos proline-rich motifs. *EMBO J.*, 13: 4011-4021.

Davis, R.J. and Czech, M.P. (1987). Stimulation of epidermal growth factor receptor threonine 654 phosphorylation by platelet-derived growth factor in protein kinase C-deficient human fibroblasts. *J. Biol. Chem.*, 262: 6832-6841.

Di Guglielmo, G.M., Baass, P.C., Ou, W., Posner, B.I. and Bergeron, J.J.M. (1994). Compartmentalization of SHC, GRB2 and mSOS, and hyperphosphorylation of Raf-1 by EGF but not insulin in liver parenchyma. *EMBO J.*, 13: 4269-4277.

Dougall, W.C., Qian, X.L., Peterson, N.C., Miller, M.J., Samanta, A. and Greene, M.I. (1994). The neu-oncogene: signal transduction pathways, transformation mechanisms and evolving therapies. *Oncogene*, 9: 2109-2123.

Downward, J., Graves, J.D., Warne, P.H., Rayter, S. and Cantrell, D.A. (1990). Stimulation of $p21^{ras}$ upon T-cell activation. *Nature*, 346: 719-723.

Downward, J., Parker, P. and Waterfield, M.D. (1984). Autophosphorylation sites on the epidermal growth factor receptor. *Nature*, 311: 483-485.

Dunn, W.A. and Hubbard, A.L. (1984). Receptor-mediated endocytosis of epidermal growth factor by hepatocytes in the perfused rat liver: ligand and receptor dynamics. *J. Cell Biol.*, 98: 2148-2159.

Ebner, R. and Derynck, R. (1991). Epidermal growth factor and transforming growth factor-α: differential intracellular routing and processing of ligand-receptor complexes. *Cell Regulation*, 2: 599-612.

Egan, S.E., Giddings, B.W., Brooks, M.W., Buday, L., Sizeland, A.M. and Weinberg, R.A. (1993). Association of SOS Ras exchange protein with GRB2 is implicated in tyrosine kinase signal transduction and transformation. *Nature*, 363: 45-50.

Escobedo, J.A., Navankasattusas, S., Kavanaugh, W.M., Milfay, D., Fried, V.A. and Williams, L.T. (1991). cDNA cloning of a novel 85 kd protein that has SH2 domains and regulates binding of PI3-kinase to the PDGF beta-receptor. *Cell*, 65: 75-82.

Fearn, J.C. and King, A.C. (1985). EGF receptor affinity is regulated by intracellular calcium and protein kinase C. *Cell*, 40: 991-1000.

Feig, L.A. (1994). Guanine-nucleotide exchange factors: a family of positive regulators of Ras and related GTPases. *Curr. Opin. Cell Biol.*, 6: 204-211.

Fischer, E.H., Charbonneau, H. and Tonks, N.K. (1991). Protein tyrosine phosphatases: a diverse family of intracellular and transmembrane enzymes. *Science*, 253: 401-406.

French, A.R. and Lauffenburger, D.A. (1996). Intracellular receptor/ligand sorting based on endosomal retention components. *Biotech. Bioeng.*, 51: 281-297.

French, A.R., Sudlow, G.P., Wiley, H.S. and Lauffenburger, D.A. (1994). Postendocytic trafficking of epidermal growth factor-receptor complexes is mediated through saturable and specific endosomal interactions. *J. Biol. Chem.*, 269: 15749-15755.

French, A.R., Tadaki, D.K., Niyogi, S.K. and Lauffenburger, D.A. (1995). Intracellular trafficking of epidermal growth factor family ligands is directly influenced by the pH sensitivity of the receptor/ligand interaction. *J. Biol. Chem.*, 270: 4334-4340.

Gale, N., Kaplan, S., Lowenstein, E.J., Schlessinger, J. and Bar-Sagi, D. (1993). Grb2 mediates the EGF-dependent activation of guanine nucleotide exchange on Ras. *Nature*, 363: 88-92.

Ghosh, R.N., Gelman, D.L. and Maxfield, F.R. (1994). Quantification of low density lipoprotein and transferrin endocytic sorting in HEp2 cells using confocal microscopy. *J. Cell Sci.*, 107: 2177-2189.

Goldschmidt-Clermont, P.J., Kim, J.W., Machesky, L.M., Rhee, S.G. and Pollard, T.D. (1991). Regulation of phospholipase C-γ1 by profilin and tyrosine phosphorylation. *Science*, 251: 1231-1233.

Heisermann, G.J., Wiley, H.S., Walsh, B.J., Ingraham, H.A., Fiol, C.J. and Gill, G.N. (1990). Mutational removal of the Thr669 and Ser671 phosphorylation sites alters substrate specificity and ligand-induced internalization of the epidermal growth factor receptor. *J. Biol. Chem.*, 265: 12820-12827.

Herbst, J.J., Opresko, L.K., Walsh, B.J., Lauffenburger, D.A. and Wiley, H.S. (1994). Regulation of postendocytic trafficking of the epidermal growth factor receptor through endosomal retention. *J. Biol. Chem.*, 269: 12865-12873.

Hu, P., Margolis, B., Skolnik, E.Y., Lammers, R., Ullrich, A. and Schlessinger, J. (1992). Interaction of phosphatidylinositol 3-kinase-associated p85 with epidermal growth factor and platelet-derived growth factor receptors. *Mol. Cell. Biol.*, 12: 981-990.

Hu, Q., Klippel, A., Muslin, A.J., Fantl, W.J. and Williams, L.T. (1995). Ras-dependent induction of cellular responses by constitutively active phosphatidylinositol-3 kinase. *Science*, 268: 100-102.

Hunter, T. and Cooper, J.A. (1981). Epidermal growth factor induces rapid tyrosine phosphorylation of proteins in A431 human tumor cells. *Cell*, 24: 741-752.

Hynes, N.E. and Stern, D.F. (1994). The biology of erbB-2/neu/HER-2 and its role in cancer. *Biochim. Biophys. Acta*, 1198: 165-184.

Kaplan, D.R., Whitman, M., Schaffhausen, B., Pallas, D.C., White, M., Cantley, L. and Roberts, T.M. (1987). Common elements in growth factor stimulation and oncogenic transformation: 85 kd phosphoprotein and phosphatidylinositol kinase activity. *Cell*, 50: 1021-1029.

Kay, D.G., Lai, W.H., Uchihashi, M., Khan, M.N., Posner, B.I. and Bergeron, J.J.M. (1986). Epidermal growth factor receptor kinase translocation and activation in vivo. *J. Biol. Chem.*, 261: 8473-8480.

Kimura, H., Fischer, W.H. and Schubert, D. (1990). Structure, expression and function of a Schwannoma-derived growth factor. *Nature*, 348: 257-260.

Klippel, A., Escobedo, J.A., Fantl, W.J. and Williams, L.T. (1992). The C-terminal SH2 domain of p85 accounts for the high affinity of the binding of phosphatidylinositol 3-kinase to phosphorylated platelet-derived growth factor beta receptor. *Mol. Cell. Biol.*, 12: 1451-1459.

Klippel, A., Escobedo, J.A., Hu, Q. and Williams, L.T. (1993). A region of the 85-kilodalton (kDa) subunit of phosphatidylinositol 3-kinase binds the 110-kDa catalytic subunit in vivo. *Mol. Cell. Biol.*, 13: 5560-5566.

Klippel, A., Reinhard, C., Kavanaugh, W.M., Apell, G., Escobedo, M. and Williams, L.T. (1996). Membrane localization of phosphatidylinositol 3-kinase is sufficient

to activate multiple signal-transducing kinase pathways. *Mol. Cell. Biol.*, 16: 4117-4127.

Knauer, D.J., Wiley, H.S. and Cunningham, D.D. (1984). Relationship between epidermal growth factor receptor occupancy and mitogenic response. *J. Biol. Chem.*, 259: 5623-5631.

Kulas, D.T., Freund, G.G. and Mooney, R.A. (1996a). The transmembrane protein-tyrosine phosphatase CD45 is associated with decreased insulin receptor signaling. *J. Biol. Chem.*, 271: 755-760.

Kulas, D.T., Goldstein, B.J. and Mooney, R.A. (1996b). The transmembrane protein-tyrosine phosphatase LAR modulates signaling by multiple receptor tyrosine kinases. *J. Biol. Chem.*, 271: 748-754.

Kurten, R.C., Cadena, D.L. and Gill, G.N. (1996). Enhanced degradation of EGF receptors by a sorting nexin, SNX1. *Science*, 272: 1008-1010.

Lai, C.C., Boguski, M., Broek, D. and Powers, S. (1993). Influence of guanine nucleotides on complex formation between Ras and Cdc25 proteins. *Mol. Cell. Biol.*, 13: 1345-1352.

Lai, W.H., Cameron, P.H., Doherty, J.I., Posner, B.I. and Bergeron, J.J.M. (1989). Ligand-mediated autophosphorylation activity of the epidermal growth factor receptor during internalization. *J. Cell Biol.*, 109: 2751-2760.

Lamaze, C. and Schmid, S.L. (1995). Recruitment of epidermal growth factor receptors into coated pits requires their activated tyrosine kinase. *J. Cell Biol.*, 129: 47-54.

Lemmon, M.A., Falasca, M., Ferguson, K.M. and Schlessinger, J. (1997). Regulatory recruitment of signalling molecules to the cell membrane by pleckstrin-homology domains. *Trends Cell Biol.*, 7: 237-242.

Lemmon, M.A., Ferguson, K.M. and Schlessinger, J. (1996). PH domains: diverse sequences with a common fold recruit signaling molecules to the cell surface. *Cell*, 85: 621-624.

Lemmon, M.A., Ladbury, J.E., Mandiyan, V., Zhou, M. and Schlessinger, J. (1994). Independent binding of peptide ligands to the SH2 and SH3 domains of Grb2. *J. Biol. Chem.*, 269: 31653-31658.

Lemmon, M.A. and Schlessinger, J. (1994). Regulation of signal transduction and signal diversity by receptor oligimerization. *Trends Biochem. Sci.*, 19: 459-463.

Lenferink, A.E.G., Pinkas-Kramarski, R., van de Poll, M.L.M., van Vugt, M.J.H., Klapper, L.N., Tzahar, E., Waterman, H., Sela, M., van Zoelen, E.J.J. and Yarden, Y. (1998). Differential endocytic routing of homo- and heterodimeric ErbB tyrosine kinases confers signaling superiority to receptor heterodimers. *EMBO J.*, 17: 3385-3397.

Li, N., Batzer, A., Daly, R., Yajnik, V., Skolnik, E., Chardin, P., Bar-Sagi, D., Margolis, B. and Schlessinger, J. (1993). Guanine-nucleotide-releasing factor hSos1 binds to Grb2 and links receptor tyrosine kinases to Ras signalling. *Nature*, 363: 85-88.

Lin, C.R., Chen, W.S., Lazar, C.S., Carpenter, C.D., Gill, G.N., Evans, R.M. and Rosenfeld, M.G. (1986). Protein kinase C phosphorylation at Thr 654 of the unoccupied EGF receptor and EGF binding regulate functional receptor loss by independent mechanisms. *Cell*, 44: 839-848.

Lowenstein, E.J., Daly, R.J., Batzer, A.G., Li, W., Margolis, B., Lammers, R., Ullrich, A., Skolnik, E.Y., Bar-Sagi, D. and Schlessinger, J. (1992). The SH2 and SH3 domain-containing protein Grb2 links receptor tyrosine kinases to Ras signalling. *Cell*, 70: 431-442.

Lund, K.A., Lazar, C.S., Chen, W.S., Walsh, B.J., Welsh, J.B., Herbst, J.J., Walton, G.M., Rosenfeld, M.G., Gill, G.N. and Wiley, H.S. (1990a). Phosphorylation of the epidermal growth factor receptor at threonine 654 inhibits ligand-induced internalization and down-regulation. *J. Biol. Chem.*, 265: 20517-20523.

Lund, K.A., Opresko, L.K., Starbuck, C., Walsh, B.J. and Wiley, H.S. (1990b). Quantitative analysis of the endocytic system involved in hormone-induced receptor internalization. *J. Biol. Chem.*, 265: 15713-15723.

Lund, K.A. and Wiley, H.S. (1994). "Regulation of the epidermal growth factor receptor by phosphorylation." in *Regulation of Cellular Signal Transduction Pathways by Desensitization and Amplification*, eds. Sibley, D. R. and Houslay, M. D. New York: John Wiley & Sons, pp. 277-303.

Margolis, B., Bellot, F., Honegger, A.M., Ullrich, A., Schlessinger, J. and Zilberstein, A. (1990). Tyrosine kinase activity is essential for the association of phospholipase C-γ with the epidermal growth factor receptor. *Mol. Cell. Biol.*, 10: 435-441.

Margolis, B.L., Lax, I., Kris, R., Dombalagian, M., Honneger, A.M., Howk, R., Givol, D., Ullrich, A. and Schlessinger, J. (1989). All autophosphorylation sites of epidermal growth factor (EGF) receptor and HER2/*neu* are located in their carboxyl-terminal tails. *J. Biol. Chem.*, 264: 10667-10671.

Masui, H., Wells, A., Lazar, C.S., Rosenfeld, M.G. and Gill, G.N. (1991). Enhanced tumorigenesis of NR6 cells which express non-downregulating epidermal growth factor receptors. *Cancer Res.*, 51: 6170-6175.

McCormick, F. (1996). Ras biology in atomic detail. *Nature Struct. Biol.*, 3: 653-655.

McGlade, C.J., Ellis, C., Reedijk, M., Anderson, D., Mbamalu, G., A.D., R., Panayotou, G., End, P., Bernstein, A., Kazlauskas, A., Waterfield, M.D. and Pawson, T. (1992). SH2 domains of the p85 alpha subunit of phosphatidylinositol 3-kinase regulate binding to growth factor receptors. *Mol. Cell. Biol.*, 12: 991-997.

Medema, R.H., De Vries-Smits, A.M.M., Zon, G.C.M., Maassen, J.A. and Bos, J.L. (1993). Ras activation by insulin and epidermal growth factor through enhanced exchange of guanine nucleotides on $p21^{ras}$. *Mol. Cell. Biol.*, 13: 155-162.

Mellman, I. (1996). Endocytosis and molecular sorting. *Annu. Rev. Cell Dev. Biol.*, 12: 575-625.

Mellman, I., Fuchs, R. and Helenius, A. (1986). Acidification of the endocytic and exocytic pathways. *Ann. Rev. Biochem.*, 55: 663-700.

Neel, B.G. and Tonks, N.K. (1997). Protein tyrosine phosphatases in signal transduction. *Curr. Opin. Cell Biol.*, 9: 193-204.

Northwood, I.C., Gonzalez, F.A., Wartmann, M., Raden, D.L. and Davis, R.J. (1991). Isolation and characterization of two growth factor-stimulated protein kinases that phosphorylate the epidermal growth factor at threonine 669. *J. Biol. Chem.*, 266: 15266-15276.

Olivier, J.P., Raabe, T., Henkemeyer, M., Dickson, B., Mbamalu, G., Margolis, B., Schlessinger, J., Hafen, E. and Pawson, T. (1993). A *Drosophila* SH2-SH3 adaptor protein implicated in coupling the Sevenless tyrosine kinase to an activator of Ras guanine nucleotide exchange, Sos. *Cell*, 73: 179-191.

Opresko, L.K., Chang, C., Will, B.H., Burke, P.M., Gill, G.N. and Wiley, H.S. (1995). Endocytosis and lysosomal targeting of epidermal growth factor receptors are mediated by distinct sequences independent of the tyrosine kinase domain. *J. Biol. Chem.*, 270: 4325-4333.

Pawson, T. (1995). Protein modules and signaling networks. *Nature*, 373: 573-580.

Pelicci, G., Lanfrancone, L., Grignani, F., McGlade, J., Cavallo, F., Forni, G., Nicolletti, I., Grignani, F., Pawson, T. and Pelicci, P.G. (1992). A novel transforming protein (SHC) with an SH2 domain is implicated in mitogenic signal transduction. *Cell*, 70: 93-104.

Pittelkow, M.R. (1992). "Growth factors and intracellular mechanisms of keratinocyte growth and differentiation." in *The Biology of the Epidermis*, eds. Ohkawara, A. and McGuire, J. Elsevier Science Publishers, pp. 109-122.

Pruss, R.M. and Herschman, H.R. (1977). Variants of 3T3 cells lacking mitogenic response to epidermal growth factor. *Proc. Natl. Acad. Sci. USA*, 74: 3918-3921.

Quilliam, L.A., Huff, S.Y., Rabun, K.M., Wei, W., Park, W., Broek, D. and Der, C.J. (1994). Membrane-targeting potentiates guanine nucleotide exchange factor Cdc25 and Sos1 activation of Ras transforming activity. *Proc. Natl. Acad. Sci. USA*, 91: 8512-8516.

Reddy, C.C., Wells, A. and Lauffenburger, D.A. (1994). Proliferative response of fibroblasts expressing internalization-deficient epidermal growth factor (EGF) receptors is altered via differential EGF depletion effect. *Biotechnol. Prog.*, 10: 377-384.

Reif, K., Nobes, C.D., Thomas, G., Hall, A. and Cantrell, D.A. (1996). Phosphatidylinositol 3-kinase signals activate a selective subset of Rac/Rho-dependent effector pathways. *Curr. Biol.*, 6: 1445-1455.

Rhee, S.G. and Choi, K.D. (1992). Regulation of inositol phospholipid-specific phospholipase C isozymes. *J. Biol. Chem.*, 267: 12393-12396.

Rordorf-Nikolic, T., Van Horn, D.J., Chen, D., White, M.F. and Backer, J.M. (1995). Regulation of phosphatidylinositol 3'-kinase by tyrosyl phosphoproteins. *J. Biol. Chem.*, 270: 3662-3666.

Rotin, D., Honegger, A.M., Margolis, B.L., Ullrich, A. and Schlessinger, J. (1992). Presence of SH2 domains of phospholipase $C\gamma_1$ enhances substrate phosphorylation by increasing the affinity toward the epidermal growth factor receptor. *J. Biol. Chem.*, 267: 9678-9683.

Rozakis-Adcock, M., Fernley, R., Wade, J., Pawson, T. and Bowtell, D. (1993). The SH2 and SH3 domains of mammalian Grb2 couple the EGF receptor to the Ras activator Sos. *Nature*, 363: 83-85.

Ruff-Jamison, S., McGlade, J., Pawson, T., Chen, K. and Cohen, S. (1993). Epidermal growth factor stimulates the tyrosine phosphorylation of SHC in the mouse. *J. Biol. Chem.*, 268: 7610-7612.

Scott, J., Urdea, M., Quiroga, M., Sanchez-Pescador, R., Fong, N., Selby, M., Rutter, W.J. and Bell, G. (1983). Structure of a mouse submaxillary messenger RNA encoding epidermal growth factor and seven related proteins. *Science*, 221: 236-240.

Shoelson, S.E., Sivaraja, M., Williams, K.P., Hu, P., Schlessinger, J. and Weiss, M.A. (1993). Specific phosphopeptide binding regulates a conformational change in the PI 3-kinase SH2 domain associated with enzyme activation. *EMBO J.*, 12: 795-802.

Simon, M., Dodson, G.S. and Rubin, G.M. (1993). An SH3-SH2-SH3 protein is required for $p21^{ras}$ activation and binds to Sevenless and Sos proteins in vitro. *Cell*, 73: 169-177.

Skolnik, E.Y., Margolis, B., Mohammadi, M., Lowenstein, E., Fischer, R., Drepps, A., Ullrich, A. and Schlessinger, J. (1991). Cloning of PI(3)kinase-associated p85 utilizing a novel method for expression/cloning of target proteins for receptor tyrosine kinases. *Cell*, 65: 83-90.

Songyang, Z. and Cantley, L.C. (1995). Recognition and specificity in protein tyrosine kinase-mediated signalling. *Trends Biochem. Sci.*, 20: 470-475.

Sorkin, A. and Carpenter, G. (1991). Dimerization of internalized epidermal growth factor receptors. *J. Biol. Chem.*, 266: 23453-23460.

Starbuck, C. and Lauffenburger, D.A. (1992). Mathematical model for the effects of epidermal growth factor receptor trafficking dynamics on fibroblast proliferation responses. *Biotechnol. Prog.*, 8: 132-143.

Sun, H. and Tonks, N.K. (1994). The coordinated action of protein tyrosine phosphatases and kinases in cell signaling. *Trends Biochem. Sci.*, 19: 480-485.

Takishima, K., Griswold-Prenner, I., Ingebritsen, T. and Rosner, M.R. (1991). Epidermal growth factor (EGF) receptor T669 peptide kinase for 3T3-L1 cells is an EGF-stimulated "MAP" kinase. *Proc. Natl. Acad. Sci. USA*, 88: 2520-2524.

Theroux, S.J., Stanley, K., Campbell, D.A. and Davis, R.J. (1992). Mutational removal of the major site of serine phosphorylation of the epidermal growth factor receptor causes potentiation of signal transduction: role of receptor down-regulation. *Molec. Endocrinol.*, 6: 1849-1857.

Toker, A. (1998). The synthesis and cellular roles of phosphatidylinositol 4,5-bisphosphate. *Curr. Opin. Cell Biol.*, 10: 254-261.

Toker, A. and Cantley, L.C. (1997). Signalling through the lipid products of phosphoinositide-3-OH kinase. *Nature*, 387: 673-676.

Tonks, N.K. and Charbonneau, H. (1989). Protein tyrosine dephosphorylation and signal transduction. *Trends Biochem. Sci.*, 14: 497-500.

Torti, M., Marti, K.B., Altschuler, D., Yamamoto, K. and Lapetina, E.G. (1992). Erythropoietin induces $p21^{ras}$ activation and p120GAP tyrosine phosphorylation in human erythroleukemia cells. *J. Biol. Chem.*, 267: 8293-8298.

Trowbridge, I.S., Collawn, J.F. and Hopkins, C.R. (1993). Signal-dependent membrane protein trafficking in the endocytic pathway. *Annu. Rev. Cell Biol.*, 9: 129-161.

van der Geer, P., Hunter, T. and Lindberg, R.A. (1994). Receptor protein-tyrosine kinases and their signal transduction pathways. *Annu. Rev. Cell Biol.*, 10: 251-337.

van der Geer, P. and Pawson, T. (1995). The PTB domain: a new protein module implicated in signal transduction. *Trends Biochem. Sci.*, 20: 277-280.

Vanhaesebroeck, B., Leevers, S.J., Panayotou, G. and Waterfield, M.D. (1997). Phosphoinositide 3-kinases: a conserved family of signal transducers. *Trends Biochem. Sci.*, 22: 267-272.

Vega, Q.C., Cochet, C., Filhol, O., Chang, C., Rhee, S.G. and Gill, G.N. (1992). A site of tyrosine phosphorylation in the C-terminus of the epidermal growth-factor receptor is required to activate phospholipase C. *Mol. Cell. Biol.*, 12: 128-135.

Vieira, A.V., Lamaze, C. and Schmid, S.L. (1996). Control of EGF receptor signaling by clathrin-mediated endocytosis. *Science*, 274: 2086-2089.

Vojtek, A.B. and Der, C.J. (1998). Increasing complexity of the Ras signaling pathway. *J. Biol. Chem.*, 273: 19925-19928.

Wada, I., Lai, W.H., Posner, B.I. and Bergeron, J.J. (1992). Association of the tyrosine phosphorylated epidermal growth factor receptor with a 55-kD tyrosine phosphorylated protein at the cell surface and in endosomes. *J. Cell Biol.*, 116: 321-330.

Walton, G.M., Chen, W.S., Rosenfeld, M.G. and Gill, G.N. (1990). Analysis of deletions of the carboxyl terminus of the epidermal growth factor receptor reveals self-phosphorylation at tyrosine 992 and enhanced in vivo tyrosine phosphorylation of cell substrates. *J. Biol. Chem.*, 265: 1750-1754.

Weber, W., Bertics, P.J. and Gill, G.N. (1984). Immunoaffinity purification of the epidermal growth factor receptor. *J. Biol. Chem.*, 259: 14631-14636.

Wells, A., Welsh, J.B., Lazar, C.S., Wiley, H.S., Gill, G.N. and Rosenfeld, M.G. (1990). Ligand-induced transformation by a non-internalizing epidermal growth factor receptor. *Science*, 247: 962-964.

Welsh, J.B., Gill, G.N., Rosenfeld, M.G. and Wells, A. (1991). A negative feedback loop attenuates EGF-induced morphological changes. *J. Cell Biol.*, 114: 533-543.

Wiley, H.S. (1985). Receptors as models for the mechanisms of membrane protein turnover and dynamics. *Curr. Topics Membranes Transport*, 24: 369-411.

Wiley, H.S. (1988). Anomalous binding of epidermal growth factor to A431 cells is due to the effect of high receptor densities and a saturable endocytic system. *J. Cell Biol.*, 107: 801-810.

Wiley, H.S. and Cunningham, D.D. (1981). A steady state model for analyzing the cellular binding, internalization and degradation of polypeptide ligands. *Cell*, 25: 433-440.

Wiley, H.S. and Cunningham, D.D. (1982). The endocytic rate constant: a cellular parameter for quantitating receptor-mediated endocytosis. *J. Biol. Chem.*, 257: 4222-4229.

Wiley, H.S., Walsh, B.J. and Lund, K.A. (1989). Global modulation of the epidermal growth factor receptor is triggered by occupancy of only a few receptors. *J. Biol. Chem.*, 264: 18912-18920.

Willumsen, B.M., Cox, A.D., Solski, P.A., Der, C.J. and Buss, J.E. (1996). Novel determinants of H-Ras plasma membrane localization and transformation. *Oncogene*, 13: 1901-1909.

Willumsen, B.M., Norris, K., Papageorge, A.G., Hubbert, N.L. and Lowy, D.R. (1984). Harvey murine sarcoma virus p21 *ras* protein: biological and biochemical significance of the cysteine nearest the carboxy terminus. *EMBO J.*, 3: 2581-2585.

Wolfman, A. and Macara, I.G. (1990). A cytosolic protein catalyzes the release of GDP from p21ras. *Science*, 248: 67-69.

Worthylake, R., Opresko, L.K. and Wiley, H.S. (1999). ErbB-2 amplification inhibits down-regulation and induces constitutive activation of both erbB-2 and epidermal growth factor receptor. *J. Biol. Chem.*, 274: 8865-8874.

Zhang, K., DeClue, J.E., Vass, W.C., Papageorge, A.G., McCormick, F. and Lowy, D.R. (1990). Suppression of c-ras transformation by GTPase-activating protein. *Nature*, 346: 754-756.

Zhou, M.M., Ravichandran, K.S., Olejniczak, E.T., Petros, A.M., Meadows, R.P., Sattler, M., Harlan, J.E., Wade, W.S., Burakoff, S.J. and Fesik, S.W. (1995). Structure and ligand recognition of the phosphotyrosine binding domain of Shc. *Nature*, 378: 584-592.

Zhu, G., Decker, S.J. and Saltiel, A.R. (1992). Direct analysis of the binding of Src-homology 2 domains of phospholipase C to the activated epidermal growth factor receptor. *Proc. Natl. Acad. Sci. USA*, 89: 9559-9563.

CHAPTER 2

Receptor-mediated Recruitment of Intracellular Signaling Proteins to the Plasma Membrane: Theoretical Analysis

Experimental observations in signal transduction have suggested that where a protein is located within a cell can be as important as its activity measured in solution for activation of a downstream pathway. The physical organization of the cell can provide an additional layer of control upon the chemical reaction networks that govern ultimately perceived signals. In this chapter, the mechanism by which subcellular location can affect the kinetics of protein-protein or protein-lipid interactions, within the framework of receptor-mediated signal transduction, was investigated. Using the cytosol and plasma membrane as relevant compartmental distinctions, I theoretically analyzed the effect of relocation on the rate of association with a membrane-associated target. This effect was quantified as an enhancement factor E in terms of measurable parameters such as the number of available targets, molecular diffusivities, and intrinsic reaction rate constants. I then formulated two simple yet relevant example models to illustrate how relocation can affect the dynamics of signal transduction pathways, in which temporal profiles and phase behavior were investigated. Experimentally observable aspects of signal transduction such as peak activation and the relative time scales of stimulus and response were also related to quantitative aspects of the relocation mechanisms in these models. In these example schemes, nearly complete relocation of the cytosolic species in the signaling pair is required to generate meaningful activation of the model pathways when the association rate enhancement factor E is as low as 10; when E is 100 or greater only a small fraction of the protein needs to be relocated.

2.1 Introduction

The behavior of living cells is regulated by chemical and/or physical cues from the extracellular environment. Most often, molecular ligands act via an appropriate repertoire of complementary cell surface receptors. Cells may respond by proliferating, differentiating, or migrating in response to receptor-ligand recognition, and may respond differently to varying magnitudes or durations of the same stimulus. A major class of cell surface receptors is the receptor tyrosine kinases (RTKs), which recognize a broad group of growth factor ligands (van der Geer et al., 1994). Because these receptors are integral membrane proteins, subsequent signaling always involves an interaction in which at least

one of the coupling molecules is associated with a two-dimensional surface. Following the ligand-dependent auto- and/or trans-phosphorylation of specific tyrosines in the cytosolic tails of RTKs, signaling molecules can be recruited from the cytosol if they possess appropriate structural domains that directly associate with certain phosphotyrosyl motifs. These include the Src-homology 2 (SH2) and phosphotyrosine-binding (PTB) modular domains (Pawson, 1995). The concept that "location matters" in cell biology recently came to the fore (Carraway and Carraway, 1995; Mochly-Rosen, 1995), particularly the notion that location or relocation of a signaling protein can directly affect its observed activity. However, this issue had not heretofore been examined using a quantitative framework.

As a specific example of a subcellular location effect on the biological activity of a signaling protein, homologs of Son of Sevenless (Sos), guanine nucleotide exchange factors (GEFs) specific for the highly conserved Ras GTPase (Bourne et al., 1991), are recruited to the plasma membrane via association with SH2 domain-containing adaptor proteins. GEFs stimulate dissociation of guanine nucleotides (GDP and GTP) from GTPases (Feig, 1994), favoring the active state of a GTPase since GTP is in excess in the cytosol. While it was discovered that the coprecipitation of Sos with the phosphorylated RTK epidermal growth factor receptor (EGFR) is required for Ras activation mediated by EGF, the GEF activity of Sos measured in solution is not affected by the interaction (Buday and Downward, 1993). But when Sos is genetically targeted to the inside face of the plasma membrane, where Ras resides constitutively, cells become transformed in a Ras-dependent fashion in the absence of growth factors (Aronheim et al., 1994; Quilliam et al., 1994). This implies that membrane association causes an increase in the GEF activity of Sos, presumably by allowing better access to its substrate.

In its GTP-bound state, Ras initiates a kinase cascade implicated in cell growth and differentiation by participating in the activation of the cytosolic Raf serine-threonine kinase (Howe et al., 1992; Hallberg et al., 1994). Oncogenic mutations in either Ras or Raf contribute to uncontrolled cellular growth, and Ras mutations in particular have been implicated in a high percentage of human tumors (Bos, 1989). Interestingly, when Raf is artificially targeted to the membrane as mentioned above for Sos, cells become transformed even when a dominant-negative Ras mutant is coexpressed (Leevers et al., 1994; Stokoe et al., 1994). Raf kinase activity is normally enriched in plasma membrane fractions of Ras-transformed cells (Jelinek et al., 1996), yet interactions with Ras or membrane lipids in solution are not sufficient to activate the kinase (Kikuchi and Williams, 1994; Force et al., 1994). Thus, relocation of pathway components could serve as a key mechanism governing signal transduction upstream and downstream of Ras.

More recent evidence indicates that plasma membrane recruitment of phosphatidylinositol 3-kinase [PI(3)K], a key enzyme that phosphorylates phosphoinositide lipids, may also be a critical event in regulating intracellular signaling. PI(3)K exists as a dimer of a catalytic p110 subunit and a regulatory p85 subunit with two SH2 domains that mediate association with activated RTKs (van der Geer et al., 1994). This interaction allows full activity of the p110 subunit on PI(3)K lipid substrates. When constitutively active p110 is artificially targeted to the membrane in the absence of growth factor stimulation, maximal activity is proffered (Klippel et al., 1996), implying that allosteric and locational effects are synergistic in the potentiation of PI(3)K activity. An interaction between p110 and Ras has also been reported, enhancing PI(3)K activity in intact cells but apparently not in solution (Rodriguez-Viciana et al., 1994).

2.2 Theory of Reaction and Diffusion in Two and Three Dimensions

2.2.1 General Considerations

If proteins are permitted to diffuse freely through space, intermolecular encounters occur randomly. While close enough to form favorable electrostatic and van der Waals interactions, associating macromolecules must align their reactive patches in the correct orientation before diffusing away (Northrup and Erickson, 1992). If k_+ is the second-order rate constant describing diffusive collisions, the observed association (forward) rate constant is

$$k_f = \gamma k_+ \qquad (2.1),$$

where γ is the average probability of capture (Shoup and Szabo, 1982). If the alignment and diffusive separation processes are described by second-order rate constants k_{on} and k_- respectively, then

$$\gamma = k_{on}/(k_{on}+k_-) \qquad (2.2).$$

When the alignment of two species is very efficient, almost all encounters result in binding ($\gamma \sim 1$ and $k_f \sim k_+$), and the association is said to be diffusion-limited. When molecules diffuse away rapidly following a collision, many collisions will occur before binding ($\gamma << 1$), and there are no detectable spatial concentration gradients of the reactants; in this limit, $k_f \sim k_{on}k_+/k_-$. In an isotropic environment, k_- and k_+ must be equivalent to satisfy the diffusion equation, so k_{on} represents the intrinsic chemical rate constant of the association. Alternatively, close-proximity alignment and separation can be modeled as first-order, unimolecular processes, imposing the existence of a non-specific encounter

complex. This restricts a target from interacting with more than one solute in close proximity, which is nonphysical.

Once associated, the bimolecular complex is not completely stable and can dissociate. If the complex has an average lifetime, molecular dissociation on a microscopic level is described by a first-order rate constant k_{off}. The probability of rebinding following dissociation is γ, and the observed dissociation rate constant is thus (Shoup and Szabo, 1982)

$$k_r = (1-\gamma)k_{off} \qquad (2.3).$$

Therefore, when diffusion matters, the observed rate constants k_f and k_r are modified from their intrinsic values, and the intracellular locations of interacting species can affect the rate of binding.

The observed affinity K, however, is not altered by a change in diffusion rates (Lauffenburger and Linderman, 1993):

$$K = k_f/k_r = (\gamma k_+)/[(1-\gamma)k_{off}] = [(1-\gamma)k_{on}]/[(1-\gamma)k_{off}] = k_{on}/k_{off} \qquad (2.4).$$

To illustrate this idea, consider a diffusion-limited interaction that has reached equilibrium. At steady state, there is no net formation of bimolecular complexes, so any concentration gradients disappear; the diffusion- and reaction-limited equilibria are therefore indistinguishable. Thus, by analyzing how k_f is affected relative to k_{on}, an analysis of dissociation resistances is not required to ascertain k_r relative to k_{off}. These issues were analyzed as they apply to interactions of cytosolic or membrane-associated proteins with a target displayed on the inside face of the plasma membrane.

2.2.2 Association of a Cytosolic Protein with a Membrane Target

In order to associate with specific targets available on the inside face of the plasma membrane, a cytosolic species must approach the membrane, find a specific site, and bind to this site before diffusing away. The diffusive aspect of this behavior is different from the capture of an extracellular protein by specific cell surface sites (Berg and Purcell, 1977; Erickson et al., 1987; Goldstein, 1989), primarily because cytosolic species are contained by the reactive boundary. A form of Poisson's equation can be employed to solve for the mean time to diffusion-limited capture in space (Berg and Purcell, 1977; Szabo et al., 1980):

$$D_c \nabla^2 W + 1 = 0 \qquad (2.5),$$

where W is the mean time to capture and D_c is the molecular diffusivity of the solute in cytosol.

The mean time for first-order diffusion to the boundary can be solved easily for spherical coordinates:

$$\bar{\tau}_1 \equiv \frac{\overline{W} D_c}{a^2} = \frac{1}{15} \qquad (2.6),$$

where $\overline{W}$ is the capture time averaged over space and a is the cell radius. Since a cytosolic protein cannot diffuse to infinity, this result is lower than that of an extracellular protein diffusing to the outside surface ($\bar{\tau} = 1/3$). When membrane sites are very sparse, diffusion-limited association relies more on finding a site once it is near the surface. The concentration gradients about each of the N uniformly distributed sinks become independent, and the cell radius can be considered semi-infinite. This contribution to the mean capture time is inversely proportional to the number of sinks and depends on the sink geometry (Hill, 1975; Berg and Purcell, 1977):

$$\bar{\tau}_2 = \frac{\pi}{3\sigma N} \quad \text{(flat)}$$

$$\bar{\tau}_2 = \frac{2}{3\sigma N} \quad \text{(hemispherical)} \qquad (2.7),$$

$$\sigma \equiv \frac{s}{a} << 1$$

where the dimension s is the sum of the associating species' radii, the distance r at which the species are in contact. For reasonably sparse sinks, this result compares fairly well with an approximate space-averaged solution of eqn. 2.5; Poisson's equation was solved with appropriate boundary conditions applied directly to the volume apportioned each sink (Appendix A), approximated as the section of a sphere cut out by the cone $\theta = \beta \equiv b/a$, where b is the mean half-distance between sinks (Figure 2.1). To a first approximation, $N = 4/\beta^2$.

The final resistance is the binding of the molecule, now in close proximity to the membrane site:

$$\bar{\tau}_3 = \frac{4\pi a D_c}{3 k_{on} N} \qquad (2.8).$$

In the absence of diffusive resistances in aqueous solution, k_{on} can be measured in the laboratory. However, this may not generalize to what is observed, since the membrane site will be restricted in its ability to orient randomly and/or sample space; thus, the entropic contribution of membrane confinement to k_{on} may aid or hinder binding.

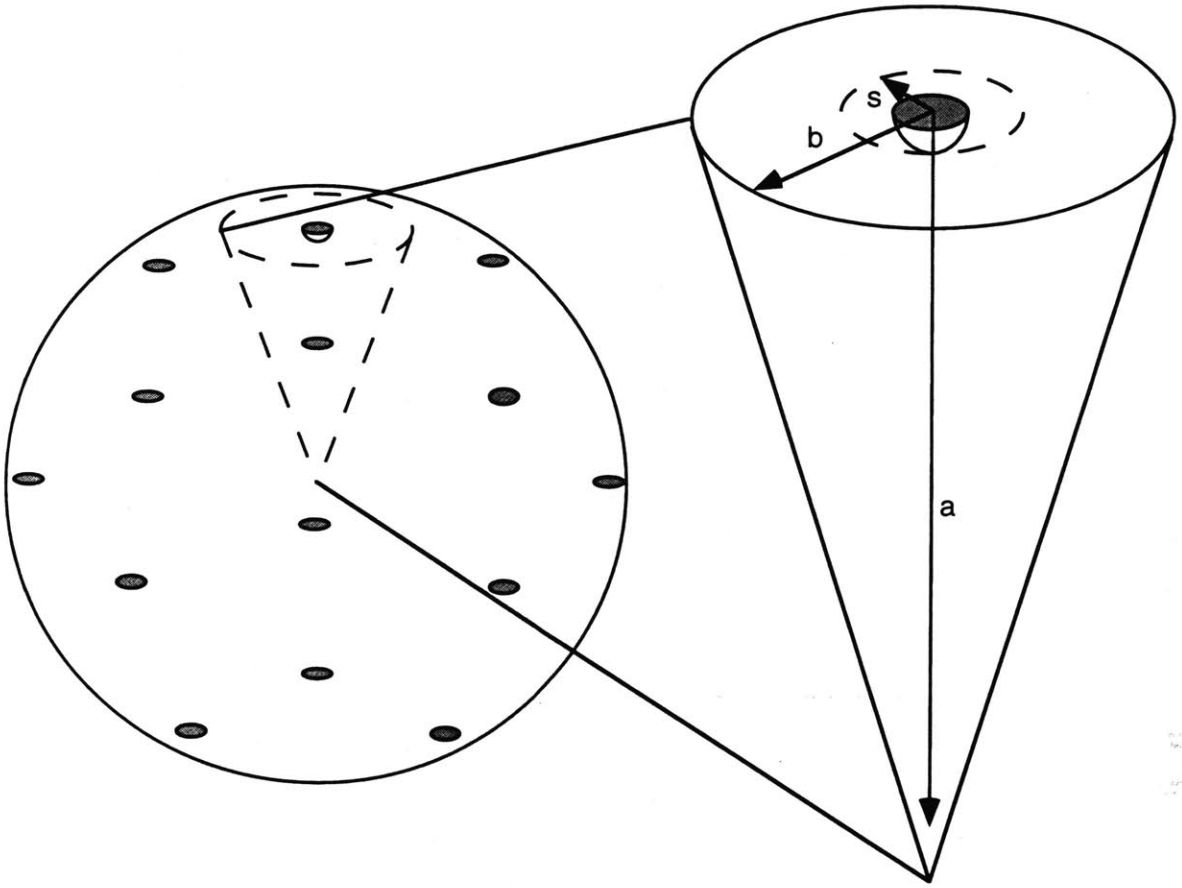

Figure 2.1 Geometry of the area and volume afforded each membrane sink. The model cell is considered spherical, with radius a and N targets evenly distributed over the inside surface of the membrane boundary. The area occupied by a single target can by approximated as a disk of radius $b = 2aN^{-1/2}$, the average distance between targets. The targets bind reactant partners at a separation s with observed second-order rate constant k_{on}; s is roughly the sum of the species' molecular radii. The corresponding volume is the section cut out by the cone $\theta = b/a$, with the sink centered at $\theta = 0$.

Constructing a second-order association rate constant $k_{c/m}$ for binding of cytosolic and membrane components (flat sink geometry; based on whole cell volume),

$$k_{c/m} = \left[\frac{N}{20\pi a D_c} + \frac{1}{4sD_c} + \frac{1}{k_{on}} \right]^{-1} \qquad (2.9).$$

One can now make order-of-magnitude estimates to gauge the relative importances of molecular processes and set a reasonable upper limit on $k_{c/m}$. The molecular diffusivity of a protein in the cytosol is about two orders of magnitude lower than in aqueous solution, ~ 10^{-8} cm^2/s (Jacobson and Wojcieszyn, 1984; Gershon et al., 1985). For typical cell parameters (a ~ 10^{-3} cm, s ~ $5x10^{-7}$ cm), $4sD_cN_{Av}$ ~ 10^7 $(Ms)^{-1}$ (N_{Av} is Avogadro's number, M denotes concentration in molarity), and the first resistance dominates the second only if N >> 30,000. As a relevant example, this reasoning can be used to analyze the recruitment of intracellular signaling proteins to RTKs phosphorylated on tyrosine. As discussed earlier, proteins generally use discrete domains to interact with membrane receptors, exhibiting very high on and off rates and dissociation constants in the 10-100 nM range (Cussac et al., 1994; Ladbury et al., 1995; Zhou et al., 1995; Mandiyan et al., 1996). Given the above analysis, recruitment is likely diffusion limited, with forward rate constant ~ 10^7 $(Ms)^{-1}$ based on the whole cell volume and a reverse rate constant in the 0.1-1 s^{-1} range. To compare these rates to those governing RTK ligand binding, the aforementioned EGF-receptor/EGF system exhibits a reverse rate constant of ~ 0.005 s^{-1}, respectively (Lauffenburger and Linderman, 1993). Recruitment of cytosolic proteins would thus respond rapidly to receptor binding, establishing new equilibria as receptor occupancy changes with time (pseudo-steady state).

2.2.3 Interaction Between Two Membrane Species

If the number of sinks, N, stays relatively constant on the time scale of membrane diffusion, the association with a second membrane species can be characterized as in the previous section. The area afforded each sink can be approximated as a flat circular disk of radius b, and the species react at a distance r = s.

One approach is to employ eqn. 2.5 to the capture time of the second membrane species. Solving for W and averaging over space:

$$\bar{\tau} \equiv \frac{\overline{W} D_m}{b^2} = \frac{1}{2}\left[\frac{\ln(1/\tilde{s})}{(1-\tilde{s}^2)} - \frac{(3-\tilde{s}^2)}{4} \right]; \quad \tilde{s} \equiv s/b = \sigma/\beta \qquad (2.10)$$

(Berg and Purcell, 1977), where D_m is the sum of the species' membrane diffusivities. With D_m in the 10^{-11}-10^{-9} cm^2/s range, proteins are less mobile in the plasma membrane than in the cytosol; however, the change in distance scales from a to b (b << a in general) and a

reduction in dimensionality mean that the transport rate is not necessarily reduced by membrane association. A more complicated expression can be used that accounts for spherical curvature:

$$\bar{\tau} = \frac{1}{2\beta^2}\left\{\frac{(1-\eta_b)^2}{(\eta_s-\eta_b)}\ln\left(\frac{1-\eta_b}{1-\eta_s}\right)-\left[2-\frac{(1+\eta_b)^2}{(\eta_s-\eta_b)}\ln\left(\frac{1+\eta_s}{1+\eta_b}\right)\right]\right\};\quad \begin{matrix}\eta_b \equiv \cos\beta \\ \eta_s \equiv \cos\sigma\end{matrix} \qquad (2.11).$$

However, even for $\beta \sim 1$ eqn. 2.10 differs from this result by < 10%.

Another determination of $\bar{\tau}$ is made by first solving the diffusion equation with appropriate boundary conditions for the dimensionless concentration profile $\theta(r,t)$, again assuming that changes in b are imperceptible on the b^2/D_m time scale (< 1 second in general):

$$\bar{\tau} \equiv \frac{\overline{W}D_m}{b^2} = \frac{2}{(1-\tilde{s}^2)}\sum_{n=1}^{\infty}\frac{2}{\lambda_n^4}\left[\frac{J_1^2(\lambda_n)}{J_0^2(\lambda_n\tilde{s})-J_1^2(\lambda_n)}\right] \qquad (2.12),$$

$$J_0(\lambda_n\tilde{s})Y_1(\lambda_n)-J_1(\lambda_n)Y_0(\lambda_n\tilde{s})=0$$

where J_n and Y_n are Bessel functions (Adam and Delbrück, 1968). Computational analysis of eqn. 2.12 shows excellent agreement with eqn. 2.10 for a wide range of target densities, and the extent that $\bar{\theta}(t) \cong \exp(-t/\overline{W})$ depends on the dominance of the first term in eqn. 2.12 ($1/\bar{\tau} \cong \lambda_1^2$). Further, modifying the boundary condition at the sink to include a second-order reactive rate constant k_2 confirms the intuition that the observed second-order rate constant between membrane species can be constructed by analogy to serial resistances in an electrical circuit:

$$\tilde{s}\left.\frac{\partial\theta}{\partial\tilde{r}}\right|_{\tilde{s}} - \kappa\theta|_{\tilde{s}} = 0;\quad \kappa \equiv \frac{k_2}{2\pi D_m}$$

$$\bar{\tau} = \frac{2}{(1-\tilde{s}^2)}\sum_{n=1}^{\infty}\frac{2}{\lambda_n^4}\left\{\frac{\kappa^2 J_1^2(\lambda_n)}{\left[(\lambda_n\tilde{s})J_1(\lambda_n\tilde{s})+\kappa J_0(\lambda_n\tilde{s})\right]^2-\left[(\lambda_n\tilde{s})^2+\kappa^2\right]J_1^2(\lambda_n)}\right\} \qquad (2.13).$$

$$\lambda_n\tilde{s}\left[J_1(\lambda_n)Y_1(\lambda_n\tilde{s})-J_1(\lambda_n\tilde{s})Y_1(\lambda_n)\right]-\kappa\left[J_0(\lambda_n\tilde{s})Y_1(\lambda_n)-J_1(\lambda_n)Y_0(\lambda_n\tilde{s})\right]=0$$

$$\bar{\tau} = \bar{\tau}(\kappa\to\infty)+\frac{(1-\tilde{s}^2)}{2\kappa}$$

Note that k_2 is analogous to k_{on} except for the change in units to reflect concentrations in two dimensions rather than three. Again, one cannot say in general how membrane association will affect the efficiency of alignment when the associating species are in close proximity. However, when associations are reaction-limited, one can argue that the primary effect of membrane confinement is a change in the effective sampling volume $V_{sampling}$ to a value much smaller than the whole cell (V_{cell}). Using order-of-

magnitude reasoning, $V_{sampling}$ can be conservatively defined as a layer adjacent to the membrane of thickness h ~ 10 nm (Lauffenburger and Linderman, 1993; McLaughlin and Aderem, 1995). The reaction-limited enhancement factor is defined as χ:

$$\chi \sim \frac{V_{cell}}{V_{sampling}} \sim \frac{a}{3h} \sim 10^2 - 10^3 \qquad (2.14).$$

Further, the dissociation rate k_{off} is unaffected by a change in volume, so the apparent affinity is enhanced by the factor χ, even when diffusive resistances are important.

Constructing an observed second-order rate constant based on the whole cell volume for association of membrane species $k_{m/m}$,

$$k_{m/m} \equiv \left\{ \frac{3}{2\pi a D_m} \left[\ln(1/\tilde{s}) - 3/4 \right] + \frac{1}{\chi k_{on}} \right\}^{-1}; \quad \tilde{s}^2 << 1 \qquad (2.15).$$

The diffusion-limited value of $k_{m/m}$ is ~ 10^6-10^8 $(Ms)^{-1}$, depending mainly on D_m and weakly on $\tilde{s} = 2\sigma N^{-1/2}$. This estimate clearly qualifies the statement that the reduction in mobility does not preclude a reduction in the frequency of collisions. For typical χk_{on} values in the range of 10^7-10^{10} $(Ms)^{-1}$, it is concluded that $k_{m/m}$ is diffusion-limited for all but the slowest reactions and/or most mobile reactants (Lauffenburger and Linderman, 1993).

2.3 Results

2.3.1 Enhancement of Association Rates

Two major implications of membrane compartmentalization, compared with cytosolic interactions, are: (1) the apparent binding affinity is enhanced by the factor χ, at least two orders of magnitude, and (2) the association rate, gauging the response time to an extracellular stimulus perceived by a membrane receptor, can be increased considerably. In any given situation, however, it is not obvious whether enhancement of the association rate is due to a reactant-concentrating effect (Nesheim et al., 1984) or to the high efficiency of diffusion in two dimensions (reduction-of-dimensionality) even when the molecular diffusivity is reduced. To address these issues, it seemed instructive to compare the second-order rate constants for cytosolic and membrane species interacting with a membrane target.

An enhancement factor E was introduced, which compares $k_{m/m}$ and $k_{c/m}$ as described in the previous section:

$$E \equiv \frac{k_{m/m}}{k_{c/m}} \qquad (2.16).$$

E thus quantifies the advantage of relocation from the cytosol to the plasma membrane conferred in the binding of a constitutively membrane-associated target. Two other dimensionless quantities were important in this analysis: a cellular Damköhler number Da comparing the contributions of reaction and diffusion to $k_{c/m}$:

$$Da \equiv \frac{k_{on}}{k_{c/m}(k_{on} \to \infty)} = \frac{k_{on}}{aD_c}\left(\frac{N}{20\pi} + \frac{1}{4\sigma}\right) \qquad (2.17),$$

and a physical parameter δ that compares the diffusion-limited values of $k_{m/m}$ and $k_{c/m}$:

$$\delta \equiv \frac{k_{m/m}(k_{on} \to \infty)}{k_{c/m}(k_{on} \to \infty)} \cong \frac{D_m}{D_c}\left[\frac{N/5 + \pi/\sigma}{6\ln(1/\tilde{s}) - 9/2}\right] \qquad (2.18).$$

By the previous order-of-magnitude reasoning, Da = 1 corresponds to $k_{on} \sim 10^7$ $(Ms)^{-1}$, or less if $N > 10^5$. Since $\tilde{s} = 2\sigma N^{-1/2}$, δ is a function of the relative mobilities in the membrane and cytosol (D_m/D_c), target availability (N), and molecular *versus* cellular dimensions (σ). The dependence of δ on N is illustrated for $D_m/D_c = 0.001\text{-}0.1$ and $\sigma = 5\times10^{-4}$ in Figure 2.2. Note that δ is often much greater than 1 even when D_m/D_c is well below 1. This again underscores the efficiency of diffusion in two dimensions.

E can be expressed in terms of Da, δ, and the previously defined χ:

$$E = \chi\left[\frac{1 + Da}{1 + (\chi/\delta)Da}\right] \qquad (2.19).$$

The curve described by eqn. 2.19 is sigmoidal in shape with asymptotic values of χ and δ as k_{on} approaches zero (reactant concentrating effect) and infinity (diffusion effects only), respectively (Figure 2.3). From Figure 2.2, δ is bounded between $\sim 0.1\text{-}10^3$. Thus, for reaction-limited associations $E = \chi$, and E can be $\sim \chi$ or < 1 for species that bind rapidly upon encounter, depending on D_m and N.

The interaction of a cytosolic protein with a membrane target can be considered reaction limited for $Da < 0.1$ and diffusion-limited for $Da > 10$. For interactions between two membrane species, $(\chi/\delta)Da \sim 0$ describes reaction-limited behavior while $(\chi/\delta)Da > 10$ describes diffusion-limited associations. Thus, the representation of E in eqn. 2.19 allows the enhancement effect to be visualized easily with a minimum of free parameters, and it allows Figure 2.3 to be segmented into regimes where chemical and physical cell parameters contribute differently to $k_{m/m}$ and $k_{c/m}$. Once the effect on the observed forward rate constant is determined, the effect on a reverse rate constant can be determined easily; the enhancement factor will be E/χ, yielding the aforementioned factor of χ enhancement of the observed affinity potentiated by membrane confinement. Figure 2.3 shows that E/χ is actually < 1 for most cases, meaning that the off-rate is generally lower when both reactants are membrane-associated.

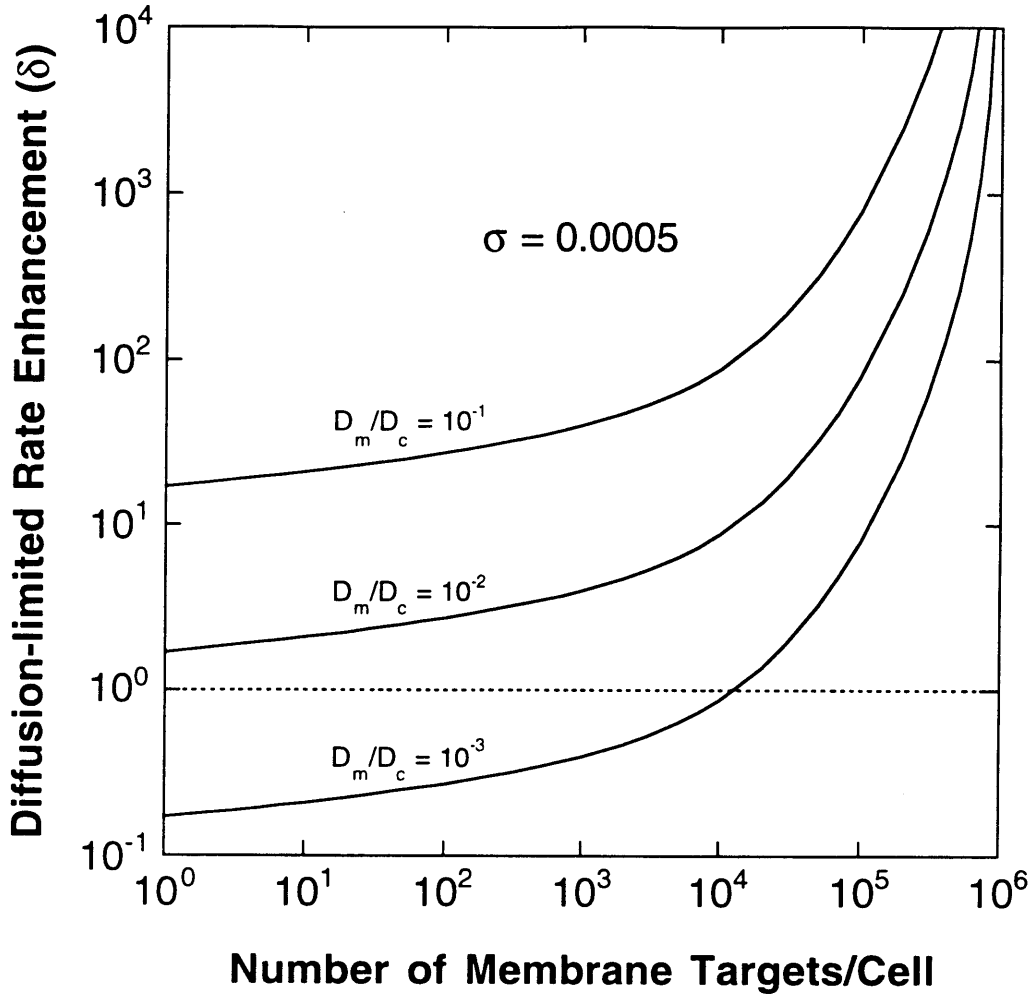

Figure 2.2 Enhancement of diffusion-limited target association rate proferred by recruitment to the plasma membrane. The physical parameter δ, as described in the text, compares the diffusion-limited rates of binding for the association of a specific membrane target with membrane-associated and cytosolic proteins. δ is a function of relative mobility (D_m/D_c), target availability (N), and molecular dimensions (σ), and is plotted versus N for $\sigma = 5 \times 10^{-4}$ and D_m/D_c values of 0.1, 0.01, and 0.001. The entire range of N is explored, and so $\tilde{s}^2$ is not neglected relative to ~ 1 as in eqn. 2.15.

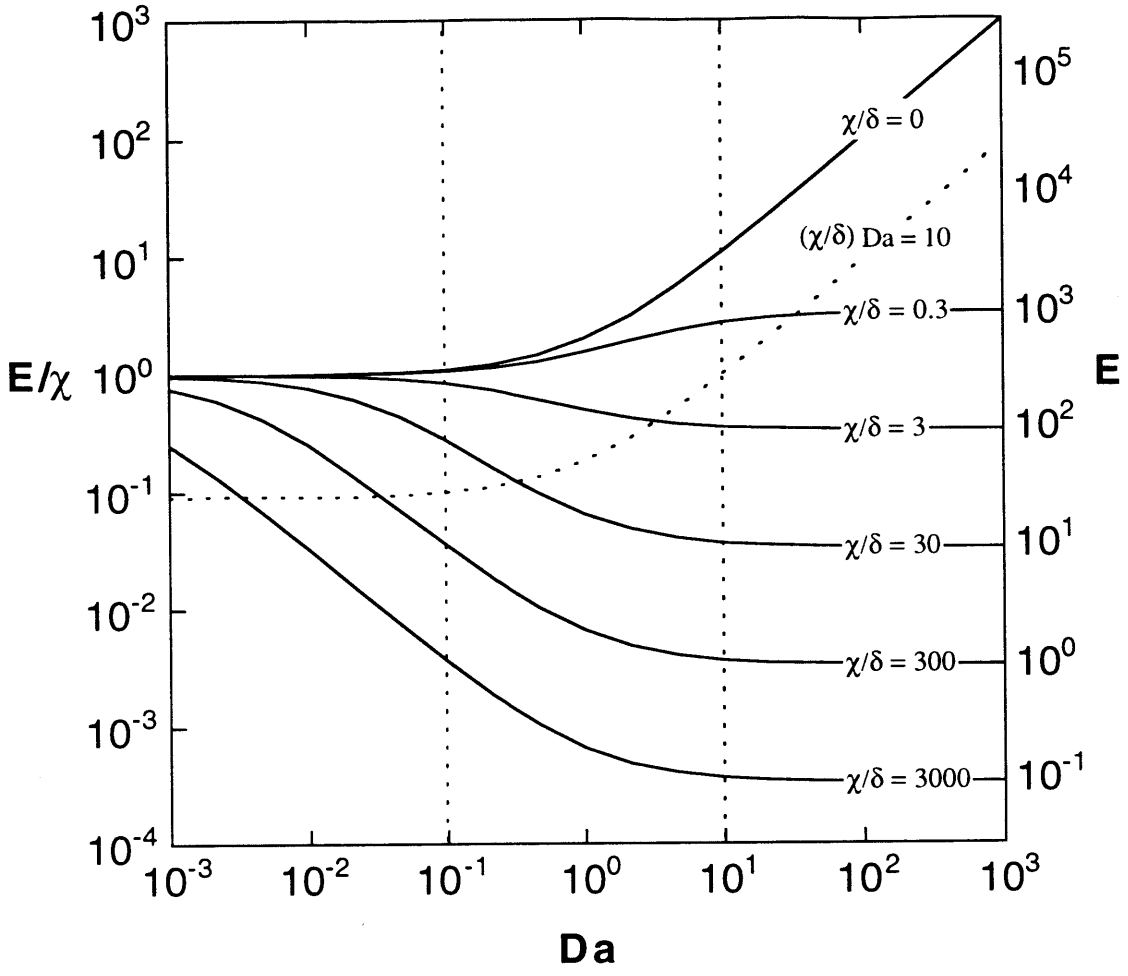

Figure 2.3 Enhancement of target association rate proferred by recruitment to the plasma membrane: reaction and diffusion limitations. The enhancement factor E compares the rates at which a membrane target is bound by membrane and cytosolic reactant partners. E is plotted versus a Damköhler number Da, the ratio of mean reaction and diffusion rates when the reactant partner is cytosolic. As Da approaches zero, E simply reflects a reduction in sampling volume, concentrating the reactant by a factor χ (taken to be 300 here). As Da approaches infinity, E approaches δ, the diffusion-limited value. While Da gauges the importance of diffusion in cytosol-membrane interactions, (χ/δ)Da serves the same purpose for membrane-membrane coupling. For reaction-limited membrane-membrane interactions, $(\chi/\delta)\text{Da} \ll 1$; for diffusion-limited membrane-membrane interactions, $(\chi/\delta)\text{Da} \gg 1$.

If one of two interacting species is permanently associated with the plasma membrane, it is apparent that the location of the second molecule can affect the dynamics of signal transduction. For more direct clarification, two simple signaling models were formulated to illustrate the potential impact of locational control (Figure 2.4). Each model involves responses to stimulation of a membrane receptor with a constant extracellular concentration of agonist. As a very well characterized system, the typical binding and internalization kinetics of EGF-receptor were used (Appendix B). EGF-receptor occupation at the surface is very dynamic on the time scale of minutes. For simplicity, receptor synthesis, recycling, and non-specific (constitutive) internalization were neglected, as was feedback attenuation of the receptor kinase. Signaling from receptor-ligand complexes in an endosomal compartment, which brings up distinct signal compartmentalization issues, was also discounted. These issues are addressed in the following chapter. The point of the receptor activation model was to be simple and dynamic, not to completely capture all the nuances of receptor trafficking and compartmentalization.

2.3.2 Upregulation of a Membrane Messenger by a Membrane Receptor-recruited Activator

The first model describes the regulation of a constitutively membrane-associated signaling target by two distinct cytosolic activating and deactivating proteins. The fraction of the signaling target in the active state is at a low baseline steady-state value for $t < 0$. In this scheme, a cell surface receptor bound to an extracellular agonist can upregulate the signal by recruiting only the activator to the plasma membrane via interactions with its intracellular tail (Figure 2.4A). This model therefore illustrates how specific relocation can mediate a signal by differentially modulating competing mechanisms that alter the activation state of a membrane-associated signaling molecule.

The levels of all species on the time scale of interest are conserved. The net rate of change in the activation state of the signaling protein is expressed in terms of activating and deactivating fluxes. The switch to the effector state occurs rapidly following the binding of activating and signaling proteins; in terms of Michaelis-Menten enzyme kinetics parameters, this means that product formation is always in the linear range, with observed second-order rate constant $k_{cat}/K_M = k_f k_{cat}/(k_r+k_{cat}) \sim k_f$. Since the specific activity of the activating protein is not constant, the activation flux is modeled as a second-order process. The specific activity of the deactivating protein is considered to be constant, so the deactivating flux is pseudo-first-order.

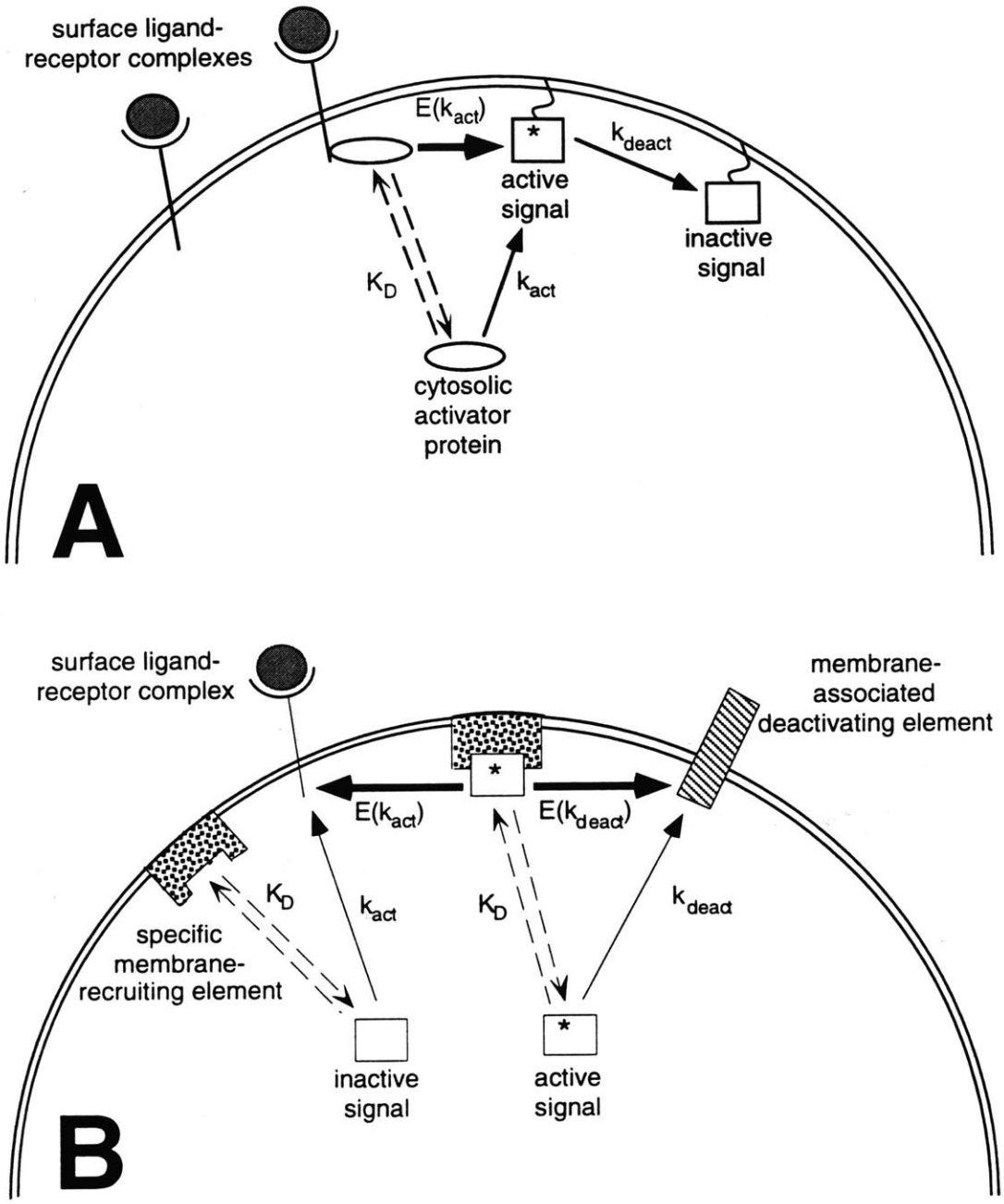

Figure 2.4 Two highly simplified signal transduction models. A, Model 1: signaling through a membrane-associated molecule regulated by distinct cytosolic activating and deactivating proteins. Only the activating element is recruited to the plasma membrane, an interaction in pseudo-equilibrium with receptor occupancy. B, Model 2: regulation of a cytosolic signaling protein by distinct, constitutively membrane-associated elements. By recruiting the signaling protein to the membrane, the activation and deactivation rates are enhanced by the same factor.

Defining α to be the fraction of the target in the activated state, the baseline activation level is

$$\alpha_0 = \frac{k_{act} A_T}{k_{act} A_T + k_{deact}} \qquad (2.20),$$

where k_{act} and k_{deact} are the rate constants of activation and deactivation observed in the absence of ligand, respectively, and A_T is the total number of activator molecules in the cell. At t = 0, a constant concentration of agonist is added, and the activator is recruited with rapid kinetics compared to agonist binding (pseudo-equilibrium). Employing mass-action kinetics, the net rate of protein activation is

$$\dot{\alpha} = k_{act} A_T \left\{ 1 + (E-1) \left[\frac{C_s(t)}{K_D + C_s(t)} \right] \right\} (1-\alpha) - k_{deact} \alpha \qquad (2.21),$$

where $C_s(t)$ is the level of receptor-agonist complexes displayed at the cell surface (see Appendix B for a description of the kinetics), and K_D is the dissociation constant describing the equilibrium between surface complexes and the recruited activator. The initial condition for eqn. 2.21 is given by eqn. 2.20. Since it is assumed that receptor function is not affected by intracellular feedback loops, $C_s(t)$ is an external, independent function of time separable from downstream signaling. E is the enhancement factor due to membrane translocation, as described by eqn. 2.19. While E can be a weak function of $C_s(t)$, it is set to a constant value for simplicity.

Since $C_s(t)$ does not depend on α, eqn. 2.21 is linear; nevertheless, it was rapidly integrated numerically to within 0.001% using the LSODE subroutine (Hindmarsh, 1980) on a Sun workstation. The activation profiles $\alpha(t)$ and phase diagrams $\alpha(t)$ *versus* $C_s(t)$ are displayed in Figure 2.5 for reasonable parameter values and various values of λ, the dimensionless extracellular ligand concentration. The activation profiles of α (Figure 2.5A) are similar to that of C_s, as to be expected if the pattern of ligand stimulation is to have a controllable effect on the resulting signal. The peak value of α saturates with λ much as C_s does.

More telling information, however, lies in the phase diagram of α *versus* C_s (Figure 2.5B). The interplay between receptor and messenger and the disparity between time scales can be visualized without seeing time pass explicitly. On extremely short time scales (seconds or less), $\Delta\alpha \sim \Delta C_s \sim 0$, and the differential equations can be approximated by difference equations:

$$\frac{\Delta\alpha}{t} \approx k_{act}A_T(E-1)(1-\alpha_0)\left(\frac{c}{\kappa+c}\right); \quad c \equiv \frac{C_s}{R_0}; \quad \kappa \equiv \frac{K_D}{R_0}$$

$$\frac{c}{t} \approx \lambda k_r \qquad (2.22),$$

$$\Delta\alpha \approx (E-1)\left(\frac{k_{act}A_T}{k_r}\right)\left(\frac{1-\alpha_0}{\lambda}\right)\left(\frac{c^2}{\kappa+c}\right) = (E-1)\left(\frac{1-\alpha_0}{\lambda}\right)\left(\frac{k_{act}A_T}{k_r}\right)\left[c-\left(\frac{\kappa c}{\kappa+c}\right)\right]$$

where R_0 is the surface receptor level per cell at t = 0, and k_r is the rate constant of ligand dissociation from receptors. Note that C_s and K_D are nondimensionalized in terms of R_0. As λ is increased, the value of C_s reached by the cell before α responds increases exponentially. The ratio $(E-1)k_{act}A_T/\kappa k_r\lambda$ can be thought of as a response coefficient, and when it is very low, signaling cannot keep up with what is perceived by the signaling machinery as a step change in the occupied receptor level.

While the above analysis is instructive, it does not capture the shape of the phase diagrams for even the shortest time scales of interest, particularly if λ is large. A more robust equation is found by linearizing eqn. 2.21 in terms of α and C_s and exploiting the fact that $C_s(t)$ can be expressed as a single exponential for short time scales (Appendix B):

$$\alpha-\alpha_0 \approx \left(\frac{E-1}{\kappa}\right)\left(\frac{k_{act}A_T}{k_r}\right)\left(\frac{1-\alpha_0}{\zeta-g(\lambda)}\right)\left\{c-\frac{\lambda}{\zeta}\left[1-\left(1-\frac{g(\lambda)}{\lambda}c\right)^{\zeta/g(\lambda)}\right]\right\} \qquad (2.23),$$

$$\zeta \equiv \frac{k_{act}A_T+k_{deact}}{k_r}; \quad g(\lambda) \equiv \sqrt{(1+\lambda+\varepsilon)^2-4\lambda\varepsilon}$$

where ε is the ratio of the endocytic rate constant k_e to k_r, as defined in Appendix B. Agreement of eqn. 2.23 with the phase diagrams at the beginning of their trajectories is illustrated in Figure 2.5B. On much longer time scales, the signal tends toward pseudo-equilibrium with C_s:

$$\alpha_{eq} = \frac{k_{act}A_T(\kappa+Ec)}{k_{act}A_T(\kappa+Ec)+k_{deact}(\kappa+c)}; \qquad (2.24).$$

$$\left(\frac{\alpha_{eq}}{1-\alpha_{eq}}\right) = \left(\frac{\alpha_0}{1-\alpha_0}\right)\left(\frac{1+Ec/\kappa}{1+c/\kappa}\right)$$

Thus, all trajectories in the model system eventually collapse onto one curve in phase space, as seen in Figure 2.5B.

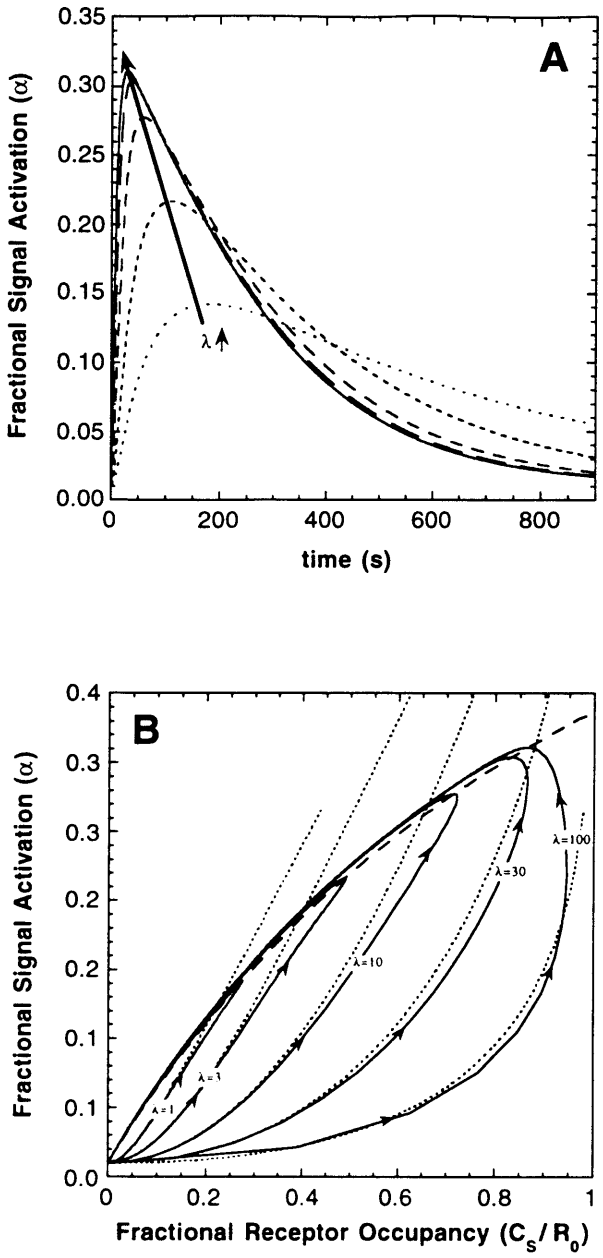

Figure 2.5 Activation of a membrane signaling target. A, solution of eqn. 2.21 for the following constant parameter values: $k_{act}A_T = 10^{-3}\ s^{-1}$; $k_{deact} = 0.1\ s^{-1}$; $E = 300$; $K_D/R_0 = 5$. The function $C_s(t)$ used is as described in Appendix B, with $k_r = 0.005\ s^{-1}$, $\varepsilon = 1$, and λ values of 1, 3, 10, 30, and 100. B, phase diagrams. The profiles of $\alpha(t)$ and $C_s(t)$ are combined to make time an implicit variable, with the direction of each trajectory marked using arrows. The dotted lines represent the analytical solution valid for short times (eqn. 2.23), and the dashed line denotes the path of pseudo-steady state (eqn. 2.24).

2.3.3 Responsive Activation of a Cytosolic Messenger by a Membrane Receptor

The second model describes a cytosolic signaling protein which is regulated by distinct membrane-associated activating and deactivating elements. Thus, compared to Model 1 the locations of the signal and regulatory proteins in the cell's resting state are reversed. The activating element is the enzymatic machinery of occupied surface receptors. This model illustrates how the relocation of the cytosolic signal to the plasma membrane can streamline its responsiveness to the regulatory elements governing its activation, particularly since the activating element $C_s(t)$ is changing dynamically with time (Figure 2.4B).

The cytosolic signal in the unactivated state and surface receptor-ligand complexes interact with second-order rate constant k_{act}, and activation is rapid following association. The specific activity of the membrane-associated deactivating protein is again constant, yielding a pseudo-first-order flux with rate constant k_{deact}. At t = 0, the concentration of extracellular agonist is stepped up from zero to a constant value. In the absence of relocation mechanisms,

$$\begin{aligned} &\dot{\alpha} = k_{act} C_s(t)(1-\alpha) - k_{deact}\alpha \\ &\alpha(0) = 0 \end{aligned} \qquad (2.25),$$

where α is again the fraction of the signaling molecule in the active state, and $C_s(t)$ is as described in Appendix B.

With recruitment of the cytosolic protein to the membrane via association with S specific sites, an interaction in pseudo-equilibrium with respect to extracellular ligand binding and characterized by dissociation constant K_D, rates of interaction with both activating and deactivating elements are modified. If the activation and deactivation flux exhibit the same enhancement factor E due to relocation of the cytosolic substrate of interest, then

$$\dot{\alpha} = \left[1 + (E-1)\left(\frac{S}{K_D + S}\right)\right]\dot{\alpha}(S=0) \qquad (2.26),$$

where $\dot{\alpha}(S = 0)$ is given in eqn. 2.25. While the recruitment of the signaling protein can certainly be regulated by the cell, S is considered to be constant for simplicity, allowing us to lump the variables in brackets into a dimensionless sensitivity parameter η:

$$\eta \equiv \left[1 + (E-1)\left(\frac{S}{K_D + S}\right)\right] \qquad (2.27).$$

Thus, the relative magnitudes of the activation and deactivation fluxes move in concert. At equilibrium of C_s and α, membrane recruitment does not affect the steady-state value of α, but rather potentiates a rapid response to the transient peak in C_s.

The dynamics of α were again determined numerically; activation profiles and phase diagrams for this case are displayed as Figure 2.6 for values of k_{act} and k_{deact} expressly chosen to be relatively unresponsive compared to the binding kinetics of EGF. This time, the sensitivity parameter η was varied while keeping $C_s(t)$ constant ($\lambda = 1$). For very short time scales, the differential equations can again be converted into approximate algebraic expressions in order to gauge the importance of the parameters in determining the phase behavior at the beginning of the trajectories in Figure 2.6B. The gain is of course proportional to η:

$$\alpha \approx \left(\frac{\eta k_{act} R_0}{\lambda k_r} \right) c^2 \qquad (2.28).$$

In this case, the response coefficient is $\eta k_{act} R_0 / \lambda k_r$. For $\eta \sim 1$, it is clear that in the characteristic time it takes to accumulate α, C_s has already gone through its dynamic. The signal fails to reach a good peak value, although the response observed is more sustained on the time scale of receptor internalization (Figure 2.6A). For $\eta k_{act} R_0 / \lambda k_r >> 1$, the signaling machinery responds immediately to what it perceives as a slow change in C_s., constantly establishing new pseudo-equilibria:

$$\alpha_{eq} = \frac{k_{act} C_s}{k_{act} C_s + k_{deact}} \qquad (2.29).$$

As η approaches infinity, the signal peaks and downregulates alongside the level of bound receptors at the surface, and the phase trajectories in Figure 2.6B get tighter and tighter about eqn. 2.29. The signal becomes a better translation of the receptors' enzymatic activity, a more efficient transducer of an extracellular instruction. Translocation in this case favors neither the activation nor the deactivation flux, but the behavior can be altered dramatically if the rate constants governing the signal in the absence of relocating mechanisms are of the same order of magnitude or less than those regulating receptor dynamics.

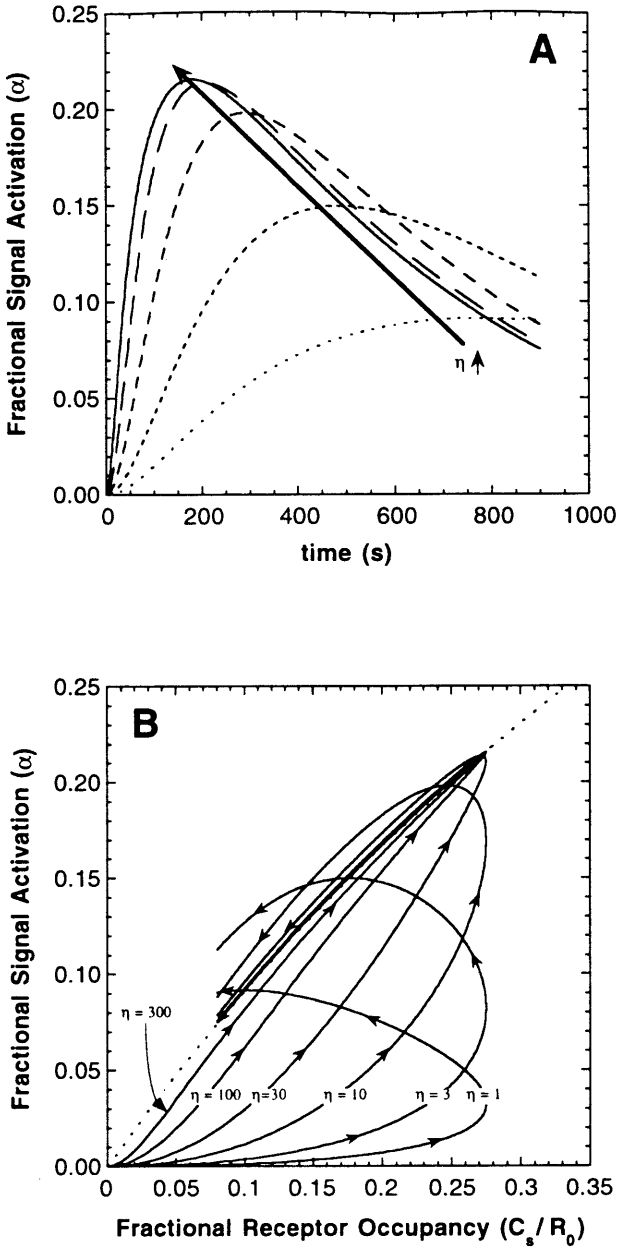

Figure 2.6 Regulation of a cytosolic signaling protein. A, solution of eqn. 2.26 for the following constant parameter values: $k_{act}R_0 = 0.001\ s^{-1}$; $k_{deact} = 0.001 s^{-1}$. The function $C_s(t)$ used is as described in Appendix B with $k_r = 0.005\ s^{-1}$, $\lambda = 1$, and $\varepsilon = 1$. The parameter η was varied using the following values: $\eta = 1$, 3, 10, 30, 100, and 300. B, phase diagrams. The profiles of $\alpha(t)$ and $C_s(t)$ are combined to make time an implicit variable, with the direction of each trajectory marked using arrows. The dashed line denotes the path of pseudo-equilibrium (eqn. 2.29).

2.3.4 Experimental Relevance

Relocation of signaling proteins from the cytosol to the plasma membrane can be used as a cellular switch to affect changes in the magnitude or responsiveness of signal activation, and these effects were theoretically quantified for typical cellular parameters. However, in an experimental situation where signal activation is measured, the relevance of this kind of analysis may not be apparent. There is often only a qualitative model of signal regulation, and the generation of multiple time courses for various conditions is often neither practical nor necessary. A singular measure of signal activation is usually sufficient to make quantitative comparisons among different variations of an experiment. Thus, it is desirable to relate experimentally accessible observables to various magnitudes of the relocation effect (quantified by the enhancement factor E) when signal activation is at least qualitatively similar to Model 1 or 2.

For signaling similar to Model 1, a convenient measure of activation is the maximum value of α attained following stimulation. The peak value α_{max} will experience the best signal:noise ratio and is most dramatic compared to the baseline level of signaling α_0. Signaling can be quantified as fold-activation relative to a control with no stimulus, measured at a common time after agonist addition which is characteristic of the peak level reached before significant receptor internalization/desensitization. The dependence of this level of activation on ligand concentration is then considered the dose-response of the signal. While the exact time of the peak will likely differ for different ligand concentrations, this type of data representation is conceptually easy to understand and experimentally feasible.

For Model 1, the fold-activation α_{max}/α_0 obeys eqn. 2.24 and is therefore a function of $k_{deact}/k_{act}A_T$, E, and the fractional recruitment experienced at the time of peak activation. The latter parameter is defined as ϕ; in Model 1, $\phi(t)$ was given a saturable dependence on $C_s(t)$:

$$\phi = \frac{c}{\kappa + c} \qquad (2.30).$$

Note that since the peaks of C_s and α do not necessarily coincide, the value of ϕ seen at α_{max} is usually not the maximum recruitment $c_{max}/(\kappa+c_{max})$. α_{max}/α_0 for Model 1 is plotted versus E for various values of ϕ and $k_{deact}/k_{act}A_T = 100$ as Figure 2.7. Also noted on the graph are dose-response values attained for E = 300 and the kinetic parameters used in Figure 2.5. While it is intuitive that as E increases, the requirement for recruitment ϕ decreases, Figure 2.7 shows the sensitivity of this requirement for an observed α_{max}/α_0. For E ~ 10, note that activation of several-fold requires significant recruitment of the activating protein. For E > 100, however, only a small percentage of the activating protein needs to be recruited to get

significant activation over baseline (For 5-fold enhancement, E = 10 requires ~ 50% recruitment, E = 100 only ~ 4%).

For signaling through a cytosolic protein as in Model 2, a sensitivity parameter η was used to quantify the responsiveness of signal activation to receptor occupancy:

$$\eta = [1 + (E-1)\phi]; \quad \phi = \frac{S}{K_D + S} \qquad (2.31).$$

Note that the fractional recruitment ϕ in this model is independent of $C_s(t)$, since S was given no dependence on receptor occupancy. Two experimentally accessible parameters characterize the responsiveness of signal activation: maximal activation and the peak time.

As stated earlier, the best responsiveness of signaling occurs when $\alpha(t)$ is in pseudo-equilibrium with $C_s(t)$. In this optimal scenario, maximal activation $\alpha_{max,eq} = k_{act}R_0c_{max}/(k_{act}R_0c_{max}+k_{deact})$ and the signal peak time t_α coincides with t_c, the peak time of receptor occupancy. For various ligand doses, signal responsiveness can be assessed through the relative peak activation $\alpha_{max}/\alpha_{max,eq}$ and the relative lag time $\Delta\tau_{peak} = (t_\alpha - t_c)/t_c$. Also, from Figure 2.6A it is apparent that for a given ligand concentration these observables are not independent; as responsiveness decreases, the lag time increases and the peak magnitude decreases.

Since the activation profile can now be sufficiently characterized with two codependent pieces of data, the dose-response behavior of Model 2 can be explored for the kinetic parameters used in Figure 2.6 and various values of η. In Figure 2.8A, lines of constant λ and η are plotted in $\alpha_{max}/\alpha_{max,eq}$ *versus* $\Delta\tau_{peak}$ space, as determined from numerical solutions of eqn. 2.26. For η = constant, two effects are apparent as saturating ligand concentrations are approached: receptor occupancy peaks increasingly earlier (see Appendix B), making the relative lag time extremely sensitive to the dose, and the relative magnitude of the peak becomes insensitive to dose. Both effects are caused by the fact that ligand association with receptors becomes less of a rate-limiting step as λ is increased.

For a given dose, however, as seen in Figure 2.6, both the magnitude and lag time of the signal peak are fairly sensitive to changes in the nature of recruitment, as manifested in the dependence of η on E and ϕ. Figure 2.8A effectively defines the requirement for recruitment to achieve certain responsiveness criteria. For example, for a cell responding to growth factor stimulation of λ = 1-10 through Model 2, a responsiveness criterion may be $\Delta\tau_{peak} < 1$, in which case η must be > 30. Another criterion may be $\alpha_{max}/\alpha_{max,eq} > 0.8$, in which case η only need be > 10. To separate the effects of E and ϕ for Model 2 as in Figure 2.7 for Model 1, $\Delta\tau_{peak}$ was plotted *versus* E for λ = 1, the kinetic parameters used in Figure 2.6, and various values of $\phi = S/(K_D+S)$ in Figure 2.8B.

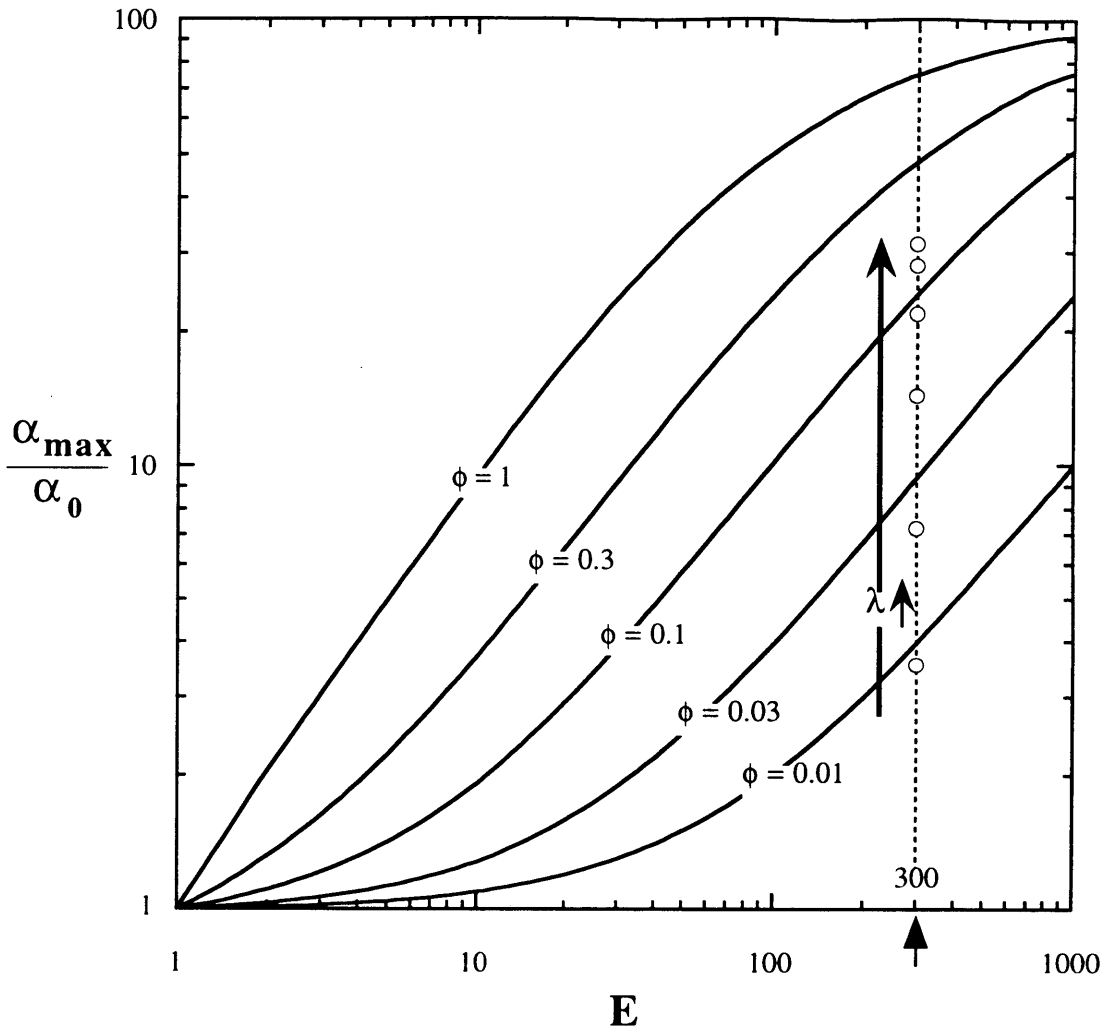

Figure 2.7 Sensitivity of Model 1 signal magnitude to aspects of membrane recruitment. The maximum level of activation in Model 1 is defined as α_{max}, and α_{max}/α_0 represents the fold-activation of the signal, a common representation of experimental data. The fraction ϕ of the cytosolic activator recruited to the membrane at the time of peak activation is directly dependent on the dose of ligand in this model. α_{max}/α_0 is plotted *versus* the rate enhancement E for various values of ϕ experienced at peak activation ($k_{deact}/k_{act}A_T = 100$). Circular symbols mark the dose-response behavior of the model for the following parameters as used in Figure 2.5: $k_{act}A_T = 0.001\ s^{-1}$; $k_{deact} = 0.1\ s^{-1}$; E = 300; $K_I/R_0 = 5$; $C_s(t)$ with $k_r = 0.005\ s^{-1}$ and $\varepsilon = 1$. Dose magnitudes are λ = 0.1, 0.3, 1, 3, 10, and infinity. Since ϕ is saturable, $\phi_{max} < 1$ for this case.

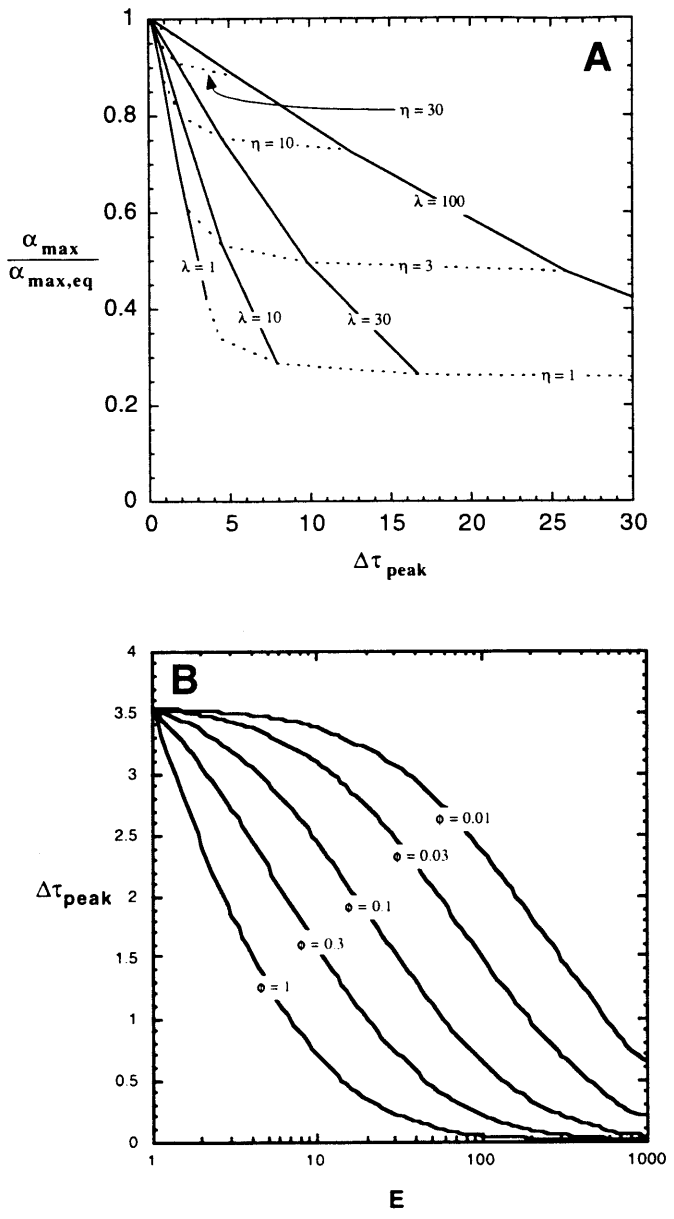

Figure 2.8 Sensitivity of Model 2 signal responsiveness to aspects of membrane recruitment. The quantitites of interest are $\alpha_{max}/\alpha_{max,eq}$, the observed peak level of activation relative to the equilibrium case, and the relative lag time $\Delta\tau_{peak} = (t_\alpha - t_c)/t_c$. A, dependence of responsiveness criteria on dose and the sensitivity coefficient η. Lines of constant λ and η are plotted in $\alpha_{max}/\alpha_{max,eq}$ vs. $\Delta\tau_{peak}$ space for the same constant parameters used in Figure 2.6. B, sensitivity of lag time to changes in relocation. $\Delta\tau_{peak}$ is plotted vs. E for the parameters used in A, $\lambda = 1$, and various $\phi = S/(K_D+S)$.

Again, there is a substantial change in the need for recruitment corresponding to values of E separated by an order of magnitude. For the criterion $\Delta\tau_{peak} < 1$, nearly complete recruitment is required for E ~ 10, while the requirement for E ~ 100 is $\phi \sim 0.05$.

2.4 Discussion

A central goal of this chapter was to explain how and why location matters in intracellular signal transduction, using plasma membrane and cytosolic compartments as relevant location categories. To this end, the physical basis for possible enhancements in association rates and equilibrium binding due to relocation of signaling components was explored. By restricting molecules to a thin layer adjacent to a surface, reactants can be greatly concentrated. They may also diffuse more efficiently and over shorter average distances (though in general less rapidly) in two dimensions to find potential targets. Transport and reaction processes involved in the binding of cytosolic and membrane-associated species to a membrane target were examined, and order-of-magnitude reasoning was employed to estimate binding parameters as they might be observed in the cell.

In the transport-limited regime, cytosolic proteins likely exhibit an observed forward rate constant ~ 10^7 $(Ms)^{-1}$ in associating with a membrane target. As a relevant example, specific recruitment of signaling proteins to phosphotyrosyl motifs of occupied RTKs may reach this limit, since the modular domains responsible for such recruitment events generally exhibit high on and off rates with targets in solution. Most but not all membrane-membrane interactions are expected to be diffusion-limited. While intuition might suggest that this is due to a reduced molecular mobility in the membrane, a reduction in distance to target and reduction-of-dimensionality often more than compensate for this effect. Rather, the diffusion limitation is caused by a significant reduction in the sampling volume, which increases by 10^2 to 10^3-fold the effective rate constant in the absence of chemical gradients. By comparing the rates of cytosol-membrane and membrane-membrane binding rates, it was concluded that relocation from the cytosol to the plasma membrane almost always confers significant enhancement in the protein association rate, by a factor E of ~ 10 - 1000. The only exception is for diffusion-limited interactions among relatively immobile membrane partners ($D_m/D_c \sim 10^{-3}$), for which E may be as low as ~ 0.1.

More importantly, the potential impact of such enhancements on the dynamics of signal activation was also investigated. To accomplish this, the enhancement in association rate for a change in location E was set to a constant, although for membrane relocation E is generally a weak function of target availability. Simple models were introduced to illustrate two potential implications of rate enhancement, using the reversible binding of a receptor as

the extracellular stimulus. In Model 1, relocation effectively boosts the activation flux of a membrane target molecule, previously at a low steady-state level. Since recruitment is directly tied to receptor occupancy, the signal responds in a dose-dependent manner and is attenuated by receptor endocytosis. This is similar to what is thought to occur in the EGF-mediated activation of Ras (Osterop et al., 1993). Model 1 may also at least qualitatively describe aspects of lipid second messenger generation through recruitment of cytosolic enzymes such as PI(3)K and phospholipase C-γ (PLC-γ) to occupied RTKs. In Model 2, both fluxes are enhanced by translocation, streamlining the response for maximum efficiency and fidelity with regard to the extracellular input. For high rate enhancements, the signal can constantly adjust to new pseudo-equilibria as the level of occupied receptors at the surface rises and falls temporally. For example, the localization of a protein regulated by RTKs and membrane phosphatases (Kulas et al., 1996b; Kulas et al., 1996a) may modulate the responsiveness of its signaling profile with time.

While the modulation of temporal sensitivity was examined in these models, with pseudo-equilibrium being the ideal response, still another issue is the sensitivity of the signal output to changes in the input (the balance between membrane-associated activating and deactivating elements). By imposing activation mechanisms that are rapid upon protein association, neglecting possible saturation of the enzymes regulating the signal, the sensitivity of α to C_s at pseudo-equilibrium is Michaelian (hyperbolic dependence; eqn. 2.29). When either or both of the regulatory elements are significantly saturated, a greater sensitivity is achieved where smaller changes in C_s above a threshold level can have a large impact on α (Goldbeter and Koshland, 1981). Since this "zero-order sensitivity" is determined by the substrate concentration relative to the Michaelis constants K_M of the regulatory enzymes, and since substrates can be concentrated by more than an order of magnitude at membrane surfaces, cells may be able to titrate the equilibrium sensitivity of a response by varying membrane recruitment (Appendix C).

It is clear from the molecular understanding of signaling that location is important, particularly at the level of membrane interactions. Many key signaling molecules are constitutively targeted to the plasma membrane by post-translational lipid modifications: the Src tyrosine kinase, heterotrimeric G proteins, other GTPases such as Ras, Rho, and Rac. These proteins are relatively inactive in solution and cannot function if membrane targeting is prevented. Still others are recruited to the membrane directly or indirectly through interactions between SH2/PTB domains and phosphotyrosine-containing motifs: Sos, PLC-γ, PI(3)K, the Syp tyrosine phosphatase (van der Geer et al., 1994). Interactions with membrane lipids themselves are also important. For example, PLC-γ hydrolyzes phosphatidylinositol (4,5)-bisphosphate (PIP_2) to inositol triphosphate and diacylglycerol

(DAG). DAG then recruits and activates isoforms of protein kinase C (PKC), a serine-threonine kinase. Other proteins can interact with acidic phospholipids and/or $\beta\gamma$ G-protein subunits courtesy of pleckstrin homology (PH) or zinc finger protein motifs (Ghosh et al., 1994; Lemmon et al., 1996), which may initiate or stabilize membrane relocation. Further compartmentalization within the plasma membrane has recently been suggested by the selective enrichment of signaling components in membrane pits containing the protein caveolin (Song et al., 1996; Liu et al., 1996; Mineo et al., 1996), which may further concentrate signaling molecules together and/or hinder association with proteins not found in these subdomains.

However, our attention need not be limited to interactions at the plasma membrane or the underlying cytoskeleton. Two associating proteins can also be anchored to any physical boundary or brought together by some scaffolding mechanism on the molecular level (Faux and Scott, 1996). Indeed, the plasma membrane generally only accounts for a small percentage of the total area associated with cellular membranes and cytoskeletal network surfaces (Gershon et al., 1985; Alberts et al., 1994). For any mechanism, molecular specificity coupled with physical considerations will determine the cellular ramifications of the relocating event. Thus, an understanding of the biophysical theory seems appropriate in the interpretation of many experiments in signal transduction.

2.5 References

Adam, G. and Delbrück, M. (1968). "Reduction of dimensionality in biological diffusion processes." in *Structural Chemistry and Molecular Biology*, eds. Rich, A. and Davidson, N. San Fransisco: W.H. Freeman and Co., pp. 198-215.

Alberts, B., Bray, D., Lewis, J., Raff, M., Roberts, K. and Watson, J.D. (1994). *Molecular Biology of the Cell, third ed.* New York: Garland Publishing.

Aronheim, A., Engelberg, D., Li, N., Al-Alawi, N., Schlessinger, J. and Karin, M. (1994). Membrane targeting of the nucleotide exchange factor Sos is sufficient for activating the Ras signaling pathway. *Cell*, 78: 949-961.

Berg, H.C. and Purcell, E.M. (1977). Physics of chemoreception. *Biophys. J.*, 20: 193-219.

Bos, J.L. (1989). Ras oncogenes in human cancer: a review. *Cancer Res.*, 49: 4682-4689.

Bourne, H.R., Sanders, D.A. and McCormick, F. (1991). The GTPase superfamily: conserved structure and molecular mechanism. *Nature*, 349: 117-127.

Buday, L. and Downward, J. (1993). Epidermal growth factor regulates p21ras through the formation of a complex of receptor, Grb2 adapter protein, and Sos nucleotide exchange factor. *Cell*, 73: 611-620.

Carraway, K.L. and Carraway, C.A.C. (1995). Signaling, mitogenesis and the cytoskeleton: where the action is. *BioEssays*, 17: 171-175.

Cussac, D., Frech, M. and Chardin, P. (1994). Binding of the Grb2 SH2 domain to phosphotyrosine motifs does not change the affinity of its SH3 domains for Sos proline-rich motifs. *EMBO J.*, 13: 4011-4021.

Erickson, J., Goldstein, B., Holowka, D. and Baird, B. (1987). The effect of receptor density on the forward rate constant for binding of ligands to cell surface receptors. *Biophys. J.*, 52: 657-662.

Faux, M.C. and Scott, J.D. (1996). Molecular glue: kinase anchoring and scaffold proteins. *Cell*, 85: 9-12.

Feig, L.A. (1994). Guanine-nucleotide exchange factors: a family of positive regulators of Ras and related GTPases. *Curr. Opin. Cell Biol.*, 6: 204-211.

Force, T., Bonventre, J.V., Heidecker, G., Rapp, U., Avruch, J. and Kyriakis, J.M. (1994). Enzymatic characteristics of the c-Raf-1 protein kinase. *Proc. Natl. Acad. Sci. USA*, 91: 1270-1274.

Gershon, N.D., Porter, K.R. and Trus, B.L. (1985). The cytoplasmic matrix: its volume and surface area and the diffusion of molecules through it. *Proc. Natl. Acad. Sci. USA*, 82: 5030-5034.

Ghosh, S., Xie, W.Q., Quest, A.F.G., Mabrouk, G.M., Strum, J.C. and Bell, R.M. (1994). The cysteine-rich region of Raf-1 kinase contains zinc, translocates to liposomes, and is adjacent to a segment that binds GTP-Ras. *J. Biol. Chem.*, 269: 10000-10007.

Goldbeter, A. and Koshland, D.E.J. (1981). An amplified sensitivity arising from covalent modification in biological systems. *Proc. Natl. Acad. Sci. USA*, 78: 6840-6844.

Goldstein, B. (1989). Diffusion limited effects of receptor clustering. *Comm. Theor. Biol.*, 1: 109-127.

Hallberg, B., Rayter, S.I. and Downward, J. (1994). Interaction of Ras and Raf in intact mammalian cells upon extracellular stimulation. *J. Biol. Chem.*, 269: 3913-3916.

Hill, T.L. (1975). Effect of rotation on the diffusion-controlled rate of ligand-protein association. *Proc. Natl. Acad. Sci. USA*, 72: 4918-4922.

Hindmarsh, A.C. (1980). LSODE and LSODI, two new initial value ordinary differential equation solvers. *ACM-Signum newsletter*, 15: 10-11.

Howe, L.R., Leevers, S.J., Gomez, N., Nakielny, S., Cohen, P. and Marshall, C.J. (1992). Activation of the MAP kinase pathway by the protein kinase raf. *Cell*, 71: 335-342.

Jacobson, K. and Wojcieszyn, J. (1984). The translational mobility of substances within the cytoplasmic matrix. *Proc. Natl. Acad. Sci. USA*, 81: 6747-6751.

Jelinek, T., Dent, P., Sturgill, T.W. and Weber, M.J. (1996). Ras-induced activation of Raf-1 is dependent on tyrosine phosphorylation. *Mol. Cell. Biol.*, 16: 1027-1034.

Kikuchi, A. and Williams, L.T. (1994). The post-translational modification of ras p21 is important for Raf-1 activation. *J. Biol. Chem.*, 269: 20054-20059.

Klippel, A., Reinhard, C., Kavanaugh, W.M., Apell, G., Escobedo, M. and Williams, L.T. (1996). Membrane localization of phosphatidylinositol 3-kinase is sufficient to activate multiple signal-transducing kinase pathways. *Mol. Cell. Biol.*, 16: 4117-4127.

Kulas, D.T., Freund, G.G. and Mooney, R.A. (1996a). The transmembrane protein-tyrosine phosphatase CD45 is associated with decreased insulin receptor signaling. *J. Biol. Chem.*, 271: 755-760.

Kulas, D.T., Goldstein, B.J. and Mooney, R.A. (1996b). The transmembrane protein-tyrosine phosphatase LAR modulates signaling by multiple receptor tyrosine kinases. *J. Biol. Chem.*, 271: 748-754.

Ladbury, J.E., Lemmon, M.A., Zhou, M., Green, J., Botfield, M.C. and Schlessinger, J. (1995). Measurement of the binding of tyrosyl phosphopeptides to SH2 domains: a reappraisal. *Proc. Natl. Acad. Sci. USA*, 92: 3199-3203.

Lauffenburger, D.A. and Linderman, J.L. (1993). *Receptors: Models for Binding, Trafficking, and Signaling.* New York: Oxford University Press.

Leevers, S.J., Paterson, H.F. and Marshall, C.J. (1994). Requirement for Ras in Raf activation is overcome by targeting Raf to the plasma membrane. *Nature*, 369: 411-414.

Lemmon, M.A., Ferguson, K.M. and Schlessinger, J. (1996). PH domains: diverse sequences with a common fold recruit signaling molecules to the cell surface. *Cell*, 85: 621-624.

Liu, P., Ying, Y., Ko, Y. and Anderson, R.G.W. (1996). Localization of platelet-derived growth factor-stimulated phosphorylation cascade to caveolae. *J. Biol. Chem.*, 271: 10299-10303.

Mandiyan, V., O'Brien, R., Zhou, M., Margolis, B., Lemmon, M.A., Sturtevant, J.M. and Schlessinger, J. (1996). Thermodynamic studies of Shc phosphotyrosine interaction domain recognition of the NPXpY motif. *J. Biol. Chem.*, 271: 4770-4775.

McLaughlin, S. and Aderem, A. (1995). The myristoyl-electrostatic switch: a modulator of reversible protein-membrane interactions. *Trends Biochem. Sci.*, 20: 272-276.

Mineo, C., James, G.L., Smart, E.J. and Anderson, R.G.W. (1996). Localization of epidermal growth factor-stimulated Ras/Raf-1 interaction to caveolae membrane. *J. Biol. Chem.*, 271: 11930-11935.

Mochly-Rosen, D. (1995). Localization of protein kinases by anchoring proteins: a theme in signal transduction. *Science*, 268: 247-251.

Nesheim, M.E., Tracy, R.P. and Mann, K.G. (1984). "Clotspeed," a mathematical simulation of the functional properties of prothrombinase. *J. Biol. Chem.*, 259: 1447-1453.

Northrup, S.H. and Erickson, H.P. (1992). Kinetics of protein-protein association explained by Brownian dynamics computer simulation. *Proc. Natl. Acad. Sci. USA*, 89: 3338-3342.

Osterop, A.P.R.M., Medema, R.H., van der Zon, G.C.M., Bos, J.L., Moller, W. and Maassen, J.A. (1993). Epidermal-growth-factor-receptors generate Ras-GTP more efficiently than insulin receptors. *Eur. J. Biochem.*, 212: 477-482.

Pawson, T. (1995). Protein modules and signaling networks. *Nature*, 373: 573-580.

Quilliam, L.A., Huff, S.Y., Rabun, K.M., Wei, W., Park, W., Broek, D. and Der, C.J. (1994). Membrane-targeting potentiates guanine nucleotide exchange factor Cdc25 and Sos1 activation of Ras transforming activity. *Proc. Natl. Acad. Sci. USA*, 91: 8512-8516.

Rodriguez-Viciana, P., Warne, P.H., Dhand, R., Vanhaesebroeck, B., Gout, I., Fry, M.J., Watersfield, M.D. and Downward, J. (1994). Phosphatidyl-3-OH kinase as a direct target of Ras. *Nature*, 370: 527-532.

Shoup, D. and Szabo, A. (1982). Role of diffusion in ligand binding to macromolecules and cell-bound receptors. *Biophys. J.*, 40: 33-39.

Song, K.S., Li, S., Okamoto, T., Quilliam, L.A., Sargiacomo, M. and Lisanti, M.P. (1996). Co-purification and direct interaction of Ras with caveolin, an integral membrane protein of caveolae microdomains. *J. Biol. Chem.*, 271: 9690-9697.

Stokoe, D., MacDonald, S.G., Cadwallader, K., Symons, M. and Hancock, J.F. (1994). Activation of Raf as a result of recruitment to the plasma membrane. *Science*, 264: 1463-1467.

Szabo, A., Schulten, K. and Schulten, Z. (1980). First passage time approach to diffusion controlled reactions. *J. Chem. Phys.*, 72: 4350-4357.

van der Geer, P., Hunter, T. and Lindberg, R.A. (1994). Receptor protein-tyrosine kinases and their signal transduction pathways. *Annu. Rev. Cell Biol.*, 10: 251-337.

Zhou, M.M., Harlan, J.E., Wade, W.S., Crosby, S., Ravichandran, K.S., Burakoff, S.J. and Fesik, S.W. (1995). Binding affinities of tyrosine-phosphorylated peptides to the COOH-terminal SH2 and NH2-terminal phosphotyrosine binding domains of Shc. *J. Biol. Chem.*, 270: 31119-31123.

CHAPTER 3

Generalized Mathematical Model of Membrane-compartmentalized Receptor-mediated Signaling

The past decade has witnessed a profound explosion of knowledge in the field of signal transduction mediated by receptor tyrosine kinases. Upon binding of cognate extracellular ligands, these receptors interact with various enzymes and other signaling molecules intracellularly. These protein substrates, which are generally freely diffusing residents of the cytoplasm, as well as the predominantly membrane-associated downstream targets that they activate, are now fairly well characterized molecules. Despite this surge in signaling research, the mechanisms that regulate signaling interactions in a dynamic fashion remain poorly understood, particularly in quantitative terms. In the previous chapter, I examined how recruitment of signaling proteins from the cytosol to the plasma membrane, via interactions with autophosphorylated receptors, can affect the dynamics of signaling reactions. Receptor trafficking effects were neglected in this analysis. In this chapter, I present a generalized mathematical model that incorporates two other factors that can influence signaling: phosphorylation of signaling proteins by the receptor, and the separation of receptor pools into potentially distinct membrane environments induced by receptor internalization and trafficking. Three major effects were analyzed: the influence of cytosolic transport in determining the rate of coupling between receptors and intracellular signaling proteins, the rates of phosphorylation and dephosphorylation reactions relative to receptor coupling rates, and the selective retention of membrane-associated molecules (lipids and lipid-tethered proteins) in different compartments.

3.1 Introduction

Signal transduction is the translation of extracellular stimuli as instructions governing cell responses. Attempts to dissect this complicated process have stimulated interesting questions. As a prominent example, it is not well understood how ligand recognition by different receptor tyrosine kinases (RTKs) can lead to distinct responses, since these receptors for the most part activate the same panel of protein substrates (Chao, 1992). Also, how can more than one response be elicited by the same receptor, and how does the cell decide among them? This has yielded speculation that the magnitude and/or duration of a particular signaling pathway can affect the nature of the cellular response (Marshall, 1995). Alternatively, the decision to respond in one manner over another may

be affected by the *relative* amounts of signaling through various pathways. Because of such issues, it is important to cast the regulatory determinants of intracellular signaling in a quantitative framework.

Signal transduction by RTKs is compartmentalized to a large degree. Allosteric and locational regulation by RTKs are concomitant with binding and are therefore compartmentalized exclusively at cellular membranes. Covalent regulation through phosphorylation is also compartmentalized, since the kinase activity is associated with membranes; on the other hand, phosphorylation is not concomitant with binding and can persist in the cytosolic compartment until the reverse modification is carried out by phosphatase activities. While much less is known about phosphatases in general, membrane phosphatases have been speculated to play a prominent role in the regulation of RTK signaling (Kulas et al., 1996b; Kulas et al., 1996a). Finally, the downstream targets of RTK substrates are, with few exceptions, membrane constituents. The enzymatic activities of phosphatidylinositol (3)-kinase [PI(3)K] and phospholipase C-gamma (PLC-γ) target membrane lipids for modification, the products of which act as second messengers. The Grb2-Sos complex, with additional coupling to phosphorylated Shc, targets the constitutively membrane-associated Ras GTPase for exchange of GDP (inactive) with GTP (active).

Besides the partitioning of RTK substrates between the cytosol and the plasma membrane, further compartmentalization is achieved through receptor endocytosis. EGFR inducibly internalize on the time scale of minutes and are delivered to endosomes in the presence of EGF (Lund et al., 1990), where they are saturably retained for degradative fates in an occupancy-dependent manner (French et al., 1994; Herbst et al., 1994). This trafficking machinery is also at work constitutively, albeit at a much slower rate, as the plasma membrane and its constituents cycle every few hours through the same internalization/recycling pathway (Mellman, 1996). Internalized EGFR that remain ligand-occupied retain kinase and substrate binding activities, and these activities maintain cytosolic orientation in early sorting endosomes. It has therefore been argued that the membrane compartment and the signaling activities previously described must further be subdivided into surface and internal membrane environments (Baass et al., 1995; Bevan et al., 1996).

Under what circumstances and to what extent does internalization of surface receptors affect a change in the magnitude or specificity of signaling? Based on current understanding, RTK-mediated signal transduction at the membrane level can be dissected in terms of discrete points of regulation (Figure 3.1): ligand binding, kinase activation and receptor autophosphorylation, substrate binding, substrate phosphorylation, and target

activation. It is conceivable that the compartmentalization of receptors between the plasma membrane and endosomal membranes could affect any of these regulation mechanisms, or impact two or more in combination. This picture of RTK regulation was used to develop a highly simplified and generalized mathematical model to analyze signal transduction mediated by these receptors.

3.2 Mathematical Model

3.2.1 General Considerations

The general solution approach was cast in terms of three distinct echelons, as illustrated in Figure 3.2. In the first echelon, the initial conditions of an experiment (e.g. ligand concentrations in the culture medium) were imposed on an appropriate trafficking model that describes the binding, internalization, and postendocytic sorting of receptors and ligands. This model determines the temporal profiles of surface and internalized receptors bound to ligand [$b_s(t)$ and $b_i(t)$, respectively]. This part of the solution is not a primary focus of this thesis, as trafficking models have been developed elsewhere (Lauffenburger and Linderman, 1993). A highly simplified trafficking model (Appendix D) was used, which was meant to capture only basic aspects of receptor dynamics. In the second echelon, the distribution of substrate molecules among various localization and phosphorylation states $s_i(t)$ was determined with time based on $b_s(t)$, $b_i(t)$. A reaction-diffusion model, solved at pseudo-steady state, was used. This is appropriate when intracellular processes governing the substrate are much faster than receptor trafficking processes. Finally, in the third echelon of the solution procedure, the total signaling activity $A_T(t)$ was calculated based on $s_i(t)$. A_T, which is proportional to the number of downstream target molecules activated per unit time, is a linear combination of s_i, with each state weighted by an activity coefficient A_i. Overall, this is a simplistic picture of signal regulation, since it is assumed that information only flows in one direction. In other words, binding of substrate does not affect receptor trafficking, and the level of downstream target activation does not affect the binding or phosphorylation of substrate.

3.2.2 General Receptor/Substrate Model

The characteristics of the general diffusion-reaction model are as follows. (i) The model cell adopts spherical axi-symmetric geometry, and the plasma membrane is an impermeable boundary defined by $r = a$. (ii) The cell displays membrane RTKs that bind only one substrate intracellularly. Once bound, the RTK can phosphorylate this substrate. (iii) There are two chemical states of the substrate: phosphorylated and unphosphorylated.

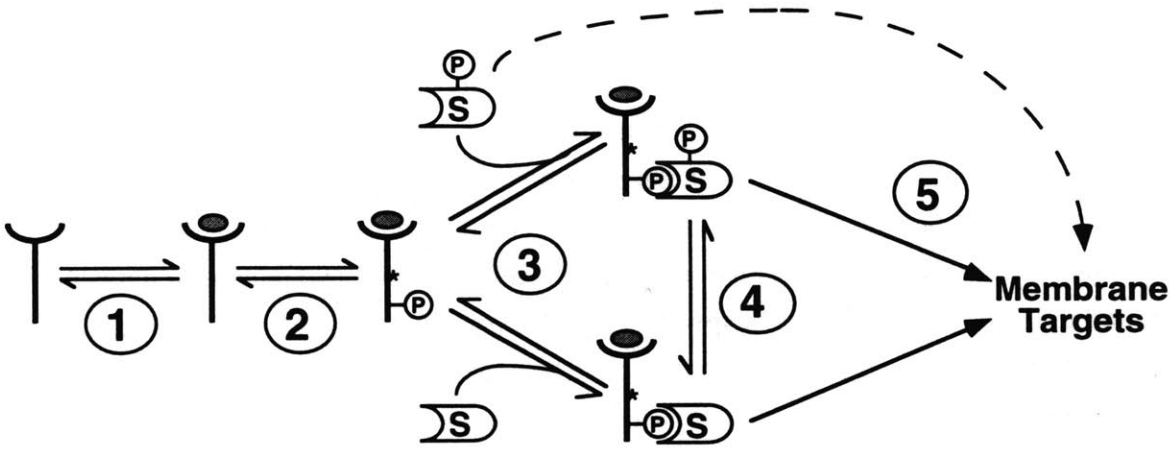

Figure 3.1 Points of Regulation in RTK-mediated Signal Transduction. Signaling mediated by receptor tyrosine kinases at the membrane level can be broken down into discrete steps: 1) reversible binding of a cognate ligand to the receptor, 2) activation of the receptor kinase and autophosphorylation, or transphosphorylation following receptor dimerization, of one or more cytoplasmic tyrosine residues of the receptor, 3) physical association of cytosolic protein substrates with receptor phosphotyrosine, mediated by SH2 and/or PTB domains of the substrate, which is concomitant with locational and allosteric regulation of the substrate, 4) potential phosphorylation of the substrate, which can further modulate substrate activity, and 5) modification of targets, generally membrane constituents, by the substrate. Receptor internalization could conceivably affect any one of these steps or multiple steps at once.

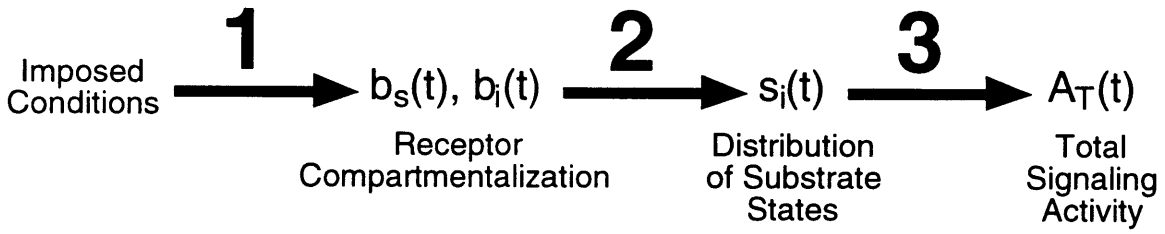

Figure 3.2 General Model Solution Approach. There are three distinct echelons in the solution of total observed signaling activity A_T with time. First, a trafficking model or experimental data describing the time evolution of ligated receptors in the two membrane compartments $b_s(t)$, $b_i(t)$ must be provided. Second, it is assumed that the intracellular processes of diffusion, substrate binding, and substrate modification are much faster than receptor trafficking, and model equations are solved at pseudo-steady state to derive the distribution of substrate states $s_i(t)$. Finally, each substrate state is weighted according to its specific activity (or activity coefficient) A_i to derive the total observed activity A_T.

(iv) RTK activity is localized in the membranes of two compartments: the plasma membrane and internal endosomal membranes. (v) The substrate, which is cytosolic in the unstimulated cell, binds to autophosphorylated receptors with 1:1 stoichiometry. The affinity of this interaction is not affected by the phosphorylation state of the substrate or the localization state of the autophosphorylated receptor. (vi) Unbound substrate is distributed in the cytosol by Fickian diffusion. Nonspecific interactions and collisions with intracellular structures are not prohibited, insofar as such interactions simply reduce the observed diffusion coefficient of the substrate in the cytosol. (vii) The total number of substrate molecules in the cell is conserved.

Thus, there are three localization states and two chemical states of the substrate, yielding six substrate species to be accounted for: $\hat{S}_c^*$ is the concentration or number density of phosphorylated substrate in the cytosol as a function of radial position r, and $\hat{S}_c$ is that of unphosphorylated cytosolic substrate; S_m^* is the number of phosphorylated substrate molecules per cell associated with receptors at the plasma membrane, and S_m is that of unphosphorylated substrate; S_e^* is the number of phosphorylated substrate molecules per cell associated with endosomal receptors, and S_e is that of unphosphorylated substrate associated with endosomes. Since allosteric regulation of substrates by RTKs is concomitant with binding to the receptor, substrate activated in this manner is not considered a distinct species. The general scheme of this model is illustrated in Figure 3.3. The conservation equations for substrate in the cytosol, with boundary conditions specified at the plasma membrane, are:

$$\frac{\partial\theta^*}{\partial\tau_c} = \nabla_{\tilde{r}}^2\theta^* - \alpha\delta_p{}^C\theta^* + R_{\theta^*}; \quad \frac{\partial\theta}{\partial\tau_c} = \nabla_{\tilde{r}}^2\theta + \alpha\delta_p{}^C\theta^* - R_{\theta^*}$$

$$-\left(\frac{1}{\gamma}\right)\left.\frac{\partial\theta^*}{\partial\tilde{r}}\right|_{\tilde{r}=1} = f_s p_s b_s \theta^*|_{\tilde{r}=1} - \kappa s_m^*; \quad -\left(\frac{1}{\gamma}\right)\left.\frac{\partial\theta}{\partial\tilde{r}}\right|_{\tilde{r}=1} = f_s p_s b_s \theta|_{\tilde{r}=1} - \kappa s_m$$

$$\theta^* \equiv \frac{V\hat{S}_c^*}{S_T}; \quad \theta \equiv \frac{V\hat{S}_c}{S_T}; \quad s_m^* \equiv \frac{S_m^*}{S_T}; \quad s_m \equiv \frac{S_m}{S_T}; \quad b_s \equiv \frac{B_s}{R_T} \tag{3.1},$$

$$\tilde{r} \equiv \frac{r}{a}; \quad \tau_c \equiv \frac{D_c t}{a^2}; \quad \alpha \equiv \frac{k_{off}a^2}{D_c}; \quad \delta_p{}^C \equiv \frac{k_p{}^C}{k_{off}}; \quad \gamma \equiv \frac{k_{on}R_T}{4\pi a D_c}; \quad \kappa \equiv \frac{k_{off}V}{k_{on}R_T}$$

where S_T and R_T are the total substrate and initial (in the absence of ligand stimulation) surface receptor molecules per cell, respectively, V is the volume of the cytosol, D_c is the observed molecular diffusivity of the substrate in the cytosol, t is time, k_{on} is the second order association rate constant of the substrate-receptor interaction, k_{off} is the first order dissociation rate constant of said interaction, and $k_p{}^C$ is the observed first order rate constant describing substrate dephosphorylation by phosphatases in the cytosol.

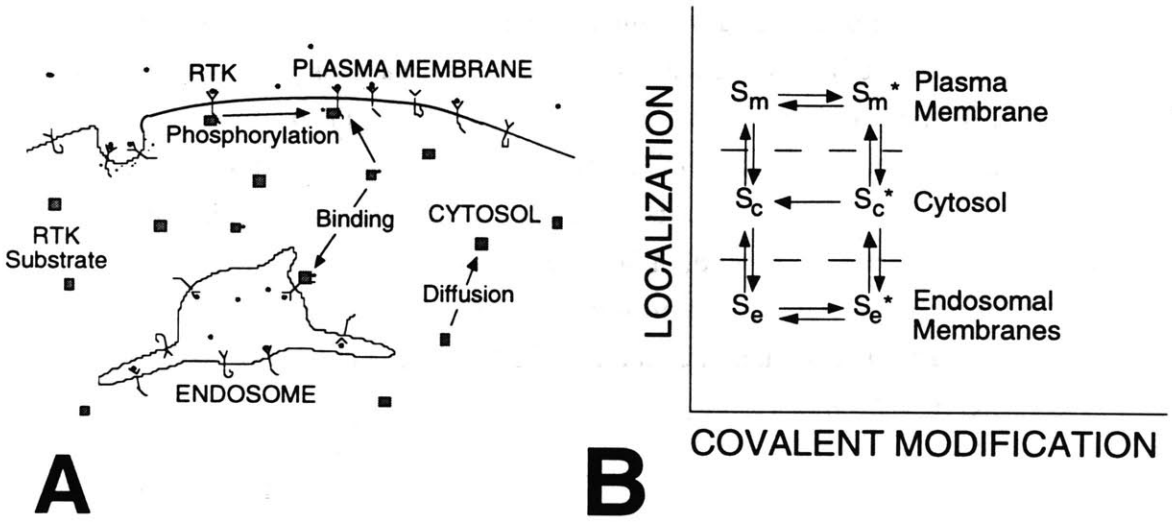

Figure 3.3 General Reaction-Diffusion RTK Signaling Model. A, cell model schematic. In the presence of ligand recognition by surface RTKs, the receptors are activated and autophosphorylated on tyrosine residues in the cytoplasmic region. Ligand binding also mediates the induced pathway of receptor-mediated endocytosis and delivery of receptors and ligand, perhaps in complex, to sorting endosomes. Intracellular substrate molecules physically associate with autophosphorylated receptors, allowing substrate phosphorylation to occur. B, summary of substrate activation states. Since localization and allostery effects but not phosphorylation state are considered concomitant with receptor binding, there are two factors that influence the signaling activity of a substrate molecule: the compartment where it is located (denoted on the y-axis) and whether it is phosphorylated (x-axis).

Thus, the dimensionless parameter γ roughly compares the rate of association with receptors to that of random collisions with the membrane boundary, and κ is a dimensionless dissociation constant (inverse affinity). In this model, substrate interacts with receptors that are ligated and autophosphorylated; B_s is the number of surface receptors that are ligand-bound, p_s is the fraction of surface receptor-ligand complexes that are phosphorylated (assumed constant), and f_s is the fraction of these receptors that are free for substrate binding (not a constant). Finally, the function R_{θ^*} includes additional source terms, if any; creation of θ^* parallels loss of θ and vice-versa, satisfying substrate conservation. To compute species profiles, one need only provide one more boundary condition each for θ^* and θ and give the form of R_{θ^*}. One or both of these should include the contribution of internalized receptors. Since the way in which the cell is organized in that regard has not yet been imposed, these are left undefined for now.

Plasma membrane-associated substrate states S_m^* and S_m are regulated by kinase and phosphatase activities, both modeled for simplicity as first order processes:

$$\left(\frac{1}{\alpha}\right)\frac{ds_m^*}{d\tau_c} = \frac{f_s p_s b_s}{\kappa}\theta^*|_{\tilde{r}=1} + \delta_k^M s_m - (1+\delta_p^M+\delta_p^C)s_m^*$$

$$\left(\frac{1}{\alpha}\right)\frac{ds_m}{d\tau_c} = \frac{f_s p_s b_s}{\kappa}\theta|_{\tilde{r}=1} + (\delta_p^M+\delta_p^C)s_m^* - (1+\delta_k^M)s_m \qquad (3.2),$$

$$\delta_k^M \equiv \frac{k_k^M}{k_{off}};\quad \delta_p^M \equiv \frac{k_p^M}{k_{off}}$$

where k_k^M is the observed rate constant of the kinase activity at the plasma membrane, and k_p^M is that of the phosphatase activity specific to the membrane. Note that the kinase-phosphatase switch at the membrane is self-contained, in that the total membrane-associated substrate ($s_m^*+s_m$) is a function of receptor binding only. Conservation equations for s_e and s_e^* will be formulated by analogy to eqn. 3.2 once it is established how internalized receptors are spatially distributed within the cell. Nevertheless, one can stipulate that ($s_e^*+s_e$) is also a function only of receptor binding, since the affinity of this interaction is not affected by substrate phosphorylation.

At steady state from the above development,

$$\frac{d}{d\tilde{r}}(\theta^*+\theta) = 0;\quad \theta^*+\theta = \frac{\kappa}{\kappa + f_s p_s b_s + f_i p_i b_i}$$

$$s_m^*+s_m = \frac{f_s p_s b_s}{\kappa + f_s p_s b_s + f_i p_i b_i};\quad s_e^*+s_e = \frac{f_i p_i b_i}{\kappa + f_s p_s b_s + f_i p_i b_i} \qquad (3.3),$$

where $f_i p_i b_i$ constitutes the dimensionless internalized receptor population per cell analogous to $f_s p_s b_s$ at the surface. Note that the fractions of complexes that are phosphorylated p_i and p_s are not necessarily equal.

The steady state level of s_m^* can now be determined in general:

$$s_m^* = \frac{\frac{f_s p_s b_s}{\kappa}\theta^*|_{\bar{r}=1} + \frac{\delta_k^M f_s p_s b_s}{\kappa + f_s p_s b_s + f_i p_i b_i}}{1 + \delta_k^M + \delta_p^M + \delta_p^C}$$

$$\frac{s_m^*}{s_m^* + s_m} = (1 - Q^M)\frac{\theta^*|_{\bar{r}=1}}{\theta^* + \theta} + \phi^M Q^M \qquad (3.4).$$

$$\phi^i \equiv \frac{\delta_k^i}{\delta_k^i + \delta_p^i + \delta_p^C}; \quad Q^i \equiv \frac{\delta_k^i + \delta_p^i + \delta_p^C}{1 + \delta_k^i + \delta_p^i + \delta_p^C}$$

The newly defined parameters ϕ^i and Q^i have convenient kinetic interpretations: ϕ^i compares the rates of kinase and phosphatase reactions in compartment i, and is thus a measure of the substrate phosphorylation stoichiometry in that compartment, and Q^i is an exchange parameter that gauges how many covalent modifications a substrate undergoes in a single encounter with compartment i. When $Q^i \sim 1$, then substrate molecules are phosphorylated and dephosphorylated many times in an encounter with compartment i, whereas when $Q^i \sim 0$, substrate molecules bind and dissociate from receptors many times before they are modified. The equation for $s_m^*/(s_m^* + s_m)$, the phosphorylation stoichiometry of substrate associated with the plasma membrane, has two terms; these correspond to distinct contributions of binding previously phosphorylated substrate from the cytosol and phosphorylating plasma membrane-associated substrate. It is clear from this formulation that the exchange parameter Q^M for the plasma membrane determines which contribution is more important.

To complete the spatial regulation model, depletion from $p_s b_s$ and $p_i b_i$ are accounted for to derive f_x and f_l, the fractions of surface and internalized phosphorylated receptors that are free for substrate binding, respectively:

$$f_x p_x b_x = p_x b_x - \sigma\left(\frac{f_x p_x b_x}{\kappa + f_s p_s b_s + f_i p_i b_i}\right); \quad \sigma \equiv \frac{S_T}{R_T}$$

$$f_s = f_i \equiv f = \frac{\kappa + f(p_s b_s + p_i b_i)}{\sigma + \kappa + f(p_s b_s + p_i b_i)} \qquad (3.5).$$

Since f can be related to molecular parameters and the receptor-ligand complex states b_s and b_i via a quadratic equation, this variable can be used in model development for brevity without loss of generality.

Two models were formulated for dealing with diffusive transport to endosomes and binding to internalized receptors: the kinetic approximation and the smear model. The differences between these models are illustrated in Figure 3.4.

3.2.3 The Kinetic Approximation

One simplified approach to the general model is to approximate the partial differential equations of eqn. 3.1 with kinetic rate equations, in which cytosolic substrate species θ^* and θ are replaced by their space-averaged values $\bar{\theta}^*$ and $\bar{\theta}$, respectively (Figure 3.4A). The disadvantage of such a method is that it yields only an approximate solution to the problem of interest. On the other hand, the major advantage of the approach is that the spatial distribution of endosomes within the cell and the degree of internalized receptor heterogeneity in the endosome population do not need to be specified. The other motivation for presenting this approach is that it allows us to lay the conceptual groundwork for more complicated models in a simplified format. For the kinetic approximation, eqn. (3.1) was replaced with

$$\left(\frac{1}{\alpha}\right)\frac{d\bar{\theta}^*}{d\tau_c} = \zeta^M s_m^* + \zeta^E s_e^* - f\left(\frac{\zeta^M p_s b_s + \zeta^E p_i b_i}{\kappa}\right)\bar{\theta}^* - \delta_p{}^c\bar{\theta}^* = 0$$
$$\left(\frac{1}{\alpha}\right)\frac{d\bar{\theta}}{d\tau_c} = \zeta^M s_m + \zeta^E s_e - f\left(\frac{\zeta^M p_s b_s + \zeta^E p_i b_i}{\kappa}\right)\bar{\theta} + \delta_p{}^c\bar{\theta}^* = 0 \qquad (3.6).$$

The radial boundary conditions and cytosolic source terms were incorporated into the conservation equations to yield ordinary differential equations in time only.

In the event that transport of substrate molecules to membrane boundaries is limiting, chemical gradients appear and affect the species concentrations seen by receptors at these boundaries. These effects were approximated by the transport coefficients ζ^M and ζ^E, which describe diffusion to the plasma membrane and endosomes, respectively:

$$\zeta^M = \frac{5}{5 + \gamma f p_s b_s}; \quad \zeta^E = \frac{N\beta}{N\beta + \gamma f p_i b_i}; \quad \beta \equiv \frac{b}{a} \qquad (3.7),$$

where b is the radius of a single endosome, considered spherical, and N is the number of endosomes in the cell, assumed constant. The space-averaged mean diffusive transport rate to the inside face of a spherical boundary from random points within the volume was derived in the previous chapter, and transport to endosomes was derived by analogy to transport of extracellular ligands to the outside surface of a spherical cell (Berg and Purcell, 1977). These diffusive barriers were then incorporated into the forward and reverse rate constants for binding to receptors, which are affected equally (Lauffenburger and Linderman, 1993).

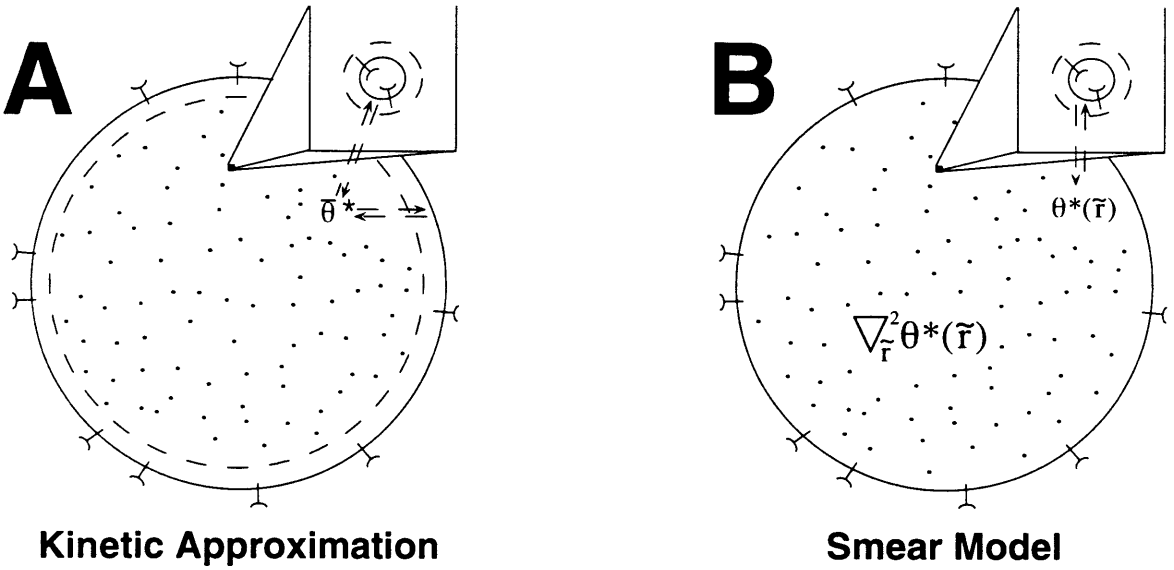

Figure 3.4 Two Model Variations. A, the kinetic approximation. The level of cytosolic substrate in the phosphorylated state is assigned its space-averaged value $\bar{\theta}^*$, and transport coefficients ζ' are incorporated into the receptor-substrate interaction rate constants. These coefficients account for the fact that receptors at the plasma membrane and endosomal membranes are not in equilibrium with $\bar{\theta}^*$ when cytosolic diffusion is controlling. Endosomes at different radial positions r are thus indistinguishable, yielding an inexact solution since proteins likely move about much faster than endosomes. B, the smear model. Endosomes are homogeneously distributed and small enough such that the concentration profile about a single endosome is symmetrical. Upon endocytosis, internalized receptors are distributed evenly among all endosomes, effectively "smearing" contributions from individual receptors over the bounded volume. Far away from endosomes, phosphorylated substrate is distributed by Fickian diffusion, denoted by the Laplacian operator ∇^2.

The kinetic equations for membrane species are

$$\begin{aligned}
&\frac{1}{\alpha}\frac{ds_m^*}{d\tau_c} = \zeta^M \frac{fp_s b_s}{\kappa}\bar{\theta}^* + \delta_k{}^M s_m - (\zeta^M + \delta_p{}^M + \delta_p{}^C)s_m^* = 0\\
&\frac{1}{\alpha}\frac{ds_m}{d\tau_c} = \zeta^M \frac{fp_s b_s}{\kappa}\bar{\theta} + (\delta_p{}^M + \delta_p{}^C)s_m^* - (\zeta^M + \delta_k{}^M)s_m = 0\\
&\frac{1}{\alpha}\frac{ds_e^*}{d\tau_c} = \zeta^E \frac{fp_i b_i}{\kappa}\bar{\theta}^* + \delta_k{}^E s_e - (\zeta^E + \delta_p{}^E + \delta_p{}^C)s_e^* = 0\\
&\frac{1}{\alpha}\frac{ds_e}{d\tau_c} = \zeta^E \frac{fp_i b_i}{\kappa}\bar{\theta} + (\delta_p{}^E + \delta_p{}^C)s_e^* - (\zeta^E + \delta_k{}^E)s_e = 0
\end{aligned} \qquad (3.8),$$

where $\delta_k{}^E$ and $\delta_p{}^E$ are the dimensionless observed first order kinase rate constants at endosomal membrane surfaces analogous to $\delta_k{}^M$ and $\delta_p{}^M$ at the plasma membrane, respectively. Note the model was simplified by representing the kinase and phosphatase activities as first order mechanisms while still allowing for differences between the two membrane compartments.

The solution to eqns. 3.6 and 3.8 is

$$\begin{aligned}
&\frac{\bar{\theta}^*}{\theta^* + \theta} = \frac{\dfrac{5\phi^M Q^M fp_s b_s}{5 + \gamma Q^M fp_s b_s} + \dfrac{N\beta\phi^E Q^E fp_i b_i}{N\beta + \gamma Q^E fp_i b_i}}{\dfrac{5Q^M fp_s b_s}{5 + \gamma Q^M fp_s b_s} + \dfrac{N\beta Q^E fp_i b_i}{N\beta + \gamma Q^E fp_i b_i} + \delta_p{}^C\kappa}\\
&\frac{s_m^*}{s_m^* + s_m} = \frac{5(1 - Q^M)\dfrac{\bar{\theta}^*}{\theta^* + \theta} + (5 + \gamma fp_s b_s)\phi^M Q^M}{5 + \gamma fp_s b_s Q^M}\\
&\frac{s_e^*}{s_e^* + s_e} = \frac{N\beta(1 - Q^E)\dfrac{\bar{\theta}^*}{\theta^* + \theta} + (N\beta + \gamma fp_i b_i)\phi^E Q^E}{N\beta + \gamma fp_i b_i Q^E}
\end{aligned} \qquad (3.9).$$

Two special cases are of note. When diffusion in the cytosol is fast ($\gamma = 0$),

$$\begin{aligned}
&\frac{\bar{\theta}^*}{\theta^* + \theta} = \frac{f(\phi^M Q^M p_s b_s + \phi^E Q^E p_i b_i)}{f(Q^M p_s b_s + Q^E p_i b_i) + \delta_p{}^C\kappa}\\
&\frac{s_m^*}{s_m^* + s_m} = (1 - Q^M)\frac{\bar{\theta}^*}{\theta^* + \theta} + \phi^M Q^M;\quad \frac{s_e^*}{s_e^* + s_e} = (1 - Q^E)\frac{\bar{\theta}^*}{\theta^* + \theta} + \phi^E Q^E
\end{aligned} \qquad (3.10a).$$

When cytosolic diffusion is limiting ($\gamma \to \infty$),

$$\frac{\bar{\theta}^*}{\theta^* + \theta} = \frac{5\phi^M + N\beta\phi^E}{5 + N\beta + \gamma\delta_p{}^C\kappa};\quad \frac{s_m^*}{s_m^* + s_m} = \phi^M;\quad \frac{s_e^*}{s_e^* + s_e} = \phi^E \qquad (3.10b).$$

In the first case, the substrate concentrations in the cytosol θ and θ^* are homogeneous; the spatial distribution of internalized receptors is not important, so eqn. 3.10a is expected to

be a general result in this case. In the latter case, the binding of cytosolic proteins to receptors at a membrane boundary is limited by the frequency of collisions with the boundary, so eqn. 3.10b shows that the phosphorylation stoichiometry of cytosolic substrate is not a function of b_s or b_i. These examples demonstrate that whether or not intracellular diffusion is limiting can be of great importance to the observed behavior.

3.2.4 The Smear Model

This spatial model explicitly accounts for Fickian diffusion of substrate in the cytosol (Figure 3.4B), and therefore assumptions must be imposed regarding the spatial arrangement of endosomes and internalized receptors: (i) There is a constant number of endosomes N in the cell at any given time, and these endosomes are evenly distributed throughout intracellular space. (ii) Endosomes are small enough such that any given endosome sees a constant bulk $\theta^*(r)$ and $\theta(r)$; cytosolic gradients are imperceptible on the distance scale of a single endosome. (iii) While a given endosome does not see a cytosolic gradient, it can have a local gradient when binding to endosomal receptors is faster than diffusive transport to the endosomal boundary. Due to (ii), this local gradient is radially symmetrical about the endosome. Endosomes are sparse enough that local gradients about different endosomes are independent. (iv) Movement of endosomes within the cell is slow relative to the equilibration of endosomes with the cytosolic milieu; in the time it takes an endosome to move a distance over which a gradient in θ^* is perceptible, the endosome has exchanged substrate molecules with the cytosol many times. (v) All N endosomes in the cell display the same number of ligated receptors $b_i R_T/N$. The density of internalized kinase activity throughout the cell is thus constant and effectively "smeared" over the volume of the cytosol. (vi) The volume of the cytosol V is closely approximated by $4\pi a^3/3$, such that the substitution $\alpha = 3\kappa\gamma$ can be made.

It should be noted that assumptions (iv) and (v) can be difficult to reconcile in certain cases. Assumption (v) is required to satisfy eqn. 3.3, but it is only valid at pseudo-steady state if endosome distribution is fast relative to internalization. One can consider the process of endosome distribution to occur on the time scale of constitutive recycling of transferrin receptor complexes, which exhibits an observed first order rate constant of ~ 0.10-0.15 min^{-1} (Wiley et al., 1991; Ghosh et al., 1994). Assumption (iv), the stationary endosome approximation, is likely appropriate then, whereas assumption (v) would be difficult to satisfy in a dynamic equilibrium situation, since endocytic rate constants for EGFR are also in the 0.1-0.3 min^{-1} range (Lund et al., 1990). This represents a drawback of this model, and its use in the simulation of many experiments incurs a notable simplification.

While the size dimension of a single endosome is considered negligible on the distance scale of cytosolic gradients, it is accounted for in terms of diffusion-limited collisions with endosomal boundaries as in the kinetic approximation:

$$\left(\frac{1}{\alpha}\right)\frac{ds_e^*(\tilde{r})}{d\tau_c} = \frac{fp_i b_i}{\kappa}\zeta^E\theta^*(\tilde{r}) + \delta_k{}^E s_e(\tilde{r}) - (\zeta^E + \delta_p{}^E + \delta_p{}^C)s_e^*(\tilde{r}) = 0$$
$$\left(\frac{1}{\alpha}\right)\frac{ds_e(\tilde{r})}{d\tau_c} = \frac{fp_i b_i}{\kappa}\zeta^E\theta(\tilde{r}) + (\delta_p{}^E + \delta_p{}^C)s_e^*(\tilde{r}) - (\zeta^E + \delta_k{}^E)s_e(\tilde{r}) = 0 \qquad (3.11),$$

as manifested in the previously defined transport coefficient ζ^E. This factor accounts for local gradients about single endosomes. Referring to eqn. 3.1, the second boundary condition is $\theta^*|_{\tilde{r}=0}$ finite, and R_{θ^*} accounts for net binding to internalized receptors:

$$R_{\theta^*} = -\alpha\zeta^E\left(\frac{fp_i b_i}{\kappa}\theta^* - s_e^*\right) = -G\left[\theta^*(\tilde{r}) + \phi^E(\theta^* + \theta)\right]$$
$$G \equiv \frac{3N\beta\gamma Q^E fp_i b_i}{N\beta + \gamma Q^E fp_i b_i} \qquad (3.12).$$

The solution for θ^* at steady state is

$$\frac{\theta^*(\tilde{r})}{\theta^* + \theta} = \frac{\gamma\phi^M Q^M fp_s b_s F(\tilde{r}) + \phi^E \dfrac{G}{Da} g(Da)}{\gamma Q^M fp_s b_s + g(Da)}; \quad Da = G + \alpha\delta_p{}^C$$
$$F(\tilde{r}) = \frac{\phi^E G}{\phi^M Da} - \left[\frac{\phi^E G}{\phi^M Da} - 1\right]\frac{\sinh\left(Da^{1/2}\tilde{r}\right)}{\tilde{r}\sinh\left(Da^{1/2}\right)}; \quad g(Da) = Da^{1/2}\coth(Da^{1/2}) - 1 \qquad (3.13),$$

and $s_m^*/(s_m^* + s_m)$ is solved by substituting eqn. 3.13 into eqn. 3.4. The notation Da was used because this grouping resembles a Damköhler number, which compares the rates of reaction and diffusion.

The average level of phosphorylated substrate in the cytosol for the smear model is

$$\bar{\theta}^* = 3\int_0^1 \theta^*(\tilde{r})\tilde{r}^2 d\tilde{r}$$

$$\frac{\bar{\theta}^*}{\theta^* + \theta} = \frac{\left\{1 + \dfrac{\phi^E G}{\phi^M Da}\left[\dfrac{Da}{3g(Da)} - 1\right]\right\}\phi^M Q^M fp_s b_s + \dfrac{N\beta\phi^E Q^E fp_i b_i}{N\beta + \gamma Q^E fp_i b_i}}{\left[\dfrac{Da}{3g(Da)}\right]Q^M fp_s b_s + \dfrac{N\beta Q^E fp_i b_i}{N\beta + \gamma Q^E fp_i b_i} + \delta_p{}^C\kappa} \qquad (3.14),$$

and it is easily shown that the relationship between the total phosphorylated substrate associated with endosomes and $\bar{\theta}^*$ is the same as eqn. 3.9.

Eqn. 3.14 can now be compared to the kinetic approximation in our limiting cases. When diffusion is fast ($\gamma = 0$), $g(Da) \approx Da/3 - Da^2/45$. Substituting, eqn. 3.14 is identical to eqn. 3.10a in this limit. This is a general result, since the spatial distribution of

endosomes is not important in the model unless there is some degree of diffusion limitation. When diffusion is limiting ($\gamma \to \infty$),

$$\frac{\bar{\theta}^*}{\theta^* + \theta} = \frac{\dfrac{(Da/3)g(Da)}{Da/3 - g(Da)}\phi^M + N\beta\phi^E}{\dfrac{(Da/3)g(Da)}{Da/3 - g(Da)} + N\beta + \gamma\delta_p{}^C\kappa} \qquad (3.15).$$

Infinite series analysis shows that eqn. 3.15 is identical to eqn. 3.10b for $Da << 1$. As Da gets large, the exactness is lost, but the inconsistencies are masked as both equations approach ϕ^E. For example, for $\phi^E/\phi^M = 2$ and $\delta_p{}^C = 0$ the maximum percent difference between eqn. 3.15 and eqn. 3.10b is only about 8%, seen at $N\beta \approx 22$.

3.2.5 Overall Signaling Activity

The phosphorylation state, binding state, and location of a signaling protein can modulate its effectiveness in downstream signaling pathways. The models formulated in the previous sections described one RTK substrate in pseudoequilibrium with receptor binding and trafficking. The final step was to sum the relative activities of substrate states into an overall observed activity exerted on downstream target molecules. If s_i is the fraction of molecules in state i, and A_i is the specific enzymatic activity [or activity coefficient (Segel et al., 1986)] observed for that state, then the total activity A_T, proportional to the number of activated downstream target molecules produced per unit time, is

$$A_T = \sum_{i=1}^{n} A_i s_i \qquad (3.16).$$

It was also assumed that locational and chemical effects are separable:

$$\Delta \equiv \frac{A_{s_c}}{A_{s_m}} = \frac{A_{s_c^*}}{A_{s_m^*}} \qquad (3.17).$$

In the case that signaling does not depend on phosphorylation ($A_{x^*} = A_x$),

$$\frac{A_T - A_\theta}{A_{s_m} - A_\theta} = \left[\frac{f(p_s b_s + p_i b_i)}{\kappa + f(p_s b_s + p_i b_i)}\right]\frac{1 + \Delta' p_i b_i / p_s b_s}{1 + p_i b_i / p_s b_s}; \quad \Delta' = \frac{\Delta A_{s_m} - A_\theta}{A_{s_m} - A_\theta} \qquad (3.18).$$

Note the implication of the newly defined parameter Δ in this case; when $\Delta < 1$, internalization of receptors acts as a signal attenuation mechanism on a per phosphorylated receptor basis, while for $\Delta > 1$ internalization amplifies signaling in this respect. The formulation of eqn. 3.18 effectively divides the expression for total activity in this case into factors that reflect total substrate binding and differences in specific activities between membrane compartments. The latter factor, which contains the fundamental information

regarding the regulation of signaling by internalization, is predictably a function of the ratio b_i/b_s. While the first factor is a complicated function of $(p_s b_s + p_i b_i)$, it approaches simple functions in limiting cases:

$\kappa >> 1$ or $\sigma >> 1$ ("linear" substrate binding); $f \approx \kappa/(\sigma+\kappa)$:

$$\frac{A_T - A_\theta}{A_{s_m} - A_\theta} \approx \left(\frac{p_s b_T}{\sigma+\kappa}\right)\frac{1+\Delta' p_i b_i / p_s b_s}{1+b_i/b_s}; \quad b_T \equiv b_s + b_i \qquad (3.19a);$$

$\kappa << 1$ and $\sigma < 1$ ("saturated" substrate binding); $\theta^* + \theta \approx 0$:

$$\frac{A_T - A_\theta}{A_{s_m} - A_\theta} \approx \frac{1+\Delta' p_i b_i / p_s b_s}{1+p_i b_i / p_s b_s} \qquad (3.19b).$$

The general case of eqn. (3.16) can also be recapitulated in terms of the special case of eqn. (3.18):

$$\frac{A_T - \hat{A}_T}{A_{s_m^*} - A_{s_m}} = \frac{\frac{A_{\theta^*} - A_\theta}{A_{s_m^*} - A_{s_m}}\left(\frac{\bar{\theta}^*}{\theta^* + \theta}\right)\kappa + f\left(\frac{s_m^*}{s_m^* + s_m} p_s b_s + \Delta \frac{s_e^*}{s_e^* + s_e^*} p_i b_i\right)}{\kappa + f(p_s b_s + p_i b_i)} \qquad (3.20),$$

where $\hat{A}_T$ is the total activity when substrate phosphorylation does not modulate signaling from eqn. (3.18). In general then, how internalization affects signaling also depends on the phosphorylation stoichiometry ratio ϕ^E/ϕ^M.

3.3 Results

3.3.1 Parameter Estimation

Generalized order-of-magnitude estimates for D_c, a, b, N, k_{on}, k_{off}, k_k^M, R_T, and S_T were derived. Estimates of these constants guided the selection of values for the dimensionless quantities employed in the model.

The physical parameters D_c, a , b, and N are important in describing the diffusion of molecules within the cell. The molecular diffusivity of the substrate protein in the cytosol D_c can be estimated based on measurements made in intact eukaryotic cells following the diffusion of proteins of various molecular weight (Wojcieszyn et al., 1981; Kreis et al., 1982; Jacobson and Wojcieszyn, 1984). The value of D_c is observed to be 0.5-2 $\times 10^{-8}$ cm^2/s, 10 - 100 times slower than in aqueous solution, and relatively insensitive to molecular size. The radius of a typical mammalian cell a is generally 5 - 10 μm. The radius of a single endosome b and the number of endosomes per cell N are estimated to be about 100-400 nm and 200/cell, respectively, based on studies in various cell types (Geuze et al., 1983; Marsh et al., 1986; Geuze et al., 1987; Griffiths et al., 1989; Benveniste et al., 1989; Kawai and Hatae, 1991; Killisch et al., 1992). Early endocytic

vesicles, which carry internalized receptors and deliver them to endosomes by fusion, are smaller than endosomes by a factor of about 3 - 6, which means the estimate of b might be revised downward. However, the residence time of nondissociative receptor-ligand complexes in these vesicles is significantly shorter than in sorting endosomes.

The second order receptor-substrate association rate constant k_{on} has two components when transport to a membrane boundary has been accounted for (by invoking transport coefficients ζ^i and/or defining proper boundary conditions); since the boundary itself is not perfectly absorbing, there is a distinct diffusion limitation associated with finding a specific reactive patch (an autophosphorylated receptor) in addition to the intrinsic chemical reaction rate of the interaction. The latter, which for most proteins is on the order of 10^6 $(Ms)^{-1}$, may also depend on aspects of motion, namely the proteins' rotation (Solc and Stockmayer, 1971; Northrup and Erickson, 1992). Thus, it is difficult to ascertain without experimental evidence whether 10^6 $(Ms)^{-1}$ remains a fair estimate of k_{on} in the reaction-limited regime. When the diffusive search for sparse reactive patches at the boundary is limiting, the second order rate constant is $k_{on} = 4sD_c$ for a flat circular patch (Hill, 1975; Berg and Purcell, 1977) and $k_{on} = 2\pi sD_c$ for a protruding hemisphere (Adam and Delbrück, 1968; Szabo et al., 1980), where s is the encounter distance, roughly the sum of the associating molecules' radii. For s ~ 3 - 10 nm and $D_c \sim 10^{-8}$ cm^2/s, $k_{on} \sim 10^7$ $(Ms)^{-1}$ in this limit. Note that γ is independent of D_c in this case: $\gamma = (1/\pi)(s/a)R_T$ (flat sink geometry). Based on an affinity of isolated SH2 and PTB domains for phosphotyrosine motifs in the 20 - 200 nM range, k_{off} was estimated to be ~ 0.1 - 1 s^{-1}, consistent with rapid kinetics in solution (Cussac et al., 1994; Ladbury et al., 1995; Zhou et al., 1995; Mandiyan et al., 1996).

For k_λ^i of the EGFR kinase, the turnover rate can be used as an upper limit, measured as ~ 1 s^{-1} for PLC-γ phosphorylation in solution (Rotin et al., 1992), with lower values for nonphysiological substrates (Weber et al., 1984). As for k_p^i, there is no specific evidence to help us estimate their magnitude, so arbitrary values were used. The cellular expression of receptors R_T varies with cell type, and can be altered experimentally by knockouts or overexpression. A fair range for EGFR is 10^4 - 10^5 receptors/cell. It would also be fair to expect S_T to be in this range.

The results of this section are summarized in Table 3.1. It is intriguing that the predicted ratios of many cellular process rates are within an order of magnitude in either direction of unity. This implies that the nature of the signaling behavior might be sensitive to modest changes in any one of the model parameters.

Parameter	Brief Description	Value Range
D_c	Substrate diffusivity in cytosol	10^{-8} cm^2/s
a	Cell radius	5 - 10 μm
b	Single endosome radius	100 - 400 nm
N	Number of endosomes per cell	100 - 300 $cell^{-1}$
k_{on}	Substrate-receptor association rate constant	10^6 - 10^7 $(Ms)^{-1}$
k_{off}	Substrate-receptor dissociation rate constant	0.1 - 1 s^{-1}
k_k^M	Rate constant, plasma membrane kinase	0.1 - 1 s^{-1}
k_k^E	Rate constant, endosomal membrane kinase	0.1 - 1 s^{-1}
k_p^M	Rate constant, plasma membrane phosphatases	no estimate
k_p^E	Rate constant, endosomal membrane phosphatases	no estimate
k_p^C	Rate constant, cytosolic phosphatases	no estimate
R_T	Surface EGFR expression per cell (intitial)	10^4 - 10^5 $cell^{-1}$
S_T	Total substrate expression per cell	10^4 - 10^5 $cell^{-1}$

Parameter	Definition	Estimated Range
β	b/a	0.02-0.04
γ	$k_{on}R_T/4\pi aD_c$	0.1 - 10
κ	$4\pi a^3k_{off}/3k_{on}R_T$	0.1 - 10
α	$k_{off}a^2/D_c$	1 - 100
δ_k^M	k_k^M/k_{off}	0.1 - 10
δ_k^E	k_k^E/k_{off}	0.1 - 10
δ_p^M	k_p^M/k_{off}	no estimate
δ_p^E	k_p^E/k_{off}	no estimate
δ_p^C	k_p^C/k_{off}	no estimate
ϕ'	$k_k'/(k_k'+k_p'+k_p^C)$	no estimate
Q'	$(k_k'+k_p'+k_p^C)/(k_{off}+k_k'+k_p'+k_p^C)$	no estimate
σ	S_T/R_T	0.1 - 10

Table 3.1 Model Parameter Estimates. Estimates for physical and kinetic constants used in the model are tabulated, based on data in the literature or calculations based on limiting cases. Ranges for the dimensionless parameters based on these estimates are also listed.

3.3.2 Static Representation of Compartmentalized RTK Signaling

In this exercise, b_s was held constant, and b_i was varied. This is deemed a static picture of receptor signaling because the imposed relationship between b_s and b_i is artificial and does not relate to a specific idea of how b_s and b_i vary with time or ligand dose. This approach can, however, be used to assess the dependence of substrate states on receptor compartmentalization at steady state. This exercise served merely to illustrate the following conclusions derived from the form of the model equations:

1. Receptor-substrate binding: The parameter κ, the dimensionless dissociation constant of the receptor-substrate interaction, controls the extent of binding to receptors from the cytosol as b_T increases. Its value relative to b_T and the stoichiometric parameter $\sigma = S_T/R_T$ also determine whether binding of substrate is saturable (whether all substrate molecules can be receptor-associated). The partitioning of substrate between the plasma membrane and endosomes is determined by the ratio b_i/b_s: $(s_e^*+s_e)/(s_m^*+s_m) = p_i b_i/p_s b_s$.

2. Phosphorylation state of substrate in the cytosol: The phosphorylation stoichiometry of cytosolic substrate $\bar{\theta}^*/(\theta^*+\theta)$ in the reaction-limited regime ($\gamma = 0$) is highly dependent on the relative numbers of active receptors in the membrane compartments, the extents to which membrane-associated substrate molecules are phosphorylated (ϕ^i), and how rapidly they exchange with the cytosol (Q^i). In the diffusion-limited regime (γ very large), the cytosolic phosphorylation stoichiometry does not depend at all on how many receptors there are in either compartment but on the transport rates to and locations of the boundaries in question. The parameter grouping $\delta_p{}^C\kappa$ gauges the relative probability that a substrate molecule will be dephosphorylated in the cytosol rather than bind a receptor; when $\delta_p{}^C\kappa$ is very large, the phosphorylation stoichiometry approaches zero, rendering the above considerations moot.

3. Phosphorylation state of substrate at membrane surfaces: The parameter ϕ^i is calculated from the relative kinase and phosphatase activities in membrane compartment i. Recall from eqn. 3.4 that there are two contributions to the level of phosphorylated substrate associated with receptors; exchange of substrate with the cytosolic pool must be significant if a phosphorylation stoichiometry higher or lower than ϕ^i is to be achieved. For $Q^i \sim 1$, substrate is modified much faster than receptors sample the cytosolic substrate pool, and $s_i^*/(s_i^*+s_i) = \phi^i$. Large γ is also sufficient for this behavior, as diffusion limitation prolongs the residence time of a boundary encounter. For Q^i, $\gamma << 1$, the phosphorylation stoichiometries in all compartments are equal, since substrate molecules exchange and sample space so rapidly. When this is the case, it is of interest that internalized kinase activity can indirectly influence the phosphorylation stoichiometry at the plasma membrane and vice-versa. This effect is buffered by cytosolic phosphatase activity. When $\delta_p{}^C\kappa$ is

large, receptors only sample unphosphorylated substrate from the cytosol, and $s_i^*/(s_i^*+s_i) = \phi^i Q^i$. There is no relationship between the phosphorylation stoichiometries at the plasma membrane and endosomal membranes in this limit.

The results of this section are presented in Figure 3.5. In Figs. 3.5A, C, and E, the fractions of total substrate that are phosphorylated and in the cytosolic, plasma membrane, and endosomal membrane compartments, respectively, were plotted versus b_i for fixed b_s = 0.2 and $\gamma = 0$. The following parameters were also fixed: $p_i = p_s = 1$, $\kappa = 1$, $\sigma = 0.2$, $\phi^M = 1/3$, $\phi^E = 2/3$, $\delta_p^C = 0$ ($p_i \neq p_s$ and $\delta_p^C \neq 0$ were not examined for the sake of simplicity). As b_i increases, the amount of substrate associated with endosomes increases, accompanied by a concomitant decrease in the levels of cytosolic and plasma membrane-associated substrate (Conclusion 1 above). Thus, $(s_e^*+s_e)$ increases while $(\theta^*+\theta)$ and $(s_m^*+s_m)$ decrease. However, there is an opposing effect on the cytosolic phosphorylation stoichiometry, since $\phi^E > \phi^M$ (Conclusion 2 above). Fig. 3.5A is thus biphasic for intermediate Q^E/Q^M. For substrate associated with membrane compartments, there is a balance between the tendency to modify substrate to a phosphorylation stoichiometry ϕ^i and the exchange of substrate with the cytosol at a potentially different phosphorylation stoichiometry (Conclusion 3 above). For example, for $\gamma << 1$, $Q^E = 1$, and $Q^M << 1$, endosomal substrate is maintained at a phosphorylation stoichiometry of ϕ^E, and the plasma membrane exchanges substrate with the cytosol so readily that $s_m^*/(s_m^*+s_m)$ also approaches ϕ^E; the system behaves as if plasma membrane-associated substrate undergoes no covalent modifications. For $Q^M = 1$, the plasma membrane maintains substrate at a phosphorylation stoichiometry of ϕ^M regardless of the Q^E value. These effects are demonstrated in Figs. 3.5C and E, for which the value of Q for the compartment in question was varied, while the value of Q for the other compartment was fixed at 1.

The effects of diffusion limitations in the cytosol, gauged by the parameter γ, on the phosphorylation state of substrate in the various compartments are explored in Figs. 3.5B, D, and F. The level of surface receptor complexes b_s was again fixed at 0.2, while b_i was varied. All fixed parameters are as specified above, and $Q^M = Q^E = 0.5$. In Fig. 3.5B, $\bar{\theta}^*$ was plotted versus b_i with $\gamma = 0$, 10, and ∞ for the kinetic approximation and smear model ($N\beta = 6$). The value of 10 represents the high end of γ in the parameter estimation. For the smear model, $\bar{\theta}^*$ for $\gamma = 10$ is not much different from $\gamma = 0$, and $\bar{\theta}^*$ for the smear model and kinetic approximation are virtually overlapping for $\gamma = 10$.

Figs. 3.5D and F illustrate the dependence on γ for s_m^* and s_e^*, respectively. For infinite γ, the phosphorylation stoichiometry is ϕ^i, since the diffusion limitation yields compartmental turnover indistinguishable from $Q^i = 1$.

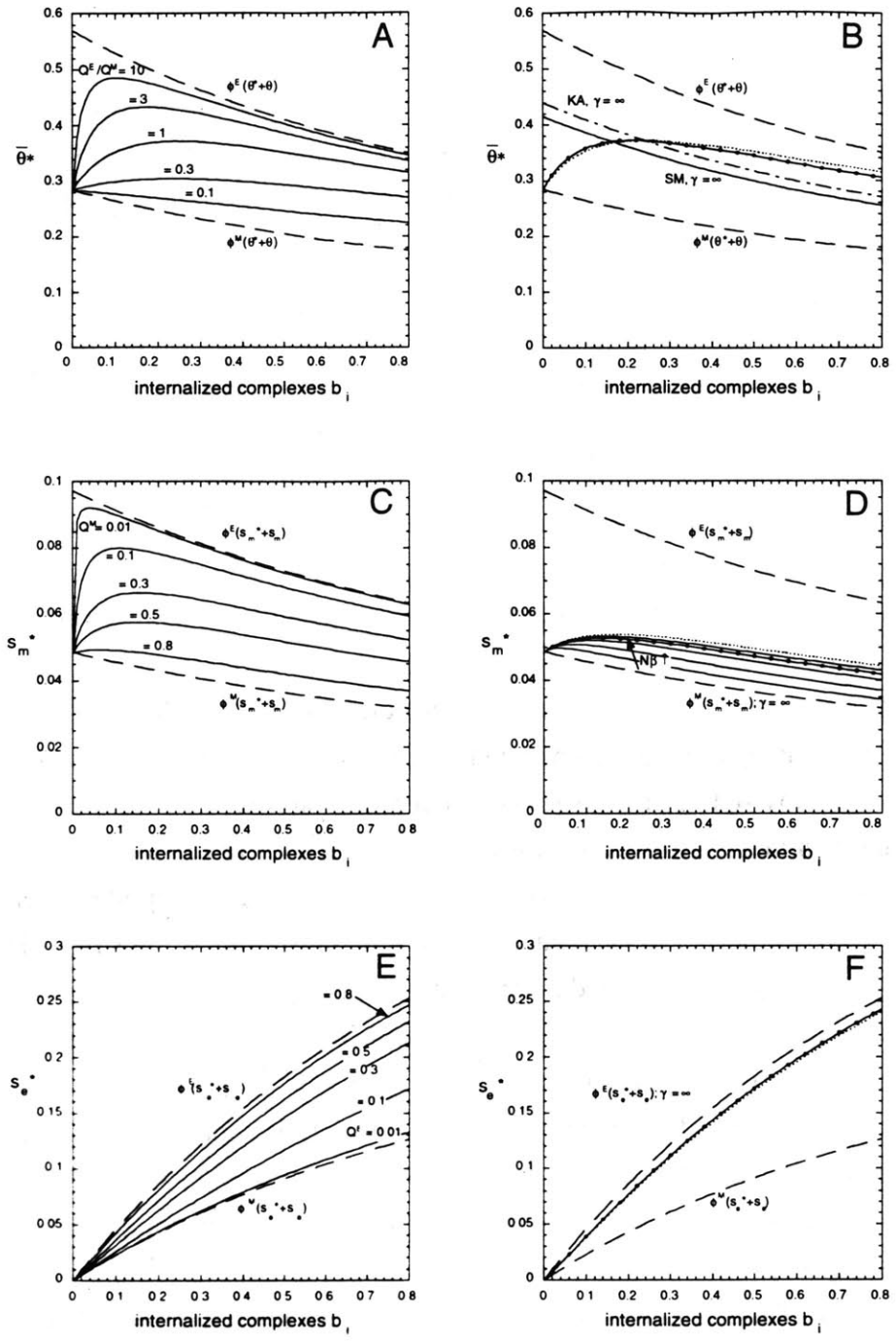

Figure 3.5 Static RTK Signaling. The normalized level of internalized receptor complexes b_i is increased while that of surface complexes b_s is fixed at 0.2. In this artificial case, b_i and b_s are temporally uncoupled, allowing for illustration of how receptors in different locations can contribute to the levels of substrate in various states. See text for details.

For $\gamma = 10$, the changes in s_m^* and s_e^* compared with $\gamma = 0$ are subtle when $N\beta$ is in the expected range (For comparison, various values of $N\beta$ are plotted for $\gamma = 10$ in Fig. 3.5D). The transport coefficients of eqn. 3.7 for the kinetic approximation demonstrate that γ must be significantly larger than 5 and $N\beta$ to have a profound effect. This implies that R_T must significantly exceed ~ 10^5/cell for diffusion limitations to manifest themselves. Overexpression of receptors can thus switch the behavior between purely kinetic and transport-controlled regimes.

3.3.3 Dynamic RTK Signaling: Insensitive to Substrate Phosphorylation

With the physicokinetic processes that drive the distribution of substrate states among cellular compartments described in detail, the potentials for signaling of these states could be investigated, as well as how they might be regulated temporally by receptor internalization. To this end, it was assumed that internalization is slow compared to receptor-substrate binding and covalent modification events (Figure 3.2), and that diffusion is not limiting ($\gamma << 1$). Recall that for homogeneous endocytic and sorting vesicles of typical size and number, a γ value as high as 10 did not yield substrate distributions markedly different from $\gamma = 0$. For signaling molecules that bind to RTKs but whose potential for transducing a signal downstream is insensitive to phosphorylation by RTKs (eqn. 3.18), the steady state equations reflect the receptor-substrate interaction only, which is concomitant with modulation of the substrate's enzymatic activity (allostery) and/or concentration seen by membrane targets (localization). This case also applies when surface and internalized receptors contribute equally to the phosphorylation of substrate. The kinetics of $b_s(t)$ and $b_i(t)$ are described in Appendix D; parameters specified in Figure D.1 are used, and the dose response of $A_T/A_0(t)$ is determined for the same dimensionless ligand concentrations as in Figure D.1.

The time- and dose-dependent behavior of eqn. 3.18 is explored in Figure 3.6. In Figs. 3.6A, B, and C, the fold-stimulation of signaling activity A_T/A_0 was plotted versus dimensionless time τ ($\tau = k_e t$, where k_e is the endocytic rate constant) for various dimensionless ligand doses λ and the following constant parameters: $p_i = p_s = 1$, $\sigma = 1$, $\kappa = 1$, $A_{\infty}/A_{\theta} = 100$. These parameters were chosen to reflect nonsaturating behavior; a fractional increase in receptor-ligand complexes yields a similar if not equal fractional increase in receptor-substrate binding. The selectivity parameter Δ, which was defined but not yet described mechanistically, was varied such that signaling correlates predominantly with surface, total, or internal complexes: Fig. 3.6A, $\Delta = 0.3$; Fig. 3.6B, $\Delta = 1$; Fig. 3.6C, $\Delta = 3$. For $\Delta < 1$ (Fig. 3.6A), substrate recruited to the plasma membrane exhibits more activity than substrate associated with endosomes, and so redistribution of active receptors

from the surface to internal compartments acts as a negative regulatory mechanism. For $\Delta > 1$ (Fig. 3.6C), substrate associated with endosomal membranes exhibits more signaling activity, which has two primary effects on the temporal signaling profiles: maximal signaling takes longer to accumulate than for $\Delta < 1$, and the ligand dose required to produce a given level of activity is lower. The latter is a consequence of the simplification that EGF does not dissociate from its receptor in endosomes. For $\Delta = 1$ (Fig. 3.6B), activated receptors at the surface and in endosomes are equal in their ability to participate in downstream signaling, and the kinetics of signaling is highly dose-dependent in this case. For low ligand doses, the accumulation of b_T is on the time scale of internalization. For high ligand doses, accumulation of b_T is much more rapid, occurring on the time scale of ligand association with receptors on the cell surface.

Figures 3.6D, E, and F are equivalent to Figs. 3.6A, B, and C, respectively, with a different set of substrate binding parameters: $\sigma = 0.2$, $\kappa = 0.01$. In this case, signaling is highly saturable; all substrate molecules can be receptor-associated for levels of ligand occupancy b_T significantly less than 1. Modulation of signaling can still be obtained in this case by redistributing substrate between the plasma membrane and endosomes for $\Delta \neq 1$ (Figs. 3.6D and F). However, the dependence of signaling on ligand concentration is markedly different, as the dose response is lacking in information as λ approaches and passes through unity. This behavior, while requiring high receptor-substrate affinity ($\kappa << 1$), is also highly dependent on the stoichiometry of substrate to receptor molecules σ. For completely stable coupling of activated receptors and substrate, increasing b_T still yields a corresponding increase in receptor-substrate binding for $\sigma = 1$ or greater. In the previous section, it was pointed out that overexpression of the receptor can potentially switch the system from purely kinetic to cytosolic diffusion-controlled behavior. Overexpression of receptors can also alter the substrate:receptor stoichiometry to switch between linear and saturable binding behavior.

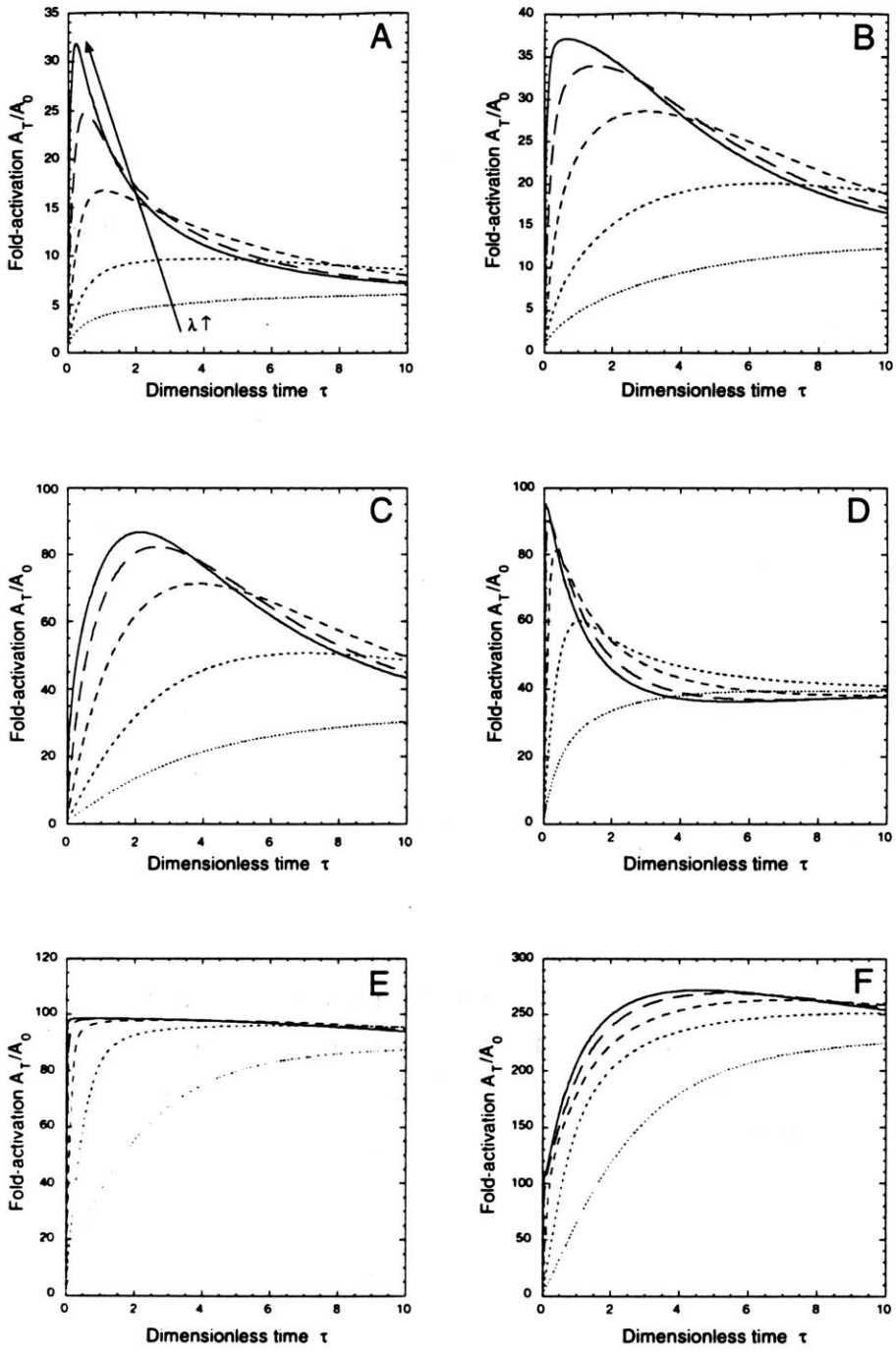

Figure 3.6 Dynamic Signaling Insensitive to Substrate Phosphorylation.
The fold-activation of signaling A_T/A_0 is plotted versus dimensionless time τ, scaled by the endocytic rate constant, for the following dimensionless ligand doses λ: 0.1, 0.3, 1, 3, 10. Substrate parameters are: A, B, and C: $\kappa = 1$, $\sigma = 1$; D, E, and F: $\kappa = 0.01$, $\sigma = 0.2$. The parameter Δ is: A and D: $\Delta = 0.3$; B and E: $\Delta = 1$; C and F: $\Delta = 3$. See text for details.

3.3.4 Dynamic RTK Signaling: Substrate Phosphorylation Required

The kinetics of signaling responses for cases in which unphosphorylated substrate has no potential for signaling can also be exmained. In Figure 3.7A-F, the same σ, κ, and Δ values were used as in Figure 3.6A-F. The diffusion parameter $\gamma = 0$, $p_s = p_i = 1$, $\delta_p^C = 0$, and $A_{s_m*} / A_{\theta*} = 100$. Thus, Figure 3.7A can be directly compared to Figure 3.6A and so on. The following additional parameters describing substrate phosphorylation were also fixed: $\phi^E/\phi^M = 2$, $Q^M = 3/4$, and $Q^E = 6/7$. These values were arrived at by assigning $\delta_k^M = 1$, $\delta_k^E = 4$, and $\delta_p^E = \delta_p^M = 2$. The assignment of $\delta_k^M = 1$ (rate of kinase turnover = rate of substrate dissociation) thus yields values of the exchange parameters Q^i that are closer to 1 than 0. The values of Q^i are such that the deviations of $s_m*/(s_m*+s_m)$ and $s_e*/(s_e*+s_e)$ from ϕ^M and ϕ^E, respectively, are subtle. In the previous section, the kinetics and dose response of signaling, as compared with those of receptor trafficking, were highly dependent on the parameter Δ. When phosphorylation is important, the relative magnitudes of $s_m*/(s_m*+s_m)$ and $s_e*/(s_e*+s_e)$ must also be integrated (eqn. 3.20), and this effect depends on b_s and b_i when $Q^i \neq 1$. When $Q^i = 1$, there is no such dependence, and the effect of differential phosphorylation in the two membrane compartments is roughly a change in Δ to $(\phi^E/\phi^M)\Delta$.

These effects are apparent when Figure 3.7 is compared to Figure 3.6. Since $\phi^E > \phi^M$, internalization amplifies signaling for $\Delta = 1$ or greater, and the kinetics and dose response of signaling activity correlate primarily with $b_i(t)$ (Figs. 3.7B, C, E, and F); for $\Delta < (\phi^E/\phi^M)\Delta < 1$, signaling at high ligand doses is attenuated by internalization, but the magnitude of the effect is tempered by the enhanced phosphorylation of substrate associated with endosomes (Fig. 3.7A and D). Finally, for $\Delta < 1 < (\phi^E/\phi^M)\Delta$, not shown here, phosphorylation rescues the cell from signal attenuation via internalization that would have occurred based on the compartmentalization of downstream signaling molecules reflected in Δ.

3.3.5 Cellular Organization and the Selectivity Parameter Δ

In the development of our single substrate models of RTK-mediated transduction of signaling activity, locational differences in the specific activities of substrate molecules in various states were allowed. Specifically, the potential for activating downstream signaling proteins or producing second messenger molecules can be different for substrate in the cytosol, substrate associated with receptors at the plasma membrane, and substrate associated with internalized receptors. As discussed previously, the downstream targets of most known RTK protein substrates reside in cellular membranes.

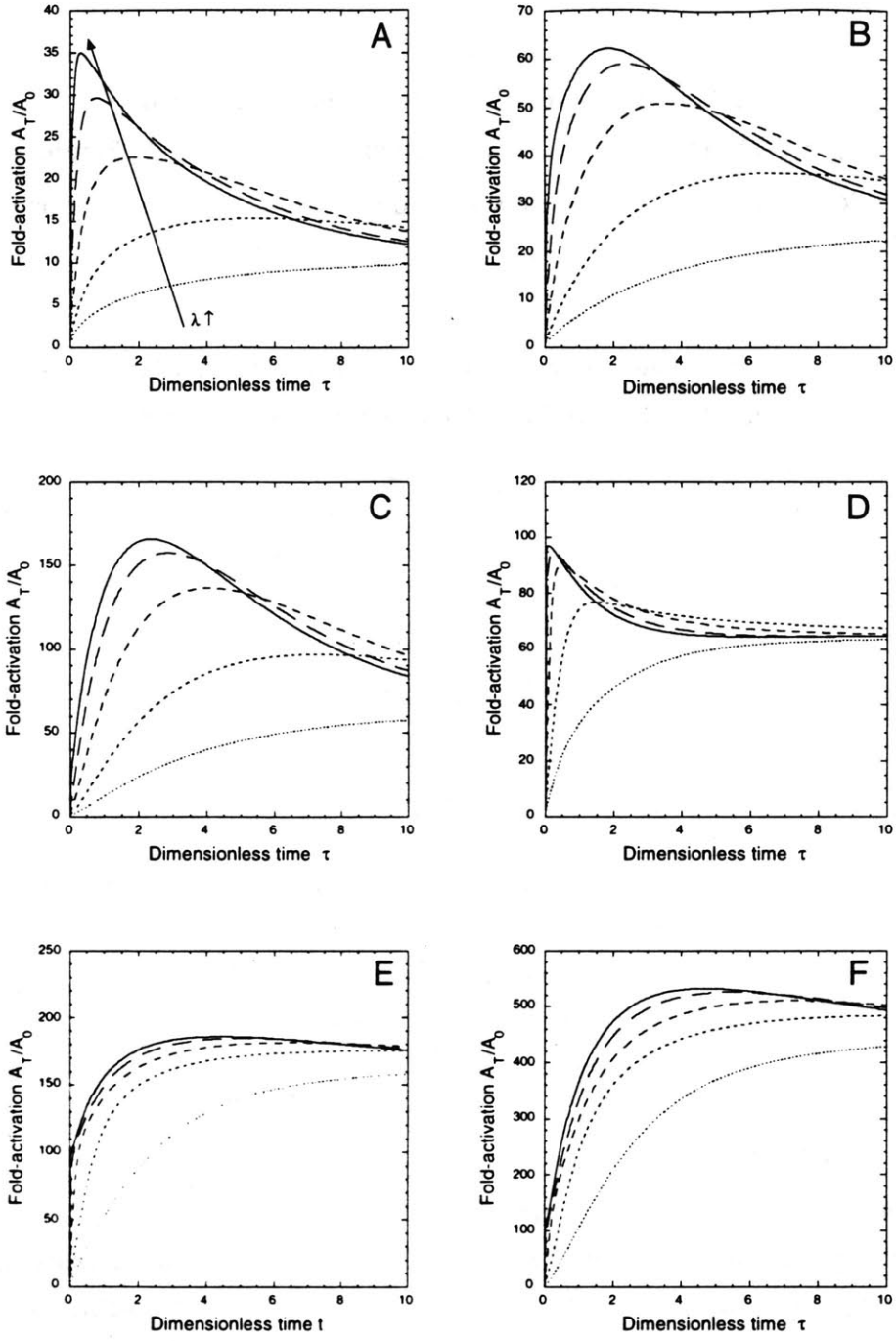

Figure 3.7 Dynamic Signaling Requiring Substrate Phosphorylation. The fold-activation of signaling A_T/A_0 is plotted versus dimensionless time τ, scaled by the endocytic rate constant, for the following dimensionless ligand doses λ: 0.1, 0.3, 1, 3, 10. Substrate parameters are: A, B, and C: $\kappa = 1$, $\sigma = 1$; D, E, and F: $\kappa = 0.01$, $\sigma = 0.2$. The parameter Δ is: A and D: $\Delta = 0.3$; B and E: $\Delta = 1$; C and F: $\Delta = 3$. See text for details.

The kinetic and equilibrium advantages of having both partners of an interaction pair associated with the membrane, as compared to having one protein membrane-associated and one cytosolic, were examined in the previous chapter. Enhancements in association rates and apparent equilibrium were predicted to be two to three orders of magnitude. Thus, the values for the parameters A_{s_m} / A_θ and $A_{s_m *} / A_{\theta *}$ were far from arbitrary when describing the activation of membrane signaling molecules. In general, these parameters must also reflect conformational changes in the substrate that may arise upon interaction with receptors, which synergize with the location effect.

Potential locational differences in the specific activities of substrate bound to surface and internalized receptors also had to be accounted for, as defined by the parameter Δ. To conceptualize such differences, a mass-action approach was considered; the downstream activation flux (*number* of downstream target molecules activated per unit time) in a membrane compartment is proportional to the product of the *surface density* of receptor-associated substrate and the *number* of unactivated target molecules in the compartment. If the differential depletion of unactivated target molecules in the two membrane compartments is disregarded, and target molecules do not interact and internalize with RTKs, then the latter is a constant determined by the partitioning of freely diffusing constituents via membrane cycling through the endocytic pathway (Appendix D). If targets are evenly distributed in membrane compartments, then the smaller collective surface area of endosomes yields opposing effects on the signaling activity of a receptor-associated substrate molecule; the surface density of substrate molecules is increased, and the number of available targets is decreased. Analysis of these surface area effects is trivial, however, as they exactly cancel: $\Delta = [(s_m N_t^M)/s_m]/[(s_e/N\beta^2)(N\beta^2 N_t^M)/s_e] = 1$, where N_t^M is the number of target molecules in the plasma membrane. Thus, $\Delta = 1$ when the target is membrane-associated and nonspecifically routed with the bulk membrane. Of course, the corollary of the above conclusion is that a portion of the membrane-associated target molecules must be specifically retained at the plasma membrane or with endosomes for $\Delta \neq 1$. Thus, the extent to which the cell controls its compartmentalization of downstream targets affects the degree of signaling control afforded by receptor internalization. This conceptual model is illustrated in Figure 3.8.

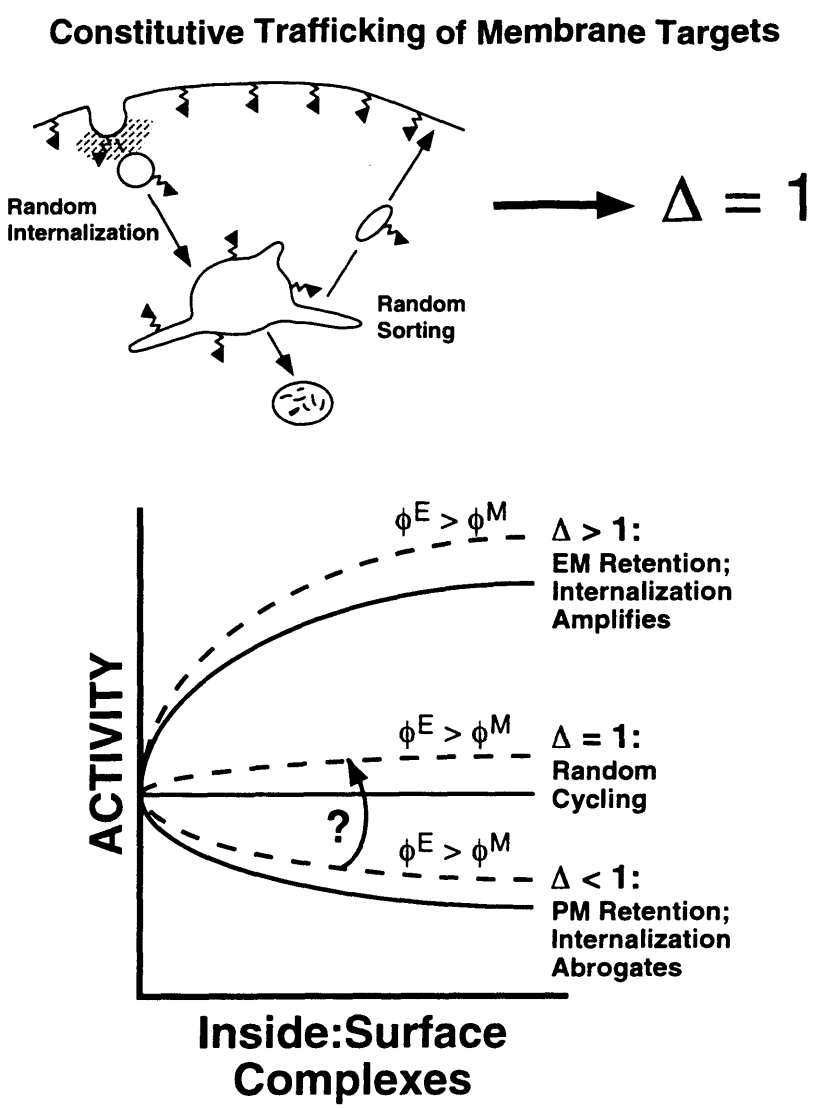

Figure 3.8 Receptor Internalization and Target Availability. The parameter Δ reflects the density of downstream targets in endosomal membranes compared to that in the plasma membrane. When a downstream target freely diffuses in membranes and undergoes the constitutive trafficking processes of random endocytosis and random endosomal sorting, $\Delta = 1$. To achieve values of $\Delta \neq 1$, the cell must preferentially retain this target at the plasma membrane or in endosomes. Thus, how the cell is organized to activate a particular target will affect whether internalization amplifies or abrogates signaling. Additional control is provided by differences in the phosphorylation efficiencies ϕ' when the activity of the substrate is sensitive to its phosphorylation state. Specifically, when $\phi^E > \phi^M$, phosphorylation effects can mitigate negative regulation imparted by $\Delta < 1$ or perhaps even overcome this effect.

3.4 Discussion

It has become increasingly clear in the last several years that the initial events in cellular signaling cascades can not be accurately reconstituted in vitro, as the eukaryotic cell is more than simply a "bag of enzymes". The function of the membrane in signal transduction goes well beyond recognizing extracellular stimuli and harboring the activation of receptor enzyme activities facing the cytoplasm. Interactions of proteins with the intracellular tails of RTKs in particular represent a paradigm in signal transduction, and the resulting subcellular relocalization of such proteins seems to be as important as modulation of protein structure in regulating signaling activity. That the organization of the cell could act as a potent control mechanism represents an experimental and theoretical challenge to elucidate how exactly the cell decides where and when signaling molecules interact, and the downstream ramifications of such events.

EGF receptors in the plasma membrane undergo a relatively rapid redistribution as they are inducibly internalized in an occupancy-dependent manner and delivered to intracellular endosomes. This allows downregulation of total cellular EGFR and consumption of extracellular ligand, which attenuate cell signaling and growth (Wells et al., 1990; Reddy et al., 1996). Regulation of this nature, however, occurs on a time scale of many hours, much longer than that of receptor internalization (~ 5-15 min.). Thus, there is no physical basis for the assumption that internalized EGFR that remain occupied can not continue to participate in meaningful cell signaling. A generalized model was formulated that, given a cellular distribution of occupied receptors, describes the corresponding distribution of protein molecules regulated by these receptors at steady or pseudo-steady state with a minimum of mathematical parameters. This model accounts for the binding and phosphorylation states of a single protein substrate, which was assumed to be sufficient to define its total observed signaling activity. The major simplifying assumptions of the model are that substrate must be bound to a receptor to be phosphorylated, and that different substrates do not compete for sites on receptor complexes. While the latter is beyond the scope of this paper, the former is addressed in Appendix E.

Two variations of the general model were investigated to describe the physical relationships among substrate molecules in three compartments: the cytosol, plasma membrane, and endosomal membranes. The smear model variation assumes that endosomes are relatively small, randomly distributed within the cell, and each display the same number of occupied receptors at any given time. As discussed previously, the latter is a noted simplification because receptor endocytosis and endosome movement are expected to occur on similar time scales. A simplified model, the kinetic approximation,

incorporates average transport characteristics into the receptor-substrate binding rate constants and is in fair agreement with the smear model. A random distribution of intracellular receptors is consistent with observations of early sorting endosomes. Fluorescently labeled, internalized transferrin and low density lipoprotein colocalize and are differentially sorted in these structures, which appear to be homogeneous (Ghosh et al., 1994). Two parameters were of special importance in these models. The potential for diffusion-limited behavior is gauged by the parameter γ; for a homogeneous distribution of typical endosomes, γ must significantly exceed 5 or $N\beta$ for substrate distributions markedly different from $\gamma = 0$. Our analysis shows that it is unlikely that cells operate in the diffusion-limited regime. An expression level of ~10^6/cell would be required, which is outside our parameter range but achievable for cell lines that greatly overexpress the receptor. Further, the fact that most adherent cells are not spherical when fully spread makes it even less likely that diffusion is rate-controlling (Berg, 1983). Q^i is an exchange parameter comparing phosphorylation/dephosphorylation rates to the rate of substrate-receptor uncoupling. It is related to the average number of covalent modifications a substrate undergoes during an encounter with membrane compartment i. Its value determines the potential degree of crosstalk or mixing of substrate molecules between the membrane compartments.

The only quantitative experiments to date that have directly addressed the distribution of EGFR substrate states among cellular compartments with time were performed by Di Guglielmo and colleagues (Di Guglielmo et al., 1994). In this study, subcellular fractions (plasma membrane, endosomes, and cytosol) were isolated from rat liver parenchyma following a bolus treatment of saturating EGF and assayed for protein and phosphotyrosine (pY) levels of EGFR and the EGFR substrate Shc. These data are satisfactory for correlating the various states of Shc defined in our model to the distribution of EGFR. Their definitive findings were: 1) The total Shc and pY-Shc associated with a membrane compartment correlate temporally with the pY-EGFR in that compartment, suggesting that the recruitment and phosphorylation of Shc are not rate-limiting steps; rather, redistribution of EGFR by internalization appears to be kinetically controlling, validating our pseudo-steady state approach. 2) The substrate phosphorylation stoichiometry (pY-Shc:total Shc) at the plasma membrane is the same at 15 min. of stimulation ($p_i b_i$ maximal) as at 0.5 min. ($p_s b_s$ maximal). This implies that events at endosomal membranes do not influence $s_m^*/(s_m^*+s_m)$, and is consistent with $Q^M \sim 1$ or $\gamma >> 5$. 3) The Shc phosphorylation stoichiometry at endosomal membranes is similar to that of the plasma membrane at 0.5 min. of stimulation, but is greatly enhanced at 15 min. This implies that $s_e^*/(s_e^*+s_e)$ could be an increasing function of b_i/b_s, which requires $\phi^E/\phi^M > 1$

and is consistent with Q^E significantly less than 1 and $\gamma << N\beta$. Comparing 2) and 3), the relation $Q^E < Q^M$ is not possible if the only parameter change is $\delta_k^E > \delta_k^M$. Thus, endosomes would have to see a reduced surface density of Shc phosphatase activity for this to be the case. Further, $5 << \gamma << N\beta$ is not consistent with our estimated range of $N\beta$ values. The models presented in this chapter, while certainly too simple to explain all aspects of substrate regulation or the potential competition among multiple substrates, provides a baseline for discussing these kinetic and physical events relevant to intracellular signaling at the receptor level.

While the above framework addresses the distribution of substrate localization and phosphorylation states, it does not complete the story of interest; the examination of downstream target activation was also desired, since the membrane localization of many such targets studied to date (e.g. small GTPases, phospholipids) allows for differential access of compartmentalized substrate to these targets. To proceed further, activity coefficients (specific activities) were assigned to all substrate states, and their effects on the kinetics and dose response of the observed total activity were determined, given typical receptor trafficking kinetics [$b_s(t)$ and $b_i(t)$] of the EGFR. This allowed the points of RTK signal regulation, as illustrated in Figure 3.1, to be examined. The parameter Δ compares the ability of plasma membrane- and endosomal membrane-associated substrate to find target molecules. Its value determines whether the kinetics and dose response of signaling activity correlates predominantly with surface, internal, or total receptor-ligand complexes. If the downstream target were cytosolic, then $\Delta = 1$ barring diffusive gradients. Not only is membrane localization alone insufficient to modulate signaling activity in this case, but localization effects due to internalization would require spatial heterogeneities of the target concentration in the cytosol, which would be relatively difficult for the cell to actively regulate. Further, if the downstream target is membrane-associated, it was shown that $\Delta = 1$ if this target is partitioned by constitutive membrane dynamics. This implies that retention mechanisms, on a molecular level, may play a significant role in regulating signaling through receptor trafficking. In addition to amplifying signaling through RTK-bound proteins, membrane localization of downstream targets readily allows for subcompartmentalization, yielding molecular distributions that are heterogeneous and potentially specific for certain proteins. As a relevant example, caveolae are ~ 50 nm plasma membrane subdomains in which many membrane-associated signaling molecules, including Ras, phosphatidylinositol (4,5)-bisphosphate (PIP_2), and the Src tyrosine kinase, are enriched (Song et al., 1996; Li et al., 1996b; Pike and Casey, 1996; Li et al., 1996a).

To adequately model signaling in any real sense would require hundreds of constant parameters, whose values in (various types of) mammalian cells will likely remain elusive.

Further, current biochemical methods used to study the activation of proteins in intact cells are generally not quantitative enough for rigorous comparisons to model predictions. That being said, a highly simplified modeling approach can be highly illustrative in understanding intracellular signal transduction on a fundamental level, and the predictive value of such an approach has been demonstrated.

3.5 References

Adam, G. and Delbrück, M. (1968). "Reduction of dimensionality in biological diffusion processes." in *Structural Chemistry and Molecular Biology*, eds. Rich, A. and Davidson, N. San Fransisco: W.H. Freeman and Co., pp. 198-215.

Baass, P.C., Di Guglielmo, G.M., Authier, F., Posner, B.I. and Bergeron, J.J.M. (1995). Compartmentalized signal transduction by receptor tyrosine kinases. *Trends Cell Biol.*, 5: 465-470.

Benveniste, M., Schlessinger, J. and Kam, Z. (1989). Characterization of internalization and endosome formation of epidermal growth factor in transfected NIH-3T3 cells by computer image-intensfied three-dimensional fluorescence microscopy. *J. Cell Biol.*, 109: 2105-2115.

Berg, H.C. (1983). *Random Walks in Biology.* Princeton, N.J.: Princeton University Press.

Berg, H.C. and Purcell, E.M. (1977). Physics of chemoreception. *Biophys. J.*, 20: 193-219.

Bevan, A.P., Drake, P.G., Bergeron, J.J.M. and Posner, B.I. (1996). Intracellular signal transduction: the role of endosomes. *Trends Endocrin. Metabol.*, 7: 13-21.

Chao, M.V. (1992). Growth factor signaling: where is the specificity? *Cell*, 68: 995-997.

Cussac, D., Frech, M. and Chardin, P. (1994). Binding of the Grb2 SH2 domain to phosphotyrosine motifs does not change the affinity of its SH3 domains for Sos proline-rich motifs. *EMBO J.*, 13: 4011-4021.

Di Guglielmo, G.M., Baass, P.C., Ou, W., Posner, B.I. and Bergeron, J.J.M. (1994). Compartmentalization of SHC, GRB2 and mSOS, and hyperphosphorylation of Raf-1 by EGF but not insulin in liver parenchyma. *EMBO J.*, 13: 4269-4277.

French, A.R., Sudlow, G.P., Wiley, H.S. and Lauffenburger, D.A. (1994). Postendocytic trafficking of epidermal growth factor-receptor complexes is mediated through saturable and specific endosomal interactions. *J. Biol. Chem.*, 269: 15749-15755.

Geuze, H.J., Slot, J.W. and Schwartz, A.L. (1987). Membranes of sorting organelles display lateral heterogeneity in receptor distribution. *J. Cell Biol.*, 104: 1715-1723.

Geuze, H.J., Slot, J.W. and Strous, G.J. (1983). Intracellular site of asialoglycoprotein receptor-ligand uncoupling: double-label immunoelectron microscopy during receptor-mediated endocytosis. *Cell*, 32: 277-287.

Ghosh, R.N., Gelman, D.L. and Maxfield, F.R. (1994). Quantification of low density lipoprotein and transferrin endocytic sorting in HEp2 cells using confocal microscopy. *J. Cell Sci.*, 107: 2177-2189.

Griffiths, G., Back, R. and Marsh, M. (1989). A quantitative analysis of the endocytic pathway in baby hamster kidney cells. *J. Cell. Biol.*, 109: 2703-2720.

Herbst, J.J., Opresko, L.K., Walsh, B.J., Lauffenburger, D.A. and Wiley, H.S. (1994). Regulation of postendocytic trafficking of the epidermal growth factor receptor through endosomal retention. *J. Biol. Chem.*, 269: 12865-12873.

Hill, T.L. (1975). Effect of rotation on the diffusion-controlled rate of ligand-protein association. *Proc. Natl. Acad. Sci. USA*, 72: 4918-4922.

Jacobson, K. and Wojcieszyn, J. (1984). The translational mobility of substances within the cytoplasmic matrix. *Proc. Natl. Acad. Sci. USA*, 81: 6747-6751.

Kawai, Y. and Hatae, T. (1991). Three-dimensional representation and quantification of endosomes in the rat kidney proximal tubule cell. *J. Electron. Micr.*, 40: 411-415.

Killisch, I., Steinlein, P., Romisch, K., Hollinshead, R., Beug, H. and Griffiths, G. (1992). Characterization of early and late endocytic compartments of the transferrin cycle. *J. Cell Sci.*, 103: 211-232.

Kreis, T., Geiger, B. and Schlessinger, J. (1982). Mobility of microinjected rhodamine actin within living chicken gizzard cells determined by fluorescence photobleaching recovery. *Cell*, 29: 835-845.

Kulas, D.T., Freund, G.G. and Mooney, R.A. (1996a). The transmembrane protein-tyrosine phosphatase CD45 is associated with decreased insulin receptor signaling. *J. Biol. Chem.*, 271: 755-760.

Kulas, D.T., Goldstein, B.J. and Mooney, R.A. (1996b). The transmembrane protein-tyrosine phosphatase LAR modulates signaling by multiple receptor tyrosine kinases. *J. Biol. Chem.*, 271: 748-754.

Ladbury, J.E., Lemmon, M.A., Zhou, M., Green, J., Botfield, M.C. and Schlessinger, J. (1995). Measurement of the binding of tyrosyl phosphopeptides to SH2 domains: a reappraisal. *Proc. Natl. Acad. Sci. USA*, 92: 3199-3203.

Lauffenburger, D.A. and Linderman, J.L. (1993). *Receptors: Models for Binding, Trafficking, and Signaling.* New York: Oxford University Press.

Li, S., Couet, J. and Lisanti, M.P. (1996a). Src tyrosine kinases, G_{α} subunits, and H-Ras share a common membrane-anchored scaffolding protein, caveolin. *J. Biol. Chem.*, 271: 29182-29190.

Li, S., Seitz, R. and Lisanti, M.P. (1996b). Phosphorylation of caveolin by Src tyrosine kinases. *J. Biol. Chem.*, 271: 3863-3868.

Lund, K.A., Opresko, L.K., Starbuck, C., Walsh, B.J. and Wiley, H.S. (1990). Quantitative analysis of the endocytic system involved in hormone-induced receptor internalization. *J. Biol. Chem.*, 265: 15713-15723.

Mandiyan, V., O'Brien, R., Zhou, M., Margolis, B., Lemmon, M.A., Sturtevant, J.M. and Schlessinger, J. (1996). Thermodynamic studies of Shc phosphotyrosine interaction domain recognition of the NPXpY motif. *J. Biol. Chem.*, 271: 4770-4775.

Marsh, M., Griffiths, G., Dean, G.E., Mellman, I. and Helenius, A. (1986). Three-dimensional structure of endosomes in BHK-21 cells. *Proc. Natl. Acad. Sci. USA*, 83: 2899-2903.

Marshall, C.J. (1995). Specificity of receptor tyrosine kinase signaling: transient versus sustained extracellular signal-related kinase activation. *Cell*, 80: 179-185.

Mellman, I. (1996). Endocytosis and molecular sorting. *Annu. Rev. Cell Dev. Biol.*, 12: 575-625.

Northrup, S.H. and Erickson, H.P. (1992). Kinetics of protein-protein association explained by Brownian dynamics computer simulation. *Proc. Natl. Acad. Sci. USA*, 89: 3338-3342.

Pike, L.J. and Casey, L. (1996). Localization and turnover of phosphatidylinositol 4,5-bisphosphate in caveolin-enriched membrane domains. *J. Biol. Chem.*, 271: 26453-26456.

Reddy, C.C., Wells, A. and Lauffenburger, D.A. (1996). Receptor-mediated effects on ligand availability determine relative mitogenic potencies of EGF and TGFα. *J. Cell. Physiol.*, 166: 512-522.

Rotin, D., Honegger, A.M., Margolis, B.L., Ullrich, A. and Schlessinger, J. (1992). Presence of SH2 domains of phospholipase $C\gamma_1$ enhances substrate

phosphorylation by increasing the affinity toward the epidermal growth factor receptor. *J. Biol. Chem.*, 267: 9678-9683.

Segel, L.A., Goldbeter, A., Devreotes, P.N. and Knox, B.E. (1986). A mechanism for exact sensory adaptation based on receptor modification. *J. Theor. Biol.*, 120: 151-179.

Solc, K. and Stockmayer, W.H. (1971). Kinetics of diffusion-controlled reaction between chemically asymmetric molecules. I. General theory. *J. Chem. Phys.*, 54: 2981-2988.

Song, K.S., Li, S., Okamoto, T., Quilliam, L.A., Sargiacomo, M. and Lisanti, M.P. (1996). Co-purification and direct interaction of Ras with caveolin, an integral membrane protein of caveolae microdomains. *J. Biol. Chem.*, 271: 9690-9697.

Szabo, A., Schulten, K. and Schulten, Z. (1980). First passage time approach to diffusion controlled reactions. *J. Chem. Phys.*, 72: 4350-4357.

Weber, W., Bertics, P.J. and Gill, G.N. (1984). Immunoaffinity purification of the epidermal growth factor receptor. *J. Biol. Chem.*, 259: 14631-14636.

Wells, A., Welsh, J.B., Lazar, C.S., Wiley, H.S., Gill, G.N. and Rosenfeld, M.G. (1990). Ligand-induced transformation by a non-internalizing epidermal growth factor receptor. *Science*, 247: 962-964.

Wiley, H.S., Herbst, J.J., Walsh, B.J., Lauffenburger, D.A., Rosenfeld, M.G. and Gill, G.N. (1991). The role of tyrosine kinase activity in endocytosis, compartmentation, and down-regulation of the epidermal growth factor receptor. *J. Biol. Chem.*, 266: 11083-11094.

Wojcieszyn, J.W., Schlegel, R.A., Wu, E. and Jacobson, K.A. (1981). Diffusion of injected macromolecules within the cytoplasm of living cells. *Proc. Natl. Acad. Sci. USA*, 78: 4407-4410.

Zhou, M.M., Harlan, J.E., Wade, W.S., Crosby, S., Ravichandran, K.S., Burakoff, S.J. and Fesik, S.W. (1995). Binding affinities of tyrosine-phosphorylated peptides to the COOH-terminal SH2 and NH2-terminal phosphotyrosine binding domains of Shc. *J. Biol. Chem.*, 270: 31119-31123.

CHAPTER 4

Epidermal Growth Factor Receptor Trafficking and Regulation of Phospholipase C Signaling

The epidermal growth factor receptor (EGFR) ligands epidermal growth factor (EGF) and transforming growth factor alpha (TGFα) elicit differential postendocytic processing of ligand and receptor molecules, which impacts long-term cell signaling outcomes. These differences arise from the higher affinity of the EGF/EGFR interaction *versus* that of TGFα/EGFR in the acidic conditions of sorting endosomes. To determine whether EGFR occupancy in endosomes might also affect short-term signaling events, I examined activation of the phospholipase C-γ1 (PLC-γ1) pathway, an event shown to be essential for growth factor-induced cell motility. I found that EGF continues to stimulate maximal tyrosine phosphorylation of EGFR following internalization, while, as expected, TGFα stimulates markedly less. The resulting higher level of receptor activation by EGF, however, did not yield higher levels of phosphatidylinositol (4,5)-bisphosphate (PIP_2) hydrolysis over those stimulated by TGFα. By altering the ratio of activated receptors between the cell surface and the internalized compartment, I found that only cell surface receptors effectively participate in PLC function. In contrast to PIP_2 hydrolysis, PLC-γ1 tyrosine phosphorylation correlated linearly with the total level of pY-EGFR stimulated by either ligand, indicating that the functional deficiency of internal EGFR can not be attributed to an inability to interact with and phosphorylate signaling proteins. I conclude that EGFR signaling through the PLC pathway is spatially restricted at a point between PLC-γ1 phosphorylation and PIP_2 hydrolysis, perhaps because of limited access of EGFR-bound PLC-γ1 to its substrate in endocytic trafficking organelles.

4.1 Introduction

Cell signaling events mediated by epidermal growth factor receptor (EGFR) regulate survival, proliferation, migration, and differentiation of many cell types. At least five ligands are known to activate EGFR, including epidermal growth factor (EGF) and transforming growth factor alpha (TGFα). Progress has been made in the last two decades in elucidating structure-function relationships for EGFR and other receptor tyrosine kinases (RTKs), particularly in how signal transduction is modulated by self-phosphorylation of cytoplasmic tyrosine residues (Lund and Wiley, 1994). This permits access to the kinase domain of EGFR (Bertics et al., 1985) and allows the receptor to bind signaling proteins

containing modular Src homology 2 (SH2) and phosphotyrosine-binding (PTB) domains (van der Geer et al., 1994; Pawson, 1995). Such interactions can affect the activity of the bound protein through transmission of conformational changes, enhancement of tyrosine phosphorylation, and/or localization in proximity to membrane-associated target molecules. One of the prominent signaling proteins activated by EGFR is the γ1 isoform of phospholipase C (PLC) (Rhee and Choi, 1992). This enzyme, which has two SH2 domains, catalyzes the hydrolysis of phosphatidylinositol (4,5)-bisphosphate (PIP_2), generating the second messengers diacylglycerol (DAG) and inositol triphosphate (IP_3) and liberating PIP_2-bound proteins (Toker, 1998). PLC-γ1 activity is positively modulated *in vivo* by association with EGFR and tyrosine phosphorylation by the receptor kinase, providing a link to ligand stimulation (Meisenhelder et al., 1989; Goldschmidt-Clermont et al., 1991; Vega et al., 1992; Chen et al., 1994b). Thus pathway is illustrated in Figure 4.1.

Another consequence of EGFR activation is clustering of ligand-receptor complexes in clathrin-coated pits, which increases the rate of receptor internalization (Chang et al., 1993). Following endocytosis, receptor-ligand complexes and other components of the plasma membrane are delivered to early endosomes, where molecules are sorted for recycling back to the cell surface or degradation in lysosomes (Trowbridge et al., 1993; Mellman, 1996). Since the degradative route can yield downregulation of total receptor mass and depletion of ligand from the extracellular milieu, endocytic trafficking has been recognized as an attenuation mechanism affecting long-term EGFR function (Wells et al., 1990; Vieira et al., 1996). An unresolved question, however, is the contribution to signaling of the steady-state EGFR pool residing in pre-degradative internal compartments. It has been demonstrated that EGF remains predominantly associated with EGFR in sorting endosomes, and that internalized EGF-EGFR retain equal or greater tyrosine phosphorylation stoichiometry as well as competency in binding and phosphorylating signaling proteins (Kay et al., 1986; Carpentier et al., 1987; Lai et al., 1989; Sorkin and Carpenter, 1991; Wada et al., 1992; Di Guglielmo et al., 1994). This suggests that meaningful signal transduction might be extended after endocytosis of EGF (Baass et al., 1995; Bevan et al., 1996). In contrast, the pH sensititivity of the TGFα/EGFR interaction and differential trafficking of TGFα compared to EGF suggest that TGFα dissociates from EGFR under the acidic conditions of endosomes (Ebner and Derynck, 1991; French et al., 1995). At the pH found at the surface, EGF and TGFα exhibit indistinguishable affinities for EGFR in an equilibrium competition assay (Ebner and Derynck, 1991).

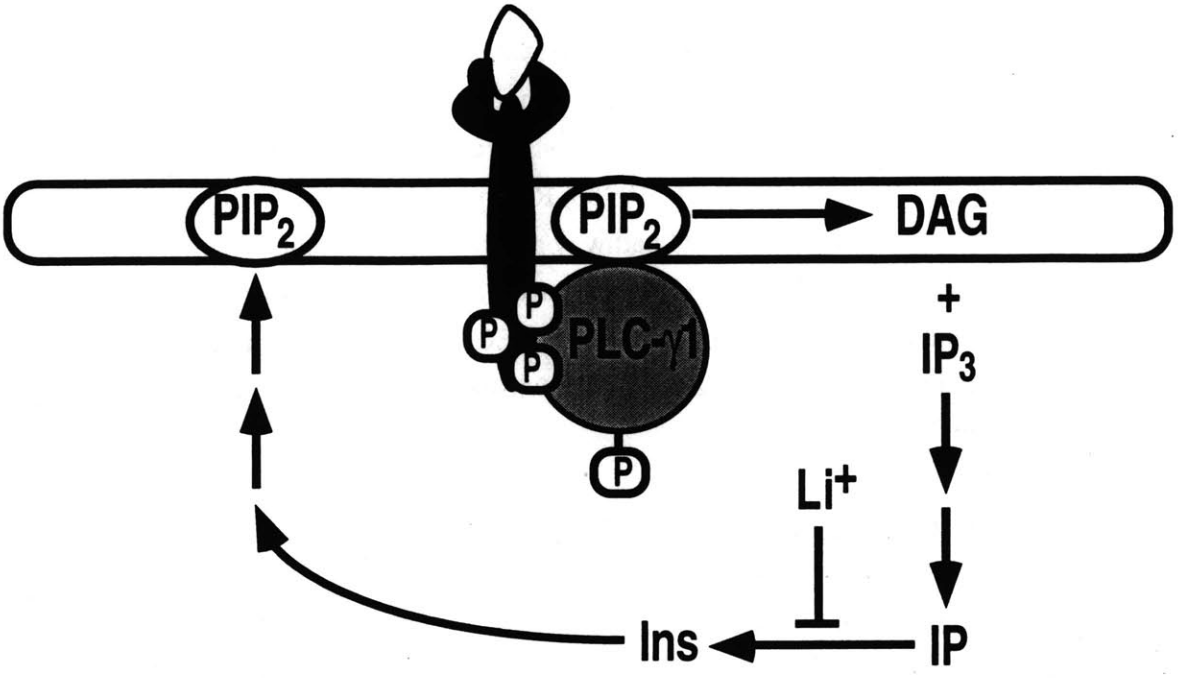

Figure 4.1 The Phospholipase C Pathway. Phosphatidylinositol (4,5)-bisphosphate (PIP_2), a membrane lipid, is hydrolyzed by phospholipase C (PLC). The γ1 isoform of PLC is recruited to the membrane and tyrosine phosphorylated by activated EGFR, yielding an increased reaction rate. One of the hydrolytic products is the soluble species inositol triphosphate (IP_3), which is successively dephosphorylated to free inositol (Ins). Exogenous addition of lithium inhibits the metabolism of inositol phosphate (IP), leading to an accumulation of IP in the cytosol.

This disparity in ligand/receptor sorting could be responsible for differences in the cell responses to EGF and TGFα. To evaluate such a possibility, it is first necessary to know whether internalized and surface complexes differ either qualitatively or quantitatively in signaling.

The effects of endocytosis and compartmentalization of EGFR on the magnitude of signaling through the PLC pathway were investigated. NR6 fibroblasts transfected with wild-type EGFR were used as the experimental system, as they have been used extensively in previous studies of both PLC-γ1 activation (Chen et al., 1994b; Chen et al., 1996a; Chen et al., 1996b; Xie et al., 1998) and endocytic trafficking of the EGFR (Wells et al., 1990; Reddy et al., 1994; Reddy et al., 1996b; Reddy et al., 1996a). A ligand-based approach was used to analyze the PLC pathway at three distinct points of regulation: tyrosine phosphorylation of EGFR, tyrosine phosphorylation of PLC-γ1, and hydrolysis of PIP_2. The results clearly show that internalized EGFR are deficient in stimulating PLC function, and that the point of regulation lies downstream of PLC-γ1 tyrosine phosphorylation.

4.2 Experimental Procudures

4.2.1 Cell Culture and Quiescence Protocol

NR6 mouse fibroblasts transfected with wild-type human EGFR (NR6 WT) (Wells et al., 1990; Chen et al., 1994a) were cultured in Corning tissue culture-treated dishes in a 5% CO_2 environment. All cell culture reagents were obtained from Life Technologies. The growth medium consisted of minimum essential medium (MEM)-α/26 mM sodium bicarbonate with 7.5% fetal bovine serum (FBS), 2 mM L-glutamine, 1 mM sodium pyruvate, 0.1 mM MEM nonessential amino acids, and the antibiotics penicillin, streptomycin, and G418 (350 μg/mL). Cells were growth arrested at subconfluence using restricted serum conditions without G418 (MEM-α/26 mM sodium bicarbonate with 1% dialyzed FBS, 2 mM L-glutamine, 1 mM sodium pyruvate, 0.1 mM MEM nonessential amino acids, and the antibiotics penicillin/streptomycin) for 18-24 h prior to experiments. Experiments were carried out in an air environment using MEM-α/13 mM HEPES (pH 7.4 at 37°C) with 0.5% dialyzed FBS, 2 mM L-glutamine, the antibiotics penicillin/streptomycin, and 1 mg/mL bovine serum albumin as the binding buffer.

4.2.2 Receptor Binding and Internalization Studies

Mouse EGF (Life Technologies) and human TGFα (Peprotech) were iodinated with ^{125}I (NEN) using Iodobeads (Pierce), according to the manufacturer's protocol. The

specific activities of labeled ligands were typically 150,000-200,000 cpm/ng (≈ 600 Ci/mmol). Quiescent cells in Corning 35 mm tissue culture dishes were equilibrated in binding buffer for 15 minutes, on a warm plate that maintains cells at 37°C, before challenge with ^{125}I-labeled ligand. Surface-bound and internalized ligand were discriminated essentially as described (Chang et al., 1993; Ware et al., 1997). Briefly, free ligand was removed by washing 6 times with ice-cold WHIPS buffer (20 mM HEPES, 130 mM NaCl, 5 mM KCl, 0.5 mM $MgCl_2$, 1 mM $CaCl_2$, 1 mg/mL polyvinylpyrrolidone, pH 7.4). Surface-bound ligand was then collected in ice-cold acid strip with urea (50 mM glycine-HCl, 100 mM NaCl, 1 mg/mL polyvinylpyrrolidone, 2 M urea, pH 3.0) for 5-8 minutes, and internalized ligand was released in 1 M NaOH overnight at room temperature. Nonspecific binding (< 2%) was assessed in the presence of 2 μM unlabeled human EGF (Peprotech) and subtracted from the total. Samples were quantified using a gamma counter.

4.2.3 Removal of Surface-bound Ligand by Mild Acid Strip

At intermediate times during an experiment, surface-bound ligand was removed without compromising cell viability, using brief (1-2 minutes) treatments of ice-cold acid strip without urea (50 mM glycine-HCl, 100 mM NaCl, 1 mg/mL polyvinylpyrrolidone, pH 3.0) as indicated. By 1 minute, this treatment is equally efficient in removing either EGF or TGFα (reproducibly 90-93%) from the surface of NR6 cells.

4.2.4 EGFR-phosphotyrosine Sandwich ELISA

High-binding ELISA plates (Corning) were coated at room temperature overnight with 10 μg/mL anti-EGFR monoclonal antibody 225 in PBS, then incubated at room temperature for 4-18 h in blocking buffer (10% horse serum/0.05% Triton X-100 in PBS). After various treatments in binding buffer as indicated, cells were washed once in ice-cold PBS supplemented with 1 mM sodium orthovanadate and 4 mM sodium iodoacetate, scraped into ice-cold lysis buffer (50 mM HEPES pH 7.0, 150 mM NaCl, 1% Triton X-100, 10% glycerol) supplemented with 1 mM sodium orthovanadate, 10 mM sodium pyrophosphate, 1 mM EGTA, 4 mM sodium iodoacetate and 10 μg/mL each of aprotinin, leupeptin, chymostatin, and pepstatin, and transferred to an Eppendorf tube. After 20 minutes of incubation on ice, cellular debris was pelleted for 10 minutes at 16,000xg, and the supernatant of each sample was transferred to a new tube and kept on ice for analysis. Total protein in each sample was assessed using a Micro BCA kit (Pierce) according to the manufacturer's protocol. Each lysate was diluted to various extents in blocking buffer supplemented with 1 mM sodium orthovanadate and incubated in anti-EGFR-coated wells

for 1 h at 37°C. The wells were then rinsed four times with wash buffer (10 mM Tris pH 8.3, 300 mM NaCl, 0.1% SDS, 0.05% NP-40) and incubated with 0.5 μg/mL alkaline phosphatase-conjugated RC20 anti-phosphotyrosine antibody (Transduction Laboratories) in blocking buffer for 1 h at 37°C. After four additional washes, the wells were reacted with 1 mg/mL p-nitrophenyl phosphate (Sigma) in 10 mM diethanolamine/0.5 mM $MgCl_2$ pH 9.5. The reaction rate was monitored by measuring absorbance at 405 nm in a 15 minute kinetic assay, using a Molecular Devices microplate reader. The relative amount of EGFR-phosphotyrosine was determined from a binding plot of reaction rate versus μg of total lysate protein for each sample. Nonspecific control lanes in which the maximum lysate load was incubated in wells without 225 antibody yielded similar activities to 225 wells incubated without lysate.

4.2.5 Immunoprecipitation and Western Blotting

Cells were lysed in 1% Triton X-100, and total cell protein was determined as detailed above. Immunoprecipitations of equivalent total protein amounts were performed at 4°C for 90 minutes using 3-5 μg primary antibody precoupled to 10 μL protein G-sepharose beads per sample. The beads were washed five times with ice-cold lysis buffer supplemented with 1 mM sodium orthovanadate, and the residual liquid was removed with a syringe. The beads in each tube were boiled for 5 minutes in 30 μL sample buffer (62.5 mM Tris pH 6.8, 2% SDS, 100 mM DTT, 10% glycerol, 0.005% bromphenol blue), then clarified by centrifugation. Proteins were separated by SDS-PAGE (Laemmli, 1970) on 7.5% acrylamide gels and transferred to nitrocellulose membranes (Towbin et al., 1979). Membranes were blotted for proteins as indicated and visualized using horseradish peroxidase-conjugated secondary antibodies and SuperSignal Ultra detection reagent (Pierce). Bands were detected and quantified using a Bio-Rad chemiluminescence screen and Molecular Imager. When reprobing of a blot was desired, bound antibodies were first removed for 1 h at 55°C in stripping buffer (62.5 mM Tris pH 6.8, 2% SDS, 100 mM β-mercaptoethanol).

4.2.6 Determination of Internal EGFR-phosphotyrosine

Internalized EGFR were isolated by labeling surface-accessible proteins for subsequent removal from cell lysates (Olayioye et al., 1998). Briefly, cells were washed 3 times with ice-cold PBS pH 8.0 after specific treatments, and surface proteins were biotinylated at 4°C with 5 mg sulfo-NHS-LC-biotin (Pierce) per 10 cm plate. Plates were washed once with PBS, once with PBS/50 mM glycine, and once again with PBS. Cells were lysed in 1% Triton X-100 as described above, and EGFR were immunoprecipitated

using 225 antibody precoupled to protein G-sepharose. Proteins were eluted by boiling for 10 minutes in TNE buffer (50 mM Tris pH 7.5, 140 mM NaCl, 5 mM EDTA) with 0.5% SDS. After adding one volume lysis buffer supplemented with 1 mM sodium orthovanadate, biotinylated (surface) EGFR were removed using immobilized streptavidin (Pierce). Supernatants were subjected to SDS-PAGE and anti-phosphotyrosine immunoblotting.

4.2.7 PIP_2 Hydrolysis Assay

In vivo PLC activity was determined essentially as described (Chen et al., 1994b). Briefly, cells were incubated with 5 μCi/mL myo-[2-^{3}H]-inositol (American Radiolabeled Chemicals) during the growth-arrest protocol. Unincorporated radioactivity was removed by two washes with PBS at 37°C just before the experiment. Following various treatments in binding buffer as indicated, cells were washed once with ice-cold WHIPS buffer, scraped into boiling dH_2O, transferred to an Eppendorf tube, and kept on ice. Samples were boiled for 5 minutes, and cellular debris was pelleted for 5 minutes at 16,000xg. The concentration of cytosolic radioactivity in dpm/mL for each supernatant was determined by liquid scintillation counting of small aliquots, and equivalent volumes of samples were loaded onto mini-columns packed with 0.5 mL anion exchange resin (AG 1-X8, formate, 100-200 mesh; Bio-Rad) each. After washing each column with 20 mL dH_2O and 20 mL 5mM sodium borate/60 mM sodium formate, inositol phosphate fractions were eluted with 200 mM ammonium formate/100 mM formic acid. The dpm of inositol phosphate that accumulated during cell treatment was normalized to the total dpm applied to the anion exchange column for each sample.

4.3 Results

4.3.1 Binding, Activation, and Internalization of the EGFR

Given the central role of EGFR autophosphorylation in initiating phospholipase C activity, it was important to determine whether the tyrosine phosphorylation stoichiometry of EGFR (pY/receptor) is altered upon internalization of EGF/ or TGFα/EGFR complexes in NR6 WT cells. Based on the differential binding affinities of these ligands at endosomal pH, it was expected that EGF would elicit a higher level of internal EGFR tyrosine phosphorylation than TGFα. Saturating doses (20 nM) of radioiodinated EGF or TGFα were used to follow the levels of surface-bound and internalized ligand with time in NR6 WT cells (Figure 4.2). A decrease in surface complexes to a level of about 60% of the total was observed within 30 minutes, with a parallel increase in internalized ligand, in

agreement with previously published results (Wells et al., 1990). The profiles of cell-associated EGF and TGFα in both compartments were indistinguishable in these experiments. This indicated that the initial trafficking of EGFR in these cells is similar following either EGF or TGFα treatment.

To distinguish between surface-associated and intracellular activated EGFR, cells were incubated briefly in a mild acid wash. This treatment rapidly removes surface-bound ligand (both EGF and TGFα are dissociated equivalently). In addition, several studies have shown that it does not compromise cell viability (Ascoli, 1982; Wahl et al., 1989; French et al., 1994). The kinetics of EGFR tyrosine phosphorylation were examined using two parallel stimulation protocols: a standard time course of stimulation with EGF or TGFα (20 nM) at 37°C, and a strip protocol (Figure 4.3). For the strip protocol, cells were stimulated with EGF or TGFα (20 nM) for 15 minutes at 37°C to allow internalization, treated with acid strip on ice for one minute, and brought back to 37°C in the absence of ligand for 9 minutes. For EGF-treated cells, ligand was then added back at 37°C to determine whether receptor binding and signaling capacities were intact following the acid wash. As shown in Figure 4.3A, EGF-treated NR6 WT cells displayed approximately 3 to 4 times higher EGFR-phosphotyrosine relative to TGFα-treated cells following the surface strip, suggesting that the former ligand is more effective in maintaining activation of EGFR in internal compartments. Following readdition of EGF, pY-EGFR returned to pre-strip levels, showing that the treatment does not compromise signaling in these cells.

4.3.2 Stoichiometry of EGFR Tyrosine Autophosphorylation

To determine the stoichiometry of EGFR tyrosine phosphorylation, the levels of surface-bound and internalized ^{125}I-ligand were determined for the same time points and stimulation conditions shown in Figure 4.3A. Since phosphorylation and dephosphorylation reactions occur very rapidly (seconds) relative to the time scale of the experiment (minutes), the total EGFR phosphorylation P_T should observe the following equation:

$$P_T = p_s L_s + p_i b_i L_i \qquad (4.1),$$

where L_s and L_i are the levels of ligand associated with surface receptors and intracellular compartments, respectively, and p_s and p_i are the phosphorylation stoichiometries (pY/receptor) of surface and internal receptor-ligand complexes, respectively (assumed constant). Because the radiolabeled ligand-binding assay does not distinguish between receptor-bound and free ligand inside cells, b_i is the fraction of L_i that is bound to intracellular receptors.

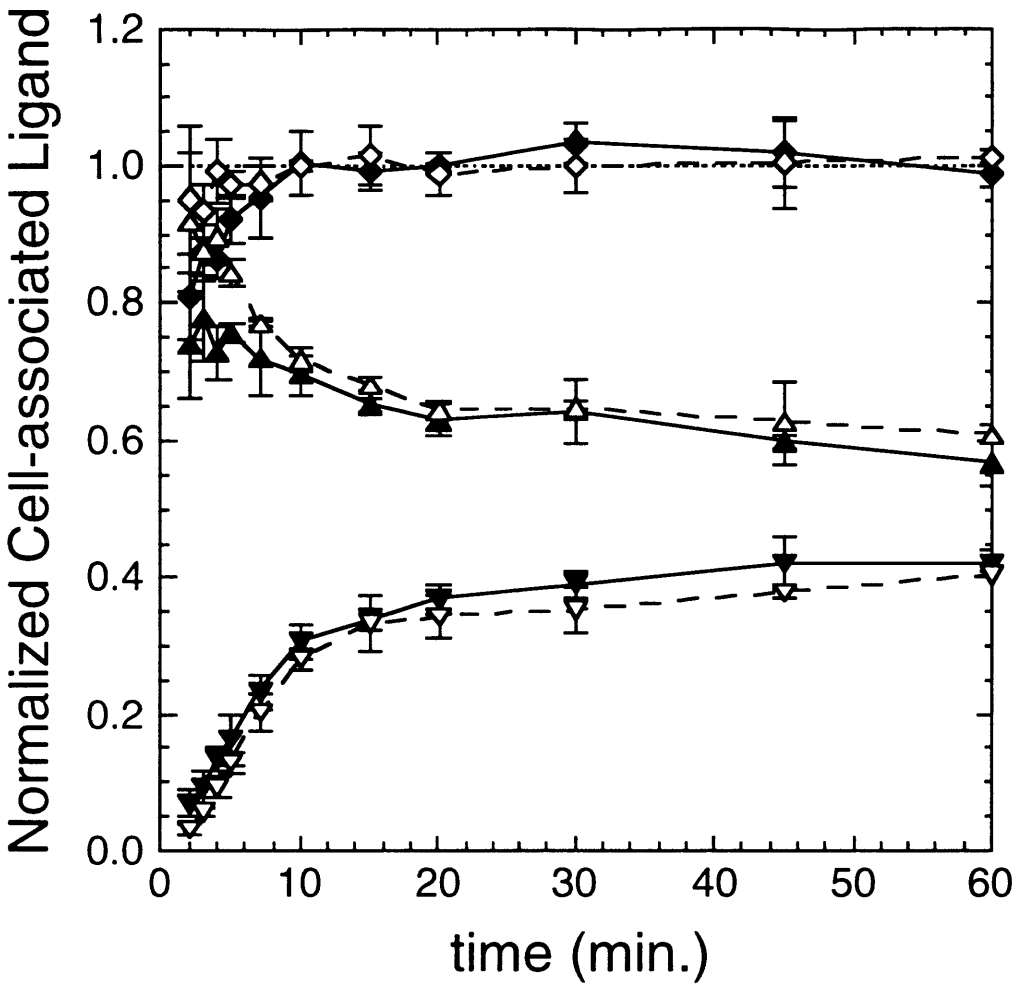

Figure 4.2 Kinetics of EGFR Internalization. Time course of 20 nM ^{125}I-EGF (closed symbols) or ^{125}I-TGFα (open symbols) binding and internalization, NR6 WT. Surface-bound (▲, △), internalized (▼, ▽) and total counts (◆, ◇) were determined in duplicate and normalized to the mean pseudo-steady state total counts (10-60 min.), and the experiment was repeated on three separate days (mean ± s.d., n = 3).

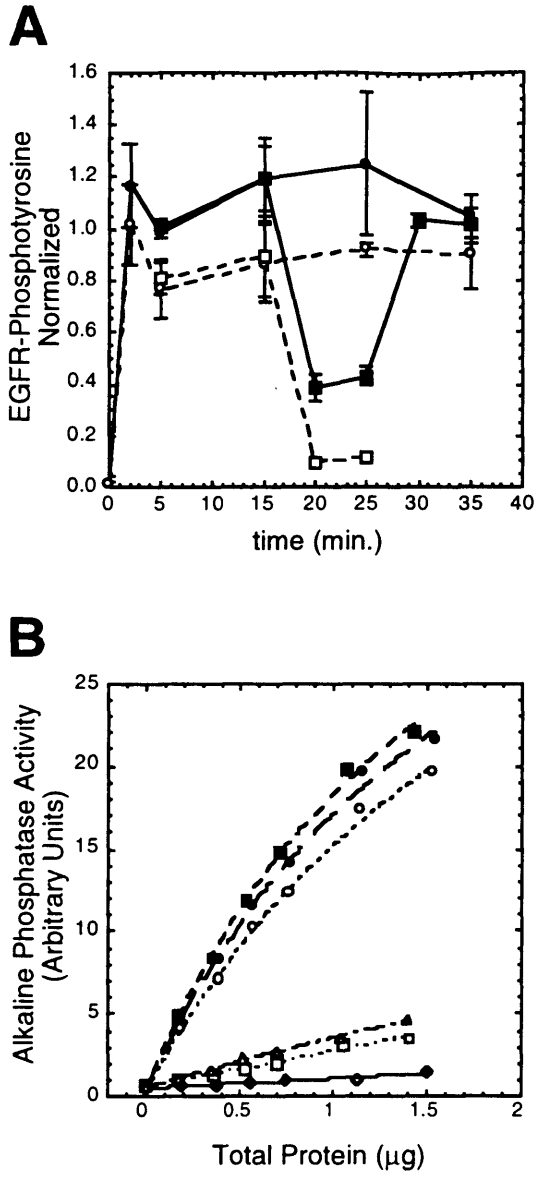

Figure 4.3 Time course of EGFR tyrosine phosphorylation. A. NR6 WT cells were stimulated with 20 nM EGF (closed symbols) or TGFα (open symbols) in a standard time course (●, ○) or using a strip protocol (■, □), as described in the text. The levels of pY-EGFR in cell extracts were determined using a sandwich ELISA and normalized to a common point (5 min. EGF stimulation); values are mean ± s.d., n = 3. B, representative analysis of pY-EGFR time course ELISA data. Alkaline phosphatase reaction rate is plotted versus total cellular protein for each well. Some of the samples processed on this day are shown: unstimulated (◇), 5 min. EGF (●, ■ duplicates), 5 min. TGFα (○), 20 min. TGFα strip protocol (□), and 25 min. TGFα strip protocol (△). The data were fit to a binding isotherm equation with background: $y = A_1 + A_2x/(1+A_3x)$, with the relative level of pY-EGFR equal to A_2 (R^2 typically > 0.99).

Rearranging,

$$\frac{P_T}{L_s + L_i} = p_s - (p_s - p_i b_i)\frac{L_i}{L_s + L_i} \qquad (4.2).$$

If p_s, p_i, and b_i are constant, a linear relationship is obtained when the ratio of (pY-EGFR/total cell-associated ligand) is plotted *versus* the ratio of (internalized ligand/total cell-associated ligand). If EGFR maintains a constant tyrosine phosphorylation stoichiometry, both with respect to time and cellular location ($p_i = p_s$), and ligand remains tightly complexed to the receptor after internalization ($b_i = 1$), such a plot will have zero slope. This seemed to be the case for EGF-treated NR6 WT cells (Figure 4.4A). EGFR maintained a nearly constant pY-EGFR/cell-associated ligand before the strip, after the strip, and following readdition of EGF. Statistical analysis showed that the slope of the least-squares best fit line through Fig. 4.4A was not significantly different from zero ($p > 0.2$; students' t-test). This type of plot can also be used to determine whether EGFR is dephosphorylated following endocytosis, since the ratio of pY/ligand would change from the surface to the internal value as the fraction of internalized ligand increased. TGFα-treated cells displayed a decrease in pY/ligand as the internal ligand fraction increased, and the extrapolated "surface" pY/ligand value was very close to the mean phosphorylation stoichiometry observed for EGF (Figure 4.4B). Statistical analysis showed that the slope of the least-squares best fit line through Fig. 4.4B was significantly less than both zero and the slope of the EGF curve of Fig. 4.4A (both $p < 0.01$; students' t-test). This suggests that in the case of cells treated with TGFα, a significant fraction of internalized EGFR are dephosphorylated, consistent with the low affinity of TGFα for the EGFR at endosomal pH ($b_i < 1$).

To examine the possibility that the receptor phosphorylation stoichiometries elicited by EGF and TGFα simply reflect differential activation of surface complexes, cell surface proteins were biotinylated and cleared from EGFR immunoprecipitates. The remaining EGFR, presumably in intracellular compartments prior to cell lysis, were then subjected to anti-phosphotyrosine immunoblotting. As shown in Figure 4.5, EGF elicited significantly higher pY-EGFR than TGFα in this assay, and phosphotyrosine levels were not altered by acid washing. This demonstrates that EGF induces a greater extent of internalized EGFR activation than TGFα, though tyrosine phosphorylation of internal EGFR in TGFα-treated cells is detectably higher than the unstimulated control. Taken together, our results indicate that tyrosine phosphorylation of internalized EGFR is strongly correlated with ligand occupancy in endosomes.

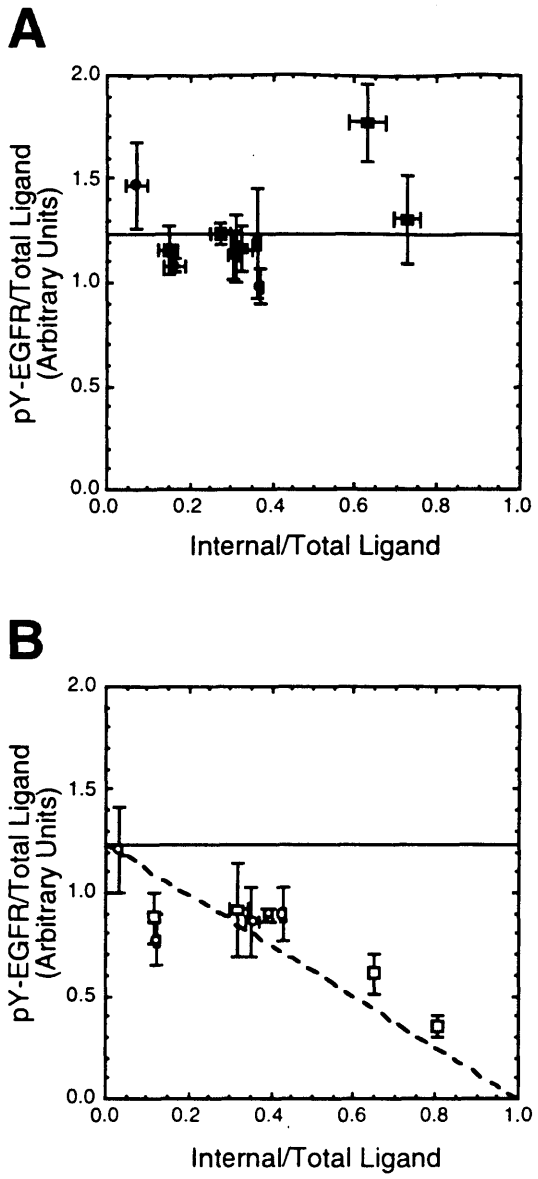

Figure 4.4 Analysis of EGFR tyrosine phosphorylation. Surface-bound and internalized ^{125}I-EGF were quantified for the same time points and conditions used in Fig. 4.3A ($n \geq 3$), and the ratio of pY-EGFR/total cell-associated ligand is plotted versus the ratio of internal/total cell-associated ligand (mean ± s.d. for both x- and y-axis values; y-value s.d. determined by propagation of error). A, EGF treatment: (●), time course; (■), strip protocol; solid line, mean of pY-EGFR/ligand. B, TGFα treatment: (○), time course; (□), strip protocol; solid line, mean of EGF-stimulated pY-EGFR/ligand from A; dashed line, theoretical line describing complete dephosphorylation of EGFR upon internalization.

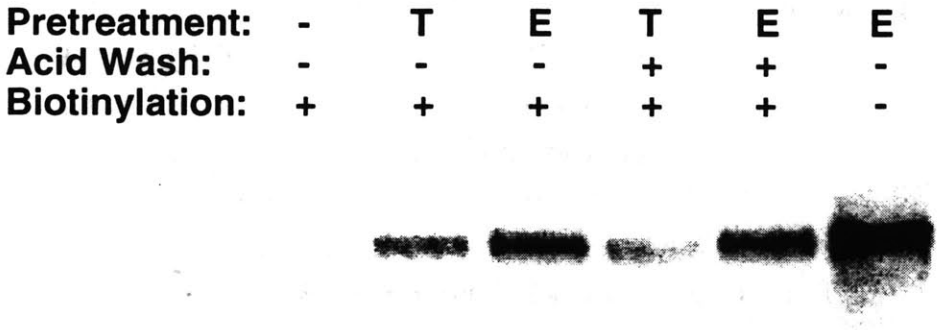

Figure 4.5 Tyrosine phosphorylation of internalized EGFR. Cells were stimulated with 20 nM TGFα (T) or EGF (E) for 15 minutes at 37°C. Where indicated, acid washing was carried out for 2 minutes on ice, followed by 5 minutes equilibration in binding buffer at 37°C. Surface biotinylation and clearance with immobilized streptavidin was employed to isolate internalized EGFR, as described under "Experimental Procedures," which was then subjected to SDS-PAGE and anti-phosphotyrosine immunoblotting.

4.3.3 Dose Responses of pY-EGFR and PIP_2 Hydrolysis

Having established that EGF yields higher levels of tyrosine phosphorylation of internalized EGFR than TGFα, it was next investigated whether these naturally occurring ligands could stimulate the PLC pathway to different extents. First, the dose responses (0-20 nM) of EGF- and TGFα-stimulated EGFR tyrosine phosphorylation were investigated, after 7.5 and 20 minutes of ligand challenge (Figure 4.6A&B). EGFR exhibited half-maximal tyrosine phoshorylation at 1-2 nM of either ligand, with TGFα values consistently and statistically lower than EGF values for the same dose. This is consistent with the previous conclusion that the two ligands activate surface EGFR to similar extents, while EGF elicits a greater degree of internalized EGFR activation.

The dose responses of EGF- and TGFα-stimulated PLC activity were also assessed. To this end, a functional assay was employed that assesses the hydrolysis of PIP_2 in intact cells. *In vitro* reactions using immunoisolated PLC-γ1 can be misleading, since the concentrations of PIP_2 and other membrane-associated signaling molecules in various compartments might be different. Following the liberation of soluble IP_3 from PIP_2, inositol phosphatases rapidly metabolize this intermediate to free inositol. Cell exposure to Li^+ inhibits the breakdown of inositol phosphate (IP), potentiating its accumulation in the cytosol. Previous studies using NR6 WT and other NR6 transfectants in conjunction with the specific PLC inhibitor U73122 demonstrated that this assay is indeed a direct readout of PIP_2 hydrolysis (Chen et al., 1994b).

NR6 cells were incubated with 20 mM LiCl for 15 minutes, followed by stimulation in the continued presence of LiCl. Control experiments indicated that IP accumulation is roughly linear with time for at least 30 minutes of 20 nM EGF stimulation, that lithium is required for observable IP accumulation, that the basal level of IP in the absence of stimulation does not increase detectably with time, and that lithium treatment does not affect EGFR internalization (data not shown). The dose responses of EGF- and TGFα-stimulated PIP_2 hydrolysis were examined for stimulation times of 15 and 30 minutes (Figure 4.7A&B). These time scales allow for sufficient internalization of ligand to occur (Figure 4.2), and for stimulated IP accumulation to achieve adequate signal:noise ratios. EGF did not gain any noticeable advantage over TGFα with respect to stimulation of the PLC pathway over the course of 30 minutes, despite higher levels of total cellular EGF-mediated EGFR activation at all doses (Figure 4.6). This might be expected if the activation of PLC were saturable, i.e. if PLC-γ1 or PIP_2 were stoichiometrically limiting at submaximal pY-EGFR. However, both ligand-induced PIP_2 hydrolysis and EGFR phosphotyrosine were half-maximal at similar EGF and TGFα concentrations (1-2 nM).

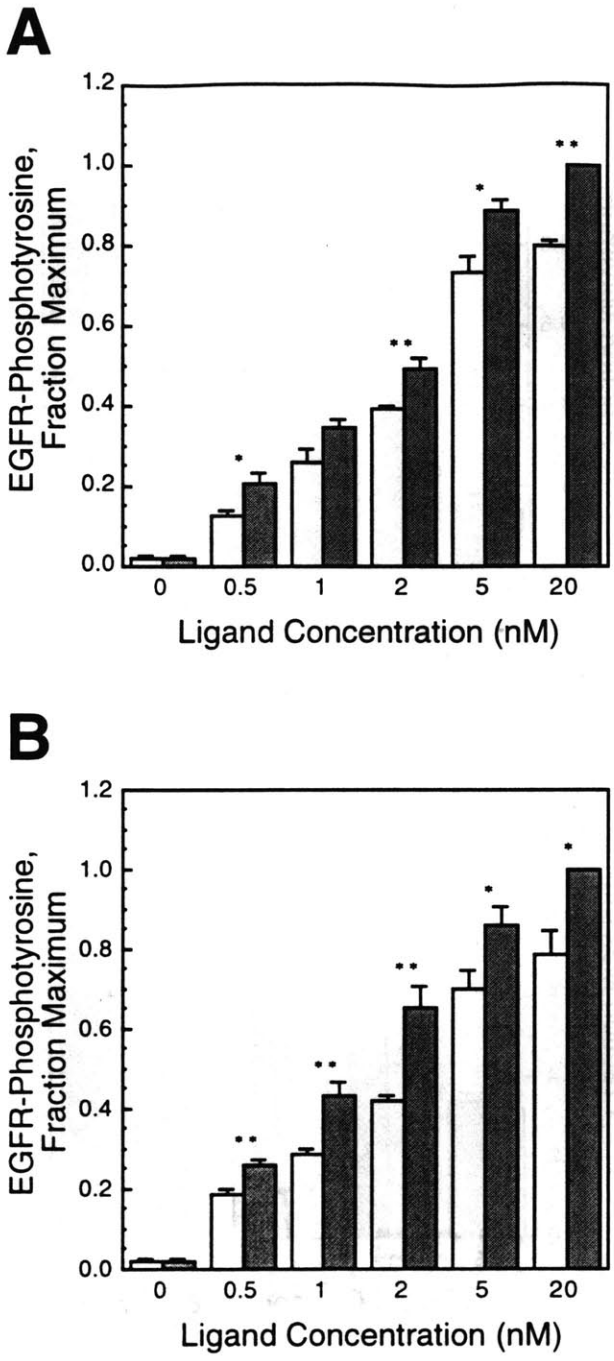

Figure 4.6 Dose response of EGFR tyrosine phosphorylation. NR6 WT cells were stimulated with the indicated doses of TGFα (□) or EGF (■) at 37°C for times of (A) 7.5 minutes or (B) 20 minutes. The levels of pY-EGFR in cell extracts were determined by sandwich ELISA and expressed relative to the maximum value obtained on the same day. Values are mean ± s.e.m., n ≥ 3; *, students' t-test, $p < 0.05$; **, students' t-test, $p < 0.01$ between EGF and TGFα at a particular ligand concentration.

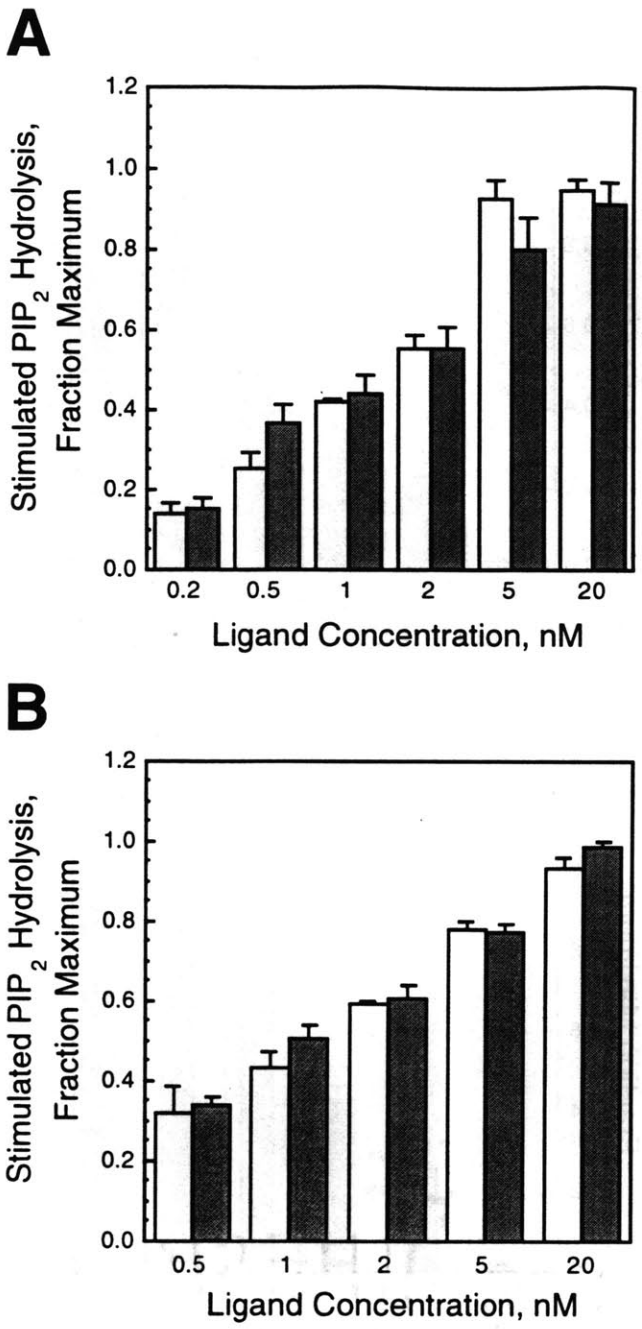

Figure 4.7 Dose response of EGFR-mediated PIP_2 hydrolysis. NR6 WT cells were stimulated with the indicated doses of TGFα (□) or EGF (■) at 37°C in the presence of 20 mM LiCl for times of (A) 15 min. or (B) 30 min. The accumulated levels of inositol phosphate resulting from hydrolysis of cellular PIP_2 were then measured as described. The unstimulated background was subtracted from stimulated values, and these are expressed relative to the maximum value obtained on the same day (mean ± s.e.m., $n \geq 3$).

Therefore, these results indirectly suggest that activated EGFR in internal compartments are deficient in stimulating PLC function.

4.3.4 Spatial Restriction of PIP_2 Hydrolysis to the Cell Surface

Although it seemed possible that active EGFR do not have access to PLC-γ1 and/or PIP_2 in intracellular trafficking compartments, our dose response results did not address this point directly. The internal pool of EGFR does not constitute a large fraction of the total cellular EGFR in the NR6 cell line, obscuring its potential contribution to PLC activation. Thus, mild acid washing was again employed to test the relationship between cell surface and intracellular receptor pools with regard to signaling.

NR6 WT cells were pretreated for 15 minutes with 20 nM EGF or TGFα at 37°C, in the absence of lithium, to saturate and permit internalization of surface EGFR. This was followed by incubation with ice-cold acid wash for 2 minutes to remove surface-bound ligand. Cells were then returned to 37°C in the presence of 20 mM LiCl and various concentrations of TGFα (0-20 nM), regardless of whether the cells were pretreated with EGF or TGFα. This "surface titration" protocol allowed us to vary the level of surface-activated EGFR, relative to a constant level of internal-activated EGFR that depends on whether the cells were pretreated with EGF or TGFα (Figure 4.8). This differs from the standard dose response experiment, in which internal receptor activation is coupled to the level of surface receptor activation. PIP_2 hydrolysis was assayed 15 minutes following LiCl addition, and pY-EGFR was assayed in separate experiments 7.5 minutes following LiCl addition as an intermediate time point. Control experiments demonstrated that accumulation of inositol phosphate was evident within 5 minutes of lithium addition (data not shown). The control protocol was 15 minutes pretreatment with no ligand at 37°C, acid wash treatment, then a return to 37°C with 20 mM LiCl and no ligand.

EGF-pretreated cells yielded statistically higher levels of total EGFR phosphotyrosine than TGFα-pretreated cells for each chase TGFα concentration (Figure 4.9A), consistent with the continued EGF-stimulated phosphorylation of internalized EGFR. In spite of this difference, PIP_2 hydrolysis activities were equivalent when EGF- and TGFα-pretreated cells were stimulated with ligand in the chase (0.5-20 nM TGFα; Figure 4.9B). For the 20 nM chase concentration, using EGF instead of TGFα in the chase did not effect the level of PIP_2 hydrolysis observed in this assay (data not shown). Further, in the absence of ligand in the chase, TGFα-pretreated cells stimulated minimal PIP_2 hydrolysis, even though tyrosine phosphorylation of some internalized EGFR was detected under these conditions (see also Figs. 4.3B and 4.5). These results are consistent with stimulation of PIP_2 hydrolysis by surface-localized EGFR only.

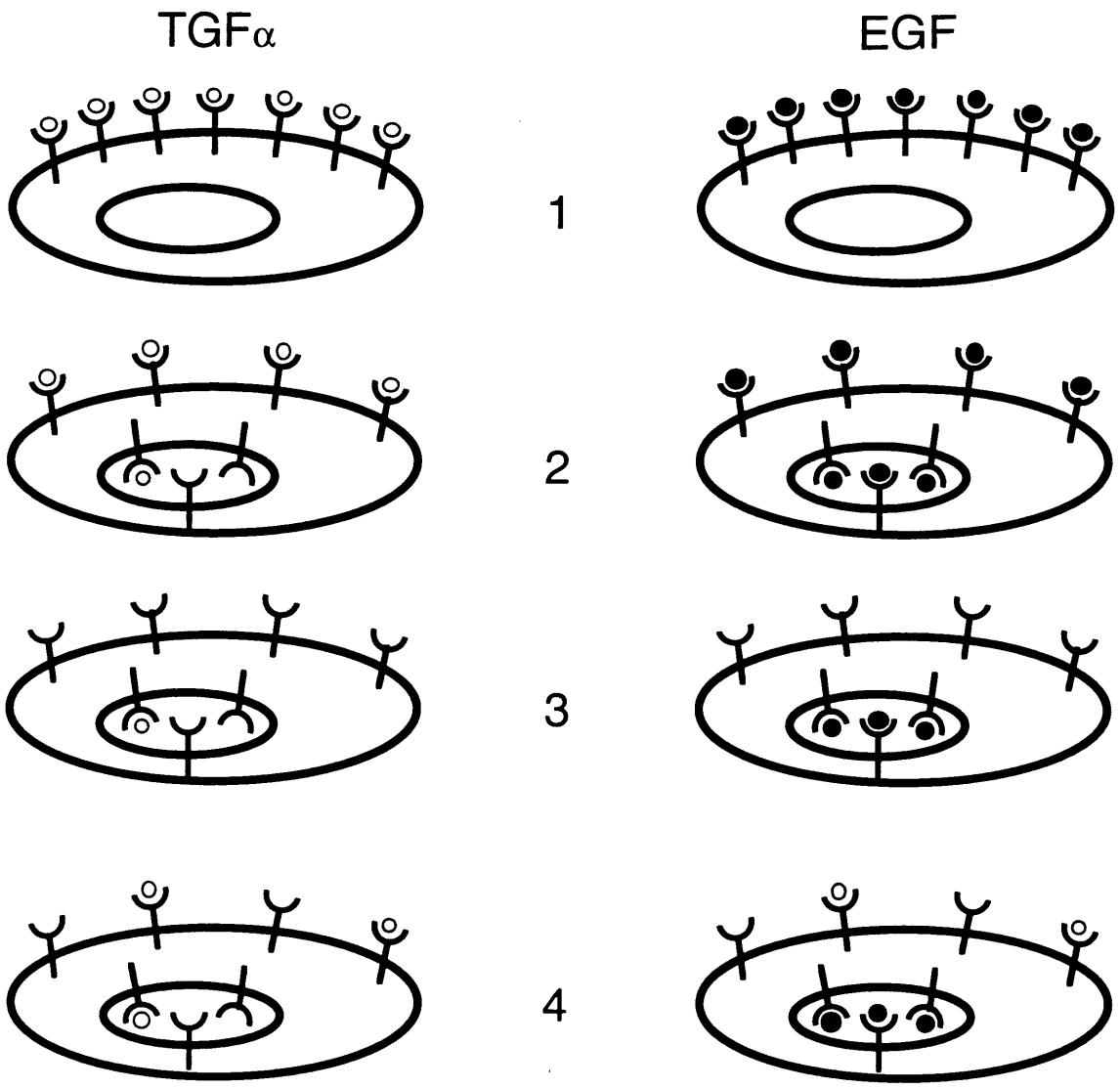

Figure 4.8 Surface titration protocol. In this procedure, cells are (1) pretreated with a saturating dose (20 nM) of either TGFα (left) or EGF (right) at 37°C. (2) A sufficient time is allowed for internalization of receptor-ligand complexes; EGF will occupy significantly more internal receptors compared to TGFα. (3) Cells are incubated in ice-cold acid wash (pH 3.0) for 2 min. to remove surface-bound ligand, and (4) cells are returned to pH 7.4, 37°C conditions in the presence of various concentrations (0-20 nM) TGFα. This protocol allows the activation of surface and internal EGFR to be manipulated independently.

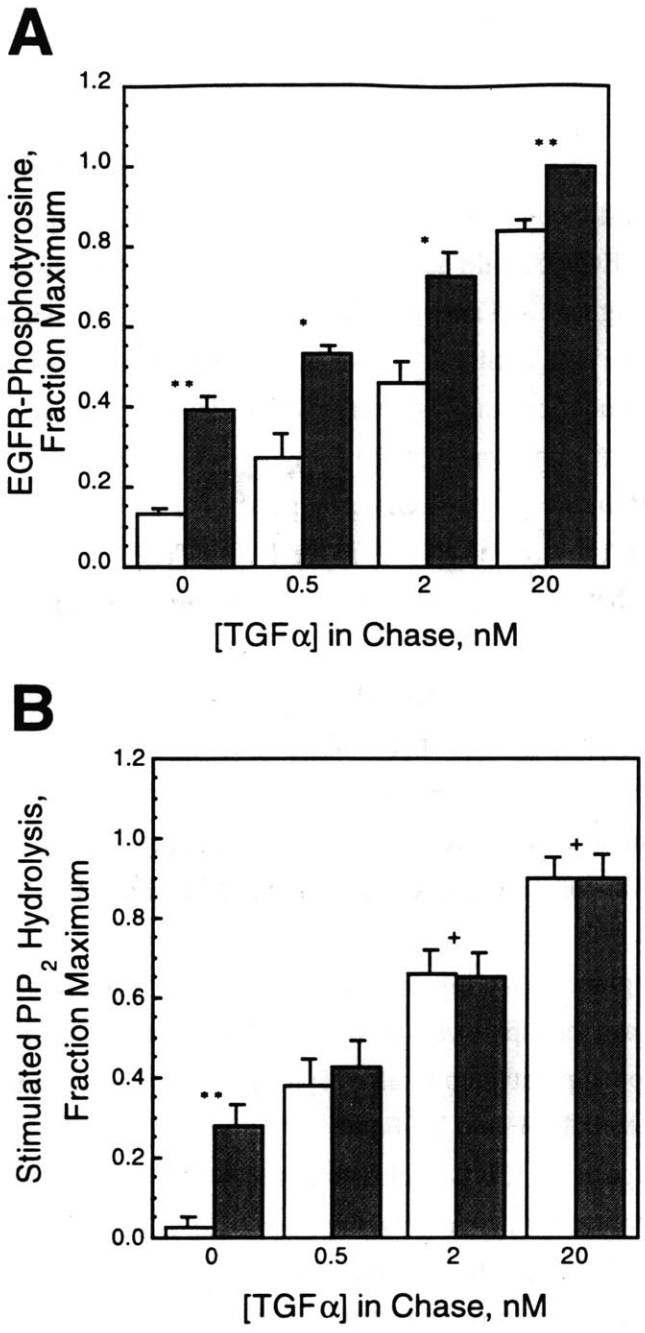

Figure 4.9 Results of surface titration experiments. NR6 WT cells were pretreated for 15 min. with 20 nM TGFα (□) or EGF (■), incubated with acid wash for 2 min. to remove surface-bound ligand, then brought back to 37°C with 20 mM LiCl and the indicated dose of TGFα in the chase. Cells were assayed for EGFR phosphotyrosine after 7.5 min. (A) or stimulated PIP_2 hydrolysis after 15 min. (B). Values are mean ± s.e.m., n ≥ 3; *, students' t-test, $p < 0.05$; **, students' t-test, $p < 0.01$; +, students' t-test, $p > 0.95$ between EGF- and TGFα-pretreated cells for the same chase conditions.

In apparent disagreement with this conclusion, however, EGF-pretreated cells exhibited statistically higher PIP_2 hydrolysis in the absence of ligand in the chase (Figure 4.9B). One possible explanation for this disparate result is that some internalized EGF, but not TGFα, is recycled back to the surface complexed with EGFR (Reddy et al., 1996a), an effect that would be masked by exogenous ligand added to the medium. To determine whether recycled EGF/EGFR could account for the enhanced PIP_2 hydrolysis, a receptor-blocking antibody (10 μg/mL 225 anti-EGFR) was included in the medium after acid wash treatment (Figure 4.10). This antibody causes accelerated dissociation of surface-bound EGF (data not shown) and therefore should reduce the level of surface signaling from recycled EGFR. Indeed, the presence of the antagonistic anti-EGFR antibody in the chase was able to inhibit PIP_2 hydrolysis in EGF-pretreated cells by 60%, but it had no effect on PIP_2 hydrolysis in TGFα-pretreated cells (Figure 4.10). Taken together, these results indicate, qualitatively, that active EGFR in internal compartments do not participate in PLC signaling.

Irrespective of the recycling effect, the dose response and surface titration data should be *quantitatively* consistent with a surface-only model of PIP_2 hydrolysis. To examine this, stimulated PIP_2 hydrolysis was plotted versus EGFR phosphotyrosine for both standard dose response and surface titration experiments. Since the extent of EGFR tyrosine phosphorylation constitutes a readout and modulator of EGFR kinase activity, in addition to the defined role of EGFR phosphotyrosine in docking PLC-γ1 and other signaling proteins, it represents the input for cell signaling at the receptor level. If signaling downstream of EGFR autophosphorylation did not depend on where receptors were located, then the relationship between total receptor phosphorylation and PIP_2 hydrolysis would be identical for both EGF and TGFα.

As shown in Figure 4.11, this is clearly not the case for the PLC pathway in NR6 cells. For the surface titration experiments, the curves for TGFα- and EGF-pretreated cells are parallel and shifted to the right by the constant level of internal pY-EGFR, indicating that these receptors are not contributing to PIP_2 hydrolysis. In the case of the standard ligand treatment (dose response) protocol, the curves of PIP_2 hydrolysis versus pY-EGFR for both TGFα and EGF overlap until intracellular EGF concentrations become high enough to start occupying receptors. At this point the curves diverge, with EGF values shifted to the right of TGFα values since EGF is more effective than TGFα in stimulating internal pY-EGFR (Figure 4.11). Finally, for high ligand concentrations (and therefore high pY-EGFR), the standard dose response and surface titration curves for the same ligand converge, confirming that the nature of signaling is not affected by differences in the two experimental designs.

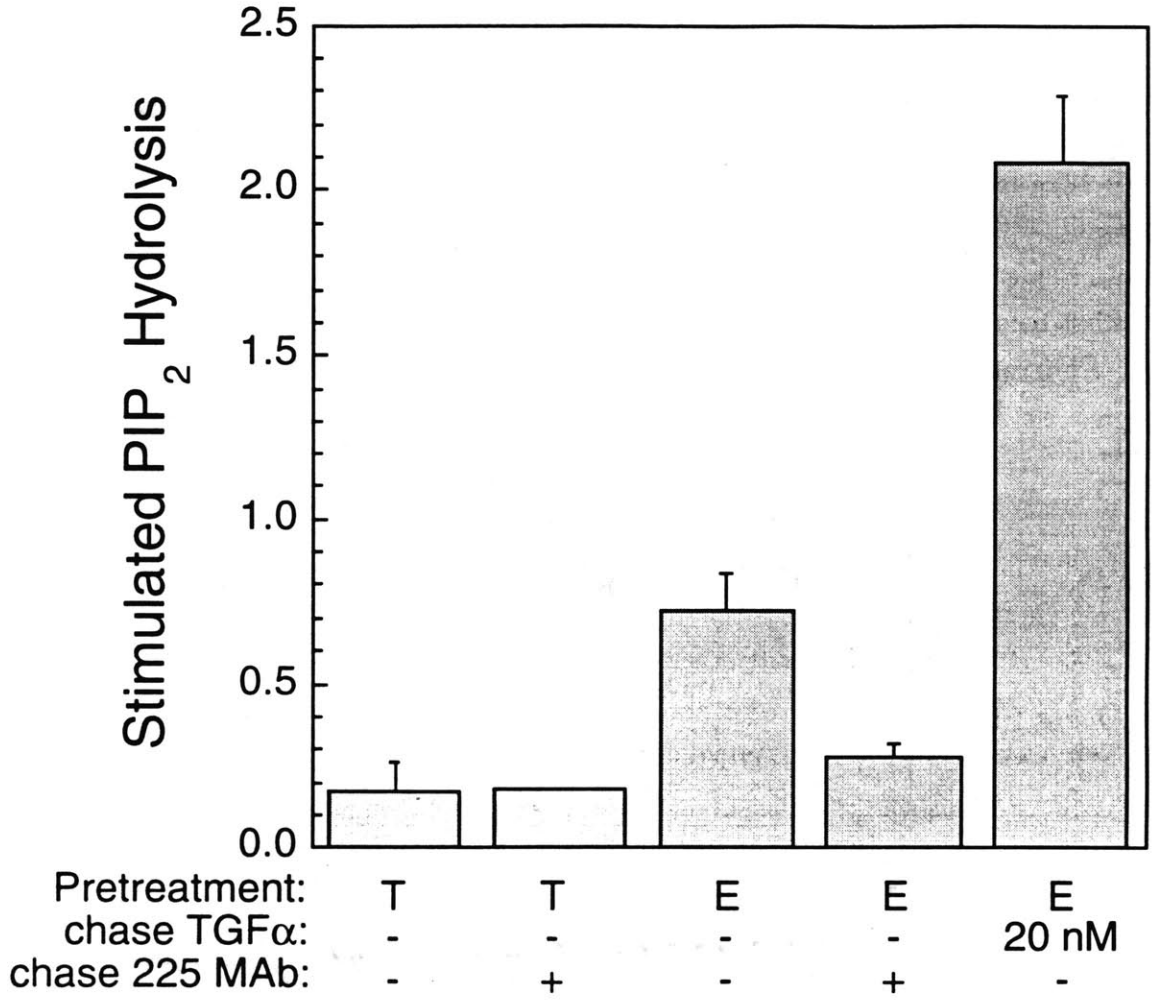

Figure 4.10 Inhibition of recycled receptor/ligand complex signaling by an anti-EGFR antibody. NR6 WT cells were treated, and PIP_2 hydrolysis was determined, as in B following pretreatment with 20 nM TGFα (T) or EGF (E). Where indicated, 10 μg/mL anti-EGFR monoclonal antibody 225 was included in the chase medium. Values are expressed as ligand-stimulated inositol phosphate accumulation normalized to the basal level (mean ± s.e.m., $n \geq 2$).

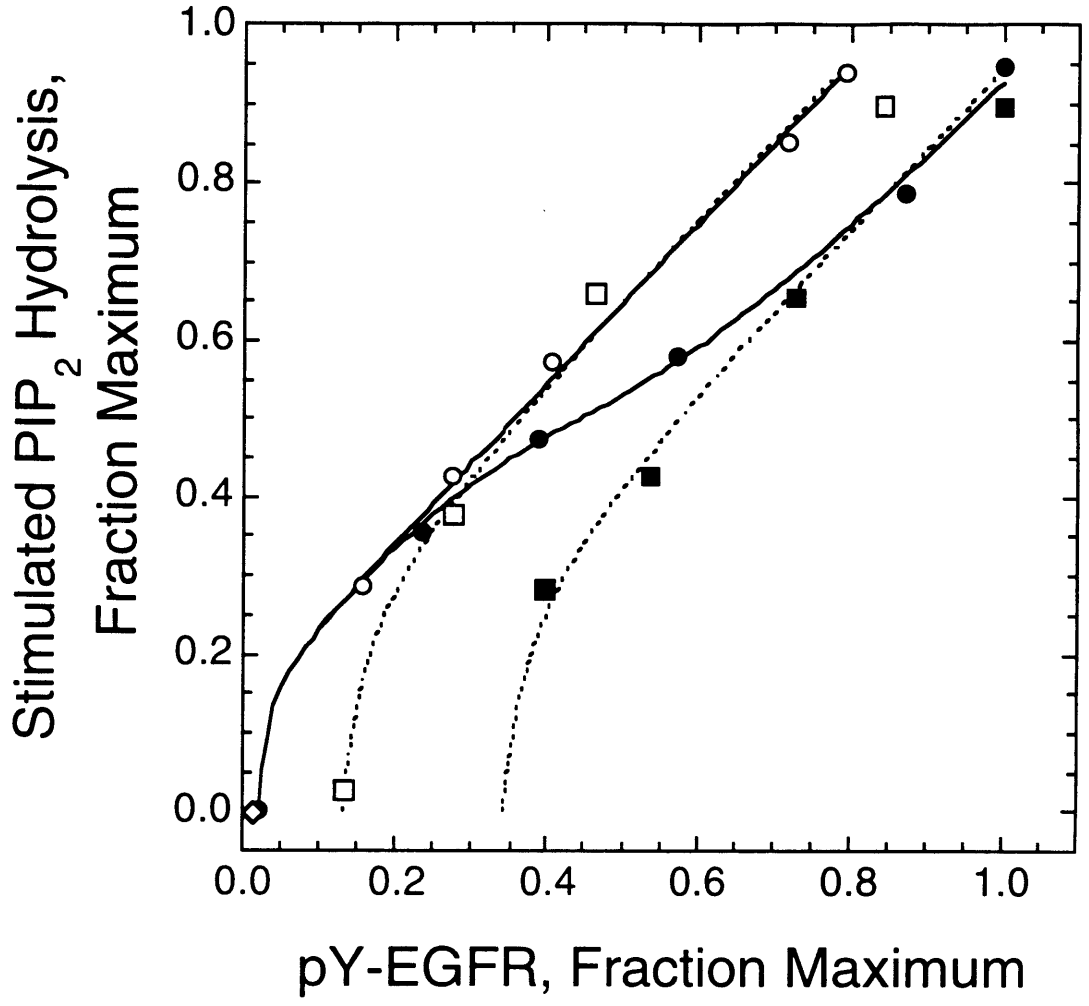

Figure 4.11 Plot of PIP_2 hydrolysis *versus* pY-EGFR for dose response and surface titration experiments. Standard dose response data for (—○—), TGFα- and (—●—), EGF-stimulated cells is taken from Figures 4.6 (x-axis values) and 4.7 (y-axis values), with values at each of the two time points averaged (7.5 and 20 minutes for pY-EGFR, 15 and 30 minutes for accumulated PIP_2 hydrolysis). Surface titration data for (···□···), TGFα- and (···■···), EGF-pretreated cells is taken from Figures 4.9A (x-axis values) and 4.9B (y-axis values); the unstimulated control (◇) is also shown.

These results are entirely consistent with the hypothesis that internalized EGFR, even when biochemically active, are far less effective than surface receptors in stimulating PLC-mediated PIP_2 hydrolysis.

These results also indicate that the relationship between surface receptor activation and PIP_2 hydrolysis has an unusual shape, with a high sensitivity of signaling to small increases in receptor activation at the low end, and a less sensitive, linear regime for moderate levels of receptor activation. This explains why the recycling effect was so pronounced in Fig. 4.9B, since small amounts of recycling to the cell surface can have a large (several-fold) impact on PIP_2 hydrolysis. The theoretical basis for the shapes of these curves will be discussed in Chapter 6.

4.3.5 Tyrosine Phosphorylation of PLC-γ1

Our dose response and surface titration experiments indicated that PLC activity is inhibited following EGFR endocytosis, and that loss of signaling occurs between EGFR activation and PIP_2 hydrolysis. To determine if this was due to an inability of the EGFR to induce tyrosine phosphorylation of PLC-γ1, the same surface titration protocol was used as above (EGF or TGFα pretreatment, surface strip, and TGFα chase). The same conditions used to measure EGFR phosphorylation in Figure 4.9A were used to examine PLC-γ1 phosphorylation.

Tyrosine-phosphorylated PLC-γ1 was immunoprecipitated using either anti-phosphotyrosine or anti-PLC-γ1 antibodies. After electrophoresis and membrane transfer, the blots were probed for the presence of PLC-γ1 or pY. Shown in Figure 4.12A is a typical experiment in which PLC-γ1 was visualized following immunoprecipitation with anti-pY antibodies. Qualitatively, PLC-γ1 tyrosine phosphorylation mirrored EGFR tyrosine phosphorylation in NR6 WT cells, in that EGF-pretreated cells always exhibited higher pY-PLC-γ1 than TGFα-pretreated cells for the same chase stimulation. Essentially identical results were obtained when PLC-γ1 was immunoprecipitated and then visualized with anti-pY antibodies.

The results of these experiments were quantified using a Bio-Rad Molecular Imager. Control experiments verified that there was a linear relationship between μg of total protein from the same lysate subjected to immunoprecipitation and the detected band intensity (data not shown). To ascertain quantitatively whether tyrosine phosphorylation of PLC-γ1 is affected by EGFR endocytosis, pY-PLC-γ1 (averaged over three experiments) was analyzed as a function of pY-EGFR for each condition (Figure 4.12B).

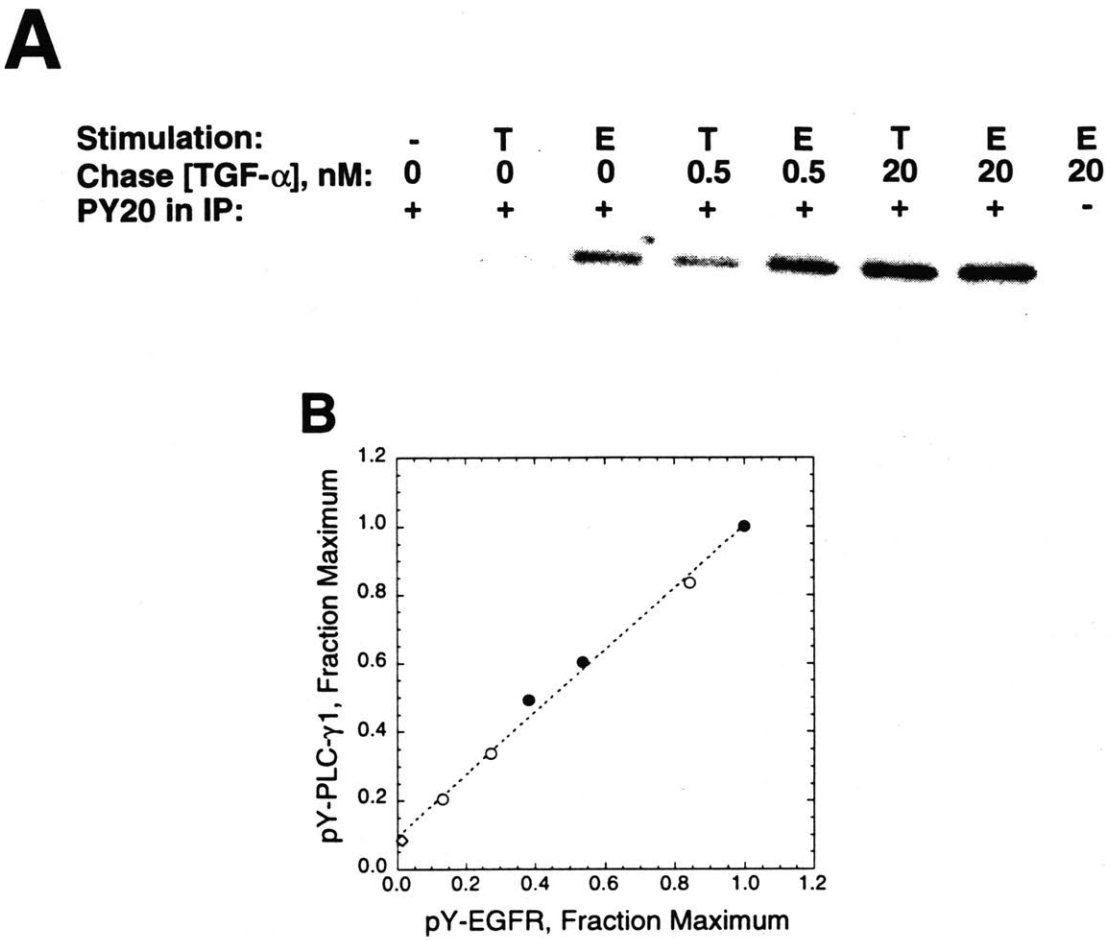

Figure 4.12 Analysis of PLC-γ1 tyrosine phosphorylation. NR6 WT extracts were prepared as for Figure 4.9A, using the surface titration protocol with TGFα (T) or EGF (E) pretreatments. Tyrosine-phosphorylated PLC-γ1 was immunoprecipitated from equal levels of total cellular protein using PY20 anti-phosphotyrosine antibody (Transduction Laboratories) and detected by immunoblotting with an anti-PLC-γ1 mixed monoclonal (Upstate Biotechnology) (n = 2; representative data shown, A). As a check, pY-PLC-γ1 was also detected once by anti-PLC-γ1 immunoprecipitation/anti-phosphotyrosine immunoblotting with similar results. B, plot of pY-PLC-γ1 *versus* pY-EGFR. For each of the three pY-PLC-γ1 experiments, the data was expressed relative to the maximum band intensity, and the mean for each condition is plotted versus pY-EGFR from Figure 4.9A to compare (○), TGFα- and (●), EGF-pretreated cells. The unstimulated point (◇) is also shown. The dotted line is the least squares linear fit of all the data points ($R^2 > 0.99$).

The relationship between tyrosine phosphorylation of the EGFR and PLC-γ1 was the same in the case of both EGF- and TGFα-pretreated cells, showing that tyrosine phosphorylation of PLC-γ1 is not affected by the localization of active receptors. As EGFR-mediated PIP_2 hydrolysis is dependent on a surface localization, this suggests a signaling restriction downstream of PLC-γ1 phosphorylation. This analysis also confirms that, on the time scale of these experiments, the tyrosine phosphorylation state (and presumably the enzymatic activity) of PLC-γ1 rapidly reaches a new pseudo-steady state during the chase with TGFα.

4.4 Discussion

While receptor downregulation and ligand depletion via the endocytic pathway are known to negatively modulate signal transduction mediated by EGFR and other RTKs (Wells et al., 1990; Vieira et al., 1996), there is no *a priori* reason to suspect that internalized receptors in sorting endosomes can not participate in signaling. Because its kinase and substrate-binding activities continue to face the cytosol in early endosomes, internalized EGFR have the potential to signal as long as they remain ligated (Wada et al., 1992). Indeed, internalized EGFR in rat liver are competent in both binding and phosphorylating the adaptor protein Shc, which helps localize the exchange factor Sos for potential interactions with the Ras GTPase (Di Guglielmo et al., 1994). In this cellular context, surface complexes are rapidly desensitized, while internal complexes somehow escape this regulation, implying that compartmentalized feedback mechanisms exist (Kay et al., 1986; Lai et al., 1989). Another possibility is that endocytosis might affect signaling specificity. Cells overexpressing a dominant-negative mutant of the dynamin GTPase are defective in both inducible endocytosis of EGFR and EGF-responsive tyrosine phosphorylation of the cytoplasmic signaling protein phosphatidylinositol (3)-kinase. This suggested that receptor internalization is required for the full manifestation of some signals but not others (Vieira et al., 1996). However, it has been reported recently that the mutant cells are also defective in high affinity EGFR/ligand binding, suggesting that dynamin might modulate aspects of signal transduction at the surface (Ringerike et al., 1998). The concept of compartmentalized "separation" of signaling pathways has also been implicated in the activation of sphingomyelinases mediated by tumor necrosis factor (Weigmann et al., 1994; Bevan et al., 1996). Thus, it is possible that signaling from the endosomal compartment *versus* the surface plays an important role in dictating the outcome of RTK stimulation.

It is now appreciated that many intracellular reactions, especially those at or just beyond the receptor level, are regulated by subcellular localization (Carraway and Carraway, 1995; Faux and Scott, 1996). Interestingly, post-receptor targets such as PIP_2 and Ras are membrane-associated, implying that they are readily compartmentalized. Since previous studies on EGFR signaling in internal compartments have not probed beyond tyrosine phosphorylation of cytoplasmic proteins, EGFR-mediated activation of the PLC pathway was examined to the level of PIP_2 hydrolysis. A physiologically relevant ligand-based approach was used, rather than comparing results from variant cell lines, based on previous studies suggesting that TGFα dissociates from EGFR in endosomes to a much greater extent than EGF (Ebner and Derynck, 1991; French et al., 1995). This study is the first to show that the magnitude of signal transduction through a specific pathway, at the level of proximal target modification, is affected by EGFR internalization.

Internalized EGF/EGFR complexes retain a maximal tyrosine phosphorylation stoichiometry, whereas EGFR internalized in response to TGFα binding are dephosphorylated to a significant extent. However, the two ligands are equipotent in stimulating PIP_2 hydrolysis, the functional outcome of PLC-γ1 activation. By manipulating the relative levels of surface and internal receptor activation independently, it was shown that active EGFR in internal compartments stimulate little if any hydrolysis of PIP_2. This deficiency was not due to a location-specific difference in PLC-γ1 tyrosine phosphorylation, since this event correlates with receptor phosphorylation in either compartment. Therefore, it is concluded that the spatial requirements for PIP_2 hydrolysis are defined at a step subsequent to PLC phosphorylation by EGFR.

The simplest interpretation of this data is that PLC-γ1 associated with EGFR in pre-degradative trafficking organelles (endocytic vesicles, early endosomes, and recycling endosomes) do not have access to PIP_2. Studies in numerous cell types have indicated that active maintenance of PIP_2 levels is required for meaningful PLC signaling. This function is carried out by phosphatidylinositol transfer protein (PITP), which directs transport of phosphatidylinositol between cellular membranes (Cockcroft, 1998). Therefore, exchange among lipid pools by membrane-phase sorting must be much slower than enzymatic turnover by PLC and other enzymes (Batty et al., 1998), indicating that the concentrations of PIP_2 and other lipids present in low amounts are not likely to be homogeneous among distinct cellular membranes. Further, PIP_2 concentrated in caveolae microdomains may comprise the EGFR-responsive substrate pool (Pike and Casey, 1996), which is probably segregrated from the bulk membrane delivered to endosomes via clathrin-coated pits.

These results also have implications regarding the functional difference between EGF and TGFα as naturally occuring agonists for the same receptor. Physiologically,

EGF and TGFα may have evolved as ligands that vary in their ability to mediate long-term receptor/ligand processing (Korc and Finman, 1989; Ebner and Derynck, 1991; Reddy et al., 1996b) but not in their compartmentalization of signal transduction. Although EGFR-transfected NR6 fibroblasts do not maintain a high percentage of internalized receptors at steady state, other cells display a rapid redistribution of receptors to internal pools (Gill et al., 1988). In these cases, internalization could act as a potent shut-off mechanism in response to chronic stimulation of EGFR. While the above situation likely applies to regulation of PLC-γ1 signaling, it is unclear whether other EGFR-mediated pathways are activated or even augmented in endosomes as has been suggested. If internalized receptors can signal through other intermediates, an important question is whether endocytosis is a requirement for signaling or if internal receptors simply continue activities initiated at the cell surface. In either case, compartmentalization of membrane-associated molecules would provide an additional level of signaling control, by affecting the spatiotemporal selectivity of enzymes that coordinate different cell functions.

4.5 References

Ascoli, M. (1982). Internalization and degradation of receptor-bound human choriogonadotropin in Leydig timor cells. *J. Biol. Chem.*, 257: 13306-13311.

Baass, P.C., Di Guglielmo, G.M., Authier, F., Posner, B.I. and Bergeron, J.J.M. (1995). Compartmentalized signal transduction by receptor tyrosine kinases. *Trends Cell Biol.*, 5: 465-470.

Batty, I.H., Currie, R.A. and Downes, C.P. (1998). Evidence for a model of integrated inositol phospholipid pools implies an essential role for lipid transport in the maintenance of receptor-mediated phospholipase C activity in 1321N1 cells. *Biochem. J.*, 330: 1069-1077.

Bertics, P.J., Weber, W., Cochet, C. and Gill, G.N. (1985). Regulation of the epidermal growth factor receptor by phosphorylation. *J. Cell. Biochem.*, 29: 195-208.

Bevan, A.P., Drake, P.G., Bergeron, J.J.M. and Posner, B.I. (1996). Intracellular signal transduction: the role of endosomes. *Trends Endocrin. Metabol.*, 7: 13-21.

Carpentier, J., White, M.F., Orci, L. and Kahn, R.C. (1987). Direct visualization of the phosphorylated epidermal growth factor receptor during its internalization in A-431 cells. *J. Cell. Biol.*, 105: 2751-2762.

Carraway, K.L. and Carraway, C.A.C. (1995). Signaling, mitogenesis and the cytoskeleton: where the action is. *BioEssays*, 17: 171-175.

Chang, C., Lazar, C.S., Walsh, B.J., Komuro, M., Collawn, J.F., Kuhn, L.A., Tainer, J.A., Trowbridge, I.S., Farquhar, M.G., Rosenfeld, M.G., Wiley, H.S. and Gill, G.N. (1993). Ligand-induced internalization of the epidermal growth factor receptor is mediated by multiple endocytic codes analogous to the tyrosine motif found in constitutively internalized receptors. *J. Biol. Chem.*, 268: 19312-19320.

Chen, P., Gupta, K. and Wells, A. (1994a). Cell movement elicited by epidermal growth factor receptor requires kinase and autophosphorylation but is separable from mitogenesis. *J. Cell Biol.*, 124: 547-555.

Chen, P., Murphy-Ullrich, J.E. and Wells, A. (1996a). A role for gelsolin in actuating epidermal growth factor receptor-mediated cell motility. *J. Cell Biol.*, 134: 689-698.

Chen, P., Xie, H., Sekar, M.C., Gupta, K. and Wells, A. (1994b). Epidermal growth factor receptor-mediated cell motility: phospholipase C activity is required, but mitogen-activated protein kinase activity is not sufficient for induced cell movement. *J. Cell Biol.*, 127: 847-857.

Chen, P., Xie, H. and Wells, A. (1996b). Mitogenic signaling from the EGF receptor is attenuated by a phospholipase C-γ/protein kinase C feedback mechanism. *Mol. Biol. Cell*, 7: 871-881.

Cockcroft, S. (1998). Phosphatidylinositol transfer proteins: a requirement in signal transduction and vesicle traffic. *BioEssays*, 20: 423-432.

Di Guglielmo, G.M., Baass, P.C., Ou, W., Posner, B.I. and Bergeron, J.J.M. (1994). Compartmentalization of SHC, GRB2 and mSOS, and hyperphosphorylation of Raf-1 by EGF but not insulin in liver parenchyma. *EMBO J.*, 13: 4269-4277.

Ebner, R. and Derynck, R. (1991). Epidermal growth factor and transforming growth factor-α: differential intracellular routing and processing of ligand-receptor complexes. *Cell Regulation*, 2: 599-612.

Faux, M.C. and Scott, J.D. (1996). More on target with protein phosphorylation: conferring specificity by location. *Trends Biochem. Sci.*, 21: 312-315.

French, A.R., Sudlow, G.P., Wiley, H.S. and Lauffenburger, D.A. (1994). Postendocytic trafficking of epidermal growth factor-receptor complexes is mediated through saturable and specific endosomal interactions. *J. Biol. Chem.*, 269: 15749-15755.

French, A.R., Tadaki, D.K., Niyogi, S.K. and Lauffenburger, D.A. (1995). Intracellular trafficking of epidermal growth factor family ligands is directly influenced by the pH sensitivity of the receptor/ligand interaction. *J. Biol. Chem.*, 270: 4334-4340.

Gill, G.N., Chen, W.S., Lazar, C.S., Glenney Jr., J.R., Wiley, H.S., Ingraham, H.A. and Rosenfeld, M.G. (1988). Role of intrinsic protein tyrosine kinase in function and metabolism of the epidermal growth factor receptor. *Cold Spring Harbor Symp. Quant. Biol.*, 53: 467-476.

Goldschmidt-Clermont, P.J., Kim, J.W., Machesky, L.M., Rhee, S.G. and Pollard, T.D. (1991). Regulation of phospholipase C-γ1 by profilin and tyrosine phosphorylation. *Science*, 251: 1231-1233.

Kay, D.G., Lai, W.H., Uchihashi, M., Khan, M.N., Posner, B.I. and Bergeron, J.J.M. (1986). Epidermal growth factor receptor kinase translocation and activation in vivo. *J. Biol. Chem.*, 261: 8473-8480.

Korc, M. and Finman, J.E. (1989). Attenuated processing of epidermal growth factor in the face of marked degradation of transforming growth factor-α. *J. Biol. Chem.*, 264: 14990-14999.

Laemmli, U.K. (1970). Cleavage of structural proteins during the assembly of the head of bacteriophage T4. *Nature*, 227: 680-685.

Lai, W.H., Cameron, P.H., Doherty, J.I., Posner, B.I. and Bergeron, J.J.M. (1989). Ligand-mediated autophosphorylation activity of the epidermal growth factor receptor during internalization. *J. Cell Biol.*, 109: 2751-2760.

Lund, K.A. and Wiley, H.S. (1994). "Regulation of the epidermal growth factor receptor by phosphorylation." in *Regulation of Cellular Signal Transduction Pathways by Desensitization and Amplification*, eds. Sibley, D. R. and Houslay, M. D. New York: John Wiley & Sons, pp. 277-303.

Meisenhelder, J., Suh, P., Rhee, S.G. and Hunter, T. (1989). Phospholipase C-γ is a substrate for the PDGF and EGF receptor protein-tyrosine kinases in vivo and in vitro. *Cell*, 57: 1109-1122.

Mellman, I. (1996). Endocytosis and molecular sorting. *Annu. Rev. Cell Dev. Biol.*, 12: 575-625.

Olayioye, M.A., Graus-Porta, D., Beerli, R.R., Rohrer, J., Gay, B. and Hynes, N.E. (1998). ErbB-1 and erbB-2 acquire distinct signaling properties dependent upon their dimerization partner. *Mol. Cell. Biol.*, 18: 5042-5051.

Pawson, T. (1995). Protein modules and signaling networks. *Nature*, 373: 573-580.

Pike, L.J. and Casey, L. (1996). Localization and turnover of phosphatidylinositol 4,5-bisphosphate in caveolin-enriched membrane domains. *J. Biol. Chem.*, 271: 26453-26456.

Reddy, C.C., Niyogi, S.K., Wells, A., Wiley, S.H. and Lauffenburger, D.A. (1996a). Engineering epidermal growth factor for enhanced mitogenic potency. *Nature Biotech.*, 14: 1696-1699.

Reddy, C.C., Wells, A. and Lauffenburger, D.A. (1994). Proliferative response of fibroblasts expressing internalization-deficient epidermal growth factor (EGF) receptors is altered via differential EGF depletion effect. *Biotechnol. Prog.*, 10: 377-384.

Reddy, C.C., Wells, A. and Lauffenburger, D.A. (1996b). Receptor-mediated effects on ligand availability determine relative mitogenic potencies of EGF and TGFα. *J. Cell. Physiol.*, 166: 512-522.

Rhee, S.G. and Choi, K.D. (1992). Regulation of inositol phospholipid-specific phospholipase C isozymes. *J. Biol. Chem.*, 267: 12393-12396.

Ringerike, T., Stang, E., Johannessen, L.E., Sandnes, D., Levy, F.O. and Madshus, I.H. (1998). High-affinity binding of epidermal growth factor (EGF) to EGF receptor is disrupted by overexpression of mutant dynamin (K44A). *J. Biol. Chem.*, 273: 16639-16642.

Sorkin, A. and Carpenter, G. (1991). Dimerization of internalized epidermal growth factor receptors. *J. Biol. Chem.*, 266: 23453-23460.

Toker, A. (1998). The synthesis and cellular roles of phosphatidylinositol 4,5-bisphosphate. *Curr. Opin. Cell Biol.*, 10: 254-261.

Towbin, H., Staehlin, T. and Gordon, J. (1979). Electrophoretic transfer of proteins from polyacrylamide gels to nitrocellulose sheets: procedure and some applications. *Proc. Natl. Acad. Sci. USA*, 76: 4350-4354.

Trowbridge, I.S., Collawn, J.F. and Hopkins, C.R. (1993). Signal-dependent membrane protein trafficking in the endocytic pathway. *Annu. Rev. Cell Biol.*, 9: 129-161.

van der Geer, P., Hunter, T. and Lindberg, R.A. (1994). Receptor protein-tyrosine kinases and their signal transduction pathways. *Annu. Rev. Cell Biol.*, 10: 251-337.

Vega, Q.C., Cochet, C., Filhol, O., Chang, C., Rhee, S.G. and Gill, G.N. (1992). A site of tyrosine phosphorylation in the C-terminus of the epidermal growth-factor receptor is required to activate phospholipase C. *Mol. Cell. Biol.*, 12: 128-135.

Vieira, A.V., Lamaze, C. and Schmid, S.L. (1996). Control of EGF receptor signaling by clathrin-mediated endocytosis. *Science*, 274: 2086-2089.

Wada, I., Lai, W.H., Posner, B.I. and Bergeron, J.J. (1992). Association of the tyrosine phosphorylated epidermal growth factor receptor with a 55-kD tyrosine phosphorylated protein at the cell surface and in endosomes. *J. Cell Biol.*, 116: 321-330.

Wahl, M.I., Nishibe, S., Suh, P., Rhee, S.G. and Carpenter, G. (1989). Epidermal growth factor stimulates tyrosine phosphorylation of phospholipase C-II independently of receptor internalization and extracellular calcium. *Proc. Natl. Acad. Sci. USA*, 86: 1568-1572.

Ware, M.F., Tice, D.A., Parsons, S.J. and Lauffenburger, D.A. (1997). Overexpression of cellular Src in fibroblasts enhances endocytic internalization of epidermal growth factor receptor. *J. Biol. Chem.*, 272: 30185-20190.

Weigmann, K., Schutze, S., Machleidt, T., Witte, D. and Kronke, M. (1994). Functional dichotomy of neutral and acidic sphingomyelinases in tumor necrosis factor signaling. *Cell*, 78: 1005-1015.

Wells, A., Welsh, J.B., Lazar, C.S., Wiley, H.S., Gill, G.N. and Rosenfeld, M.G. (1990). Ligand-induced transformation by a non-internalizing epidermal growth factor receptor. *Science*, 247: 962-964.

Xie, H., Pallero, A., Gupta, K., Ware, M.F., Chang, P., Witke, W., Kwiatkowski, D.J., Lauffenburger, D.A., Murphy-Illrich, J.E. and Wells, A. (1998). EGF receptor regulation of cell-substratum interactions: EGF induces disassembly of focal adhesions independently of the motility-associated PLCγ signaling pathway. *J. Cell Sci.*, 111: 616-625.

CHAPTER 5

Influence of Epidermal Growth Factor Receptor Trafficking and Feedback Desensitization on the Activation of Ras

Normal activation of the highly conserved Ras GTPase is a central event in the stimulation of cell proliferation, motility, and differentiation elicited by receptor tyrosine kinases such as the epidermal growth factor receptor (EGFR). In fibroblasts, this involves formation and membrane localization of Shc-Grb2-Sos complexes, which increases the rate of Ras guanine nucleotide exchange. In order to control Ras-mediated cell responses, this activity is regulated by receptor downregulation and a feedback loop involving the dual specificity kinase MEK. The role of EGFR endocytosis in the regulation of Ras activation was investigated. Of fundamental interest is whether activated receptors in endosomes can participate in the stimulation of Ras guanine nucleotide exchange. I found that activated EGFR at the cell surface and in internal compartments contribute equally to the membrane recruitment and tyrosine phosphorylation of Shc in NR6 fibroblasts expressing wild-type EGFR. Importantly, both the rate of Ras-specific guanine nucleotide exchange and the level of Ras-GTP were depressed to near basal values on the time scale of receptor trafficking. Using the selective MEK inhibitor PD098059, I was able to block the feedback desensitization pathway and maintain activation of Ras. Under these conditions, the generation of Ras-GTP was not significantly affected by the subcellular location of activated EGFR. In conjunction with the previous analysis of the phospholipase C pathway in the same cell line (Chapter 4), this suggests selective continuation of signaling activities that affect cell function.

5.1 Introduction

The 170 kDa epidermal growth factor receptor (EGFR) is the best studied member of the erbB family of receptor tyrosine kinases. The EGFR exerts its biological effects in response to binding of specific polypeptide ligands, including epidermal growth factor (EGF) and transforming growth factor alpha (TGFα). This leads to activation of the EGFR catalytic domain, autophosphorylation of specific residues in its carboxyl terminus, and recruitment and phosphorylation of heterologous signaling proteins (van der Geer et al., 1994). The EGFR can also transactivate other members of the erbB receptor family via

heterodimerization, enhancing the diversity of potential signaling interactions (Lemmon and Schlessinger, 1994).

Abnormal expression and mutations of EGFR and other erbB family members, in conjunction with other permissive mutations, have been widely implicated in transformation and tumorigenesis. Acquisition of increased ligand secretion and autocrine signaling through the EGFR can also contribute to cell transformation. In particular, secretion of TGFα is potently mitogenic, since its dissociation from EGFR after endocytosis spares the receptor from proteolysis (Gangarosa et al., 1997; Ouyang et al., 1999). In contrast, the interaction of EGF with the receptor persists after internalization by virtue of its relative insensitivity to decreases in pH, yielding continued tyrosine phosphorylation and, later, receptor downregulation (Ebner and Derynck, 1991; French et al., 1995; Baass et al., 1995).

Another broad determinant of cell transformation involves dysregulation of the 21 kDa Ras GTPase, a ubiquitous and highly conserved signaling protein normally activated in response to stimulation of receptor tyrosine kinases (Bos, 1989; Bourne et al., 1991). Interruption of its GTPase activity yields a constitutively active Ras and unregulated cell proliferation. The biological activity of Ras is completely dependent on post-translational modifications that lead to its insertion into the plasma membrane. In its GTP-bound state, Ras recruits other signaling proteins to the membrane via its effector loop. These include the Raf serine/threonine kinase, phosphatidylinositol 3-kinase, and activators of the Rho and Rac GTPases (Vojtek and Der, 1998). Activation of Raf initiates the well-studied cascade involving successive activation of the dual specificity MAPK and Erk kinase (MEK) and extracellular signal-related kinase (Erk). This signaling pathway, illustrated in Figure 5.1, is required for both cell cycle progression and cell motility in fibroblasts; another signaling pathway involving phospholipase C-γ1 (PLC-γ1) is required for cell motility but is dispensable for mitogenesis (Chen et al., 1994; Klemke et al., 1997; Xie et al., 1998).

Ras is positively modulated by guanine nucleotide exchange factors (GEFs), which accelerate the dissociation of bound nucleotides. This favors the subsequent binding of the more abundant GTP from the cytosol. Stimulation of receptor tyrosine kinases leads to the recruitment of Ras-GEF activity to the membrane, which is sufficient to elicit Ras activation (Aronheim et al., 1994; Quilliam et al., 1994). For example, the Grb2 adaptor protein interacts via its SH3 domains with the Ras-GEF Sos; the SH2 domain of Grb2 mediates membrane recruitment of the complex through interactions with certain phosphotyrosine motifs, including the Y1068 minor autophosphorylation site of the EGFR (Buday and Downward, 1993). However, the Grb2 SH2 domain has a five-fold higher affinity for the

tyrosine-phosphorylated Shc adaptor protein (Cussac et al., 1994), which binds to autophosphorylated EGFR and erbB-2 using both SH2 and PTB domains (Pawson, 1995). Given that Shc uses two high affinity phosphotyrosine recognition domains, and also that its preferred binding sites on the EGFR are more extensively phosphorylated than Y1068 *in vivo* (Downward et al., 1984; Batzer et al., 1994; Okabayashi et al., 1994), it is likely that coupling to tyrosine-phosphorylated Shc is the predominant mechanism governing the EGFR-mediated localization of the Grb2-Sos complex (Sasaoka et al., 1994).

Two distinct mechanisms have been identified that attenuate EGFR-mediated Ras activation. These are desensitization by a MEK-dependent negative feedback loop, which prevents complexation of Sos with tyrosine-phosphorylated Shc (de Vries-Smits et al., 1995a; Langlois et al., 1995; Rozakis-Adcock et al., 1995; Porfiri and McCormick, 1996; Holt et al., 1996), and internalization and downregulation of the EGFR (Osterop et al., 1993; Klarlund et al., 1995). With regard to the latter mechanism, however, it is unclear when Ras activation is silenced during the trafficking of the EGFR. Shc can associate with endosomal membranes in response to EGF stimulation, and this Shc pool is efficiently tyrosine phosphorylated in rat liver (Di Guglielmo et al., 1994; Lotti et al., 1996). However, the fact that Ras is a membrane-associated protein suggests that it might be compartmentalized. For example, activated EGFR in internal compartments effectively participate in the tyrosine phosphorylation of PLC-γ1, but not in the hydrolysis of its membrane lipid substrate phosphatidylinositol (4,5)-bisphosphate (Chapter 4). It was therefore of interest to determine whether active, internalized EGFR could participate in the activation of Ras.

To deconvolute the two modes of Ras regulation, the specific inhibitor PD098059 was employed to block the MEK-dependent feedback loop in NR6 fibroblasts expressing wild-type EGFR, which prolonged Ras-GEF activity on the time scale of receptor internalization. The tyrosine phosphorylation and recruitment of Shc and the activation of Ras were then quantitatively related to the total level of EGFR autophosphorylation, under conditions that manipulated the relative numbers of EGFR activated at the surface and in internal compartments. Under these conditions, internal receptors were at least as potent as surface receptors in stimulating all of these signaling determinants. Given the previous investigation of phospholipase C regulation in the same cell line, this demonstrates that internalized EGFR can, in a selective manner, continue signaling through certain pathways, and that Ras activation mediated by EGFR is attenuated primarily by feedback desensitization.

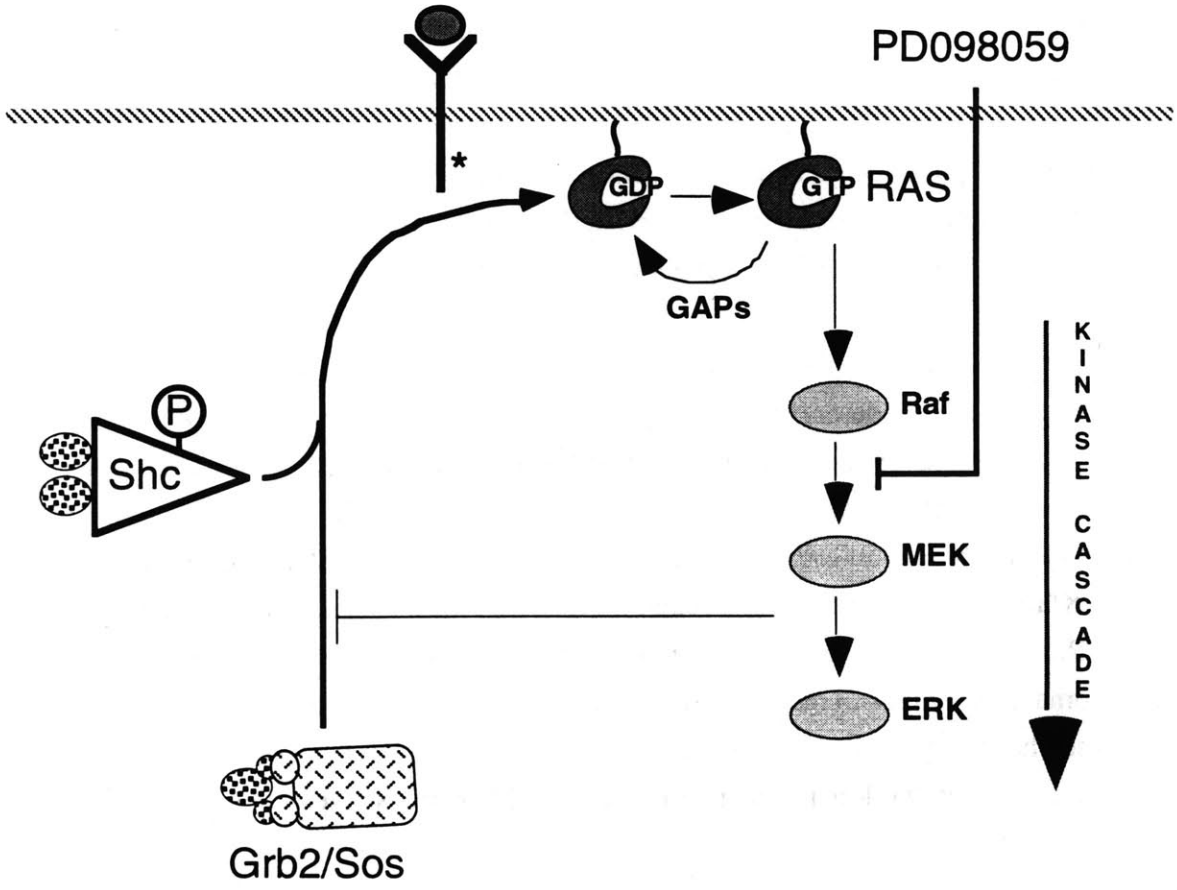

Figure 5.1 The Ras/Erk Pathway. Ras is a ubiquitous, highly conserved, and membrane-associated GTPase centrally involved in the normal and aberrant progression of the cell growth cycle. Ras is activated by guanine nucleotide exchange factors (GEFs), including Sos, which is recruited in complex with the Grb2 adaptor to the membrane via associations with autophosphorylated receptors. In fibroblasts and other cell types, this linkage is primarily mediated by tyrosine-phosphorylated Shc, another adaptor protein. Ras is deactivated by GTPase-accelerating proteins (GAPs). In its GTP-bound (active) state, Ras initiates a kinase cascade that involves the serial activation of Raf, MEK, and Erk, which mediates cell growth and other functional responses. This pathway regulates itself through a negative feedback loop that prevents Sos recruitment and therefore desensitizes the Ras activation mechanism. This feedback loop can be blocked by the pharmacological agent PD098059, a selective inhibitor of MEK.

5.2 Experimental Procedures

5.2.1 Cell Culture and Quiescence Protocol

NR6 mouse fibroblasts transfected with wild-type human EGFR (NR6 WT) (Wells et al., 1990; Chen et al., 1994) were cultured using minimum essential medium (MEM)-α/26 mM sodium bicarbonate with 7.5% fetal bovine serum (FBS), 2 mM L-glutamine, 1 mM sodium pyruvate, 0.1 mM MEM nonessential amino acids, and the antibiotics penicillin, streptomycin, and G418 (350 μg/mL) as the growth medium. All cell culture reagents were obtained from Life Technologies. Cells were quiesced at subconfluence using restricted serum conditions without G418 (MEM-α/26 mM sodium bicarbonate with 1% dialyzed FBS, 2 mM L-glutamine, 1 mM sodium pyruvate, 0.1 mM MEM nonessential amino acids, and the antibiotics penicillin/streptomycin) for 18-24 h prior to experiments. Experiments were carried out in an air environment using MEM-α/13 mM HEPES (pH 7.4 at 37°C) with 0.5% dialyzed FBS, 2 mM L-glutamine, the antibiotics penicillin/streptomycin, and 1 mg/mL bovine serum albumin as the binding buffer.

5.2.2 Use of Pharmacological Inhibitor PD098059

The activation of MEK was selectively blocked using PD098059 (Alessi et al., 1995). The agent, purchased from Calbiochem, was dissolved to a stock concentration of 50 mM in DMSO and stored in aliquots at -20°C. Just before use, an aliquot was warmed to 37°C and diluted 1,000-fold in warm binding buffer. In all cases, cells were preincubated with PD098059 for 60 minutes at 37°C before stimulation.

5.2.3 Surface Titration Protocol

This stimulation procedure allows the numbers of activated EGFR at the plasma membrane and in intracellular compartments following endocytosis to be varied independently. After preincubation with either PD098059 or 0.1% DMSO only, mouse EGF (Life Technologies) or human TGFα (Peprotech) was added to 20 nM in the same medium for 20 minutes. Cells were then washed once with ice cold WHIPS buffer (20 mM HEPES, 130 mM NaCl, 5 mM KCl, 0.5 mM $MgCl_2$, 1 mM $CaCl_2$, 1 mg/mL polyvinylpyrrolidone, pH 7.4) and incubated in an acid wash (50 mM glycine-HCl, 100 mM NaCl, 1 mg/mL polyvinylpyrrolidone, pH 3.0) on ice for 2 minutes. By 1 minute, this treatment is equally efficient in dissociating EGF and TGFα from surface EGFR of NR6 cells. After another wash with ice cold WHIPS, cells were reequilibrated for 5 min. in 37°C binding buffer containing various concentrations of TGFα (0-20 nM) in the continued presence of either PD098059 or DMSO only. Thus, a constant level of internal

receptor activation, depending only on whether cells were pretreated with EGF or TGFα, is titrated with various levels of surface receptor activation following the acid wash.

5.2.4 EGFR Autophosphorylation

Tyrosine phosphorylation of the EGFR was assessed using a quantitative sandwich ELISA assay. High-binding 96-well plates were precoated with 10 μg/mL anti-EGFR monoclonal antibody 225 in PBS, then with blocking buffer (10% horse serum/0.05% Triton X-100 in PBS), at room temperature. After various treatments, cells were washed with ice cold PBS supplemented with 1 mM sodium orthovanadate, scraped into ice cold lysis buffer (50 mM HEPES pH 7.0, 150 mM NaCl, 1% Triton X-100, 10% glycerol) supplemented with 1 mM sodium orthovanadate, 10 mM sodium pyrophosphate, 1 mM EGTA, 4 mM sodium iodoacetate and 10 μg/mL each of aprotinin, leupeptin, chymostatin, and pepstatin A, transferred to an Eppendorf tube, and incubated on ice for 20 minutes. Clarified lysates were diluted to various extents in blocking buffer supplemented with 1 mM sodium orthovanadate and incubated in the ELISA wells for 1 h at 37°C. The amount of associated phosphotyrosine was determined using alkaline phosphatase-conjugated RC20 anti-phosphotyrosine antibody (Transduction Laboratories) and p-nitrophenyl phosphate (Sigma) substrate.

5.2.5 Shc Tyrosine Phosphorylation and Coprecipitation with the EGFR

1% Triton X-100 cell lysates were generated as detailed above. For pY-Shc, total cell protein was determined (Micro BCA; Pierce), and immunoprecipitations of equivalent total protein amounts were performed (4°C for 90 minutes) using 5 μg PY20 anti-phosphotyrosine antibody (Transduction Laboratories) precoupled to protein G-sepharose. For coprecipitation with the EGFR, recovery was enhanced by immunoprecipitating equal lysate volumes (4°C for 60 minutes) with 5 μg 225 anti-EGFR antibody precoupled to protein G-sepharose, with total protein amounts determined subsequently. In both cases, beads were washed five times with ice-cold lysis buffer supplemented with 1 mM sodium orthovanadate, and the residual liquid was removed with a syringe. Precipitated proteins were subjected to SDS-PAGE on 10% acrylamide gels and transferred to PVDF membranes. Membranes were blotted using anti-Shc polyclonal antibodies (Transduction Laboratories), horseradish peroxidase-conjugated anti-rabbit IgG, and SuperSignal Ultra detection reagent (Pierce). Bands were detected and quantified using a Bio-Rad chemiluminescence screen and molecular imager. For EGFR coprecipitation, band intensities were normalized to total cell protein amounts.

5.2.6 Ras Immunoprecipitation and Elution of Guanine Nucleotides

After various treatments, cells were lysed in ice-cold Ras extract buffer (50 mM Tris-HCl pH 7.4, 150 mM NaCl, 1% Nonidet P-40, 20 mM $MgCl_2$) supplemented with 1 mM phenylmethylsulfonyl fluoride and 10 μg/mL each of aprotinin, leupeptin, chymostatin, and pepstatin A. After incubation on ice for 20 minutes, each lysate was clarified, transferred to a new tube, adjusted to 500 mM NaCl, 0.5% deoxycholate, and 0.05% SDS, and subjected to 2 hours immunoprecipitation at 4°C using 3 μg Y13-259 anti-Ras monoclonal antibody precoupled with 30 μg rabbit anti-rat IgG and 10 μL protein A-sepharose beads. The immune complexes were washed 10 times with high salt buffer (50 mM Tris HCl pH 7.4, 500 mM NaCl, 10 mM $MgCl_2$, 0.1% Triton X-100, and 0.005% SDS) and 3 times with 20 mM Tris phosphate pH 7.8, and residual liquid was removed using a syringe. The beads of each sample were resuspended in 40 μL elution buffer (5 mM Tris phosphate pH 7.8, 2 mM EDTA, 2 mM DTT), boiled for 3 minutes, cooled briefly on ice, and pelleted for 5 minutes at 16,000xg. The supernatants, containing guanine nucleotides dissociated from the immunoprecipitated Ras, were collected and either analyzed immediately or stored at -80°C.

5.2.7 Ras Guanine Nucleotide Exchange

Ras-GEF activity was measured by permeabilization of cells with digitonin and uptake of [α-^{32}P]-GTP (de Vries-Smits et al., 1995b). Cells quiesced in 150 mm plates were washed once with ice-cold permeabilization buffer (10 mM PIPES-KOH, pH 7.4, 120 mM KCl, 30 mM NaCl, 5 mM $MgCl_2$, 0.8 mM EGTA, 0.64 mM $CaCl_2$, and 1 mM ATP) after various treatments, then incubated with 0.5 mL permabilization buffer supplemented with freshly added 0.1% digitonin (Boehringer Mannheim) and 25 μCi [α-^{32}P]-GTP (NEN) for 2 min. at 37°C. The liquid was aspirated carefully. Cells were lysed, Ras was immunoprecipitated, and nucleotides were eluted as described above, except that 1 mM ATP and 100 μM each of GTP and GDP were included in the lysis buffer, and clarified lysates were precleared using 50 μL protein A-sepharose beads for 5 min. at 4°C. Radioactivity eluted from Ras was quantified by liquid scintillation counting.

5.2.8 GTP and GDP Determination

The extent of Ras activation was determined using quantitative assays developed by Scheele and colleagues that independently assess absolute, fmol amounts of GDP and GTP eluted from Ras immunoprecipitates (Scheele et al., 1995). Ras was immunoprecipitated from cell lysates, and guanine nucleotides were eluted, as described above. The absolute amount of GTP eluted from immunoprecipitated Ras was determined using a kinetic assay,

in which GTP is converted to ATP by nucleoside 5' diphosphate kinase (NDP kinase) in the presence of excess ADP, and ATP is consumed by the highly sensitive firefly luciferase reaction to produce light (Scheele et al., 1995). The reaction, monitored in a photon-counting luminometer (MGM Instruments), contained equal volumes of eluate sample and an enzyme mixture. The latter consisted of ATP Assay Mix (Sigma; FL-AAM), supplemented with 1 μM ADP (purified by HPLC to remove ATP contamination) and 1 unit/mL NDP kinase (Sigma; purified by dialysis). Levels of GTP in samples were determined by integrating photon counts over 10 minutes, and subtracting counts obtained for a control sample in which Y13-259 anti-Ras antibody was omitted from the immunoprecipitation. The amount of GDP was determined by equilibrium conversion of GDP and radioactive ATP to ADP and radioactive GTP using NDP kinase, with subsequent separation of GTP and ATP by TLC. 5 μL of sample was reacted with 250 fmol unlabeled ATP, 0.1 μCi [γ-^{32}P]-ATP (purified by TLC), and 25 milliunits of NDP kinase in the presence of 50 mM Tris-HCl pH 7.4 and 10 mM $MgCl_2$ (15 μL total reaction volume) for 90 minutes at 37°C. 10 μL of each reaction mixture was spotted onto a plastic-backed cellulose TLC plate (Baker). After being developed as in (Scheele et al., 1995), the plate was exposed to a Bio-Rad phosphor screen overnight for subsequent imaging and analysis.

5.3 Results

5.3.1 Feedback Desensitization of Ras Guanine Nucleotide Exchange

Activation of Ras is transient in fibroblasts, achieving a maximum after only 2 minutes or so of EGFR stimulation. On the other hand, trafficking of the EGFR between the surface and intracellular compartments reaches a pseudo-steady state after about 20 minutes in NR6 WT cells (Chapter 4). While receptor internalization may play a role in the deactivation of Ras, it is also known that a MEK-dependent feedback loop, acting downstream of receptor activation and upstream of Ras activation, is a potent regulatory mechanism in this pathway.

In order to deconvolute the potential contributions of the MEK-dependent negative feedback loop and EGFR trafficking to Ras deactivation in NR6 WT fibroblasts, the pharmacological agent PD098059 (Alessi et al., 1995) was employed to block the former mechanism. PD098059 selectively binds to MEK and prevents its activation by Raf, and its biological effects exhibit an IC_{50} of approximately 10 μM in NR6 WT cells (Xie et al., 1998). It was first determined whether PD098059 treatment would lead to prolonged activation of Ras, as it does in other fibroblast lines. An assay that assesses Ras guanine

nucleotide exchange was used, as this activity is the proposed target of MEK-dependent desensitization. NR6 WT cells were permeabilized with 0.1% digitonin, in the presence of [α-^{32}P]-GTP, and Ras-associated radioactivity was immunoprecipitated. After two minutes of maximal (20 nM) EGF stimulation, a 3.6-fold increase in Ras-specific GNP exchange was observed when the nonspecific cpm was subtracted (Fig. 5.2). This is in agreement with translocation of exchange activity (measured *in vitro*) to the plasma membrane in NR6 WT, which is elevated about 3-fold after 2 minutes stimulation (Sasaoka et al., 1996). After 20 minutes of EGF stimulation, GNP exchange activity decreased to nearly the basal level, consistent with the desensitization of Ras activation seen in other fibroblast lines. However, treatment with PD098059 led to maintenance of elevated Ras-GNP exchange activity (2.8-fold above basal) after 20 minutes (Figure 5.2). PD098059 had no effect on the basal activity (data not shown). Thus, on the time scale of EGFR trafficking, Ras activation is desensitized in a MEK-dependent manner in NR6 WT cells.

5.3.2 Compartmentalization and Desensitization of pY-EGFR

In the previous chapter, it was demonstrated that the EGFR remains maximally tyrosine-phosphorylated after internalization of EGF, but not TGFα, in NR6 WT cells. This was shown using both pH 3 dissociation of surface-bound ligand and clearance of surface-biotinylated proteins from anti-EGFR immunoprecipitates. The difference in internal receptor activation was not surprising, since TGFα exhibits a much lower affinity than EGF for the EGFR at the acidic pH typically found in sorting endosomes (French et al., 1995). A method for varying the levels of activated EGFR at the surface and in internal compartments independently was also described. In this surface titration protocol, described under *Experimental Procedures*, cellular EGFR saturated with either EGF or TGFα are allowed to internalize, then surface-bound ligand is rapidly dissociated by acid washing. The remaining level of internal receptor is then titrated with varying levels of surface activation, achieved by chasing cells with different concentrations of TGFα.

To assess whether activation of Ras is compartmentalized, the same experimental design was employed in conjunction with inhibition of Ras-GEF desensitization. When the surface titration protocol was performed on PD098059-treated NR6 WT cells, EGF-pretreated cells again yielded higher levels of EGFR activation than TGFα-pretreated cells for each chase concentration of TGFα (Fig. 5.3). However, for the 20 nM TGFα chase condition, the difference in total pY-EGFR between EGF- and TGFα-pretreated cells, while still statistically significant, was diminished relative to that seen without PD098059.

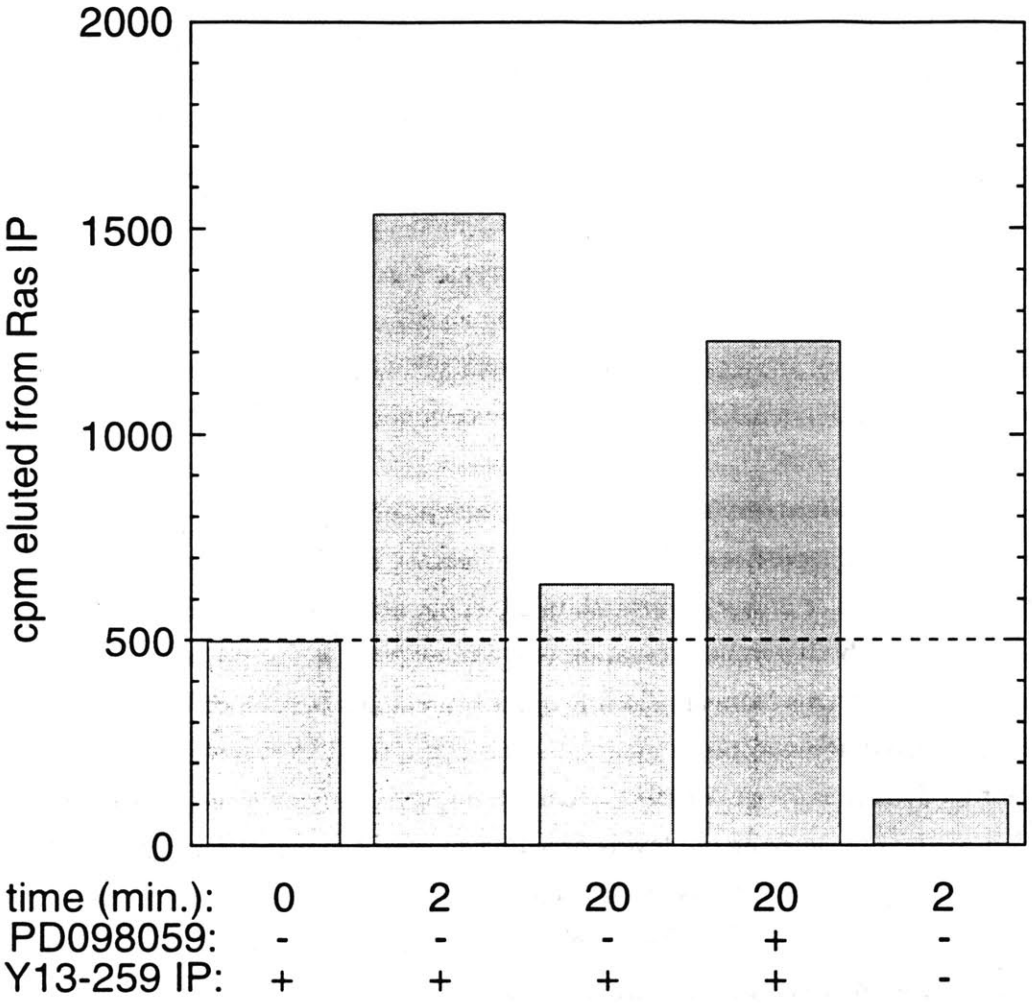

Figure 5.2 MEK-dependent Desensitization of Ras Guanine Nucleotide Exchange. NR6 WT fibroblasts were pretreated with 50 μM PD098059 or vehicle only for 60 minutes, then challenged with 20 nM EGF for the times indicated. The cells were permeabilized with digitonin in the presence of [α-^{32}P]-GTP for 2 minutes, and Ras was immunoprecipitated using Y13-259 monoclonal antibodies. The associated radioactivity reflects the rate of Ras GNP exchange.

This is attributed to changes in feedback mechanisms regulating EGFR kinase and/or tyrosine phosphatase activities (Morrison et al., 1996), rather than to a loss of internal EGFR phosphorylation relative to the surface. That such mechanisms are affected by MEK inhibition is evidenced by comparing EGF-internalized cells chased with 20 nM TGFα that were preincubated with either PD098059 or vehicle only. PD098059 yielded an 18% increase in total EGFR tyrosine phosphorylation (Fig. 5.3). That PD098059 treatment does not drastically affect the surface/internal ratio of cell-associated ligand, after a 20 minute challenge with 20 nM ^{125}I-EGF, was also confirmed. The percent internal was 37% for both no treatment and 0.1% DMSO preincubation, and 32% for PD098059 preincubation. This is expected because the specific pathway of EGFR internalization is largely saturated under these stimulation conditions (Figure 1.4).

5.3.3 Tyrosine Phosphorylation of Shc

Tyrosine phosphorylation of Shc, which affects the ability of Shc to couple Grb2-Sos complexes with Ras activation, was measured in detergent lysates of NR6 WT cells. This was achieved by immunoprecipitation with PY20 anti-phosphotyrosine antibodies, in the presence of phosphatase inhibitors, followed by immunoblotting of separated proteins with polyclonal anti-Shc antibodies. To confirm that the assay procedure was quantitative, NR6 WT cells were treated with or without 20 nM EGF, and different amounts of lysate from EGF-treated cells were subjected to immunoprecipitation and immunoblotting. The detected band intensity was proportional to the amount of lysate used for immunoprecipitation, and phosphorylation of all three Shc isoforms was detected (Fig. 5.4).

To test whether compartmentalization of activated EGFR affects the ability of the receptor to stimulate tyrosine phosphorylation of Shc, cell lysates were generated for the same surface titration conditions used in Fig. 5.3, and equal protein amounts were subjected to immunoprecipitation and Western blotting. A typical immunoblot is shown in Fig. 5.5A. Since Shc is maximally phosphorylated by 1 minute of EGF stimulation in NR6 WT cells (Sasaoka et al., 1996), it was reasoned that pY-Shc is in equilibrium with activation of EGFR on the time scale of the experiments. The level of tyrosine phosphorylated Shc was plotted *versus* pY-EGFR for each experimental condition (Fig. 5.5B). Phosphorylation of the 66 kDa Shc isoform, which has been reported to antagonize signaling through the 46 and 52 kDa isoforms (Okada et al., 1997), is shown as a separate curve. If a signaling readout such as Shc phosphorylation does not depend on the location of activated receptors, then all points would lie on the same curve when the data is plotted in this manner.

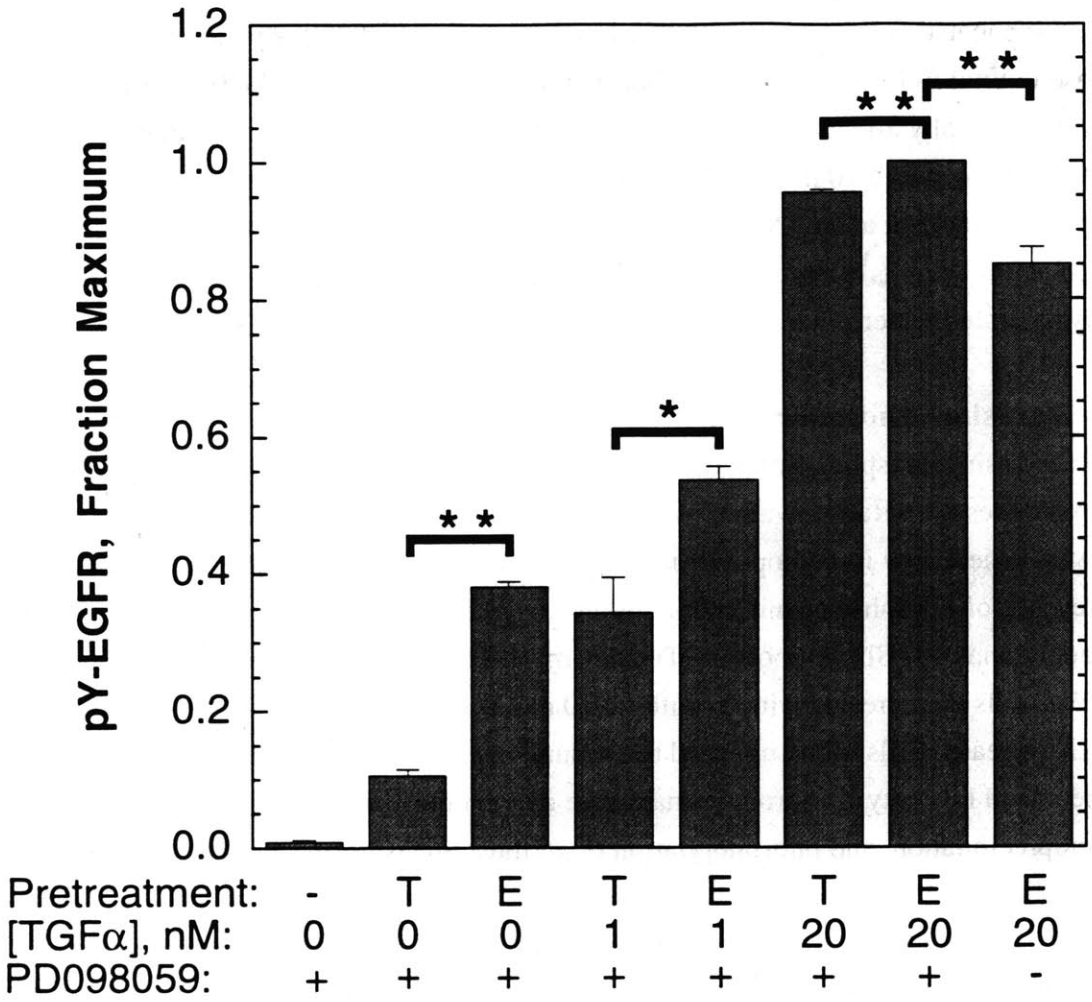

Figure 5.3 Compartmentalization of Activated EGFR. Cells were treated according to the surface titration protocol, and the levels of tyrosine-phosphorylated EGFR in cell extracts were determined using a sandwich ELISA. After preincubation with PD098059 or vehicle only, cells were allowed to internalize TGFα (T) or EGF (E) for 20 minutes. Surface-bound ligand was removed by acid washing, and the indicated concentration of TGFα was subsequently added for 5 minutes before cell lysis. Values are mean ± s.e.m., n = 3; *, students' t-test, $p < 0.05$; **, students' t-test, $p < 0.01$.

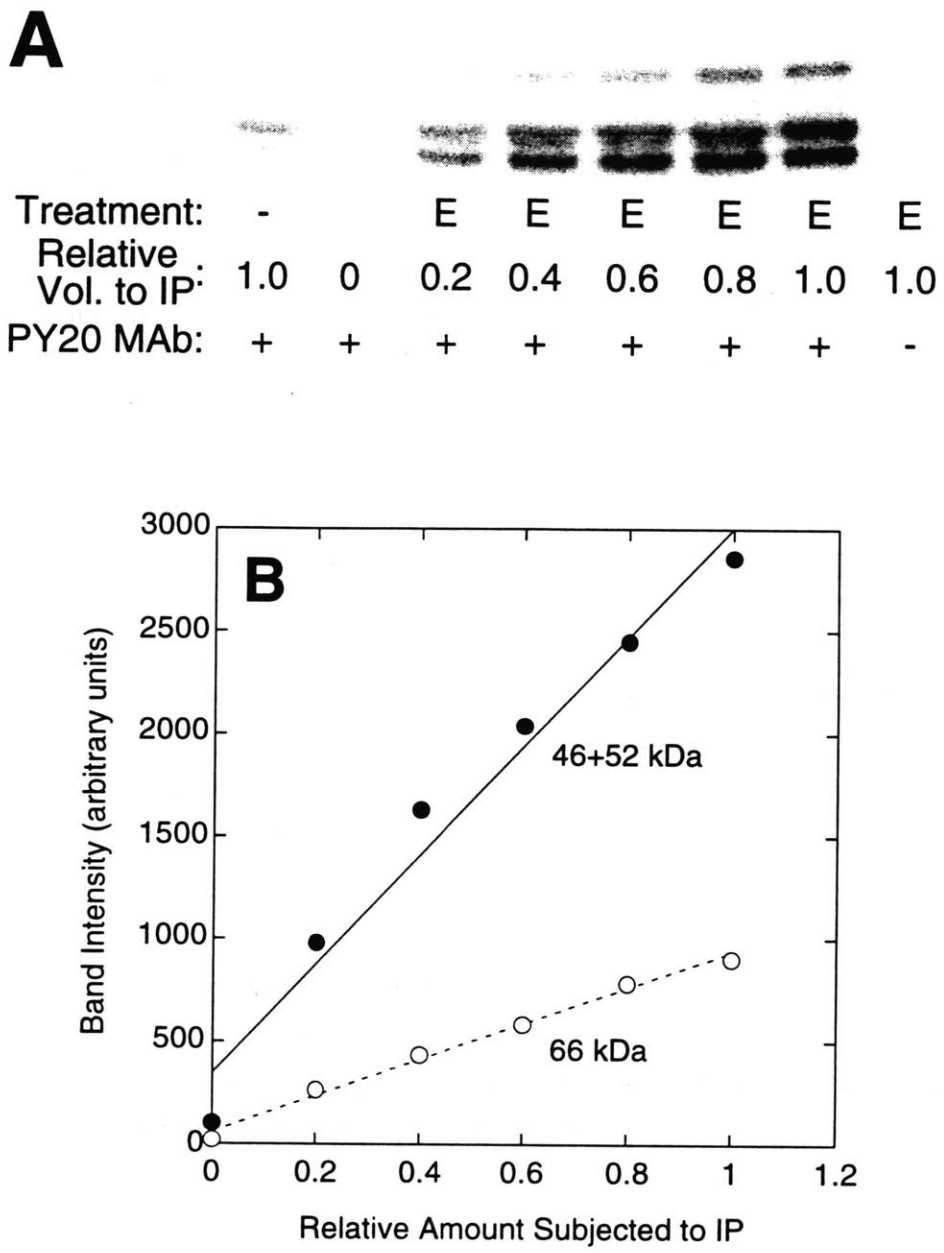

Figure 5.4 Quantitative Immunoblotting of Tyrosine-phosphorylated Shc. Cells were either unstimulated (-) or treated with EGF (E) and lysed. Tyrosine-phosphorylated proteins were immunoprecipitated from the indicated relative volumes of lysate using PY20 monoclonal antibodies, separated by SDS-PAGE, and subjected to immunoblotting with anti-Shc polyclonal antibodies. A, chemiluminescent bands were visualized using a molecular imager. B, analysis of the detected bands for EGF-treated cells confirmed that the assay is quantitative.

For the surface titration protocol, EGF- and TGFα-pretreated cells differ greatly with respect to activation of internal EGFR, yet points for both ligand pretreatments fall on the same curve in Fig. 5.5B. This is consistent with activated EGFR at the plasma membrane and in endosomes contributing equally to Shc phosphorylation. Also, treatment with PD098059 did not affect tyrosine phosphorylation of the 46 and 52 kDa Shc isoforms. This is consistent with the proposed MEK-dependent mechanism of Ras exchange activity desensitization, which acts downstream of Shc phosphorylation by tyrosine kinases.

The relationship between pY-Shc and pY-EGFR is saturable, as Shc phosphorylation was insensitive to receptor autophosphorylation when greater than a third of the EGFR were activated (Fig. 5.5B). This was not due to phosphorylation of all cellular Shc molecules, as only about 10% of cellular Shc could be immunoprecipitated by PY20 antibodies (data not shown). Whether this observed relationship was an artifact of slow Shc dephosphorylation following the acid wash was also tested, by performing a 20 minute dose response with 0.5 - 20 nM EGF or TGFα. Treatment with 0.5 nM TGFα for 20 minutes yields approximately 18% maximal EGFR autophosphorylation (Chapter 4). In this range, Shc phosphorylation was again insensitive to receptor activation (Fig. 5.5C), in accord with a dose response performed by others (Sasaoka et al., 1996). Shc phosphorylation was the same for EGF- and TGFα-treated cells.

5.3.4 Complexation of Shc with EGFR

In addition to tyrosine phosphorylation, recruitment to Ras-containing membranes is expected to play a critical role in the biological activity of Shc. This localization could be mediated by direct binding of Shc to autophosphorylated EGFR, or by binding to erbB-2 transactivated by heterodimerization with EGFR, which may be affected by internalization of the EGFR. The extent of coprecipitation between EGFR and Shc was therefore quantified for the same surface titration conditions used in Figs. 5.3 and 5.5.

Fig. 5.6A shows a typical experiment in which proteins immmunoprecipitated from cell lysates using anti-EGFR antibody 225 were separated by SDS-PAGE, transferred to a PVDF membrane, and probed using anti-Shc antibodies. To maximize recovery of Shc, equal volumes of cell lysate were subjected to immunoprecipitation, with subsequent measurement of total protein concentrations for normalization of detected band intensities. All three Shc isoforms were again detected, but the 66 kDa bands were too weak to be accurately quantified when 500 μg lysate protein or less was subjected to immunoprecipitation. The quantitative relationship between EGFR/Shc (46 and 52 kDa isoforms) coprecipitation and EGFR activation was determined by again plotting the variables for each experimental condition, with pY-EGFR on the x-axis (Fig. 5.6B).

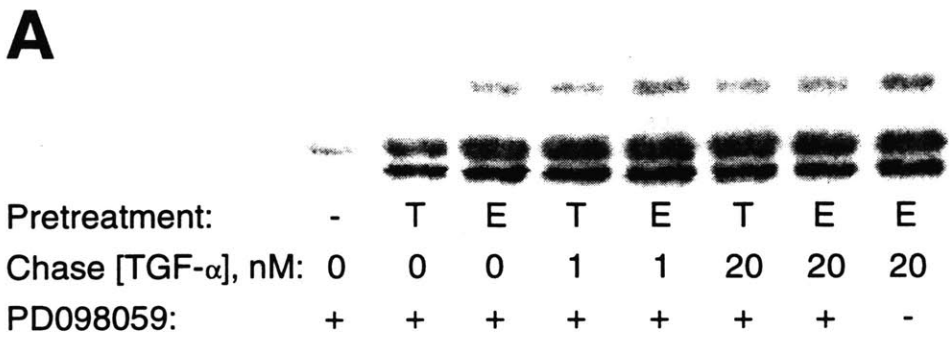

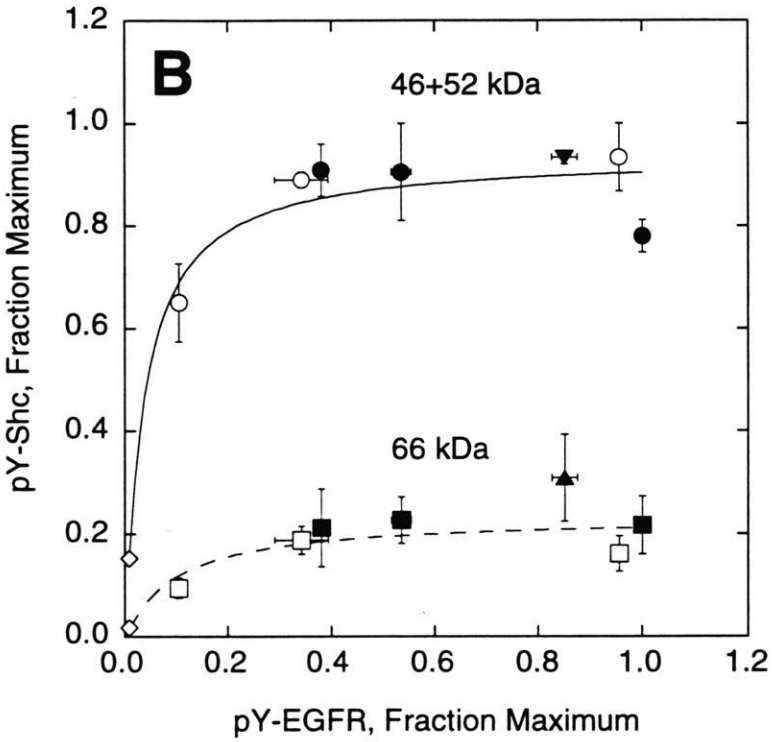

Figure 5.5 Compartmentalization of Shc Tyrosine Phosphorylation. Cells were treated according to the surface titration protocol, and tyrosine-phosphorylated Shc was quantified as in Fig. 5.4. A, representative immunoblot. After preincubation with PD098059 or vehicle only, cells were allowed to internalize TGFα (T) or EGF (E) for 20 min. After acid washing, the indicated concentration of TGFα was added for 5 min. before cell lysis. B, relationship to receptor activation. x-axis values are from Fig. 5.3 (mean ± s.e.m.), and y-axis values are mean ± s.e.m., n = 2. (◇), unstimulated. (○) and (□), pretreatment with TGFα; all closed symbols, pretreatment with EGF. (▼) and (▲), preincubation with 0.1% DMSO only; all others, preincubation with 50 μM PD098059.

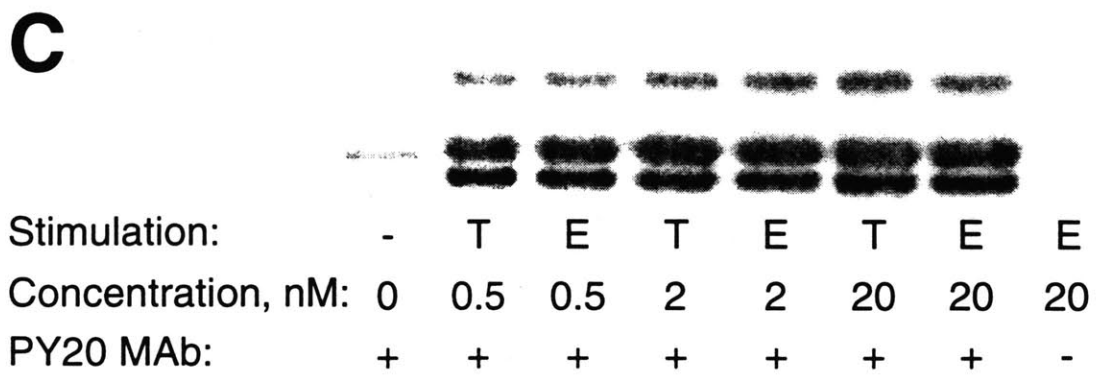

Figure 5.5C Dose Responses of Ligand-stimulated Shc Tyrosine Phosphorylation. Cells were treated with the indicated concentration of TGFα (T) or EGF (E) for 20 minutes, and the levels of pY-Shc in cell lysates were assayed as in A.

Since the surface titration protocol was used, the results indicate that coprecipitation is not affected by EGFR trafficking, since points for EGF- and TGFα-pretreated cells fall on the same curve. Also, PD098059 treatment did not affect the complexation of Shc with activated EGFR (Fig. 5.6B), again consistent with the nature of the proposed MEK-dependent feedback loop. Finally, it was apparent that coprecipitation (and presumably *in vivo* complexation) of EGFR and Shc was more sensitive to changes in receptor activation than tyrosine phosphorylation of Shc (Fig. 5.6C).

5.3.5 Activation of Ras

It has thusfar been established that the ability of the EGFR to elicit membrane recruitment and tyrosine phosphorylation of Shc is not affected by the subcellular location of the activated receptor. However, Shc-dependent activation of Ras could still depend on compartmentalization of the EGFR if the membranes of internal trafficking compartments contained two-dimensional concentrations of Ras that differed from that of the plasma membrane. To ascertain whether generation of Ras-GTP in intact cells is affected by EGFR internalization, an assay described by Scheele and colleagues was employed, which independently measures fmol quantifies of GTP and GDP eluted from Ras immunoprecipitates (Scheele et al., 1995), in conjunction with the surface titration protocol.

GTP was quantified using a kinetic, coupled enzyme assay in which GTP is converted to ATP by NDP kinase in the presence of excess ADP, and ATP is consumed by firefly luciferase in the presence of luciferin to produce light. Measurements using GTP standards confirmed that the kinetics of the reaction were quantitatively consistent with first order conversion of GTP to ATP and first order consumption of ATP. Consistent with that mechanism, integrated photon counts were proportional to the initial amount of GTP in the sample, and the assay could detect as little as 1 fmol GTP (data not shown). Representative kinetic results for surface titration samples are shown in Fig. 5.7A. Control samples in which Y13-259 antibody was omitted from the immunoprecipitation exhibited much lower photon counts and single exponential decay of reaction rate with time, consistent with the absence of GTP (Fig. 5.7A), as did samples in which NDP kinase was excluded from the reaction mixture (data not shown).

GDP was quantified by NDP kinase-mediated conversion to radioactive GTP in a reaction allowed to come to equilibrium, using [γ-^{32}P]-ATP as the phosphate donor. GTP and ATP were then separated by thin layer chromatography. Fig. 5.7B shows a phosphorimage of a typical TLC plate spotted with reacted GDP standards and eluates of Ras immunoprecipitates.

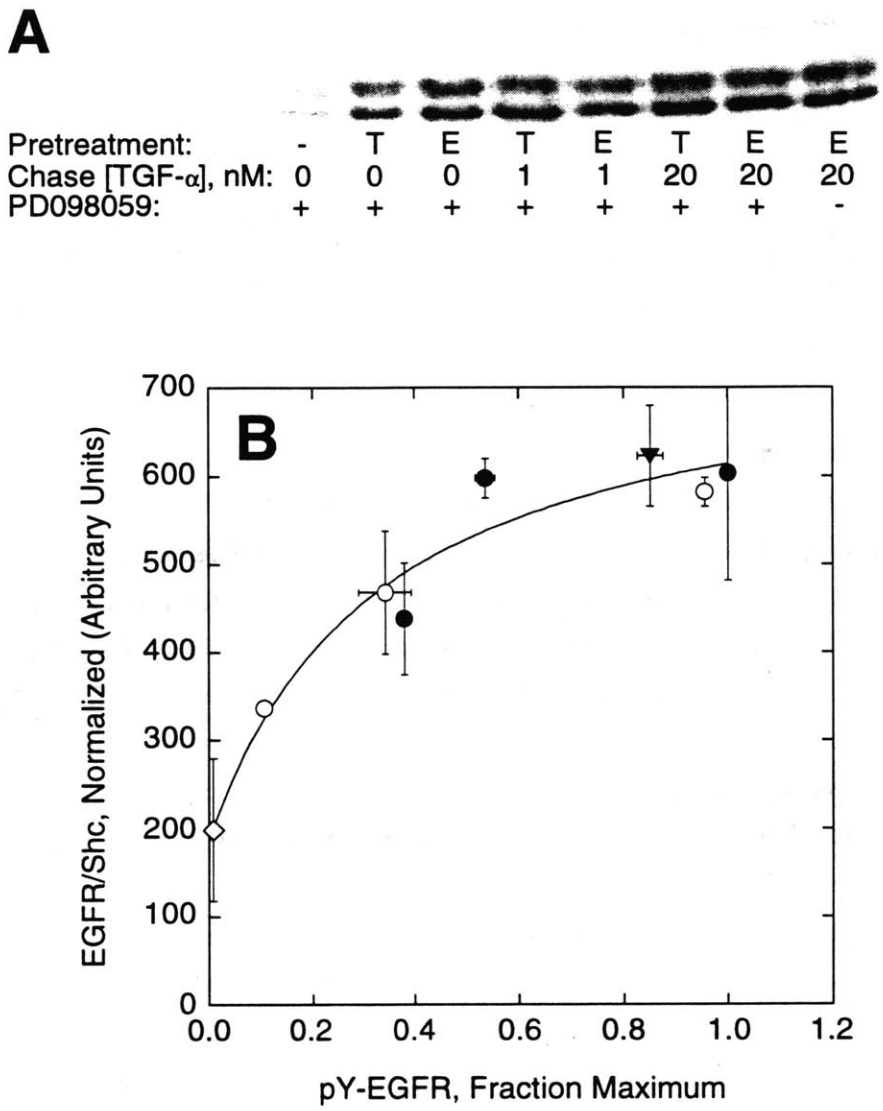

Figure 5.6 Coprecipitation of Shc with Surface and Internal EGFR. Cells were treated according to the surface titration protocol, and the amount of EGFR-associated Shc was assessed by quantitative immunoblotting. A, representative immunoblot. After preincubation with PD098059 or vehicle only, cells were allowed to internalize TGFα (T) or EGF (E) for 20 minutes. Surface-bound ligand was removed by acid washing, and the indicated concentration of TGFα was subsequently added for 5 minutes before cell lysis. B, relationship to receptor activation. x-axis values are from Fig. 5.3 (mean ± s.e.m.), and y-axis values are mean ± s.e.m., n = 2. (◇), no ligand before or after acid wash. (○), pretreatment with TGFα; all closed symbols, pretreatment with EGF. (▼), preincubation with 0.1% DMSO only; all others, preincubation with 50 μM PD098059.

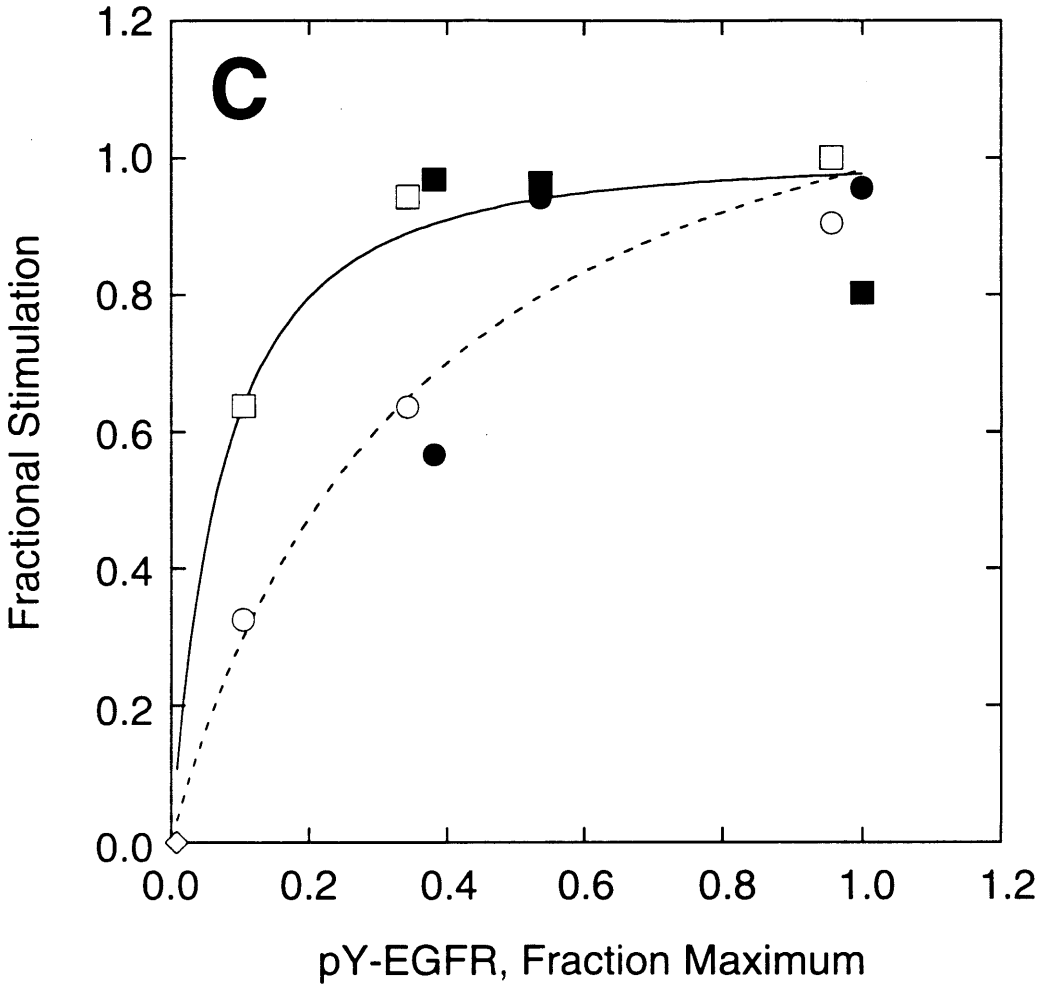

Figure 5.6C EGFR-Shc Coprecipitation and Shc phosphorylation: Comparison of Sensitivity to Receptor Activation. Coprecipitation of Shc with EGFR (circle symbols) is from B, and pY-Shc (square symbols) is from Fig. 5.5B .

For the amounts of ATP added to the reactions, standard curves of fractional conversion *versus* fmol GDP were linear up to 100 fmol GDP. Control samples in which Y13-259 antibody was omitted from the immunoprecipitation yielded no conversion to [γ-^{32}P]-GTP. Based on experiments using GTP and GDP standards, it was estimated that there are approximately 20,000 Ras molecules per NR6 WT cell, in agreement with the amount reported for NIH 3T3 fibroblasts (Scheele et al., 1995). However, roughly 10% of the Ras molecules were GTP-bound in the basal state for NR6 WT, over an order of magnitude higher than in NIH 3T3 cells.

The quantitative relationship between Ras activation, expressed as the ratio of GTP/GDP eluted from cellular Ras, and autophosphorylation of EGFR in surface titration experiments was elucidated by the plot shown in Fig. 5.8. Activation of Ras at maximal EGFR stimulation correlated quantitatively with the GTP loading experiment described in Fig. 5.2. Without inhibition of MEK activation, both the level of Ras-GTP and the rate of Ras GNP exchange desensitized to near basal levels by 20 minutes, whereas PD098059 treatment yielded Ras GTP/GDP and GNP exchange of about 2.8 times the basal level. This is consistent with a Ras activation mechanism in which exchange of GDP for GTP is enhanced while acceleration of GTPase activity is relatively unaffected. As noted for the tyrosine phosphorylation of Shc, the activation of Ras was saturable with respect to pY-EGFR and, importantly, did not seem to depend on compartmentalization of the EGFR. While EGF-pretreated cells exhibited a higher level of Ras-GTP relative to TGFα-pretreated cells, which would be consistent with even more efficient activation of Ras elicited by internal receptors compared to surface receptors, the difference was not significant. It was also confirmed that the saturability of Ras-GTP reflected the true equilibrium relationship at submaximal EGFR activation and not a slow decay after acid washing: PD098059-treated cells stimulated for 20 minutes with 0.5, 2, or 20 nM EGFR (26%, 66%, and 100% EGFR activation respectively) exhibited similar increases in Ras-GTP above the basal level (data not shown).

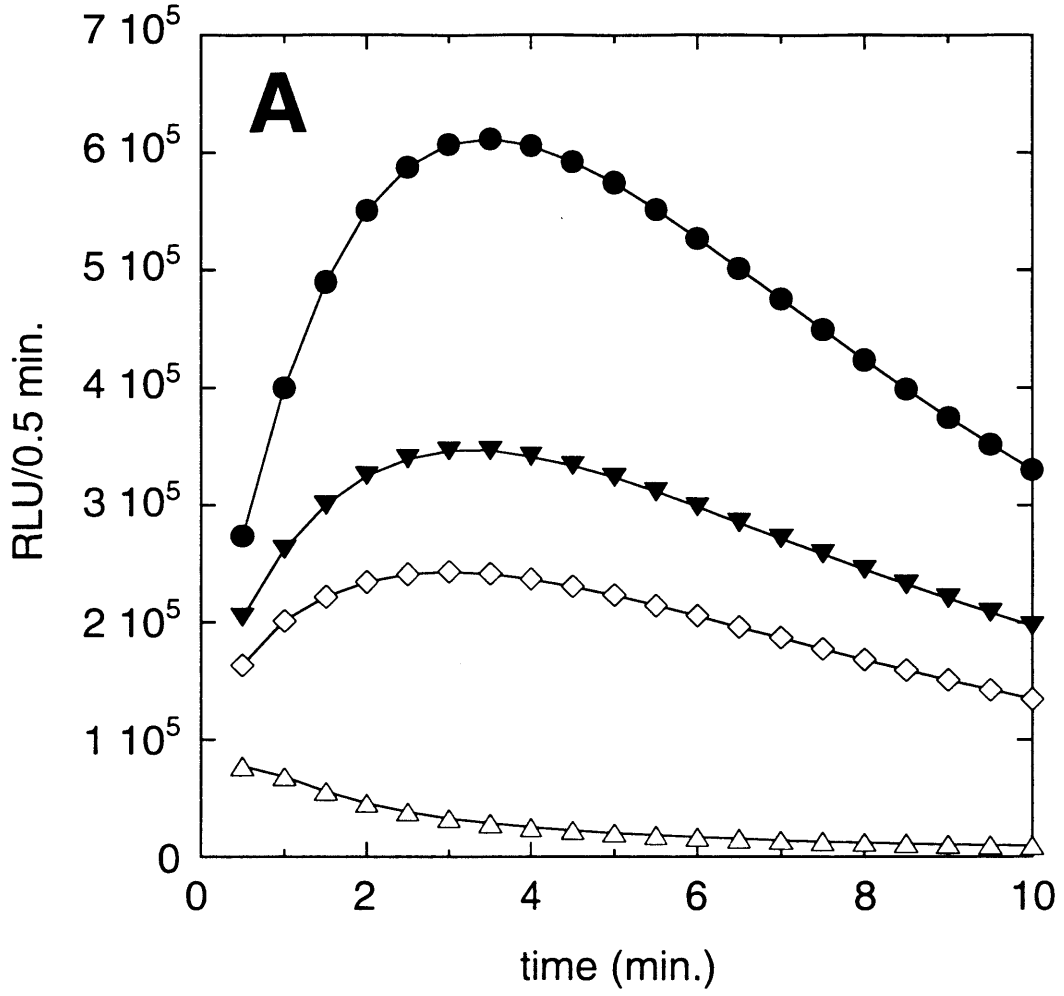

Figure 5.7A GTP Determination. GTP was converted to GDP and ATP by NDP kinase in the presence of excess ADP, and ATP was consumed by firefly luciferase to produce light. The progress of the coupled enzymatic reaction was monitored in a photon-counting luminometer. Shown are representative samples corresponding to cells treated according to the surface titration protocol. (◇), PD098059 preincubation, no ligand stimulation before or after acid wash. (●), PD098059, EGF pretreatment, 20 nM TGFa chase. (▼), same as (●) but PD098059 was omitted. (△), same as (●) but Y13-259 antibody was omitted from the immunoprecipitation.

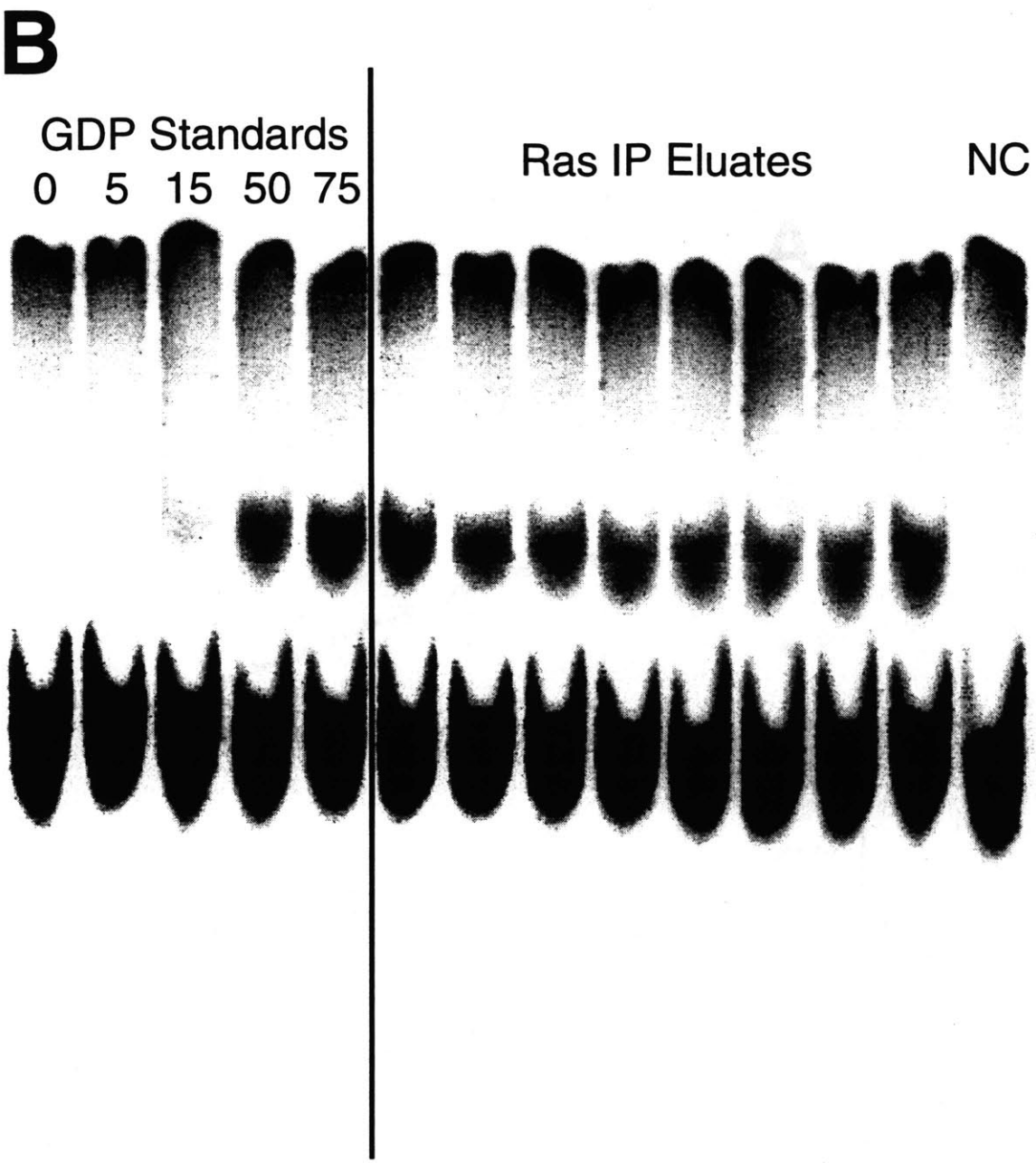

Figure 5.7B GDP Determination. GDP was converted to radioactive GTP by NDP kinase, using [γ-32P]-ATP as the phosphate donor. GTP and ATP were separated by TLC, and the radioactive spots were visualized using a molecular imager. GDP standards, with the initial amount of GDP in fmol indicated, and eluates of Ras immunoprecipitations are shown. The negative control (NC) was maximal cell stimulation conditions and omission of Y13-259 antibody in the immunoprecipitation.

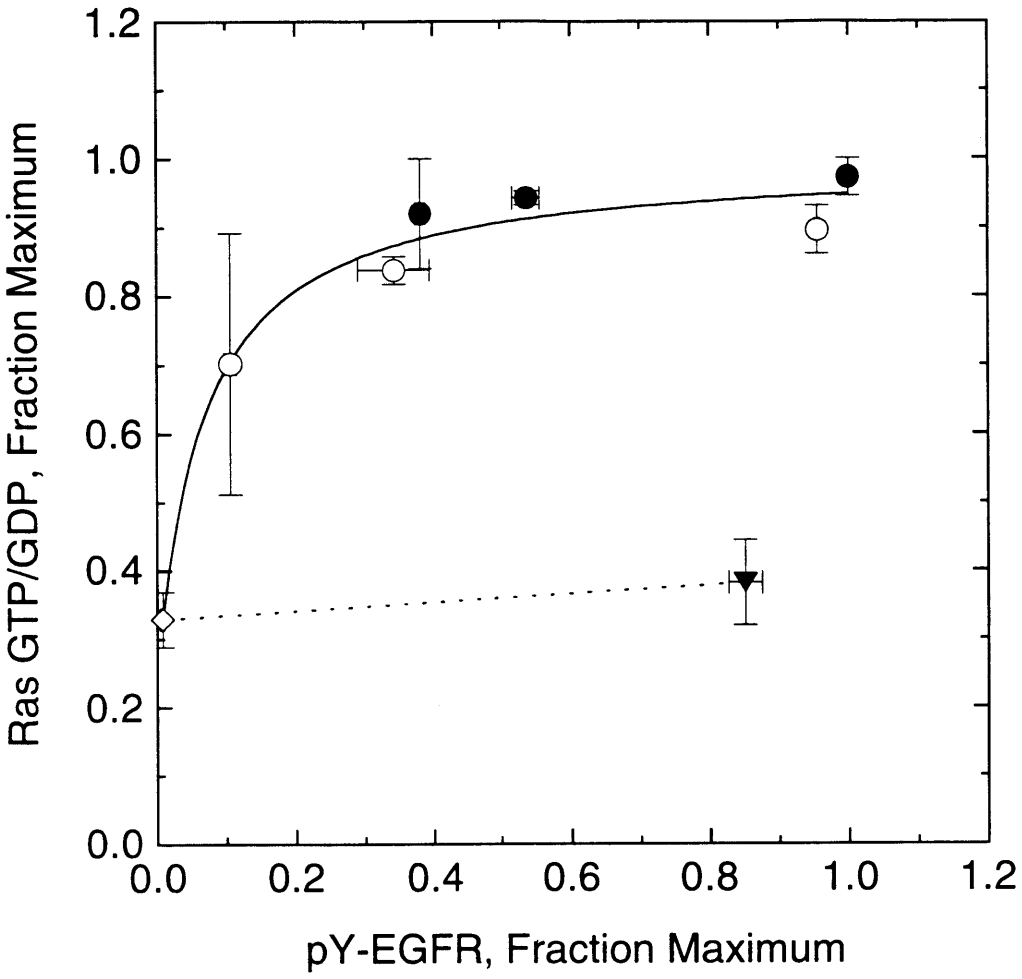

Figure 5.8 Participation of Surface and Internal EGFR in the Activation of Ras. Cells were treated according to the surface titration protocol, and the ratio of GTP/GDP eluted from Ras immunoprecipitates was determined using methods described in Fig. 5.7. The results are plotted as a function of total receptor activation. x-axis values are from Fig. 5.3 (mean ± s.e.m.), and y-axis values are mean ± s.e.m., n = 2. (◇), no ligand before or after acid wash. (○), pretreatment with TGFα; all closed symbols, pretreatment with EGF. (▼), preincubation with 0.1% DMSO only; all others, preincubation with 50 μM PD098059.

5.4 Discussion

The importance of erbB receptor endocytosis and intracellular sorting in controlling cell growth and transformability has been demonstrated in numerous studies, including many using EGFR-expressing NR6 fibroblasts (Wells et al., 1990; Masui et al., 1991; Reddy et al., 1994; Lenferink et al., 1998). However, the regulation of signal transduction via receptor trafficking is complex, since it is not obvious whether signaling ceases immediately after internalization, or if it continues while receptor-ligand complexes remain intact in early endosomes (Baass et al., 1995). In the previous chapter, it was demonstrated that EGFR-mediated PLC-γ1 signaling does not occur in intracellular compartments of NR6 cells, in spite of continued tyrosine phosphorylation of EGFR and PLC-γ1. This is probably because the membrane lipid target of the pathway phosphatidylinositol (4,5)-bisphosphate (PIP_2) is compartmentalized. To extend this concept, the possible effects of subcellular location on the activation of the membrane-associated intermediate Ras were examined.

In fibroblasts, the primary linkage between EGFR and Ras activation is achieved through the tyrosine phosphorylation of Shc. In cells expressing variant EGFR that lack autophosphorylation sites, efficient tyrosine phosphorylation of Shc, activation of the Ras/Erk pathway, and stimulation of mitogenesis have been observed in response to EGF (Gotoh et al., 1994; Soler et al., 1994). This initially suggested that Shc phosphorylation and subsequent binding of Grb2-Sos complexes are sufficient for increased Ras-GNP exchange. Three lines of evidence suggest that membrane localization of Shc-Grb2-Sos complexes is also important. First, since Ras is expected to be mobile in cellular membranes, recruitment of Ras-GEF activity to the membrane would theoretically enhance its association with Ras by at least 1,000-fold (Chapter 2). Second, when the c'973 EGFR truncation mutant is expressed in NR6 cells, membrane recruitment of GEF activity is still observed, as is tyrosine phosphorylation of erbB-2 in trans (Sasaoka et al., 1996). Finally, while EGF elicits Shc phosphorylation, localization of Shc to the plasma membrane, and Erk activation in NR6 cells expressing an EGFR/erbB-2 chimera, cells expressing a kinase-positive, autophosphorylation-negative chimera exhibit efficient tyrosine phosphorylation of Shc but not membrane recruitment of Shc or Erk activation (Lotti et al., 1996). This last result also suggests that tyrosine phosphorylation of receptors is at least permissive for if not directly mediating Shc recruitment. It is also known that EGF treatment can induce recruitment of Shc to endosomal membranes (Di Guglielmo et al., 1994; Lotti et al., 1996), presumably mediated by internalized EGFR-EGF complexes. In rat liver, the time course of Shc recruitment to endosomal membranes parallels that of

internal EGFR autophosphorylation, and the endosome-associated Shc is efficiently tyrosine phosphorylated. Accumulation of tyrosine-phosphorylated Shc in the cytosol is also observed on the same time scale, and it was speculated that this pool could participate in activating Ras at the plasma membrane (Di Guglielmo et al., 1994).

By exploiting the different tendencies of EGF and TGFα to remain associated with the EGFR in endosomes, it was determined that autophosphorylated EGFR at the surface and in internal compartments of NR6 cells expressing wild-type EGFR (NR6 WT) are equal in their ability to form a complex with Shc and, presumably, localize Shc to membranes *in vivo*. Compared to EGFR/Shc coprecipitation, tyrosine phosphorylation of Shc was relatively insensitive to EGFR activation, and the level of pY-Shc did not depend on the surface/internal ratio of activated receptors. In Chapter 3, a mathematical model was formulated that relates the localization and phosphorylation states of soluble receptor tyrosine kinase substrates to the numbers of activated receptors at the cell surface and inside the cell. Since most Shc molecules in the system are not phosphorylated, the relative sensitivities of Shc receptor binding and phosphorylation suggested by Fig. 5.6C are only explained by the theoretical model if: 1) surface and internal receptors do not differ in their Shc binding and phosphorylation properties, 2) Shc is phosphorylated predominantly by an 'intracomplex' mechanism, and 3) Shc-specific tyrosine phosphatase activity in the cytosol is weak, such that pY-Shc persists in the cytosol after dissociation from the receptor (Appendix E). As noted above, EGF-stimulated generation of cytosolic pY-Shc has been observed in rat liver. However, this analysis does assume that coprecipitation accurately reflects binding *in vivo*. Because cell lysis greatly dilutes cellular proteins, coprecipitation is dependent on the stability of a complex in the lysate at 4°C.

The generation of Ras-GTP was also investigated. On the time scale of EGFR trafficking, Ras activation in NR6 WT was desensitized by a MEK-dependent negative feedback loop. This feedback loop, which can be blocked by PD098059 treatment, has been reported to disrupt the complexation of Sos with tyrosine-phosphorylated Shc. Consistent with this model, the upstream events of EGFR/Shc complexation and Shc phosphorylation were not affected by MEK activation. Like Shc phosphorylation, there was an insensitive relationship between stimulation of Ras-GTP and total receptor activation when cells were treated with PD098059. The level of Ras-GTP did not significantly depend on the surface/internal ratio of activated receptors, and certainly internal receptors were no less efficient than surface receptors in contributing to generation of Ras-GTP. This is in direct contrast to hydrolysis of PIP_2 by the PLC pathway in the same cell line.

Two fairly detailed conceptual models adequately explain these findings and tie them in with evidence from other reports, as illustrated in Figure 5.9. In the first model (Fig. 5.9A), Sos is recruited to both the plasma membrane and internal membranes, where Ras is activated. For this model to be quantitatively consistent with the data, the different cellular membranes would have to contain, on average, roughly equal concentrations of Ras. Modeling work showed that this criterion would be satisfied if newly translated Ras proteins were only delivered to the plasma membrane, and if Ras was internalized and sorted with the bulk membrane (Appendix D). If EGFR/Shc coprecipitation is quantitatively related to membrane recruitment of Shc, then two other stipulations must be made: the amount of Sos would have to be limiting with respect to localization of Ras-GEF activity, and Shc-Grb2-Sos complexes would have to be much more stable at the membranes than in the cytosol. The latter would corroborate the observation that formation of Grb2-Sos is often inducible (Buday and Downward, 1993; Ravichandran et al., 1995; Hu and Bowtell, 1996), and stabilization of the complex could be mediated by the PH domain of Sos (McCollam et al., 1995; Karlovich et al., 1995). The main feature of this model is that, with respect to this pathway, the plasma membrane and endosomal membrane environments are equivalent.

In the second model (Fig. 5.9B), Ras-GEF activity simply reflects the total level of pY-Shc in the cell, and Ras is activated at the plasma membrane. If membrane localization of Shc-Grb2-Sos complexes is required, then this would be mediated by a mechanism that is insensitive to or independent of EGFR activation. For example, upon formation of a receptor-Shc-Grb2-Sos complex, an interaction between the Sos PH domain and membrane lipids would be stabilized by analogy to the effect of Sos localization on its association with Ras-GDP. This complex might then allow the Shc PTB domain to rapidly exchange its phosphotyrosine ligand for a lipid (Ravichandran et al., 1997), generating an assembly that could exist transiently as an independent species. The Sos PH domain and Shc PTB domain both bind PIP_2 *in vitro* (Kubiseski et al., 1997; Zhou et al., 1995), and the results of the previous chapter suggest that activated EGFR only have access to this lipid at the plasma membrane. An important feature of this model is that Ras can in principle be deficient or even absent in endosomal membranes, and the contribution of internal EGFR to Ras activation is simply to phosphorylate its fair share of Shc molecules. By immunofluorescence, wild-type Ras is predominantly seen at the plasma membrane (Willumsen et al., 1996), but fractionation of endosomes suggests the presence of Ras (Pol et al., 1998). Indeed, endosomes isolated from EGF-treated A431 cells can activate Erk in cytosolic preparations from unstimulated cells (Xue and Lucocq, 1998).

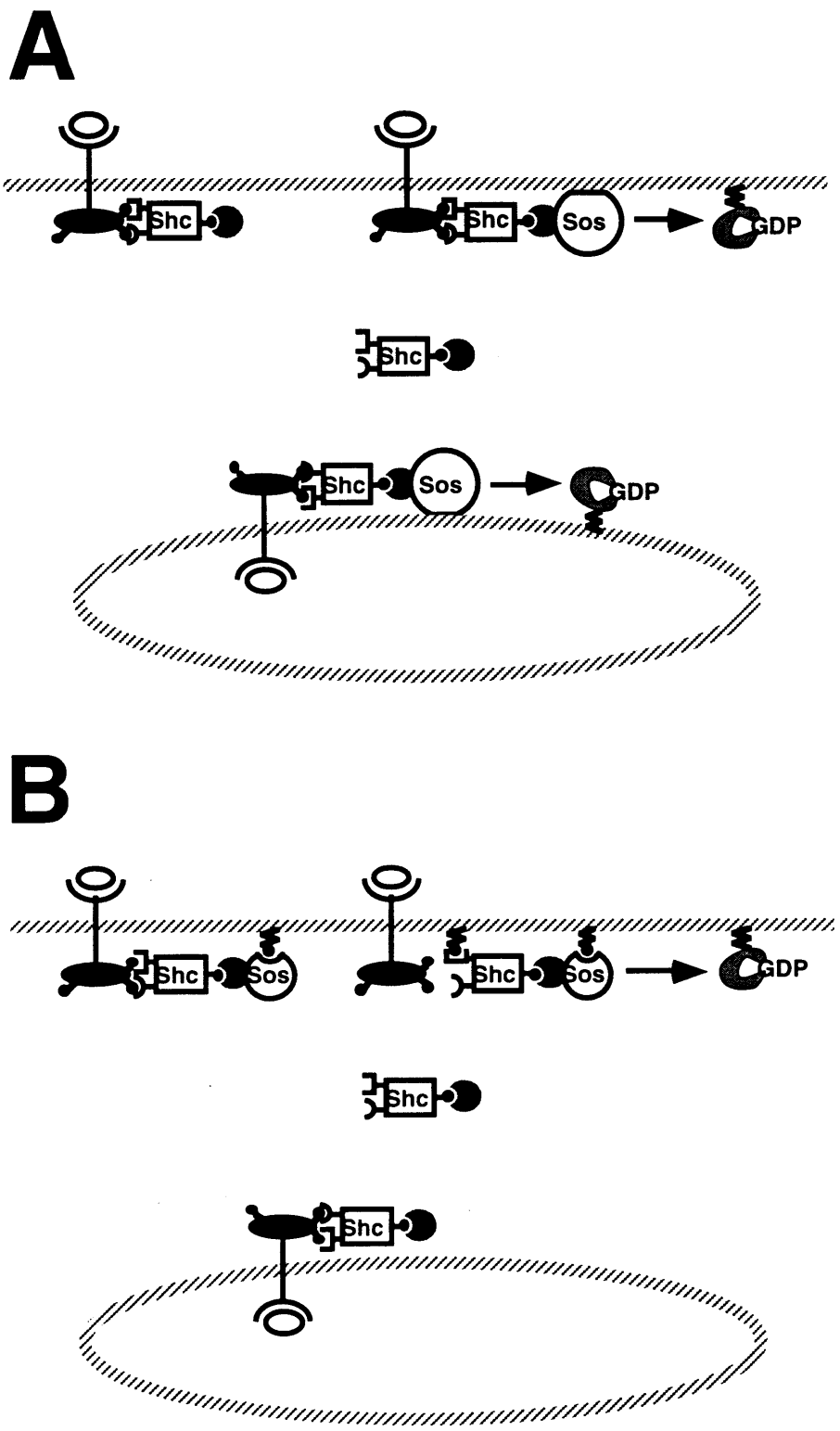

Figure 5.9 Two Models of EGFR-mediated Activation of Ras. See text for details.

5.5 References

Alessi, D.R., Cuenda, A., Cohen, P., Dudley, D.T. and Saltiel, A.R. (1995). PD 098059 is a specific inhibitor of the activation of mitogen-activated protein kinase kinase in vitro and in vivo. *J. Biol. Chem.*, 270: 27489-27494.

Aronheim, A., Engelberg, D., Li, N., Al-Alawi, N., Schlessinger, J. and Karin, M. (1994). Membrane targeting of the nucleotide exchange factor Sos is sufficient for activating the Ras signaling pathway. *Cell*, 78: 949-961.

Baass, P.C., Di Guglielmo, G.M., Authier, F., Posner, B.I. and Bergeron, J.J.M. (1995). Compartmentalized signal transduction by receptor tyrosine kinases. *Trends Cell Biol.*, 5: 465-470.

Batzer, A.G., Rotin, D., Urena, J.M., Skolnik, E.Y. and Schlessinger, J. (1994). Hierarchy of binding sites for Grb2 and Shc on the epidermal growth factor receptor. *Mol. Cell. Biol.*, 14: 5192-5201.

Bos, J.L. (1989). Ras oncogenes in human cancer: a review. *Cancer Res.*, 49: 4682-4689.

Bourne, H.R., Sanders, D.A. and McCormick, F. (1991). The GTPase superfamily: conserved structure and molecular mechanism. *Nature*, 349: 117-127.

Buday, L. and Downward, J. (1993). Epidermal growth factor regulates p21ras through the formation of a complex of receptor, Grb2 adapter protein, and Sos nucleotide exchange factor. *Cell*, 73: 611-620.

Chen, P., Xie, H., Sekar, M.C., Gupta, K. and Wells, A. (1994). Epidermal growth factor receptor-mediated cell motility: phospholipase C activity is required, but mitogen-activated protein kinase activity is not sufficient for induced cell movement. *J. Cell Biol.*, 127: 847-857.

Cussac, D., Frech, M. and Chardin, P. (1994). Binding of the Grb2 SH2 domain to phosphotyrosine motifs does not change the affinity of its SH3 domains for Sos proline-rich motifs. *EMBO J.*, 13: 4011-4021.

de Vries-Smits, A.M.M., Pronk, G.J., Medema, J.P., Burgering, B.M.T. and Bos, J.L. (1995a). Shc associates with an unphosphorylated form of the $p21^{ras}$ guanine nucleotide exchange factor mSos. *Oncogene*, 10: 919-925.

de Vries-Smits, A.M.M., van der Voorn, L., Downward, J. and Bos, J.L. (1995b). Measurements of GTP/GDP exchange in permeabilized fibroblasts. *Methods Enzymol.*, 255: 156-161.

Di Guglielmo, G.M., Baass, P.C., Ou, W., Posner, B.I. and Bergeron, J.J.M. (1994). Compartmentalization of SHC, GRB2 and mSOS, and hyperphosphorylation of Raf-1 by EGF but not insulin in liver parenchyma. *EMBO J.*, 13: 4269-4277.

Downward, J., Parker, P. and Waterfield, M.D. (1984). Autophosphorylation sites on the epidermal growth factor receptor. *Nature*, 311: 483-485.

Ebner, R. and Derynck, R. (1991). Epidermal growth factor and transforming growth factor-α: differential intracellular routing and processing of ligand-receptor complexes. *Cell Regulation*, 2: 599-612.

French, A.R., Tadaki, D.K., Niyogi, S.K. and Lauffenburger, D.A. (1995). Intracellular trafficking of epidermal growth factor family ligands is directly influenced by the pH sensitivity of the receptor/ligand interaction. *J. Biol. Chem.*, 270: 4334-4340.

Gangarosa, L.M., Sizemore, N., Graves-Deal, R., Oldham, S.M., Der, C.J. and Coffey, R.J. (1997). A Raf-independent epidermal growth factor receptor autocrine loop is necessary for Ras transformation of rat intestinal epithelial cells. *J. Biol. Chem.*, 272: 18926-18931.

Gotoh, N., Tojo, A., Muroya, K., Hashimoto, Y., Hattori, S., Nakamura, S., Takenawa, T., Yazaki, Y. and Shibuya, M. (1994). Epidermal growth factor-receptor mutant lacking the autophosphorylation sites induces phosphorylation of Shc protein and

Shc-Grb2/ASH association and retains mitogenic activity. *Proc. Natl. Acad. Sci. USA*, 91: 167-171.

Holt, K.H., Waters, S.B., Okada, S., Yamauchi, K., Decker, S.J., Saltiel, A.R., Motto, D.G., Koretsky, G.A. and Pessin, J.E. (1996). Epidermal growth factor receptor targeting prevents uncoupling of the Grb2-Sos complex. *J. Biol. Chem.*, 271: 8300-8306.

Hu, Y.L. and Bowtell, D.D.L. (1996). Sos1 rapidly associates with Grb2 and is hypophosphorylated when complexed with the EGF receptor after EGF stimulation. *Oncogene*, 12: 1865-1872.

Karlovich, C.A., Bonfini, L., McCollam, L., Rogge, R.D., Daga, A., Czech, M.P. and Banerjee, U. (1995). In vivo functional analysis of the Ras exchange factor son of sevenless. *Science*, 268: 576-579.

Klarlund, J.K., Cherniak, A.D. and Czech, M.P. (1995). Divergent mechanisms for homologous desensitization of $p21^{ras}$ by insulin and growth factors. *J. Biol. Chem*, 270: 23421-23428.

Klemke, R.L., Cai, S., Giannini, A.L., Gallagher, P.J., de Lanerolle, P. and Cheresh, D.A. (1997). Regulation of cell motility by mitogen-activated protein kinase. *J. Cell Biol.*, 137: 481-492.

Kubiseski, T.J., Chook, Y.M., Parris, W.E., Rozakis-Adcock, M. and Pawson, T. (1997). High affinity binding of the pleckstrin homology domain of mSos1 to phosphatidylinositol (4,5)-bisphosphate. *J. Biol. Chem.*, 272: 1799-1804.

Langlois, W.J., Sasaoka, T., Saltiel, A.R. and Olefsky, J.M. (1995). Negative feedback regulation and desensitization of insulin- and epidermal growth factor-stimulated $p21^{ras}$ activation. *J. Biol. Chem.*, 270: 25320-25323.

Lemmon, M.A. and Schlessinger, J. (1994). Regulation of signal transduction and signal diversity by receptor oligimerization. *Trends Biochem. Sci.*, 19: 459-463.

Lenferink, A.E.G., Pinkas-Kramarski, R., van de Poll, M.L.M., van Vugt, M.J.H., Klapper, L.N., Tzahar, E., Waterman, H., Sela, M., van Zoelen, E.J.J. and Yarden, Y. (1998). Differential endocytic routing of homo- and heterodimeric ErbB tyrosine kinases confers signaling superiority to receptor heterodimers. *EMBO J.*, 17: 3385-3397.

Lotti, L.V., Lanfrancone, L., Migliaccio, E., Zompetta, C., Pelicci, G., Salcini, A.E., Falini, B., Pelicci, P.G. and Torrisi, M.R. (1996). Shc proteins are localized on endoplasmic reticulum membranes and are redistributed after tyrosine kinase receptor activation. *Mol. Cell. Biol.*, 16: 1946-1954.

Masui, H., Wells, A., Lazar, C.S., Rosenfeld, M.G. and Gill, G.N. (1991). Enhanced tumorigenesis of NR6 cells which express non-downregulating epidermal growth factor receptors. *Cancer Res.*, 51: 6170-6175.

McCollam, L., Bonfini, L., Karlovich, C.A., Conway, B.R., Kozma, L.M., Banerjee, U. and Czech, M.P. (1995). Functional roles for the pleckstrin and Dbl homology regions in the Ras exchange factor Son-of-sevenless. *J. Biol. Chem.*, 270: 15954-15957.

Morrison, P., Saltiel, A.R. and Rosner, M.R. (1996). Role of mitogen-activated protein kinase kinase in regulation of the epidermal growth factor receptor by protein kinase C. *J. Biol. Chem.*, 271: 12891-12896.

Okabayashi, Y., Kido, Y., Okutani, T., Sugimoto, Y., Sakaguchi, K. and Kasuga, M. (1994). Tyrosines 1148 and 1173 of activated human epidermal growth factor receptors are binding sites of Shc in intact cells. *J. Biol. Chem.*, 269: 18674-18678.

Okada, S., Kao, A.W., Ceresa, B.P., Blaikie, P., Margolis, B. and Pessin, J.E. (1997). The 66-kDa Shc isoform is a negative regulator of the epidermal growth factor-stimulated mitogen-activated protein kinase pathway. *J. Biol. Chem.*, 272: 28042-28049.

Osterop, A.P.R.M., Medema, R.H., van der Zon, G.C.M., Bos, J.L., Moller, W. and Maassen, J.A. (1993). Epidermal-growth-factor-receptors generate Ras-GTP more efficiently than insulin receptors. *Eur. J. Biochem.*, 212: 477-482.

Ouyang, X.M., Gulliford, T., Huang, G.C. and Epstein, R.J. (1999). Transforming growth factor-alpha short-circuits downregulation of the epidermal growth factor receptor. *J. Cell. Physiol.*, 179: 52-57.

Pawson, T. (1995). Protein modules and signaling networks. *Nature*, 373: 573-580.

Pol, A., Calvo, M. and Enrich, C. (1998). Isolated endosomes from quiescent rat liver contain the signal transduction machinery: differential distribution of activated Raf-1 and Mek in the endocytic compartment. *FEBS Lett.*, 441: 34-38.

Porfiri, E. and McCormick, F. (1996). Regulation of epidermal growth factor receptor signaling by phosphorylation of the Ras exchange factor hSos1. *J. Biol. Chem.*, 271: 5871-5877.

Quilliam, L.A., Huff, S.Y., Rabun, K.M., Wei, W., Park, W., Broek, D. and Der, C.J. (1994). Membrane-targeting potentiates guanine nucleotide exchange factor Cdc25 and Sos1 activation of Ras transforming activity. *Proc. Natl. Acad. Sci. USA*, 91: 8512-8516.

Ravichandran, K.S., Lorenz, U., Shoelson, S.E. and Burakoff, S.J. (1995). Interaction of Shc with Grb2 regulates association of Grb2 with mSos. *Mol. Cell. Biol.*, 15: 593-600.

Ravichandran, K.S., Zhou, M., Pratt, J.C., Harlan, J.E., Walk, S.F., Fesik, S.W. and Burakoff, S.J. (1997). Evidence for a requirement for both phospholipd and phosphotyrosine binding via the Shc phosphotyrosine-binding domain in vivo. *Mol. Cell. Biol.*, 17: 5540-5549.

Reddy, C.C., Wells, A. and Lauffenburger, D.A. (1994). Proliferative response of fibroblasts expressing internalization-deficient epidermal growth factor (EGF) receptors is altered via differential EGF depletion effect. *Biotechnol. Prog.*, 10: 377-384.

Rozakis-Adcock, M., van der Geer, P., Mbamalu, G. and Pawson, T. (1995). MAP kinase phosphorylation of mSos1 promotes dissociation of mSos-Shc and mSos1-EGF receptor complexes. *Oncogene*, 11: 1417-1426.

Sasaoka, T., Langlois, W.J., Bai, F., Rose, D.W., Leitner, J.W., Decker, S.J., Saltiel, A.R., Gill, G.N., Kobayashi, M., Draznin, B. and Olefsky, J.M. (1996). Involvement of ErbB2 in the signaling pathway leading to cell cycle progression from a truncated epidermal growth factor receptor lacking the C-terminal autophosphorylation sites. *J. Biol. Chem.*, 271: 8338-8344.

Sasaoka, T., Langlois, W.J., Leitner, J.W., Draznin, B. and Olefsky, J.M. (1994). The signaling pathway coupling epidermal growth factor receptors to activation of $p21^{ras}$. *J. Biol. Chem.*, 269: 32621-32625.

Scheele, J.S., Rhee, J.M. and Boss, G.R. (1995). Determination of absolute amounts of GDP and GTP bound to Ras in mammalian cells: comparison of parental and Ras-overproducing NIH 3T3 fibroblasts. *Proc. Natl. Acad. Sci. USA*, 92: 1097-1100.

Soler, C., Alvarez, C.V., Beguinot, L. and Carpenter, G. (1994). Potent SHC tyrosine phosphorylation by epidermal growth factor at low receptor density or in the absence of receptor autophosphorylation sites. *Oncogene*, 9: 2207-2215.

van der Geer, P., Hunter, T. and Lindberg, R.A. (1994). Receptor protein-tyrosine kinases and their signal transduction pathways. *Annu. Rev. Cell Biol.*, 10: 251-337.

Vojtek, A.B. and Der, C.J. (1998). Increasing complexity of the Ras signaling pathway. *J. Biol. Chem.*, 273: 19925-19928.

Wells, A., Welsh, J.B., Lazar, C.S., Wiley, H.S., Gill, G.N. and Rosenfeld, M.G. (1990). Ligand-induced transformation by a non-internalizing epidermal growth factor receptor. *Science*, 247: 962-964.

Willumsen, B.M., Cox, A.D., Solski, P.A., Der, C.J. and Buss, J.E. (1996). Novel determinants of H-Ras plasma membrane localization and transformation. *Oncogene*, 13: 1901-1909.

Xie, H., Pallero, A., Gupta, K., Ware, M.F., Chang, P., Witke, W., Kwiatkowski, D.J., Lauffenburger, D.A., Murphy-Illrich, J.E. and Wells, A. (1998). EGF receptor regulation of cell-substratum interactions: EGF induces disassembly of focal adhesions independently of the motility-associated PLCγ signaling pathway. *J. Cell Sci.*, 111: 616-625.

Xue, L.Z. and Lucocq, J. (1998). ERK2 signalling from internalised epidermal growth factor receptor in broken A431 cells. *Cell. Signal.*, 10: 339-348.

Zhou, M.M., Ravichandran, K.S., Olejniczak, E.T., Petros, A.M., Meadows, R.P., Sattler, M., Harlan, J.E., Wade, W.S., Burakoff, S.J. and Fesik, S.W. (1995). Structure and ligand recognition of the phosphotyrosine binding domain of Shc. *Nature*, 378: 584-592.

CHAPTER 6

Receptor-mediated Supply and Hydrolysis of Phosphoinositide Lipids: a Second Generation Mathematical Model

Growth factor-induced cell motility is an important determinant in wound invasion and contraction. The migratory response of fibroblasts to ligands of the epidermal growth factor receptor (EGFR) is dependent on the ability of the receptor to stimulate the intracellular enzyme phospholipase C-γ1 (PLC-γ1). This leads to the hydrolysis of a specific membrane lipid, phosphatidylinositol (4,5)-bisphosphate (PIP_2), an activity modulated positively by membrane localization and tyrosine phosphorylation of the enzyme. In Chapter 4, I described how the internalization of activated EGFR interrupts this signaling pathway, and I quantitatively characterized the relationship between PIP_2 hydrolysis and receptor activation. While a generalized mathematical model had been designed to relate receptor activation to modification of membrane-associated signaling targets such as Ras or PIP_2 (Chapter 3), this model could not adequately explain what was observed experimentally. For this reason, I formulated a second generation mechanistic model that simplifies certain aspects of the generalized model, yet accounts for known or speculated molecular events specific to the PLC pathway. This model, while mathematically very tractable, was sufficiently complex to explain all of the experimental results. Further, I used this model to examine the molecular events necessary to mimic the shapes of experimental activation-response curves, and implications for molecular intervention strategies designed to modulate lipid hydrolysis were elucidated.

6.1 Introduction

Cell surface receptors with intrinsic tyrosine kinase activity such as epidermal growth factor receptor (EGFR) elicit multiple cell responses as a consequence of specific polypeptide ligand recognition. For example, ligation of EGFR stimulates proliferation in cells of epithelial origin, and promotes their enhanced motility on a substratum (Blay and Brown, 1985; Barrandon and Green, 1987; Chen et al., 1994a). This is a critical event in the physiological response to trauma, as dermal fibroblasts migrate into the wound and aid in its repair and closure. Thus, engagement of transmembrane receptors provides quantitative information about the immediate environment and instructions that guide cellular decisions to respond in an appropriate manner.

The molecular bases for signaling of EGFR-stimulated responses, including cell motility in fibroblasts, have been the subject of intense study. In response to ligand binding, the domain responsible for the enzymatic kinase function of EGFR is activated, and multiple tyrosine residues in the intracellular tail of the receptor are autophosphorylated. This promotes intracellular association with soluble, cytosolic proteins that possess SH2 and PTB phosphotyrosine-recognition domains (van der Geer et al., 1994; van der Geer and Pawson, 1995). One such protein is phospholipase C-γ1 (PLC-γ1), an enzyme that catalyzes the hydrolysis of the membrane lipid phosphatidylinositol (4,5)-bisphosphate (PIP_2). This reaction yields two products, the second messengers diacylglycerol and inositol triphosphate, and releases PIP_2-sequestered proteins into the cytosol (Toker, 1998). A link between this signaling pathway and EGFR-mediated fibroblast motility has been clearly established. Manipulation of phospholipase C activity was achieved in the Swiss 3T3-derived NR6 fibroblast line by genetic and pharmacological interventions, and in each case PLC activity correlated positively with cell invasion into an acellular area. Activation of the PLC pathway was an absolute requirement for EGFR-mediated cell migration (Chen et al., 1994b). A subsequent study indicated that PIP_2 hydrolysis is required for liberation of PIP_2-bound gelsolin, an actin-modifying protein, in these cells. Blocking the function of gelsolin also inhibited EGFR-mediated cell motility, confirming a relationship between PLC activity and cytoskeletal modifications that induce cell movement (Chen et al., 1996).

Coupling of PLC-γ1 to activated EGFR modulates the activity of the enzyme, in part, by recruiting it to the membrane. Since PIP_2 is a membrane lipid, the analysis of Chapter 2 predicts that membrane recruitment alone would enhance the observed activity of PLC-γ1 by at least 1000-fold. Coupling to EGFR also enhances the tyrosine phosphorylation of PLC-γ1 by the receptor (Rotin et al., 1992), which positively affects enzymatic activity as well (Goldschmidt-Clermont et al., 1991). This suggests that the model described in Chapter 3, which accounts for both membrane localization and phosphorylation effects, could be used to analyze experimental data relating the rate of PIP_2 hydrolysis and the level of PLC-γ1 phosphorylation to the extent of receptor activation. PIP_2 hydrolysis is assessed experimentally by measuring the accumulation of inositol phosphate (IP) recovered from the cytosol of cells incubated with exogenous lithium, which blocks the dephosphorylation of IP to inositol. PLC-γ1 phosphorylation can be assessed by quantitative Western blotting. In Chapter 4, this kind of data was generated for NR6 fibroblasts expressing wild-type EGFR. Activation-response curves of PIP_2 hydrolysis *versus* EGFR autophosphorylation had an unusual shape, with a sensitive response at low levels of stimulation and a linear response at moderate to high levels of

receptor activation, with no apparent saturation (Figure 6.1A). While the model described in Chapter 3 can mechanistically explain purely linear or saturable relationships, it could not mimic results similar to Fig. 6.1A under any parameter conditions. While the experimental curve could have been caused by a change in the pattern of EGFR autophosphorylation on different sites, this was ruled out when tyrosine phosphorylation of PLC-γ1 was also examined. The activation-response curve for this intermediate molecular event is purely linear (Figure 6.1B).

Implicit in the formulation of the generalized mathematical model described in Chapter 3 is the assumption of constant target molecule concentrations in the membrane compartments. This would be valid if the target modification was reversible and the fraction of modified molecules was small. For example, the activation of the membrane-anchored Ras GTPase in many cell types would be amenable to this assumption. However, experimental evidence overwhelmingly indicates that this assumption is not valid for the hydrolysis of PIP_2 by phospholipase C. The hydrolysis reaction can not be reversed in one step to reform PIP_2 in the plasma membrane. Rather, phosphatidylinositol (PI) is reassembled by PI synthase in the ER (Hsuan and Tan, 1997). PI is then actively transported to the plasma membrane by phosphatidylinositol transfer protein (PITP) (Cockcroft, 1998). That this latter activity is a requirement for maintenance of meaningful PLC signaling indicates that enzymatic activities rapidly turn over PIP_2 (Thomas et al., 1993; Batty et al., 1998). After being delivered to the plasma membrane, PI is phosphorylated by the membrane-associated enzymes PI (4)-kinase and PI(4)P (5)-kinase to generate PIP_2 (Hsuan and Tan, 1997). PIP_2 can then act as the substrate for phospholipase C and other enzymes. The most widely studied signaling protein that competes with PLC for PIP_2 is PI (3)-kinase, an activity linked to prevention of apoptosis in multiple cell types (Toker and Cantley, 1997). Consistent with its role in PIP_2 supply, PITP is also required for maintainence of PI (3)-kinase signaling (Kular et al., 1997).

When PITP and PLC-γ1 are depleted from the cytosol of A-431 cells, both proteins must be added exogenously to reconstitute EGFR-mediated PLC activity. Interestingly, PITP forms a signaling complex with EGFR, PI (4)-kinase, and PLC-γ1 in response to EGF in these cells, suggesting that PIP_2 supply and hydrolysis are coupled (Kauffman-Zeh et al., 1995). This has led to speculation that EGFR-PITP coupling can mediate a direct transfer of PIP_2 to PLC-γ1 bound to the same receptor. Alternatively, the analysis of Chapter 2 indicates that coupling to EGFR might simply function to enhance the ability of PITP to insert PI into the plasma membrane.

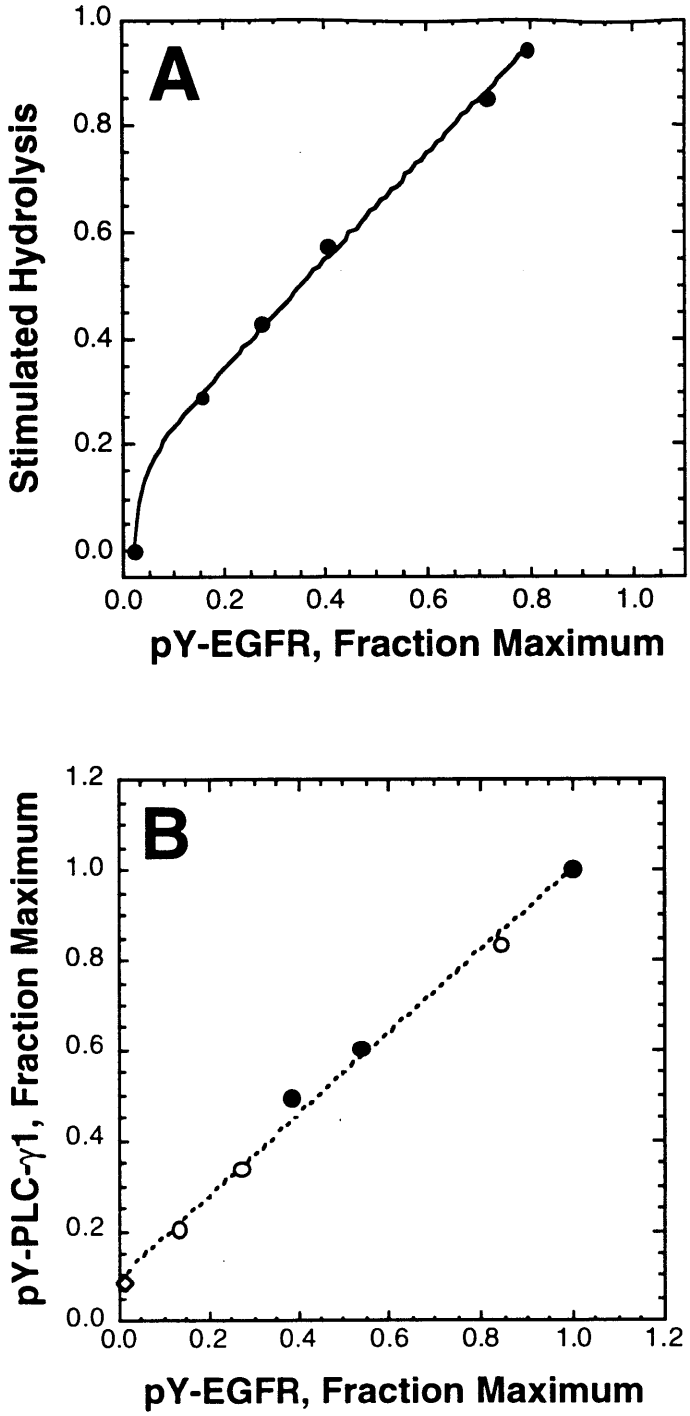

Figure 6.1 Experimental Activation-response Relationships for Wild-type EGFR-expressing NR6 Fibroblasts. A, PIP_2 hydrolysis versus receptor activation, adapted from Fig. 4.11. B, Tyrosine phosphorylation of PLC-γ1 *versus* receptor activation, adapted from Fig. 4.12B.

A second generation mathematical model was formulated that accounts for the supply of PIP_2 available to EGFR-associated PLC-γ1 and its regulation by receptor activation. This model includes only known or widely speculated molecular mechanisms. To simplify the model, only EGFR at the plasma membrane are considered. In Chapter 4, it was determined that receptors associated with internal subcellular compartments do not participate in the modulation of PIP_2 hydrolysis. Activation of predominantly surface receptors can be achieved experimentally by stimulating cells with the EGFR agonist TGFα, which dissociates from the receptor after internalization.

6.2 Mathematical Model

6.2.1 General Considerations

The idealized cellular reaction of interest involves the accumulation of a soluble species, with instantaneous concentration y(t) above the basal level in the cytosol, mediated by an enzyme E that is modulated by active receptors. The precursor for this reaction is an insoluble species found in the plasma membrane, with instantaneous density x(t), which is supplied from an infinite intracellular store by a transfer protein T. The precursor is also depleted by competitive enzymes C. Finally, a direct, receptor-mediated transfer of the precursor to the enzyme E is considered, a pathway that bypasses the insertion of the precursor in the membrane. A schematic of this model is shown in Figure 6.2. For the EGFR-stimulated PLC pathway, y(t) and x(t) represent the levels of IP in the cytosol and PIP_2 in the plasma membrane, respectively. E represents PLC-γ1, T signifies PITP as well as PI 4-kinase and PIP 5-kinase activities, and C represents enzymes like PI 3-kinase that also use PIP_2 as a substrate.

Ordinary differential equations describing x(t) and y(t) are

$$\frac{dx}{dt} = r_T^{\bullet} - \left(k_E^{\bullet} + \sum k_C^{\bullet}\right)x$$

$$\frac{dy}{dt} = r_{T/E}^{\bullet} + k_E^{\bullet}x \qquad (6.1).$$

$$x(0) = \frac{r_T^0}{k_E^0 + \sum k_C^0}; \quad y(0) = 0$$

The asterisk superscripts indicate functions of receptor activity and therefore time. Zero superscripts indicate values in the absence of receptor activity. r_T and $r_{T/E}$ are precursor transfer rates to the plasma membrane and directly to E, respectively, and k_i are observed rate constants describing precursor depletion from the membrane.

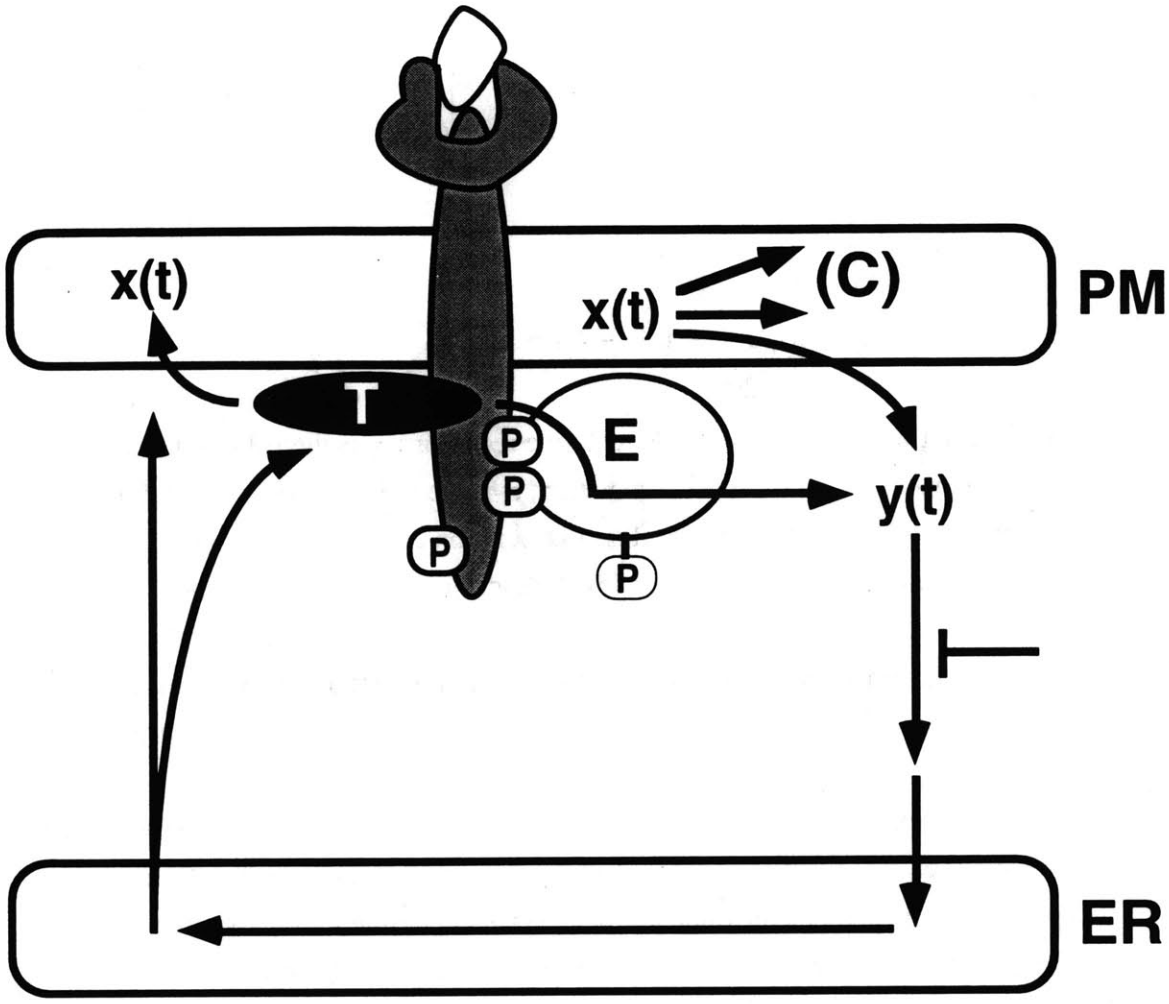

Figure 6.2 Schematic of Model Signaling Pathway. A hydrolytic enzyme E catalyzes the consumption of a plasma membrane (PM) precursor x to form a soluble product y. Experimentally, the metabolism of y is blocked, leading to accumulation in the cytosol. The activity of E is modulated by coupling to activated receptors, as are the activities of competitive enzymes C that also deplete x. The precursor is synthesized in the endoplasmic reticulum (ER), and it is delivered to the plasma membrane by a transfer protein T. The function of T is also modulated by receptor coupling, which may also mediate a direct transfer of the precursor to E on the same receptor.

Rate constants and transfer rates are modulated by binding of the relevant proteins to sites on active receptors. By invoking the simplifying assumptions that proteins associate with active receptors noncompetitively and with 1:1 stoichiometry,

$$
\begin{aligned}
k_i^* &= k_i^0\left(1-\phi_i+\chi_i\phi_i\right) \\
r_T^* &= r_T^0\left\{1-\phi_T+\chi_T\left[1-\left(\frac{r_{T/E}^{max}}{\chi_T r_T^0+r_{T/E}^{max}}\right)\sigma_E\phi_E/p_s\right]\phi_T\right\} \\
r_{T/E}^* &= r_{T/E}^{max}\left(\frac{r_{T/E}^{max}}{\chi_T r_T^0+r_{T/E}^{max}}\right)\sigma_E\phi_E\phi_T/p_s \\
\phi_i &= \frac{\sigma_i+\kappa_i+p_s-\left[(\sigma_i+\kappa_i+p_s)^2-4\sigma_i p_s\right]^{1/2}}{2\sigma_i}
\end{aligned}
\qquad (6.2),
$$

where ϕ_i is the fraction of protein i bound to active receptors, χ_i is the fold-enhancement of protein function proferred by receptor association, σ_i is the ratio of species i/receptor expression levels, and κ_i is the dimensionless dissociation constant (inverse of the affinity), normalized to the total receptor expression level, describing the strength of the species i interaction with active receptors. The key variable here is p_S, the fraction of total receptors that are tyrosine-phosphorylated at the cell surface (and therefore active with respect to this reaction). Implicit in eqn. 6.2 is the assumption that the receptor coupling of intracellular proteins rapidly responds to changes in p_S over time (see Chapter 3).

In line with experimental observations, if the accumulation of y is observed to be linear with time [i.e., x(t) reaches a pseudo-steady state value rapidly and $p_S(t)$ does not deviate appreciably from its mean value on the experimental time scale], then the normalized net rate of y accumulation stimulated by receptor activation is

$$
\begin{aligned}
\frac{\Delta y}{r_T^0 t} &\cong \frac{(1-\phi_E+\chi_E\phi_E)\left\{1-\phi_T+\chi_T\left[1-\frac{\rho\sigma_E\phi_E}{(\chi_T+\rho)p_s}\right]\phi_T\right\}}{1-\phi_E+\chi_E\phi_E+\sum\beta_C(1-\phi_C+\chi_C\phi_C)} \\
&\quad+\frac{\rho\sigma_E\phi_E\phi_T}{(\chi_T+\rho)p_s}-\frac{1}{1+\sum\beta_C} \\
\beta_C &\equiv \frac{k_C^0}{k_E^0};\quad \rho\equiv\frac{r_{T/E}^{max}}{r_T^0}
\end{aligned}
\qquad (6.3).
$$

Given values for the constant parameters, we can thus assess the theoretical dependence of the observed reaction rate as a function of p_S, the pseudo-steady state *activation-response* relationship.

6.2.2 Case 1.1: E binding saturated, T and C binding linear

In this case all E molecules are bound to active receptors ($\phi_E = 1$). Conversely, only a small fraction of transfer protein T and competitive protein C molecules are receptor-associated, such that $\phi_T, \phi_C \propto p_S$. Substituting into eqn. 6.3,

$$\frac{\Delta y}{r_T^0 t} \cong \frac{\chi_E(1+\alpha_T p_s)}{\chi_E+\beta_C(1+\alpha_C p_s)} + \eta\left(\frac{\kappa_E+\sigma_E}{\kappa_T+\sigma_T}\right)\left[\rho - \frac{\chi_E\chi_T}{\chi_E+\beta_C(1+\alpha_C p_s)}\right] - \frac{1}{1+\beta_C} \qquad (6.4a),$$

$$\alpha_i \equiv \frac{\chi_i - 1}{\kappa_i+\sigma_i}; \quad \eta \equiv \left(\frac{\rho}{\chi_T+\rho}\right)\left(\frac{\sigma_E}{\kappa_E+\sigma_E}\right)$$

where from now on the summation over potentially many competing C proteins is implied. A linear dependence on p_S is achieved when receptor stimulation of competitive pathways is not significant ($\chi_E+\beta_C >> \beta_C\alpha_C$):

$$\frac{\Delta y}{r_T^0 t} \cong \frac{\beta_C(\chi_E - 1)}{(1+\beta_C)(\chi_E+\beta_C)} + \eta\left(\frac{\kappa_E+\sigma_E}{\kappa_T+\sigma_T}\right)\left(\rho - \frac{\chi_E\chi_T}{\chi_E+\beta_C}\right) + \left(\frac{\chi_E\alpha_T}{\chi_E+\beta_C}\right)p_s \qquad (6.4b)$$

$$\alpha_i \equiv \frac{\chi_i - 1}{\kappa_i+\sigma_i}; \quad \eta \equiv \left(\frac{\rho}{\chi_T+\rho}\right)\left(\frac{\sigma_E}{\kappa_E+\sigma_E}\right)$$

6.2.3 Case 1.2: E and C binding saturated, T binding linear

Here, all E and C molecules are receptor-associated ($\phi_E = \phi_C = 1$), and $\phi_T \propto p_S$. Substituting,

$$\frac{\Delta y}{r_T^0 t} \cong \frac{\beta_C(1-\gamma_C)}{(1+\beta_C)(1+\beta_C\gamma_C)} + \eta\left(\frac{\kappa_E+\sigma_E}{\kappa_T+\sigma_T}\right)\left(\rho - \frac{\chi_T}{1+\beta_C\gamma_C}\right) + \frac{\alpha_T p_S}{1+\beta_C\gamma_C} \qquad (6.5).$$

$$\gamma_C \equiv \frac{\chi_C}{\chi_E}$$

The relationship in this case is a straight line under all parameter conditions. The saturability of the E and C interactions with active receptors requires high affinities ($\kappa_E, \kappa_C << p_S$) and active receptors in excess of E and C levels ($\sigma_E, \sigma_C < p_S$). Obviously, this is not true when $p_S = 0$, so the sensitivity of the transition between no stimulation and the behavior described by eqn. 6.5 as p_S increases depends on the values of κ_E and κ_C. Thus, the mechanistic basis for the shape of the activation-response curve in these first two cases is fairly intuitive: the steep increase in signaling at low p_S is due to saturation of protein-receptor interactions, and the linear response of the signal at moderate to high p_S is due to linear binding of distinct proteins to active receptors.

6.2.4 Case 2.1: T binding saturated, E and C binding linear

In this case, all T molecules are bound to active receptors, and only a small fraction of E and C molecules are receptor-associated. Substituting into eqn. 6.3,

$$\frac{\Delta y}{r_T^0 t} \cong \left[\frac{\chi_T(1+\alpha_E p_S)(1-\eta)}{1+\beta_C+(\alpha_E+\beta_C\alpha_C)p_S}\right] - \frac{1}{1+\beta_C} + \eta\rho \qquad (6.6a).$$

This is a sigmoidal function of p_S, for which the sensitivity relies on the influence of competing reactions. If $\beta_C = 0$, then the hydrolysis rate exhibits an insensitivity to p_S, reflecting the saturation of transfer protein T association with active receptors. This is also true if the enzyme E and competitive proteins exhibit the same responsiveness to receptor activation ($\alpha_E = \alpha_C$).

The greatest sensitivity of eqn. 6.6a to changes in p_S is achieved when the competitive enzymes are not activated by receptor stimulation, and receptor potentiation of the hydrolytic enzyme does not affect the level of precursor in the membrane [$x \approx \chi_T(1-\eta)r_T^0/\Sigma k_C^0$; requires $\alpha_C << 1$, $\beta_C >> 1+\alpha_E$], which is modulated by the constant factor $\chi_T(1-\eta)$:

$$\frac{\Delta y}{r_T^0 t} \cong \eta\rho - \beta^{-1} + \chi_T(1-\eta)\beta^{-1}(1+\alpha_E p_S) \qquad (6.6b).$$

In this case, the activation-response relationship is linear.

6.2.5 Case 2.2: T and C binding saturated, E binding linear

If we modify the above case by saturating the binding of competitive proteins, y accumulation is given by

$$\frac{\Delta y}{r_T^0 t} \cong \frac{(1+\alpha_E p_s)\chi_T(1-\eta)}{1+\alpha_E p_s+\beta_C\chi_C} + \eta\rho - \frac{1}{1+\beta_C} \qquad (6.7a).$$

The greatest sensitivity of eqn. 6.7a to receptor stimulation again occurs when x(t) is not affected by modulation of its hydrolysis [$x \approx \chi_T(1-\eta)r_T^0/\Sigma\chi_C k_C^0$; requires $\beta_C\chi_C >> 1+\alpha_E$]:

$$\frac{\Delta y}{r_T^0 t} \cong \eta\rho - \frac{1}{1+\beta_C} + \frac{\chi_T(1-\eta)}{\chi_C\beta_C}(1+\alpha_E p_s) \qquad (6.7b),$$

but in this case the sensitivity of competitive pathway activities to p_S is a nonissue.

6.2.6 Case 3.1: All protein-receptor interactions linear

In this case, the fraction of each protein that is receptor-associated is proportional to p_S. Will it still be possible for the activation-response curve to exhibit a steep increase at low p_S, followed by linear behavior? Substituting,

$$\frac{\Delta y}{r_T^0 t} \cong \frac{\left[\frac{\beta_C(\alpha_E-\alpha_C)}{1+\beta_C}\right]p_s + (1+\alpha_E p_s)\left[\frac{\chi_T(1-\eta)-1}{\kappa_T+\sigma_T}\right]p_s}{1+\beta_C+(\alpha_E+\beta_C\alpha_C)p_s} + \left(\frac{\eta\rho}{\kappa_T+\sigma_T}\right)p_s \qquad (6.8a).$$

For $\alpha_E >> 1+\beta_C$, eqn. 6.8a simplifies to

$$\frac{\Delta y}{r_T^0 t} \cong \frac{\beta_C(1-\mu_C)}{(1+\beta_C)(1+\beta_C\mu_C)} + \left[\frac{\chi_T(1-\eta)-1}{1+\beta_C\mu_C} + \eta\rho\right]\frac{p_s}{\kappa_T+\sigma_T}; \quad \mu_C \equiv \frac{\alpha_C}{\alpha_E} \qquad (6.8b).$$

A straight line with (potentially) nonzero y-intercept can therefore be obtained, requiring only that α_E be sufficiently large. Eqn. 6.8b is much like eqn. 6.5, for which all E and C molecules are coupled to active receptors, except that the direct transfer of the precursor to receptor-associated E molecules enhances the magnitude of the slope rather than the y-intercept. Thus, competition for membrane-associated precursor is an absolute requirement for a nonzero intercept in this case. For the intercept to be positive, it is apparent that μ_C must be less than one; competitive proteins must be less responsive to receptor activation than the enzyme E.

6.2.7 Case 3.2: E and T binding linear, C binding saturated

Modifying the above case with saturated binding of competitive proteins to active receptors,

$$\frac{\Delta y}{r_T^0 t} \cong \frac{(1+\alpha_E p_s)\left\{1+\left[\frac{\chi_T(1-\eta)-1}{\kappa_T+\sigma_T}\right]p_s\right\}}{1+\alpha_E p_s+\beta_C\chi_C} + \left(\frac{\eta\rho}{\kappa_T+\sigma_T}\right)p_s - \frac{1}{1+\beta_C} \qquad (6.9a).$$

A linear activation-response relationship is achieved when $1+\alpha_E >> \beta_C\chi_C$; this parameter inequality is exactly the opposite of that which is required for linearity when transfer protein binding to the receptor is also saturated (case 2.2). Substituting,

$$\frac{\Delta y}{r_T^0 t} \cong \frac{\beta_C}{1+\beta_C} + \left[\alpha_T + \frac{\eta(\rho-\chi_T)}{\kappa_T+\sigma_T}\right]p_s \qquad (6.9b).$$

With α_E sufficiently large, the accumulation rate loses all dependence on this parameter as well as χ_C. Compared to eqn. 6.8, the saturation of competitive activities relaxes the parameter constraint on competition pathway responsiveness to receptor stimulation (the dependence on α_C in eqn. 6.8). The existence of a positive intercept is solely dependent on the existence of competitive pathways, and the magnitude of the intercept is positively related to their influence.

6.3 Results

6.3.1 Qualitative Assessment of Special Cases

Thusfar, a mathematical model has been described that addresses the dynamic nature of PIP_2 hydrolysis mediated by phospholipase C. Importantly, this model was formulated to address inconsistencies between a more general model, described in Chapter 3, and experimental data obtained for fibroblasts stimulated with EGFR agonists. In particular, the previous model could not explain why, for moderate levels of EGFR stimulation, the relationship between accumulated PIP_2 hydrolysis and receptor autophosphorylation is described by a straight line with positive y-intercept. As the rest of this section will detail, the new model is complex enough to adequately explain the shapes of these activation-response curves, yet it is mathematically simple in that there are a minimum of adjustable parameters. These are summarized in Table 6.1. To reduce the number of parameters even further, special cases of the model were described in which intracellular protein-receptor interactions are linear (the fraction of a protein species that is receptor-bound is proportional to receptor activation) or saturated (all molecules of a protein species are receptor-bound).

A summary of these special cases is provided as Table 6.2. Of particular interest in the analysis of the model equations were (1) parameter requirements for a linear activation-response relationship between hydrolysis rate and receptor activation, and (2) the effects of certain molecular mechanisms on attributes of this curve (magnitudes of the slope and y-intercept). The latter includes the effects of receptor-mediated enhancement of precursor transfer to the plasma membrane, receptor-mediated transfer directly to the hydrolytic enzyme, and depletion of the membrane precursor by competitive pathways. Thus, the more controversial aspects of PIP_2 regulation can be critically examined in the context of the model.

With respect to the experimental observations in NR6 fibroblasts, cases 1.1 and 1.2 can be ruled out because the tyrosine phosphorylation of PLC-γ1 is proportional to receptor activation (Fig. 6.1B). Referring to Table 6.2, we can therefore conclude that competitive pathways must have a significant influence in order for the activation-response curve to be linear with positive slope and y-intercept. The stimulated activity of the hydrolytic enzyme in the model is proportional to p_S, with coefficient $\alpha_E = (\chi_E - 1)/(\kappa_E + \sigma_E)$. We can also rule out cases for which the parameter requirement for a linear activation-response relationship is unreasonable. Case 2.1 can be ruled out because the modulation of E is expected to be significant, so the requirement for the magnitude of β_C is likely to be too high; also, the restriction on α_C may not be realistic.

	Definition	Comments
σ_i	Number of i molecules per receptor molecule	Must be < 1 to saturate binding of i to the receptor
κ_i	Inverse affinity of i-receptor interaction, scaled to total receptor expression	Must be << 1 to saturate binding of i to the receptor
χ_i	Enhancement of protein function proferred by receptor binding	Includes membrane recruitment and structural changes; expected to be >> 1
β_C	Ratio of competitive/hydrolytic activities in the unstimulated cell	Reflects expression levels and catalytic efficiencies
ρ	Ratio of direct precursor transfer rate to E/basal transfer rate to membrane	For mechanism to be significant, $\rho \sim \chi_T$ or greater.

Table 6.1 Summary of Adjustable Model Parameters.

Case	Sat'ed	Parameter requirement(s) for linearity	R-med. xfer req'ed?	Direct xfer req'ed?	Direct xfer: slope	Direct xfer: y-int	Comp. req'ed?	Comp: slope	Comp: y-int.
1.1	E	$\chi_E+\Sigma\beta_C >> \Sigma\beta_C\alpha_C$	Y	N*	none	+	N*	-	+/-
1.2	E,C	none	Y	N*	none	+	N*	-	+/-
2.1	T	$\alpha_C << 1$ $\Sigma\beta_C >> 1+\alpha_E$	N	N	-	+	Y	-	-
2.2	T,C	$\Sigma\beta_C\chi_C >> 1+\alpha_E$	N	N	-	+	Y	-	-
3.1	none	$\alpha_E >> 1+\Sigma\beta_C$	N*	N*	+	none	Y	-	+/-
3.2	C	$1+\alpha_E >> \Sigma\beta_C\chi_C$	N*	N*	+	none	Y	none	+

* one of these is required

Table 6.2 Molecular Requirements for Model Agreement with Experiment.

The requirement for case 3.2 is not feasible because the value of β_C must be significant for a positive y-intercept, χ_C is expected to greatly exceed 1, and $\alpha_E << \chi_E$ for linear E-receptor coupling. The cases of interest are therefore 2.2 and 3.1, for which the coupling of both T and C molecules to activated receptors are saturated or linear, respectively.

6.3.2 Parameter Analysis: Linear Receptor-protein Interactions

As stated previously, it was somewhat intuitive that the shape of the activation-response relationship observed experimentally could be obtained if either the intracellular interaction of the hydrolytic enzyme or the transfer protein with the receptor was highly saturable, with the other interaction proportional to receptor activation. However, the experimental result could also be mimicked using the second generation model even when all interactions are linear (special case 3.1). The analysis of Table 6.2 shows that competition parameters are very important for this case. To investigate further, certain parameters were set constant: $\sigma_E = 1$, $\sigma_T = \sigma_C = 0.1$, $\kappa_E = \kappa_T = 100$, $\chi_E = 10^4$, $\chi_C = 10^3$, and $\chi_T = 10^2$. The values of χ_i were chosen to reflect membrane recruitment ($\chi_i \sim 10^2$-10^3, Chapter 2), except χ_E was given a higher value to reflect the effect of tyrosine phosphorylation. The other values are somewhat arbitrary, because what matters are the values of the lumped parameters α_i. The above parameters fix $\alpha_E = 99$ and $\alpha_T = 0.99$. For simplicity, a direct precursor transfer mechanism was not considered ($\rho = 0$), because Table 6.2 indicates that it is not a strict requirement for agreement with experiment.

The influence of competition was probed by varying the basal parameter β_C and the dissociation constant κ_C in Figure 6.3. In the absence of competition or direct transfer ($\beta_C = \rho = 0$), the activation-response is a straight line through the origin with slope α_T. Thus, the modulation of precursor hydrolysis is directly related to the modulation of precursor transfer to the membrane elicited by receptor activation. In the presence of competition, the behavior of the curve depends on the relative extents to which receptor activation modulates the hydrolytic and competitive pathways, which depends on the value of κ_C. In Fig. 6.3A, competitive pathways are more responsive to receptor activation ($\mu_C = \alpha_C/\alpha_E > 1$), and the curves have a negative y-intercept in the presence of competition. Interestingly, the value of the y-intercept is a biphasic function of β_C under these conditions (Table 6.2). The slope of the curves is a sensitive function of β_C, decreasing to zero as β_C increases. In Fig. 6.3B, the hydrolytic and competitive pathways are equally responsive ($\mu_C \approx 1$). The curves are lines through the origin with slopes again negatively dependent on β_C. In Fig. 6.3C, the hydrolytic pathway is more responsive to receptor activation ($\mu_C < 1$), and the curves have a positive y-intercept in the presence of competition that is a biphasic function of β_C (Table 6.2). As in Figs. 6.3A&B, the slope decreases from α_T to zero as β_C increases, but the

sensitivity is reduced. In Fig. 6.3D, the competitive pathway is not modulated by receptor activation ($\mu_C = 0$). The y-intercept of the curve is a monophasic, positive function of β_C, and the slope is always equal to α_T.

It is interesting to note that the value of the y-intercept in this nondimensional representation has an upper limit of unity for this case. Therefore the slope, which has as its upper limit α_T, cannot be greater than O(10) or else the positive y-intercept could not be distinguished experimentally.

6.3.3 Parameter Analysis: T and C Binding Saturable

The other case of interest arises when all T and C molecules can be recruited to the membrane at $p_S << 1$. As was seen for the previous case, an analysis of the ratio of the slope to y-intercept of the activation-response curve yields important parameter information. In the absence of direct transfer ($\rho = 0$),

$$\frac{\text{slope}}{\text{intercept}} \approx \alpha_E \left[1 - \frac{\chi_C}{\chi_T} \left(\frac{\beta_C}{1+\beta_C} \right) \right]^{-1} \qquad (6.10).$$

Since this quantity is either greater than α_E or negative, α_E cannot exceed O(10) or else the positive y-intercept could not be distinguished experimentally. In Figure 6.4A, the activation-response curves were determined for $\rho = 0$, $(\chi_T/\chi_C)\chi_E = 10^3$ and α_E equal to 4.95 or 50. For the latter, the y-intercept is too small to distinguish.

In general, if receptor-mediated direct precursor transfer to the hydrolytic enzyme is allowed,

$$\frac{\text{slope}}{\text{intercept}} \approx \alpha_E \left[1 + \frac{\chi_C \beta_C}{\chi_T} \left(\frac{\eta}{1-\eta} \right) \rho - \frac{\chi_C}{\chi_T (1-\eta)} \left(\frac{\beta_C}{1+\beta_C} \right) \right]^{-1} \qquad (6.11a).$$

The addition of the added positive term in the denominator reveals that direct precursor transfer can in principle relax the upper limits on both α_E and χ_C/χ_T. If each activated receptor molecule is coupled to an E molecule ($\sigma_E/\kappa_E >> 1$), then

$$\frac{\text{slope}}{\text{intercept}} \approx \alpha_E \left[1 + \chi_C \beta_C \left(\frac{\rho}{\chi_T} \right)^2 - \frac{\chi_C}{\chi_T} \left(\frac{\beta_C}{1+\beta_C} \right) \left(1 + \frac{\rho}{\chi_T} \right) \right]^{-1} \qquad (6.11b).$$

It is apparent that the relaxation of the upper limit on α_E is not robust; for $\alpha_E >> 10$ the value of ρ/χ_T must be within a narrow range to mimic experimental activation-response curves. This is illustrated in Figure 6.4B, in which $\chi_E = \chi_T = \chi_C = 10^3$ and $\alpha_E = 50$, while ρ is varied.

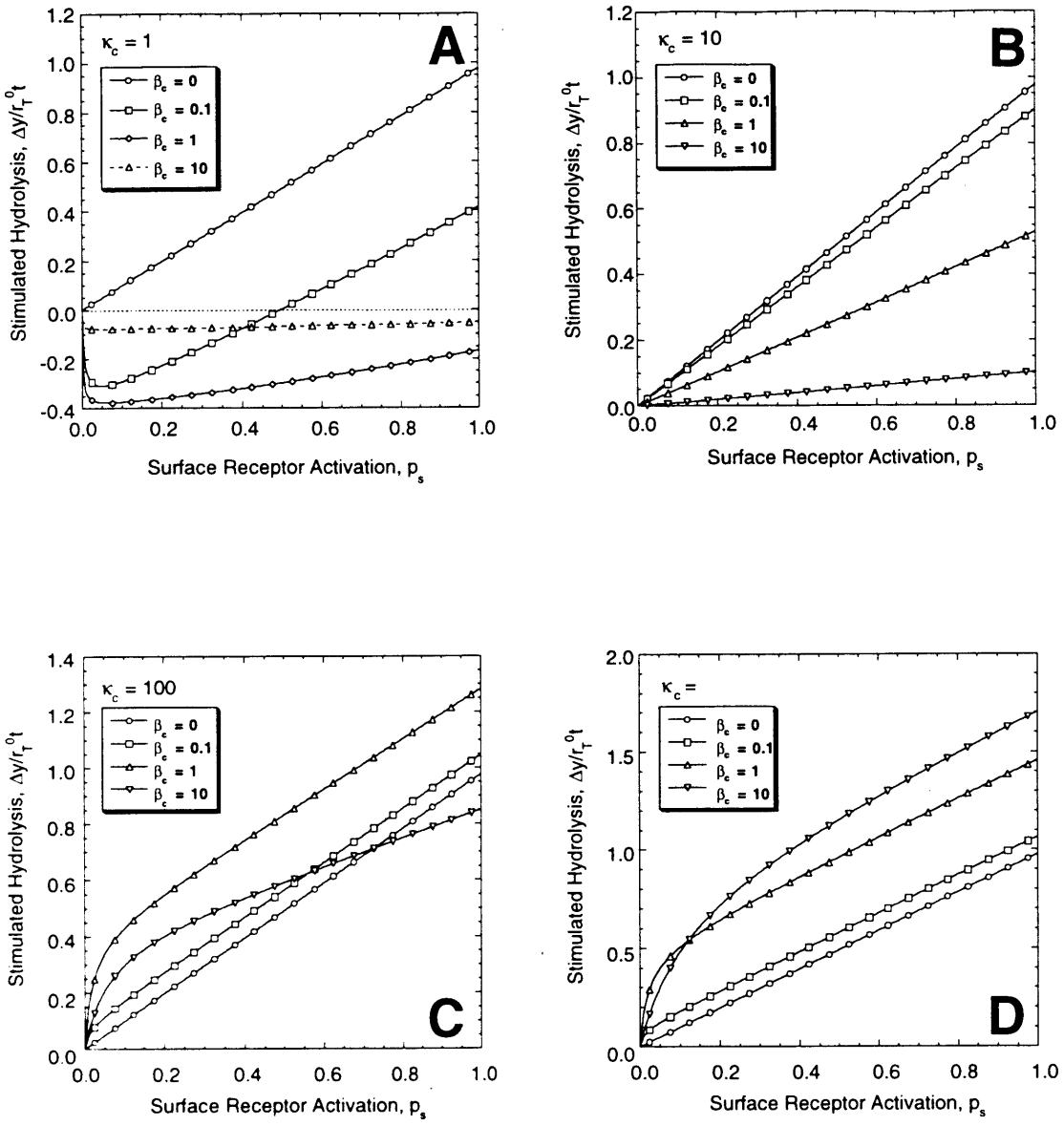

Figure 6.3 Analysis of Presursor Hydrolysis: All Receptor Interactions Linear. Constant parameters are $\sigma_E = 1$, $\sigma_T = \sigma_C = 0.1$; $\kappa_E = \kappa_T = 100$. $\chi_E = 10^4$, $\chi_C = 10^3$, $\chi_T = 10^2$. Direct precursor transfer is not considered ($\rho = 0$), and β_C values are as indicated. A, $\kappa_C = 1$ ($\mu_C = 9.2$); B, $\kappa_C = 10$ ($\mu_C = 1$); C, $\kappa_C = 100$ ($\mu_C = 0.1$); D, $\kappa_C = \infty$ ($\mu_C = 0$).

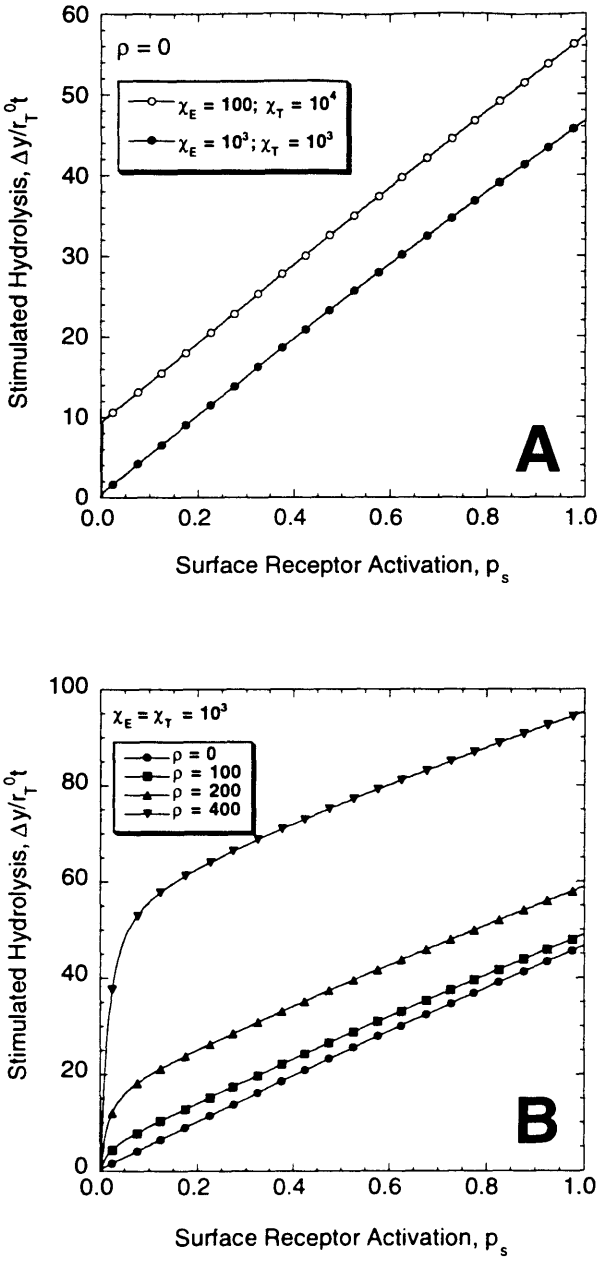

Figure 6.4 Analysis of Precursor Hydrolysis: Transfer Protein- and Competitive Enzyme-receptor Interactions Saturable. Constant parameters are $\sigma_E = \kappa_E = 10$; $\sigma_T = \sigma_C = 0.01$; $\kappa_T = \kappa_C = 0.01$; $\chi_C = 10^3$. Basal competition is moderate ($\beta_C = 1$). A, $\rho = 0$, and χ_E and χ_T values are as indicated; B, $\chi_E = \chi_T = 10^3$, and ρ values are as indicated.

6.4 Discussion

A relatively simple mathematical model of a signaling pathway, incorporating both supply and depletion of the major substrate, was formulated. The supply of the reactant level by a delivery mechanism was included because a more generalized model, which only considered the modulation of enzyme activity, failed to capture the relationship between receptor activation and reaction rate (the *activation-response* curve) seen experimentally. The second generation model does capture the observed behavior, and only known or speculated molecular events were modeled. These included competitive pathways that also deplete the reactant, receptor modulation of precursor transfer to the membrane, and the use of a receptor as a scaffold for a direct transfer of the precursor to the enzyme.

The reaction of interest involves the hydrolysis of an insoluble precursor to generate a soluble second messenger. When the modulation of the hydrolytic enzyme is proportional to receptor activation, as suggested by experimental data (Fig. 6.1B), precursor depletion via competitive pathways is required to mimic the hydrolysis data of Fig. 6.1A. Analysis of the model parameters suggested that two special cases were worthy of further study; these included the case in which the interactions of all intracellular proteins with the receptor are proportional to p_S: $\phi_i \propto p_S$, $<< 1$, and the case in which modulation of transfer and competitive activities are saturable.

For the former, the sensitive increase in hydrolysis seen in Fig. 6.1A is obtained when the hydrolytic pathway is more responsive to receptor activation ($\alpha_E > \alpha_C$). The linear portion that follows the sharp increase relies on the interaction between the transfer protein and activated receptors. The slope is affected both by transfer to the membrane and direct transfer to the enzyme, but only the former is also affected by competition for the precursor. For α_E of sufficient magnitude and no direct transfer ($\rho = 0$), this case was fairly robust with respect to mimicking the experimental results; the quantity $\alpha_T(1+\beta_C^{-1})$ should be within an order of magnitude of unity. One interesting observation was that the magnitude of the hydrolysis rate for a given value of p_S could be a biphasic function of the basal competition parameter β_C. This yields a fairly nonintuitive result: inhibition of the competitive catalytic activities can yield a *decrease* in the net stimulation of hydrolysis, by increasing the basal rate. With respect to drug design and therapeutic strategies, it makes more sense to cripple the binding of competitive enzymes to the receptor. This is made possible by the modular nature of signaling proteins; substrate catalysis and interactions with receptors are usually mediated by independent domains. For the other special case, in which all transfer and competitive proteins are bound to receptors at low p_S, a minimal requirement to mimic Fig. 6.1A in the absence of direct transfer ($\rho = 0$) was $\alpha_E < 10$, $<<$

$\chi_C\beta_C$. The presence of direct transfer relaxed the restriction of α_E to < O(10), but the shape of the activation-response curve was very sensitive to the value of ρ. Thus, when direct transfer must be invoked, the model is not robust.

All of the results outlined here call into serious question the necessity of a direct transfer mechanism to explain the regulation of PIP_2 hydrolysis by phospholipase C. Since it is known that PITP transfers phosphatidylinositol to cellular membranes, and it is currently unknown whether PI can be phosphorylated or PIP_2 can be hydrolyzed while bound to PITP (Cockcroft, 1998; Kearns et al., 1998), it is likely that the primary function of the PITP-EGFR interaction is to modulate transfer to the plasma membrane. Structured modeling of signaling pathways, formulated with a minimum of adjustable parameters, offers a potentially powerful tool for elucidating molecular interventions that manipulate cell function.

6.5 References

Barrandon, Y. and Green, H. (1987). Cell migration is essential for sustained growth of keratinocyte colonies: the roles of transforming growth factor-α and epidermal growth factor. *Cell*, 50: 1131-1137.

Batty, I.H., Currie, R.A. and Downes, C.P. (1998). Evidence for a model of integrated inositol phospholipid pools implies an essential role for lipid transport in the maintenance of receptor-mediated phospholipase C activity in 1321N1 cells. *Biochem. J.*, 330: 1069-1077.

Blay, J. and Brown, K.D. (1985). Epidermal growth factor promotes the chemotactic migration of cultured rat intestinal epithelial cells. *J. Cell. Physiol.*, 124: 107-112.

Chen, P., Gupta, K. and Wells, A. (1994a). Cell movement elicited by epidermal growth factor receptor requires kinase and autophosphorylation but is separable from mitogenesis. *J. Cell Biol.*, 124: 547-555.

Chen, P., Murphy-Ullrich, J.E. and Wells, A. (1996). A role for gelsolin in actuating epidermal growth factor receptor-mediated cell motility. *J. Cell Biol.*, 134: 689-698.

Chen, P., Xie, H., Sekar, M.C., Gupta, K. and Wells, A. (1994b). Epidermal growth factor receptor-mediated cell motility: phospholipase C activity is required, but mitogen-activated protein kinase activity is not sufficient for induced cell movement. *J. Cell Biol.*, 127: 847-857.

Cockcroft, S. (1998). Phosphatidylinositol transfer proteins: a requirement in signal transduction and vesicle traffic. *BioEssays*, 20: 423-432.

Goldschmidt-Clermont, P.J., Kim, J.W., Machesky, L.M., Rhee, S.G. and Pollard, T.D. (1991). Regulation of phospholipase C-γ1 by profilin and tyrosine phosphorylation. *Science*, 251: 1231-1233.

Hsuan, J.J. and Tan, S.K. (1997). Growth factor-dependent phosphoinositide signalling. *Int. J. Biochem. Cell Biol.*, 29: 415-435.

Kauffman-Zeh, A., Thomas, G.M.H., Ball, A., Prosser, S., Cunningham, E., Cockcroft, S. and Hsuan, J.J. (1995). Requirement for phosphatidylinositol transfer protein in epidermal growth factor receptor signaling. *Science*, 268: 1188-1190.

Kearns, B.G., Alb, J.G. and Bankaitis, V.A. (1998). Phosphatidylinositol transfer proteins: the long and winding road to physiological function. *Trends Cell Biol.*, 8: 276-282.

Kular, G., Loubtchenkov, M., Swigart, P., Whatmore, J., Ball, A., Cockcroft, S. and Wetzker, R. (1997). Co-operation of phosphatidylinositol transfer protein with phosphoinositide 3-kinase(γ) in the formylmethionylleucylphenylalanine-dependent production of phosphatidylinositol 3,4,5 trisphosphate in human neutrophils. *Biochem. J.*, 325: 299-301.

Rotin, D., Honegger, A.M., Margolis, B.L., Ullrich, A. and Schlessinger, J. (1992). Presence of SH2 domains of phospholipase $C\gamma_1$ enhances substrate phosphorylation by increasing the affinity toward the epidermal growth factor receptor. *J. Biol. Chem.*, 267: 9678-9683.

Thomas, G.M.H., Cunningham, E., Fensome, A., Ball, A., Totty, N.F., Truong, O., Hsuan, J.J. and Cockcroft, S. (1993). An essential role for phosphatidylinositol transfer protein in phospholipase C-mediated inositol lipid signaling. *Cell*, 74: 919-928.

Toker, A. (1998). The synthesis and cellular roles of phosphatidylinositol 4,5-bisphosphate. *Curr. Opin. Cell Biol.*, 10: 254-261.

Toker, A. and Cantley, L.C. (1997). Signalling through the lipid products of phosphoinositide-3-OH kinase. *Nature*, 387: 673-676.

van der Geer, P., Hunter, T. and Lindberg, R.A. (1994). Receptor protein-tyrosine kinases and their signal transduction pathways. *Annu. Rev. Cell Biol.*, 10: 251-337.

van der Geer, P. and Pawson, T. (1995). The PTB domain: a new protein module implicated in signal transduction. *Trends Biochem. Sci.*, 20: 277-280.

APPENDICES

A. Mean Diffusion Time within a Bounded Cone to a Sink at the Center of its Top Surface

For moderate surface coverages of uniformly distributed, perfectly absorbing sinks on the inside surface of a sphere, the volume afforded each sink can reasonably be defined by a range of angle θ values. For a sink centered on θ = 0, the volume is defined by $|\theta| \le b/a$, where b and a are the half-distance of separation between sink centers and the sphere radius, respectively. Following eqn. 2.5 for the dimensionless mean time to capture τ(r,θ) of randomly distributed molecules contained in the volume,

$$\frac{\partial}{\partial \tilde{r}}\tilde{r}^2\left(\frac{\partial \tau}{\partial \tilde{r}}\right)+\frac{1}{\sin\theta}\frac{\partial}{\partial\theta}\left(\sin\theta\frac{\partial\tau}{\partial\theta}\right)=-\tilde{r}^2$$

$$\left.\frac{\partial\tau}{\partial\theta}\right|_{\theta=0}=\left.\frac{\partial\tau}{\partial\theta}\right|_{\theta=\beta}=0$$

$$\tau|_{\tilde{r}=0} \quad \text{finite} \qquad \text{(A.1)},$$

$$\begin{cases}\left.\dfrac{\partial\tau}{\partial\tilde{r}}\right|_{\tilde{r}=1}=0; & \sigma<\theta<\beta \\ \tau|_{\tilde{r}=1}=0; & 0<\theta<\sigma\end{cases}$$

$$\tau\equiv\frac{WD}{a^2};\quad \tilde{r}\equiv\frac{r}{a};\quad \beta\equiv\frac{b}{a};\quad \sigma\equiv\frac{s}{a}<<1$$

where D is the molecular diffusivity of molecules in the volume and s is the sum of the reacting species radii. The mixed boundary condition at $\tilde{r} = 1$ can be modified by assuming an average "flux" at the sink, its value set to counter the source term (conservation):

$$\left.\frac{\partial\tau}{\partial\tilde{r}}\right|_{\tilde{r}=1}=\begin{cases}0; & \sigma<\theta<\beta \\ -\dfrac{(1-\cos\beta)}{3(1-\cos\sigma)}; & 0<\theta<\sigma\end{cases} \qquad \text{(A.2)}.$$

The PDE can now be solved to within an additive constant, set by stipulating that the mean capture time averaged over the sink area is zero. The resulting mean capture time averaged over space is:

$$\bar{\tau} = \frac{1}{15} + \sum_{n=1}^{\infty} \left(\frac{(1-\eta_b)}{3m_n \int_{\eta_b}^{1} P_{m_n}{}^2(\eta)d\eta} \right) \left(\frac{\int_{\eta_s}^{1} P_{m_n}(\eta)d\eta}{(1-\eta_s)} \right)^2$$

$$= \frac{1}{15} + \sum_{n=1}^{\infty} \left[\frac{(2+1/m_n)}{3(1+\eta_b)P_{m_n}(\eta_b)} \left(\frac{d^2 P_{m_n}}{d\eta dm_n}\bigg|_{\eta_b} \right)^{-1} \right] \left[\frac{(1+\eta_s)}{m_n(m_n+1)} \left(\frac{dP_{m_n}}{d\eta}\bigg|_{\eta_s} \right) \right]^2 \qquad \text{(A.3)},$$

$$\eta = \cos\theta; \quad \eta_b = \cos\beta; \quad \eta_s = \cos\sigma$$

$$\left. \frac{dP_{m_n}}{d\eta} \right|_{\eta_b} = 0$$

where P_{m_n} are Legendre polynomials and m_n are positive but need not be integral.

Unfortunately, this series does not have desirable convergence properties, and the roots of the transcendental equation become increasingly difficult to determine as terms are collected. A simplifying assumption is to solve eqn. A.1 with the modification in eqn. A.2 and $\sin\theta \cong \theta$ ($\beta >> O(\beta^3)$). The resulting PDE is then scalable ($\tilde{q} \equiv \theta/\beta$), a major computational advantage:

$$\beta^2 \frac{\partial}{\partial \tilde{r}} \tilde{r}^2 \left(\frac{\partial \tau}{\partial \tilde{r}} \right) + \frac{1}{\tilde{q}} \frac{\partial}{\partial \tilde{q}} \left(\tilde{q} \frac{\partial \tau}{\partial \tilde{q}} \right) = -\beta^2 \tilde{r}^2$$

$$\left. \frac{\partial \tau}{\partial \tilde{q}} \right|_{\tilde{q}=0} = \left. \frac{\partial \tau}{\partial \tilde{q}} \right|_{\tilde{q}=1} = 0$$

$$\left. \frac{\partial \tau}{\partial \tilde{r}} \right|_{\tilde{r}=1} = \begin{cases} 0; & \tilde{s} < \tilde{q} < 1 \\ -\dfrac{1}{3\tilde{s}^2}; & 0 < \tilde{q} < \tilde{s} \end{cases} \qquad \text{(A.4)}.$$

$$\tilde{s} \equiv \frac{\sigma}{\beta} = \frac{s}{b}$$

This result is identical to a PDE formulated in conical coordinates, and

$$\bar{\tau} \cong \frac{1}{15} + \sum_{n=1}^{\infty} \frac{4}{3(\lambda_n \tilde{s})^2 f_n(\lambda_n)} \left(\frac{J_1(\lambda_n \tilde{s})}{J_0(\lambda_n)} \right)^2$$

$$J_1(\lambda_n) = 0 \qquad \text{(A.5)},$$

$$f_n(\lambda_n) = \frac{-1 + \sqrt{1 + 4(\lambda_n/\beta)^2}}{2} \cong \frac{\lambda_n}{\beta}$$

where J_n are Bessel functions. Since

$$\frac{1}{\sigma N} = \frac{2(1-\cos\beta)}{4\sigma} \cong \frac{\beta^2}{4\sigma} = \frac{\beta}{4\tilde{s}} \qquad \text{(A.6)},$$

a mean time can be constructed that is the sum of a constant and a term inversely proportional to N, as predicted by eqn. 2.7:

$$\bar{\tau} \cong \frac{1}{15} + \frac{1}{3\sigma N}\sum_{n=1}^{\infty} \frac{16}{\tilde{s}(\lambda_n)^3}\left[\frac{J_1(\lambda_n \tilde{s})}{J_0(\lambda_n)}\right]^2 \qquad \text{(A.7)}.$$

This comparison is demonstrated in graphical form as Figure A.1. The apparent advantage of this method is that it allows for interference of the concentration profiles by adjacent sinks of finite separation, and thus may be more accurate than eqn. 2.7 for intermediate sink densities. However, an obvious disadvantage is that eqn. A.7 fails to predict exactly the sparse sink limit; since the depletion zone is close to the sink, the approximations made for the concentration profile at the sink introduce noticeable errors. While the mean capture time averaged over the sink is zero, it is slightly less at $\tilde{q} = 0$ and slightly greater at $\tilde{q} = \tilde{s}$. Since capture favors molecules near reflective boundaries, this results in an overestimate (~ 8%) of $\bar{\tau}(\tilde{s} \rightarrow 0)$. Using the approximate boundary conditions of eqn. A.4, the second term of eqn. A.7 in the sparse sink limit approaches $(32/3\pi)/3\sigma N$ (Shoup et al., 1981) rather than $\pi/3\sigma N$ as in eqn. 2.7.

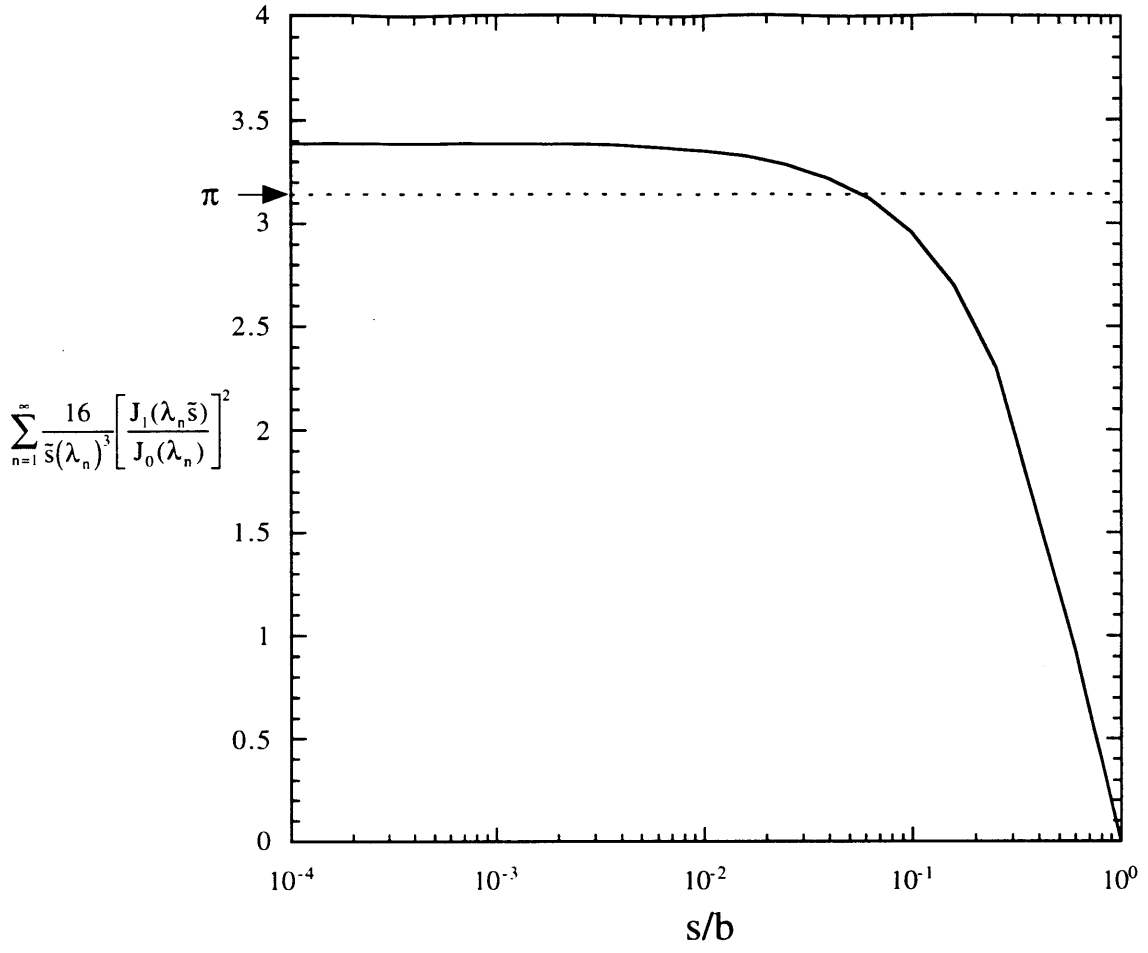

Figure A.1 Computational Analysis of Equation A.7. To determine the approximate mean time to capture of molecules in a conical volume to a sink in the center of the top surface (eqn. A.7), the infinite series

$$\sum_{n=1}^{\infty} \frac{16}{\tilde{s}(\lambda_n)^3}\left[\frac{J_1(\lambda_n\tilde{s})}{J_0(\lambda_n)}\right]^2$$

was estimated, where λ_n are the positive roots of $J_1(\lambda_n) = 0$ and $\tilde{s} \equiv s/b$ as defined in the text. Truncation of the series occurred when the magnitude of a term dropped below 10^{-15}. For sparse sinks ($\tilde{s} << 1$), the concentration gradients around adjacent sinks are independent, and this series converges to a constant. Assuming that the volume is of semi-infinite size yields oblate spheroidal coordinate surfaces and predicts this constant to be π by eqn. 2.7.

B. Receptor-ligand binding and internalization kinetics

An extremely simplified model describing the dynamics of surface receptor-ligand complexes C_s and total surface receptors R_T is

$$\begin{aligned} \dot{C}_s &= k_f[L]R_T - (k_f[L] + k_r + k_e)C_s \\ \dot{R}_T &= -k_e C_s \\ C_s(0) &= 0 \\ R_T(0) &= R_0 \end{aligned} \qquad \text{(B.1)},$$

where k_f, k_r, k_e are rate constants describing ligand association, ligand dissociation, and specific complex internalization, respectively, and [L] is the extracellular ligand concentration, assumed to be constant. Such a model neglects *de novo* receptor synthesis, non-specific (constitutive) internalization, and intracellular receptor sorting; these are fair simplifications for short periods of stimulation. Also neglected is the saturation of the induced endocytic pathway (Lund et al., 1990). The solution is

$$\begin{aligned} \frac{C_s(t)}{R_0} &= \left(\frac{\lambda}{f_1}\right)\sinh(f_1 k_r t)e^{-f_2 k_r t} \\ \frac{R_T(t)}{R_0} &= \left[\left(\frac{f_2}{f_1}\right)\sinh(f_1 k_r t) + \cosh(f_1 k_r t)\right]e^{-f_2 k_r t} \\ f_1 &= \frac{\sqrt{(1+\lambda+\varepsilon)^2 - 4\lambda\varepsilon}}{2} \\ f_2 &= \frac{1+\lambda+\varepsilon}{2} \\ \lambda &\equiv \frac{k_f[L]}{k_r}; \quad \varepsilon \equiv \frac{k_e}{k_r} \end{aligned} \qquad \text{(B.2)}.$$

The activation of the receptor and subsequent auto/transphosphorylation is assumed to be relatively instantaneous upon binding of ligand, and deactivation is considered instantaneous upon ligand dissociation.

The dynamics of $C_s(t)$ follows a biphasic activation profile with time; C_s rises as ligand becomes associated with free receptors, then falls as specific internalization of receptors depletes the total number of surface receptors. The peak value of C_s occurs at a characteristic time t_{peak}:

$$C_{s,peak} = C_s(t_{peak})$$

$$t_{peak} = \frac{\tanh^{-1}\left(\frac{f_1}{f_2}\right)}{f_1 k_r} \qquad \text{(B.3).}$$

Typical parameters for the well-characterized epidermal growth factor (EGF)/EGF-receptor are k_r, $k_e \sim 0.3\ min^{-1}$ ($\varepsilon = 1$) (Lauffenburger and Linderman, 1993). The kinetics of $C_s(t)$ for various values of dimensionless ligand concentration λ are displayed as Figure B.1.

For short time scales ($k_r t$ significantly less than f_1-f_2), note that the level of receptor-ligand complexes can be approximated as a single exponential:

$$\frac{C_s}{R_0} = \left(\frac{\lambda}{2f_1}\right)\left(1 - e^{-2f_1 k_r t}\right)e^{(f_1 - f_2)k_r t} \approx \left(\frac{\lambda}{2f_1}\right)\left(1 - e^{-2f_1 k_r t}\right) \qquad \text{(B.4),}$$

which can simplify the mathematics when the time scale of interest warrants it.

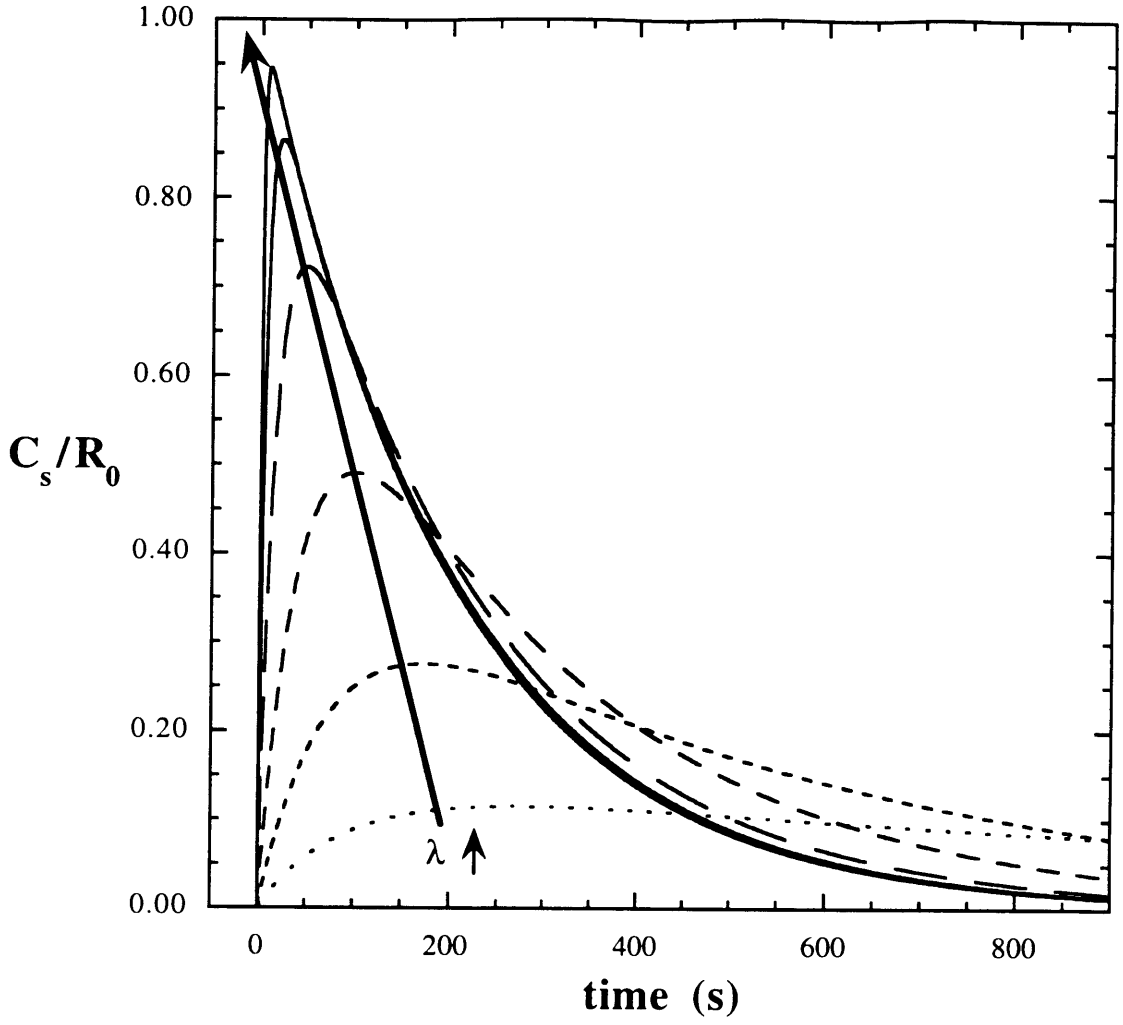

Figure B.1 Time Profiles of C_s, the Level of Surface Receptor-ligand Complexes per Cell. Equation B.2 is plotted for the following parameter values: ligand dissociation rate constant $k_r = 0.005\ s^{-1}$; endocytic rate constant $k_e = 0.005\ s^{-1}$; dimensionless ligand concentrations λ, scaled to the receptor-ligand affinity, of 0.3, 1, 3, 10, 30, and 100. R_0 is the number of free receptors per cell at t = 0.

C. Membrane Recruitment and Zero-order Sensitivity

Model 2 of membrane signaling in Chapter 2 involved membrane-associated regulatory elements that activate and deactivate a signaling protein of interest. By imposing a model in which the modification of the protein is concomitant with association of the regulatory elements, the equilibrium response is hyperbolic (eqn. 2.29). However, in systems in which the signaling protein is covalently modified by positive and negative regulatory enzymes, such as Model 2, the state of the signal can achieve a more sensitive, "switch-like" response to changes in the relative activities of the regulatory elements when either or both enzymes are significantly saturated. How membrane recruitment may be able to reversibly modulate a response between hyperbolic and ultrasensitive behaviors was explored.

Consider a signaling protein expressed intracellularly at ~ 10^4 molecules/cell. At this level, the cytosolic concentration in a typical mammalian cell is ~ 10 nM. Thus, for significant saturation, one or both of the Michaelis constants K_M must in the 1 nM range or lower. However, this is hard to achieve for most signaling molecules. Employing the nomenclature of Goldbeter and Koshland (Goldbeter and Koshland, 1981), K_1 and K_2 are the Michaelis constants of the activating and deactivating enzymes, respectively, and ε_1 and ε_2 are the total enzyme concentrations of the activating and deactivating enzymes, respectively, all scaled to the total substrate concentration W_T. The balance of maximal positive and negative regulatory activities V_1/V_2 is α (not to be confused with the definition of α used in the main text). The mole fraction of unbound, unactivated protein W is then governed by

$$\begin{aligned} &W^3(1-\alpha)+W^2\{(K_1+K_2\alpha)+(1-\alpha)[K_1+\varepsilon_1+\varepsilon_2\alpha-1]\} \\ &\quad +K_1W\{(K_1+\alpha K_2)+(\alpha-2)+(\varepsilon_1+\varepsilon_2\alpha)\}-{K_1}^2=0 \end{aligned} \qquad (C.1),$$

with the mole fractions of other species in terms of W; this equation, which accounts for depletion of free substrate due to binding of the enzymes, is taken directly from Figure 3 of Goldbeter and Koshland. If equilibrium partitioning of the substrate between the cytosol and membrane is allowed, part of the substrate population will experience a significant reduction in K_1 and K_2 if the regulatory enzymes are both membrane-associated. For example, an observed Michaelis constant (based on whole cell volume) is reduced by the factor E (see main text) when the substrate is modified much more rapidly than it dissociates from the enzyme, whereas it is reduced by the factor χ when the reverse is true. If the former is assumed, and the partition coefficient μ describes the membrane/cytosol ratio of unbound substrate regardless of activation state, eqn. C.1 becomes

$$
\begin{aligned}
&W_c^3[(1+\mu)(1+\mu E)^2](1-\alpha) \\
&\quad + W_c^2\{[(1+\mu)(1+\mu E)](K_1 + K_2\alpha) \\
&\qquad + (1-\alpha)[(1+\mu)(1+\mu E)K_1 + (1+\mu E)^2(\varepsilon_1 + \varepsilon_2\alpha - 1)]\} \\
&\quad + K_1 W_c\{(1+\mu)(K_1 + \alpha K_2) + (1+\mu E)[(\alpha-2) + (\varepsilon_1 + \varepsilon_2\alpha)]\} - K_1^2 = 0
\end{aligned}
\qquad \text{(C.2)},
$$

where W_c is the mole fraction of cytosolic, unbound, unactivated substrate. The fraction of the substrate in the active state is $W^*_T = W^*_c + W^*_m + E_2 W^*_c + E_2 W^*_m$, the sum of cytosolic and unbound, membrane-associated and unbound, cytosolic and bound, and membrane-associated and bound substrates in the active state. This output of interest can be calculated in terms of W_c:

$$
W^*_T = \alpha W_c\left[\frac{K_2(1+\mu)}{K_1 + W_c(1-\alpha)(1+\mu E)} + \frac{\varepsilon_2(1+\mu E)}{K_1 + W_c(1+\mu E)}\right] \qquad \text{(C.3)}.
$$

If a case where $K_1 = K_2 = 3$ (near hyperbolic behavior) and $E = 300$ is considered, the cell can achieve observed values of $K_1/E = K_2/E = 0.01$ when all the substrate is recruited to the membrane ($\mu >> 1$). If $\varepsilon_1, \varepsilon_2 > 1$, Goldbeter and Koshland showed that an ultrasensitive response is seen under these conditions as α is modulated from less than to greater than 1. The interesting contribution of membrane recruitment, however, is not simply that zero-order ultrasensitivity can be achieved, but that hyperbolic sensitivity, switchlike sensitivity, and any responses in between can be accessed by modulating the membrane partition coefficient μ.

D: Simplified Receptor Trafficking and Membrane Dynamics

Expressions for $b_s(t)$ and $b_i(t)$ from Chapter 3 are derived that capture the kinetics of receptor internalization and sorting yet remain mathematically tractable. In this model, ligand binds its receptor reversibly via a one-site model, and receptor-ligand complexes are specifically internalized via concentration in clathrin-coated pits. Upon endocytosis, the ligand remains complexed with its receptor, and complexes are retained in endosomes for eventual degradation in lysosomes. This is a fairly accurate representation of trafficking for nondissociative ligands such as murine EGF.

The initial value problem of interest is

$$\frac{db_s}{dt} = k_f[L]r_{sT} - (k_f[L] + k_r + k_e)b_s$$
$$\frac{dr_{sT}}{dt} = v_s - k_e b_s \qquad \text{(D.1)},$$
$$\frac{db_i}{dt} = k_e b_s - k_{deg} b_i$$
$$b_s(0) = b_i(0) = 0; \quad r_{sT}(0) = 1$$

where r_{sT} is the total surface receptors (bound and unbound) per cell scaled to R_T, [L] is the extracellular ligand concentration introduced at time t = 0 (assumed constant for t > 0), k_f and k_r are the forward and reverse rate constants of ligand binding at the cell surface, respectively, k_e is the endocytic rate constant of receptor-ligand complexes, v_s is the rate of *de novo* receptor synthesis scaled to R_T, and k_{deg} is the degradation rate constant of internal complexes. With the following dimensionless variable substitutions:

$$\tau \equiv k_e t$$
$$\lambda \equiv \frac{k_f[L]}{k_r}; \quad \rho \equiv \frac{k_r}{k_e}; \quad \nu \equiv \frac{v_s}{k_e}; \quad \delta \equiv \frac{k_{deg}}{k_e} \qquad \text{(D.2)},$$

the solution to eqn. D.1 is

$$b_s(\tau) = \left[\left(\frac{\rho\lambda - f_2\nu}{f_1}\right)\sinh(f_1\tau) - \nu\cosh(f_1\tau)\right]e^{-f_2\tau} + \nu$$
$$b_i(\tau) = f_3\left[e^{-(f_2+f_1)\tau} - e^{-\delta\tau}\right] - f_4\left[e^{-(f_2-f_1)\tau} - e^{-\delta\tau}\right] + \frac{\nu}{\delta}\left(1 - e^{-\delta\tau}\right) \qquad \text{(D.3)}.$$
$$f_1 = (f_2^2 - \rho\lambda)^{1/2}; \quad f_2 = \frac{1 + \rho(1+\lambda)}{2}$$
$$f_3 = \frac{\rho\lambda - (f_2 - f_1)\nu}{2f_1(f_2 + f_1 - \delta)}; \quad f_4 = \frac{\rho\lambda - (f_2 + f_1)\nu}{2f_1(f_2 - f_1 - \delta)}$$

The kinetics and dose response of b_s, b_i, and $b_T = b_s + b_i$ are displayed as Figure D.1 for parameter values typical of the EGF/EGFR system.

In the derivation of eqn. D.3, constitutive endocytosis was neglected. When the clathrin-coated pit retention elements are not saturated, the observed rate of receptor-ligand complex internalization is several-fold greater than that of the bulk plasma membrane. However, for membrane proteins/lipids that are not concentrated in clathrin-coated pits, constitutive endocytosis and endosomal trafficking processes are the mechanisms by which these molecules are distributed among the plasma membrane, endosomes, and other organelles along the sorting pathway.

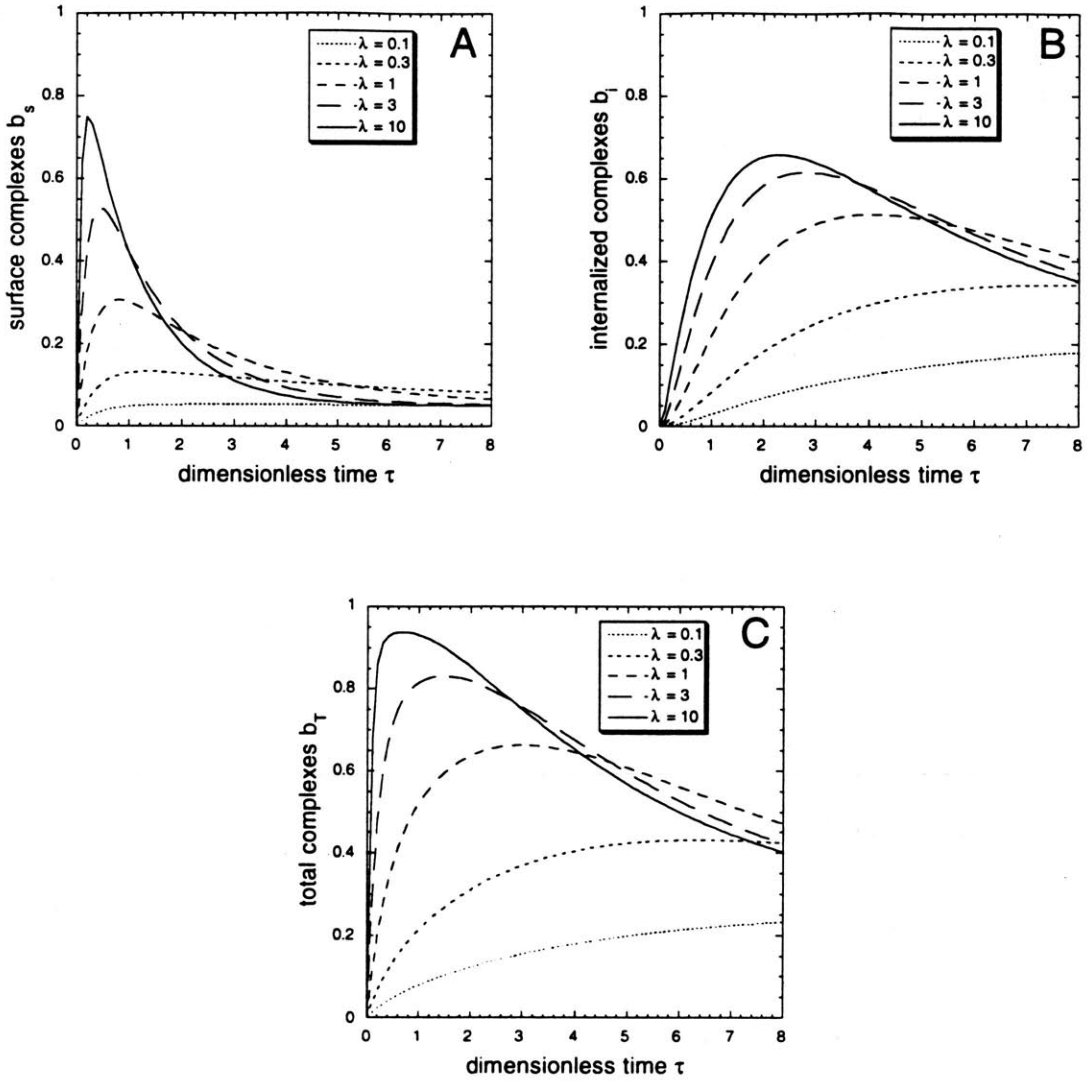

Figure D.1 Simplified RTK Binding and Trafficking Kinetics. Surface, internal, and total receptor complexes are plotted versus dimensionless time $\tau = k_e t$, where k_e is the endocytic rate constant, according to eqn. D.3. The following dimensionless parameters are used: $\rho = 5/4$; $\nu = 1/20$, $\delta = 1/4$, and λ as indicated. A, surface receptor ligand complexes b_s. B, internalized receptor complexes b_i. C, total receptor complexes $b_T = b_s + b_i$.

First, the conservation of "membrane" is considered. The appropriate equations at steady state are:

$$\begin{aligned} V_m - k_t M^M + k_{rec} M^E &= 0 \\ k_t M^M - (k_{rec} + k_{deg}) M^E &= 0 \end{aligned} \qquad \text{(D.4)},$$

where M^M is the amount of membrane comprising the plasma membrane of a cell and M^E is that of endosomes collectively. The rate constants k_t, k_{rec}, and k_{deg} describe random membrane endocytosis, recycling of membrane from endosomes back to the plasma membrane, and movement of membrane out of endosomes to degradative compartments, respectively, and V_m is the rate of membrane synthesis (delivered to the plasma membrane). Rearranging,

$$\frac{M^E}{M^M} = \frac{k_t}{k_{rec} + k_{deg}} \equiv N\beta^2 \qquad \text{(D.5)},$$

where N and β are as defined in the main text. Substituting values for rate constants reported in the literature [$k_t \approx 0.03 - 0.05\ s^{-1}$, $k_{rec} + k_{deg} \approx 0.2 - 0.3\ s^{-1}$ (Lauffenburger and Linderman, 1993; Ghosh et al., 1994; Thilo et al., 1995)], $N\beta^2 \approx 0.2 - 0.25$, in agreement with direct measurements and independent estimates of N and β (Table 3.1).

For protein/lipid targets that reside in membranes, equations can be formulated as in eqn. D.4. If these targets diffuse freely in membranes such that their trafficking is indeed random, then

$$\frac{N_t^E}{N_t^M} = \frac{k_t}{k_{rec} + k_{deg}} = N\beta^2 \qquad \text{(D.6)},$$

where N_t^i are the number of targets of interest residing in compartment i. The implication is that $N_t^M/M^M = N_t^E/M^E$; the density of freely diffusing membrane components in endosomes is the same as that in the plasma membrane. This is in spite of the likelihood that synthesis rates of "membrane" and its constituents are various. Equations D.5 and D.6 hold as long as newly synthesized molecules are not delivered to endosomes.

E. Secondary Effects on Substrate Phosphorylation State

An aspect of substrate-receptor interactions neglected in the model equations of Chapter 3 is the possible direct interaction of substrate molecules with the receptor kinase domain, irrespective of the interaction of substrate with receptor phosphotyrosine. Likewise, it is also possible for the substrate to interact with membrane phosphatases. Referring to eqn. 3.1, the new radial boundary condition at the plasma membrane is

$$-\left(\frac{1}{\gamma}\right)\frac{\partial\theta}{\partial\tilde{r}}\bigg|_{\tilde{r}=1} = (fp_s + \varepsilon^M)b_s\theta|_{\tilde{r}=1} - \kappa\left(s_m + \chi^{-1}\delta_p{}^M\theta^*|_{\tilde{r}=1}\right)$$
$$\frac{\partial(\theta^*+\theta)}{\partial\tilde{r}}\bigg|_{\tilde{r}=1} = 0; \quad \varepsilon^M \equiv \frac{k_k{}^{CM}}{k_{on}} \qquad \text{(E.1)},$$

where $k_k{}^{Ci}$ is the observed second order rate constant of cytosolic substrate phosphorylation by receptors in compartment i, and the parameter χ is defined as the enhancement factor of membrane-membrane protein association over cytosol-membrane association; this factor is expected to be two to three orders of magnitude (Chapter 2). Note that it has been somewhat arbitrarily stipulated for simplicity that cytosolic substrate can interact with the kinase domains of all ligated surface receptors in this model. An analogous modification is also made at endosomal boundaries, depending on the spatial variation of the model used, with ε^E being the dimensionless rate constant describing direct phosphorylation of cytosolic substrate by active endosomal receptors.

Another effect examined here is the potential transphosphorylation of receptor-bound substrate by other active receptors diffusing laterally in cellular membranes. This is done by simply adding second order reaction terms into the $\delta_k{}^i$ component of ϕ^i and Q^i:

$$\hat{\phi}^M = \frac{\phi^M(1+\psi b_s)}{1+\phi^M\psi b_s}; \quad \hat{\phi}^E = \frac{\phi^E(N\beta^2+\psi b_i)}{N\beta^2+\phi^E\psi b_i}$$
$$\hat{Q}^M = \frac{Q^M(1+\phi^M\psi b_s)}{1+\phi^M Q^M\psi b_s}; \quad \hat{Q}^E = \frac{Q^E(N\beta^2+\phi^E\psi b_i)}{N\beta^2+\phi^E Q^E\psi b_i} \qquad \text{(E.2)},$$
$$\psi \equiv \frac{k_{xk}{}^M R_T}{k_k{}^M} = \frac{N\beta^2 k_{xk}{}^E R_T}{k_k{}^E}$$

where $k_{xk}{}^i$ is the second order crossphosphorylation rate constant observed for compartment i, in units of [(#/cell)*time]$^{-1}$.

With these added effects sufficiently defined, one can resolve the model equations to see if complex behaviors arise with their inclusion. The kinetic approximation is employed, since it is the most tractable, with abbreviated notation:

$$\frac{\bar{\theta}^*}{\bar{\theta}} = \frac{\hat{\phi}^M m(\hat{Q}^M\pi_s) + \hat{\phi}^E e(\hat{Q}^E\pi_i) + m(\varepsilon^M b_s) + e(\varepsilon^E b_i)}{(1-\hat{\phi}^M)m(\hat{Q}^M\pi_s) + (1-\hat{\phi}^E)e(\hat{Q}^E\pi_i) + m(\chi^{-1}\mu^M) + e(N\beta^2\chi^{-1}\mu^E) + \mu^C} \qquad \text{(E.3a)}.$$
$$m(x) = \frac{5x}{5+\gamma x}; \quad e(x) = \frac{N\beta x}{N\beta+\gamma x}; \quad \pi_x = fp_x b_x; \quad \mu^i \equiv \delta_p{}^i\kappa$$

Note the expression above is in the form of phosphorylated:unphosphorylated, rather than phosphorylated:total, because the solution posed in this way is more compact. The phosphorylation stoichiometries of receptor-bound species are then

$$\frac{s_m^*}{s_m^* + s_m} = \frac{(1-\hat{Q}^M)\bar{\theta}^*/(\theta^* + \theta) + (1+\gamma f p_s b_s/5)\hat{\phi}^M \hat{Q}^M}{1+(\gamma f p_s b_s/5)\hat{Q}^M}$$
$$\frac{s_e^*}{s_e^* + s_e} = \frac{(1-\hat{Q}^E)\bar{\theta}^*/(\theta^* + \theta) + (1+\gamma f p_s b_s/N\beta)\hat{\phi}^E \hat{Q}^E}{1+(\gamma f p_s b_s/N\beta)\hat{Q}^E} \qquad \text{(E.3b).}$$

In order to impact substrate phosphorylation, $\chi^{-1}\delta_p{}^i\kappa$, ε^i, and/or ψ must be of significant magnitude. For the phosphatase effect, $\delta_p{}^i\kappa$ must be at least ~ χ ~ 10^2 - 10^3. This is unlikely based on our parameter estimations, so dephosphorylation of cytosolic substrate by membrane phosphatases is probably not significant under normal circumstances. As for ε^i, one can get a sense of its magnitude by analyzing the bound substrate case. If one conservatively considers a substrate bound to a receptor to be restrained by a 10 nm tether with no further restrictions, then the concentration of this single molecule is ~ 1 mM. By comparison, the concentration of a cytosolic protein with 10^4 - 10^5 copies in a typical cell S_T/V is ~ 10 - 100 nM. Thus, $\varepsilon^i\sigma/\delta_k{}^i\kappa$ may be as low as 10^{-5} to 10^{-4}. In the presence of kinase saturability, the concentration to compare S_T/V to is the value of the Michaelis constant K_M. For example, for a K_M of ~ 100 μM (Bertics and Gill, 1985; Rotin et al., 1992), $\varepsilon^i\sigma/\delta_k{}^i\kappa$ can be as high as ~ 10^{-3}. Given our estimates of $k_k{}^M$ and k_{on}, ε^i ~ 10^{-3} to 10^{-2} in this limit. This suggests that it may be appropriate to neglect phosphorylation of substrate in the cytosol under normal conditions. Many investigators have noted that when the phosphorylable tyrosines of EGFR are removed ($p_i = p_s = 0$), substrates are still phosphorylated to a measurable extent (Vega et al., 1992; Gotoh et al., 1994; Soler et al., 1994). Our analysis suggests that this is an artificial situation that likely alters both the phosphorylation and dephosphorylation fluxes by orders of magnitude.

The other model modification is the potential for transphosphorylation of bound substrate by other receptors. It is difficult to conceive of this mechanism being important, given the much higher proximity of the substrate to its binding partner's kinase in relation to all other active receptors. This point is illuminated when one tries to estimate ψ by invoking $\psi \sim \chi\varepsilon^M/\delta_k{}^M\kappa$, which our previous analysis argues should be ~ 0.01 to 1. Obviously, the high end of this estimate is achieved through kinase saturability, implying that substrate bound to receptor phosphotyrosine is also interacting with the kinase domain of the same receptor at any given time with high probability. Thus, additional conformational aspects of the substrate-kinase interaction must be significantly different for transphosphorylation of substrate to be important. Nevertheless, an order-of-magnitude upper bound on $k_{xk}{}^M$ can be estimated in the diffusion limit: $k_{xk}{}^M(\max) \sim D_m/a^2 \sim 10^{-4}$ $(\text{cell}^*\text{s})^{-1}$, where D_m is the membrane diffusivity of the receptor. Based on this limit and our other parameter estimates, it is at least *possible* to achieve ψ ~ 1 or greater.

To analyze these effects, eqn. E.3 was simplified by not allowing ligation of internalized receptors ($b_i = 0$). In Figure E.1, δ_p^C/δ_p^M, χ, ε^M, and ψ are varied, with fixed $\gamma = 0$, $\delta_k^M = 1$, $\delta_p^M+\delta_p^C = 2$, and $p_s = 1$, and the sensitivity of total substrate phosphotyrosine ($\theta^*+s_m^*$) to b_s is examined. In Figure E.1A, more or less linear substrate binding parameter values are used ($\sigma = \kappa = 1$), whereas more saturable values are used for Figure E.1B ($\sigma = \kappa = 0.1$). For the base case, $\chi = \infty$ and $\varepsilon^M = \psi = 0$, corresponding to the model used in the main text. We then varied these parameters one at a time, using a reasonable value for χ ($\chi = 300$), an exaggerated value for ε^M ($\varepsilon^M = 0.1$), or the maximum conceivable value of ψ ($\psi = 1$). From this analysis we conclude that the $\chi^{-1}\delta_p^M$ and ε^M effects, which directly affect θ^*, can be prominent if $\delta_p^C << \delta_p^M$ and substrate-receptor binding is low ($s_m^*+s_m << 1$). In contrast, the relative effect of ψ, which directly impacts s_m^*, can be prominent if $\delta_p^C << \delta_p^M$ or substrate-receptor binding is high. Again, it should be noted that exaggerated values of ε^M and ψ were used in Figure E.1 for illustrative purposes.

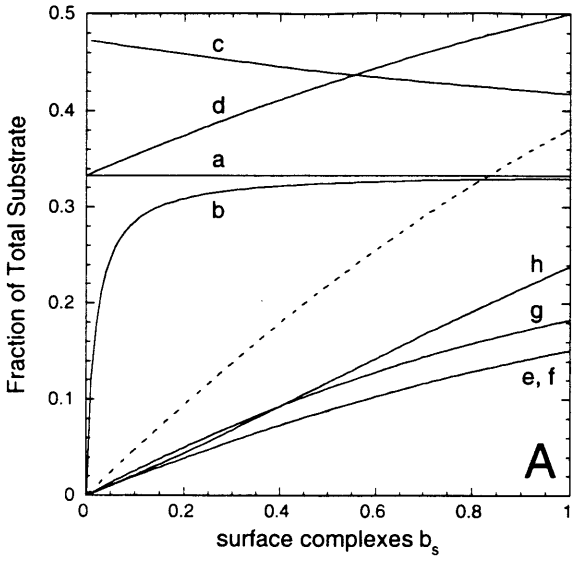

	δ_p^M	δ_p^C	χ	ε^M	ψ
a	2	0	$>>10^3$	0	0
b	2	0	300	0	0
c	2	0	$>>10^3$	0.1	0
d	2	0	$>>10^3$	0	1
e	0.5	1.5	$>>10^3$	0	0
f	0.5	1.5	300	0	0
g	0.5	1.5	$>>10^3$	0.1	0
h	0.5	1.5	$>>10^3$	0	1

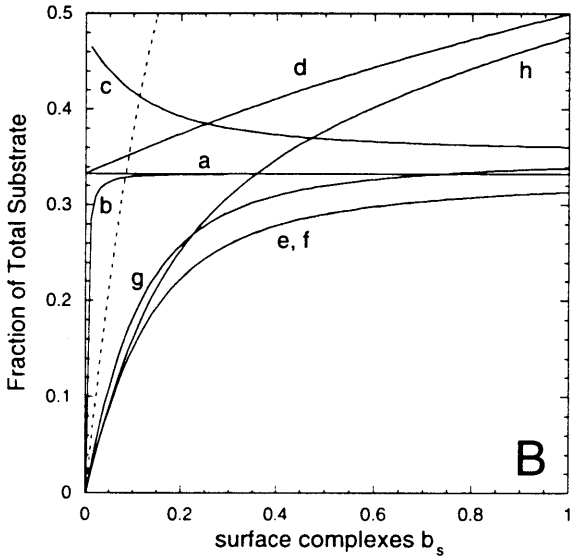

Figure E.1 Secondary Substrate Phosphorylation/Dephosphorylation Mechanisms. Equation E.3 was simplified by not allowing internal receptors to be active ($b_i = 0$), and substrate phosphorylation states were calculated as a function of b_s. Dashed lines indicate receptor-substrate binding ($s_m^* + s_m$) and solid lines indicate substrate phosphotyrosine ($\theta^* + s_m^*$). The following parameters were held constant: $\gamma = 0$, $\delta_k^M = 1$, $\delta_p^M + \delta_p^C = 2$, and $p_s = 1$. Values for δ_p^C/δ_p^M, χ, ε^M, and ψ for each curve are as indicated, and receptor-substrate binding parameters are: A, $\sigma = \kappa = 1$; B, $\sigma = \kappa = 0.1$.

References

Bertics, P.J. and Gill, G.N. (1985). Self-phosphorylation enhances the protein-tyrosine kinase activity of the epidermal growth factor receptor. *J. Biol. Chem.*, 260: 14642-14647.

Ghosh, R.N., Gelman, D.L. and Maxfield, F.R. (1994). Quantification of low density lipoprotein and transferrin endocytic sorting in HEp2 cells using confocal microscopy. *J. Cell Sci.*, 107: 2177-2189.

Goldbeter, A. and Koshland, D.E.J. (1981). An amplified sensitivity arising from covalent modification in biological systems. *Proc. Natl. Acad. Sci. USA*, 78: 6840-6844.

Gotoh, N., Tojo, A., Muroya, K., Hashimoto, Y., Hattori, S., Nakamura, S., Takenawa, T., Yazaki, Y. and Shibuya, M. (1994). Epidermal growth factor-receptor mutant lacking the autophosphorylation sites induces phosphorylation of Shc protein and Shc-Grb2/ASH association and retains mitogenic activity. *Proc. Natl. Acad. Sci. USA*, 91: 167-171.

Lauffenburger, D.A. and Linderman, J.L. (1993). *Receptors: Models for Binding, Trafficking, and Signaling.* New York: Oxford University Press.

Lund, K.A., Opresko, L.K., Starbuck, C., Walsh, B.J. and Wiley, H.S. (1990). Quantitative analysis of the endocytic system involved in hormone-induced receptor internalization. *J. Biol. Chem.*, 265: 15713-15723.

Rotin, D., Honegger, A.M., Margolis, B.L., Ullrich, A. and Schlessinger, J. (1992). Presence of SH2 domains of phospholipase $C\gamma_1$ enhances substrate phosphorylation by increasing the affinity toward the epidermal growth factor receptor. *J. Biol. Chem.*, 267: 9678-9683.

Shoup, D., Lipari, G. and Szabo, A. (1981). Diffusion-controlled bimolecular reaction rates: the effect of rotational diffusion and orientation constraints. *Biophys. J.*, 36: 697-714.

Soler, C., Alvarez, C.V., Beguinot, L. and Carpenter, G. (1994). Potent SHC tyrosine phosphorylation by epidermal growth factor at low receptor density or in the absence of receptor autophosphorylation sites. *Oncogene*, 9: 2207-2215.

Thilo, L., Stroud, E. and Haylett, T. (1995). Maturation of early endosomes and vesicular traffic to lysosomes in relation to membrane recycling. *J. Cell Sci.*, 108: 1791-1803.

Vega, Q.C., Cochet, C., Filhol, O., Chang, C., Rhee, S.G. and Gill, G.N. (1992). A site of tyrosine phosphorylation in the C-terminus of the epidermal growth-factor receptor is required to activate phospholipase C. *Mol. Cell. Biol.*, 12: 128-135.